TV / COMPUTER MOTION ANALYSIS SYSTEMS

THE FIRST TWO DECADES

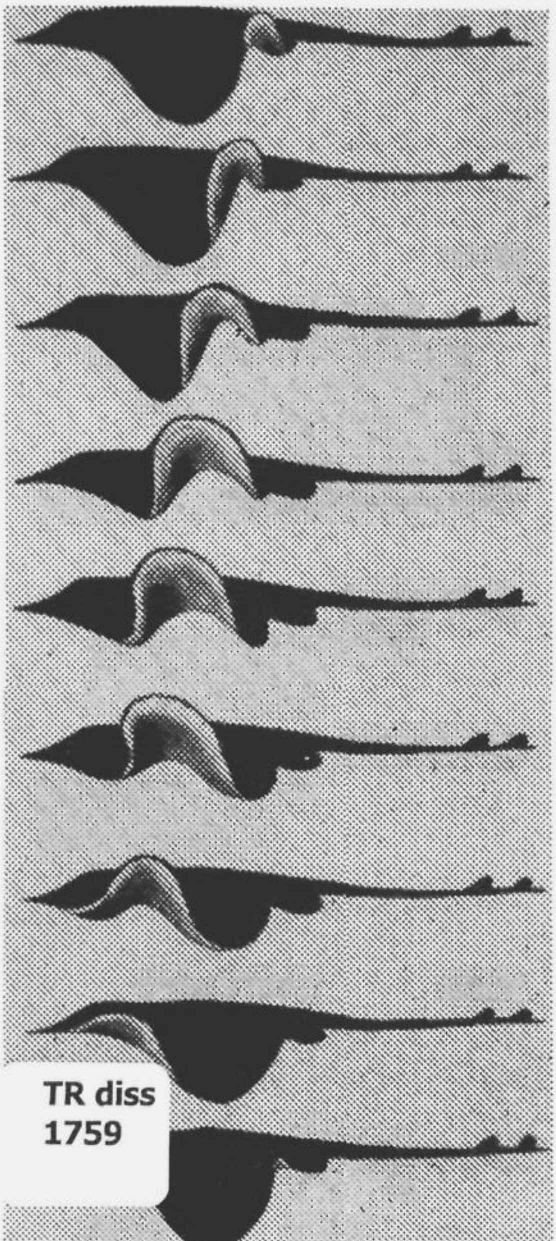

E.H. Furnée

TV / COMPUTER MOTION ANALYSIS SYSTEMS

THE FIRST TWO DECADES

E.H. Furnée

PhD thesis october 1989
Delft University of Technology

Cover: swimming Manta ray, recorded by E.J. Marey, 1884.

CIP-gegevens Koninklijke Bibliotheek, den Haag
Furnée, Egbert Hans
TV / computer motion analysis systems : the first two decades / Egbert Hans Furnée. - [S.l. : s.n.]. - Ill.
Proefschrift Delft. - Met lit. opg. - Met samenvatting in het Nederlands, Frans en Duits.
ISBN 90-9003095-6
SISO 666.7 UDC 681.3:621.397.13(043.3)
Trefw.: bewegingsstudie.

Signal Processing Department, Faculty of Applied Physics
Delft University of Technology, FAX 31-15 786081
PO Box 5046, 2600 GA Delft, the Netherlands

TV / COMPUTER MOTION ANALYSIS SYSTEMS
THE FIRST TWO DECADES

TV / COMPUTER SYSTEMEN VOOR BEWEGINGSANALYSE
DE EERSTE TWINTIG JAAR

PROEFSCHRIFT
ter verkrijging van de graad van doctor
aan de Technische Universiteit Delft,
op gezag van de Rector Magnificus, prof. drs P.A. Schenck,
in het openbaar te verdedigen ten overstaan van een
commissie aangewezen door het College van Dekanen op
maandag 30 oktober 1989 te 14.00 uur door

EGBERT HANS FURNÉE,

geboren te den Haag,
elektrotechnisch ingenieur.

*Dit proefschrift is goedgekeurd
door de promotoren*

*Prof. ir B.P.Th. Veltman
Prof. J.P. Paul PhD.*

To my wife Lidy

to my students

Dick de Graaff *
Piet Venemans *
Ab Pasman *
Max Dil *
Paul Steilberg
John Bijlsma
Ko Rozema *
Siebren Gombert
Peter Dirkson *
Jacques Hendriks
Jan Schimmel *
Anton van Gent *
Gert-Jan van Ingen Schenau
Jetse Molenaar *
Hans van Stokrom
Kaj Nieukerke
Jûnt Halbertsma
Jan Bakker *
Bob Andriesse
Jelte Feenstra *
Rolf de Boer *
Johan de Bie
Arie Lodder *
Pieter Oostinjen
Martin Loose *
Gert van Antwerpen
Erwin Serlé
Ben Kleiss *
Axel Zandbergen
Henk Demper
Jan Melein
Hein Sikkenk
Jan Cees Sabel
Marcel Zuidhof
Bart Schilt
Hans Brinkman
Dirk-Jan Toet

* *on other than the video projects*

Abstract

TV-based motion analysis systems are described, that perform real-time non-contacting coordinate data acquisition of contrasting markers, attached as landmark points to unobstructed moving objects. The account ranges from our original prototype to the recent PRIMAS Precision Motion Analysis System. A review of literature discusses derived and alternative systems, developments are positioned within a historical framework. Performance criteria are formulated, PRIMAS test results are given and a comparison of this and commercial systems is provided.

Acknowledgements: schematic drawings F. van 't Hof and H.K. Nagtegaal
photographs ch. 4 A.R. Suiters.

Summary

This book concerns TV-based systems interfaced to digital computers for motion analysis.

Real-time data acquisition, at normal or elevated TV rates, pertains to the projected or spatial coordinates of markers, which are attached to strategic points of interest at the subject in motion.
The landmarks may be chosen such that all relevant points in a kinematic chain are defined, like in articulating segments of the human or animal body or of a technical construction. In other applications, the landmarks may define a surface grid, such as for the dynamic strain analysis in metallurgy or artificial and biological tissue mechanics. Though some drawbacks are well recognized, reducing the moving subject to one or more representative marker clusters is essential with all past and present automated motion recording systems.
Landmarking the subject already played a role in historic development, such as sketched in the introductory chapter 1, where the emphasis is on the introduction of photographic methods and the invention in 1888 of the filmcamera by the French engineer-physiologist E.-J. Marey.
Since the invention of the digital computer, several methods, reviewed in chapter 1, were developed for the manual or semi-automatic transfer of photographic or film data for subsequent motion analysis. Automatic systems for direct-view on-line computer input, without intermediary cine-film recording, had been lacking.

Chapter 2 is concerned with our original TV-based real-time coordinate data acquisition system. This introduced the so-called video-digital coordinate converter. In this device, above-threshold video from the marker image triggers the instantaneous read-out of two running binary counters, one for the line number or Y-coordinate, the other for the horizontal sweep increment or X-coordinate.
The first operational and documented multi-marker 50 Hz system (1967) hooked up to the early IBM-1130 disk-based minicomputer.
It already offered the choice of markers between subminiature lamps or passive, reflective paper stickers.
Also, this first automated motion recording system had the feature of data reduction, in that a contour suppressor inhibited all but one points on each of the marker contours. Later versions had the option of digitizing two or four diagonal points on the marker contour. To alleviate host computer transfer and storage, real-time data reduction has remained a hallmark of further system development.
Equidistant and simultaneous sampling of the markers was accomplished with the early prototypes by introducing a synchronously rotating shutter in front of the TV camera, while stroboscopic pulse illumination of reflective markers was used as early as 1974.
Concurrently with the hardware, the characteristic software required with TV-based systems was pioneered, such as the marker identification routine which assigns coordinate pairs to markers, by tracking their relative position shifts across the successive TV fields.

Chapter 3 reviews the collaborative project, started at Strathclyde University, Glasgow, on the basis of our TV-system prototypes. This Strathclyde system, with the improvements achieved and based upon a dedicated DEC-PDP-11 minicomputer, in its turn gave birth to the first commercial system VICON (1981) by Oxford Instruments, UK.
Next to a literature review of derived or alternative TV-based systems chapter 3 reviews competing opto-electronic motion analysis systems, based on non-TV sensors like the Position Sensitive Device, emerging in the 1975 SELSPOT system, and linear CCD arrays such as with CoStel (1979) and OPTOTRAK (1988), all using active switched LED markers.

Chapter 4 returns to the author's work, with a discussion of further development in the TV/computer motion analysis system. Here the focus is on real-time estimation of the centroid coordinates of full marker contours, on camera improvements and hooking up to personal computers. The real-time marker centroid estimation by an on-board microprocessor subsystem achieves data reduction as well as sub-pixel resolution.
The dedicated CCD cameras achieve 100 fields/s operation and low-noise system performance, with typically better than 1:10000 precisions.
Moreover, as these cameras feature the option of reduced-integration-time or electronically-shuttered stroboscopy, this front-end offers a 100-fold improved contrast of the synchronously illuminated retro-reflective markers, allowing daylight operation. As from 1986, the system acronym is PRIMAS for Precision Motion Analysis System.

After discussing contemporary competing systems such as VICON, ELITE (1985), ExpertVison (1986) and Hentschel (the latter, 1988, using an unconventional random access image dissector camera) this chapter ends with a review of the system performance aspects such as sampling rate and the figure or merit for spatio-temporal resolution.
The final systems comparison, inclusive of non-TV commercial devices, is unequivocal as to the merit of the PRIMAS specifications.

Chapter 5 focuses on an alternative approach to a high-speed low-noise system which, while using the same PSD camera improves on some aspects of the SELSPOT system. Using the LED markers in frequency-multiplex and applying synchronous detection to the PSD signals, the advantage is regained of simultaneous sampling of the moving markers. Moreover, background or ambient light, plaguing other PSD systems, is drastically suppressed. In its turn, this allows visible light LED markers, so to obviate the problems of spurious reflections with infrared LED's in the competing systems. A closer analysis has yielded the requirement of tapered windowing for the synchronous detection signals, to improve the low-pass filter characteristic for motion frequency components and totally suppress the electric light interference.

The application chapter 6 reviews some of the collaborative projects with investigations of human, animal and industrial motion phenomena, and is followed by a recapitulation, conclusion and future prospects.

Sommaire

Cet ouvrage concerne les systèmes à TV, joints à des ordinateurs, pour l'analyse du mouvement.

L'acquisition des données en temps réel, aux cadences TV normaux ou élevés, regarde les coordonnées projetées ou spatiales des repères ou marques attacheés à des points stratégiques au sujet en mouvement.
Les marques peuvent être choisies tant que tous les points d'intérêt dans une chaine kinématique soient définis, comme dans les membres articulants du corps humain ou animal ou dans une construction technique. Dans d'autres applications les marques peuvent definir un réseau en surface, comme pour l'analyse dynamique d'étirage en métallurgie ou dans la méchanique des tissus artificiels ou biologiques.
Bien que des inconvénients soient reconnus, la réduction du sujet vers un ou plusieurs ensembles de marques est essentiel avec tous systèmes d'enrégistrement de mouvement au passé et à présent.
Le marquage des sujet se faisait déjà dans le dévéloppement historique comme dépeint en premier chapitre, où l'accent est mis sur l'introduction des méthodes photographiques et l'invention en 1888 de l'appareil de prises de vue par l'ingénieur-physiologiste français E.-J. Marey, ce qu'est devenu le premier ciné-caméra.
Depuis l'invention de l'ordinateur, plusieurs méthodes, décrites en chapitre 1, furent dévéloppées pour le transfert à main ou en semi-automatique des données photographiques ou cinematographiques pour l'analyse de mouvements. Il manquaient des systèmes automatiques pour le transfert en directe à l'ordinateur, sans l'intermédiare du film.

Chapitre 2 concerne notre système original à TV pour l'acquisition des coordonnées en temps réel. Cela a introduit le soi-disant convertisseur video-digital des coordonnées. Dans cet appareil le signal video, passant un valeur seuil, provoque la lecture instantanée du contenu de deux compteurs binaires, l'un pour le numéro de lignes ou coordonnée Y, et l'autre pour l'incrément de balayage horizontal ou la valeur X.
Le premier système opérationnel et documenté (1967), à plusieurs marques et à 50 Hz, s'accouplait au mini-ordinateur précoce IBM-1130.
Déjà cet ensemble offrait le choix de marques entre des ampoules sous-miniatures ou des réflecteurs passifs en papier gommé.
Aussi, ce premier système automatique pour l'enrégistrement de mouvement avait l'attribut de la réduction des données, en tant qu'un soi-disant suppresseur de contours prévoyait l'inhibition de tous les points sauf un sur le contour de chacun des marques. Des versions suivantes offraient de digitaliser deux ou quatre points en diagonale sur le contour des marques. Pour faciliter le transfert et l'emmagasinage des données en ordinateur, la réduction des données en temps réel a resté l'un des caractéristiques du dévéloppement ultérieur.
L'échantillonnage équidistante et simultanée des marques fut, avec les premiers prototypes, accompli par un obturateur rotatif synchronisé, introduit en face du caméra, tandis que l'illumination stroboscopique des marques réflecteurs fut introduit déjà en 1974.

En même temps que l'appareillage nous avons pionné le soft typiquement nécessaire avec les systèmes en TV. Ainsi le programme pour l'identification des marques, qui doit attribuer les paires de coordonnées aux marques annexes, en utilisant la poursuite et la prédiction de leur déplacements relatifs dans les champs TV successifs.

Le chapitre 3 parcourt le projet collaboratif mis en marche à Glasgow au Strathclyde University, s'appuyant sur nos prototypes de systèmes à TV. C'est ce système Strathclyde, avec son fonctionnement à plusieurs caméras et basé sur le mini-ordinateur dédié du type DEC-PDP-11, qui à son tour a engendré le VICON, le premier système commercial (1981), par Oxford Instruments, RU.
Après une revue de la littérature de systèmes à TV dérivés ou alternatifs, le chapitre 3 survole les systèmes concurrents optoélectroniques pour l'analyse des mouvements, basés sur des capteurs non-TV. Ainsi le Position Sensitive Device (PSD) dans le système SELSPOT, mis au jour 1975, et le capteur CCD linéaire comme avec CoStel (1979) et OPTOTRAK (1988), tous ceux utilisant les marques actifs sous forme de LED's (diodes émettants la lumière) commutés.

Le chapitre 4 retourne au travail de l'auteur même avec une discussion des développements parcourus dans les systèmes TV/ordinateur d'analyse de mouvements. Les points focaux sont a) l'estimation des coordonnées du centre géometrique à partir des contours complètes des marques, b) les améliorations des caméras TV et c) l'accouplage aux PC. L'estimation des coordonnées des centres de marques, par un microprocesseur à bord du système intelligent, parvient à la réduction des données et à une résolution qui s'exprime à l' échelle sous-pixel.
Les caméras TV dédiés atteignent la cadence de 100 Hz et l'opération à bruit abaissé, la précision du système typiquement surpassant 1:10000. En plus, comme ces caméras TV offrent l'attribut d'un temps d'intégration réduit ou bien la stroboscopie en obturateur électronique, c'est ce capteur du système qui réalise un perfectionnement à 100 fois du contraste des marques rétro-réflecteurs, illuminés en synchronisme.
Cela permet l'opération au lumière du jour. Depuis 1986 le système se nomme PRIMAS (Precision Motion Analysis System).

Après avoir discutés les systèmes commerciaux contemporains VICON, ELITE (1985), ExpertVision (1986) et Hentschel (ce dernier, de 1988, utilisant un caméra inconventionnel du type dissecteur d'images avec l'accès aléatoire) le chapitre en finit avec un survol des points de vue de performance de système, notamment la cadence d'échantillonnage et l'indicatif de mérite en résolution spatio-temporelle.
La comparaison finale des systèmes, y compris les systèmes commerciaux non-TV, est sans équivoque sur les mérites des spécifications PRIMAS.

Le chapitre 5 se met à décrire une approche alternative à un système à haute cadence et à bruit abaissé qui, bien qu'utilisant le même caméra à PSD, surpasse le système SELSPOT dans quelques points de vue.

C'est en utilisant les marques LED en multiplex de fréquence (donc pas commutés) et en appliquant la méthode de détection synchrone, que l'avantage est récupéré de l'échantillonnage simultanée des marques. En outre, la lumière de fond ou de l'ambiance, si nocif au système SELSPOT, est radicalement supprimé. A son tour cela permet les marques LED en lumière visible, afin de réduire les problèmes des réflections fausses avec les marques LED infrarouges des systèmes compétiteurs. Une analyse plus avancée a révélé l'exigence d'une envéloppe décroissante ("windowing") des signaux de détection synchrone, pour améliorer la caractéristique du filtre passe-bas en ce qui concerne les composants de fréquence du mouvement, ainsi que pour la suppression totale des parasites de lumière électriques.

Le chapitre 6 sur les applications fait voir des exemples de projets collaboratifs à la recherche de phénomènes de mouvement humaines, animales et industrielles, et est enfin dans le chapitre 7 suivi d'une récapitulation, de conclusions et de perspectives futures.

Zusammenfassung [1]

Dieses Buch befaßt sich mit auf Videokameras basierende, rechnergekoppelte Bewegungsanalysesysteme.

Die Echtzeit-Datenerfassung erfolgt anhand der Raumkoordinaten (oder deren Projektionen) von Markierungen, die an strategisch wichtigen Punkte am bewegten Subjekt befestigt sind. Hierbei wird die normale oder eine erhöhte Video-Abtastrate benutzt.
Die Meßmarken sind so zu wählen, daß alle relevante Punkte der kinematischen Kette, wie zum Beispiel bei gelenkverbundene Teile der menschlichen oder tierischen Körpers, oder bei technischen Konstruktionen, definiert sind. Bei anderen Anwendungen können die Markierungen ein Flächennetz bilden, wie z.B. bei der dynamischen Verzerrungsanalyse im Bereich der Metallurgie oder bei der Mechanik künstlicher oder biologischer Gewebe. Obwohl bei diesem Verfahren einige Nachteile bekannt sind, ist das Verfahren der Reduktion des sich bewegenden Subjektes auf eine oder mehrere repräsentative Gruppen von Markierungspunkte *typisch für alle früheren und heutigen Bewegungserfassungs* Systeme. Das Verfahren der Markierung, also Abstrahierung, eines Subjektes spielte schon in der historischen Entwicklung der Bewegungsanalyse eine Rolle, wie im einleitendem Kapitel 1 dargestellt. Hierin wird besonders auf die Einführung von fotografische Verfahren sowie auf die Erfindung der Filmkamera im Jahre 1888 durch den französischen Ingenieur-Physiologen E.-J. Marey eingegangen.
Kapitel 1 skizziert des weiteren, daß seit der Erfindung des Digitalrechners verschiedene Verfahren entwickelt wurden, die der manuellen oder halb-automatischen Eingabe von fotografischen oder Filmdaten zur Bewegungsanalyse dienen.

[1] *Uebersetzt von dipl.ing. U. Pohl, Aachen.*

Es fehlten automatische Systeme für die direkt-Sicht Datengewinnung, das heißt, ohne Zwischenstufe von Filmaufname und Bearbeitung.

Kapitel 2 befaßt sich mit unserem originellen, auf Video-Kameras basierenden, Echtzeit-Koordinatenerfassungssystem. Dieses Verfahren introduzierte den sogenannten video-digital Koordinatenwandler.
In diesem Gerät löst das, einem Schwellwert überschreitendes, Videosignal, das die kontrastierende Bilder von Markierungen repräsentiert, das sofortige Ablesen zweier mitlaufender binärer Zähler aus. Der eine Zähler stellt die Zeilenzahl oder die Y-Koordinate, der andere das horizontale Abtast-Inkrement oder die X-Koordinate dar.
Das erste betriebsfähige und dokumentierte Multi-Marker-50-Hz-System (1967) benutzte eine Schnittstelle zum früheren IBM-1130 Minicomputer, der bereits mit einer Festplatte ausgerüstet war.
Schon dieses System bot für die Markierungen die Wahl zwischen subminiatur-Lampen oder passiven, reflektierenden Papierscheibchen.
Außerdem besaß dieses erste automatisierte Bewegungseingabesystem als Besonderes eine Einrichtung zur Datenreduktion, indem ein sogenannter Umrißunterdrücker aus eine Vielzahl von Punkte pro Kontur, bei jedes Marker-Bildes, nur eine zum Umwandlung auswählte. Spätere Versionen hatten die Option, zwei oder vier Diagonalpunkte auf dieser Marker-Kontur zu digitalisieren. Zur Reduzierung des Datentransfers und der Speicherbedarfs im übergeordneten Rechner wurde bei der Weiterentwicklung dieser Systeme der Schwerpunkt bleibend auf die Datenreduzierung im Echtzeitbereich gelegt.
Für die äquidistante und gleichzeitige Stichprobenmessung der Markierungs-Positionen war bei den früheren Prototypen ein synchron vor der Kamera rotierender Verschluß vorgesehen. Die stroboskopische Synchronbeleuchtung von reflektierenden Markierungen wurde schon im Jahre 1974 eingesetzt.
Gleichzeitig mit dem Hardware wurde auch Pionierarbeit auf dem Gebiet der benötigten speziellen Software für Video-gestutzte Systeme so wie der Markierungsidentifikation geleistet. Diese ordnet neu eingewonnene Koordinatenpaare den Markierungen zu durch Verfolgen der relativen Positionsabweichungen über das laufenden Videobild.

Kapitel 3 gibt einen Ueberblick über das gemeinsame Projekt, das, auf der Basis unseres Video-Systems, an der Strathclyde Universität, Glasgow, begonnen hat. Aus diesem Strathclyde-System mit sein Mehr-Kamerabetrieb, das außerdem ein zugeordneter DEC-PDP-11 Minicomputer mit Festplatte besaß, wurde das erste Handelssystem VICON (1981) entwickelt von Oxford Instruments, GB.
Neben ein Literaturübersicht über abgeleitete oder alternative Video-Systeme, gibt das Kapitel 3 auch eine Uebersicht über konkurrierende opto-elektronische Bewegungsanalysesysteme die nicht mit Video sondern mit anderen Bildaufnahmeverfahren arbeiten. Zum Beispiel das Position Sensitive Device PSD, das eingesetzt wird im SELSPOT System (1975), und die lineare CCD Zeilenaufnehmer, wie sie in CoStel- (1979) und OPTOTRAK- (1988) Systemen eingesetzt werden. All diese Systeme verwenden aktiv geschaltete LED Markierungen.

Das Kapitel 4 wendet sich wieder der Arbeit des Autors zu, mit einer Erörterung der Weiterentwicklung im Video/Computer-Bewegungsanalyse-System. Zentrale Fragen sind hier a) Abschätzung der Schwerpunktskoordinate von vollständige Markerungs-Konture im Echtzeitbetrieb, b) Kameraverbesserung, c) Ankupplung an Personal-Computer.
Die Schwerpunktsbestimmung bedeutet wieder eine Datenreduktion, sowie eine Steigerung der Auflösung in den Sub-Pixel Bereich. Die dem System zugeordneten CCD-Kameras erlauben 100 Hz Operationen und eine starke Verringerung des Rauschens, bis auf eine typische 1:10000 Präzision. Zudem haben diese Kameras eine reduzierte Integrations-zeit, also eine stroboskopische Arbeitsweise, mit Vollelektronikverschluß. Das gewährleistet eine 100-fach verbesserten Kontrast der synchron angestrahlte *retro-reflektierende Markierungen, was die Tageslichtbenutzung ermög*licht. Seit 1986 gibt es die Bezeichnung PRIMAS (Precision Motion Analysis System) für das System.

Nach einer Diskussion der gegenwärtig konkurrierenden Systeme wie VICON, ELITE (1985), ExpertVison (1986) und Hentschel (1988, benutzt eine unkonventionelle sogenannte Image Dissector Kamera mit freiwählbarem Zugriff) schließt dieses Kapitel mit einem Ueberblick über Systemleistungsaspekte wie Abtastfrequenz und die spatio-temporare Auflösungsleitzahl.
Der Endvergleich, der auch die nicht-video-gestützten kommerziellen Systeme einbezieht, ist eindeutich hinsichtlich des Verdienstes der *PRIMAS Spezifizierungen.*

Das 5. Kapitel geht auf eine alternativer Annäherung an ein niedrigrauschendes Hochgeschwindigkeits-System ein, das, obwohl dieselbe PSD-Kamera benutzt wird, das SELSPOT System in mehrerer Hinsicht verbessert. Mit der Anwendung von LED Markierungen im Frequenz-Multiplex statt im Zeit-Multiplex und der Verwendung eines synchronen Detektors wird der Vorteil gleichzeitiger Stichprobenmessungen der bewegten Markierungen wiedergewonnen. Außerdem wird das Problem des Hintergrund- und Umgebungslichtes (die Schwierigkeiten der anderen PSD-Systeme) drastisch zurückgedrängt. Deswegen wird die Benutzung sichbarer-Licht LED-Markierungen wieder ermöglicht. Damit werden die Probleme der *störender Reflektionen der Infrarot-LED's ausgeschaltet, womit konkur*rierende PSD-Systeme noch zu kämpfen haben.
Eine eingehendere Analyse hat gezeigt, daß für die synchronen Detektor Signale eine sich verjüngende Einhüllende ("windowing") benötigt wird, um die Tiefpaß-Filterkennlinie für die Bewegungsfrequenzkomponente zu verbessern. Nebenbei gelingt es dann, die Interferenz von elektrischem Fremdlicht völlig zu beseitigen.

Das Anwendungskapitel 6 gibt eine Uebersicht und Auswahl über und von einigen kollaborativen Forschungsprojekte bezüglich menschlicher, tierischer und technischer Bewegungsvorgänge.

Das abschließende Kapitel 7 rekapituliert, gibt Schlußfolgerungen und eine Ausblick auf künftige Entwicklungen.

CONTENTS

CHAPTER 1. INTRODUCTION

The pursuit of non-axiomatic science is not the only endeavour where there is no substitute for observation. On the other hand one bears in mind that, however much measurement science and technology has through the ages boosted the modalities of human observation, even the keenest observation is not a substitute for science. Yet it is no artefact that one activity occurs twice in the perennial cycles of science: observation for new phenomena, inference, hypothesizing, prediction and observation for validation. With these reflections we will in the present thesis account for some contributions towards quantitative observation methods for position and movement. This concerns a data acquisition system with non-contacting, real-time digitizing of moving landmark coordinates, in what began as a study of certain aspects of human motion.

1.1 Historical background

Direct visual observation has until the mid-nineteenth century been the sole tool to provide the data-base for scientific description of, and enquiry into, the nature of animal and human movement.

Supplemented by palpation or dissection, it was only detailed visual observation of the human and animal body in motion that was available to a long line of scientists from Aristotle, through da Vinci, Harvey, Borelli and Boerhaave. These nonetheless compiled meticulous, often comparative descriptions of muscle action and performed geometric and kinematic analyses on locomotion, jumping, and other motion patterns. An actual experiment for instance was performed by Borelli (1679), who noted that he could not keep two vertical posts, put up at a distance, in line of sight while directing his walk straight towards them. This self-experiment demonstrated the cycle of lateral sway in human gait. Boerhaave (1703) was one of the first advocates of applying, after Newton's Principia, methods of mechanics to observations in medicine.

The German brother physiologist and physicist W. and E. Weber (1836) were perhaps the first to attempt some quantitative measurement of locomotion. They used clocks, measuring lines and optical surveying gear, and evolved a theory which in the swing phase of gait considered the leg as a pure pendulum.
The German physician K.H. Vierordt (1881) developed an ink-jet method with multiple nozzles attached to the subject to deliver direct though not too accurate traces on suspended paper strips. On these records he could base a descriptive classification of a number of pathologies.

These non-contacting methods contrasted with the **myograph**, the device which in physiology addressed skeletal or isolated muscle movement by mechanical transmission to a pointer, which traced time-records of its excursion on the soot-blackened surface of a rotating drum. This and similar contraptions were used and improved by the French engineer-physiologist E.-J. Marey, who in 1868 recorded the wing-beat of a dove flying in a carousel with a pneumatic linkage to this apparatus. The myograph or kymograph, originally due to Helmholz, considerably pre-dates Edisons phonograph of 1888 which recorded sound-induced membrane motion on a waxed drum. Human walking patterns were already studied by M.G. Carlet (1872) with tiny balloon pads for sensing displacements of parts of the body, foot pressure and periods of muscular activity. Again these sensors had pneumatic transmission to the kymograph, that early precursor of the electric penrecorder.

It was not until the advent of **photography** that significant advances were made in the quantifying of locomotion and, in due time, many other aspects of human and animal motion. Methods and instruments developed in this field, as the following will show, have ever since found widening application. They led to the consumers' cinema, and with improvements all along, from observatory to Wilson chamber, they have within a century been used for recording most of the moving macro- and microcosm of physical bodies and particles.
To return to locomotion, it was the British photographer E. Muggeridge (later Muybridge) who in Sacramento CA USA demonstrated the ability of photography to arrest motion by a sequence of pictures. With an array of 12 cameras, with trip-wired shutters to secure properly ordered delays, he in 1872 proved the unsupported transit phase of the horse in trot: a wager had been laid on the number of hooves in contact with the turf, cf. (Willman 1882, Muybridge 1899, Mozley et al. 1972).

With perfected methods, with up to 24 cameras and a rotary commutator for the progressive electromagnetic release of the shutters (cf. Haas 1976), Muybridge (1899, 1901) pursued his **serial photography**. This heritage consists of some 100.000 plates of animal and human motion, recorded at Palo Alto CA and, from 1884, at the University of Pennsylvania. Already Dercum (1888) presents displacement/time curves for normal and pathological gait, derived from Muybridge's recordings.

The invention of the film-camera is due to the earlier-mentioned Marey who in 1888 [1] presented the **chronophotographic box**, in which a strip of photographic paper was transported behind a lens with an interposed rotary shutter mechanism at 20 exposures/s. Marey describes the necessity of the film being at rest during each of the successive exposures as well as the mechanism employed, <u>cf. fig. 1.1</u>. In his 1990 book, he mentions a sensitive celluloid film, employed at of 50 pictures/s, and a 1/4000 s aperture time.
This invention as a scientific instrument predates by three years the first sprocketed filmcamera, the **kinetoscope** which was built by W.K.L. Dickson at the Edison factory. Here, George Eastman's 70 mm celluloid film for his 1889 Kodak camera was used, cut in half by Dickson and perforated at the edges, thus giving rise to the 35 mm format of cine and miniature cameras. In its turn, the kinetoscope dates three years prior to the more publicised **cinematograph** of the Lumière brothers.

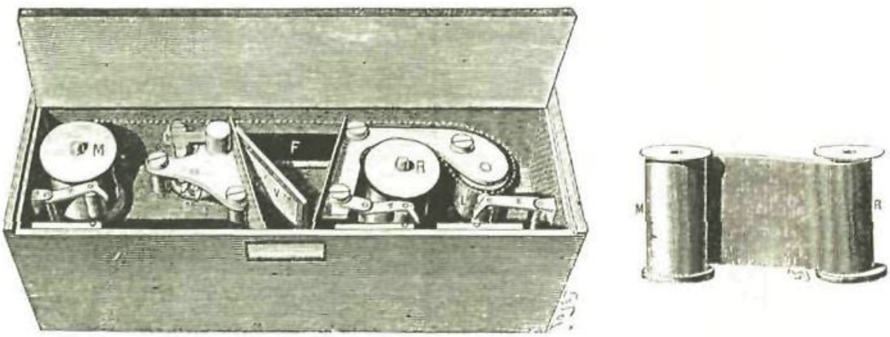

Fig. 1.1. The image box and film of Marey's chronophotograph.

note
1 Presentation to the Académie des Sciences, Paris: "J'ai l'honneur de vous présenter aujourdhui une bande de papier sensible sur laquelle une série d'images a été obtenue à raison de vingt images par seconde."

Before his primordial filmcamera, Marey had in two ways improved upon the multicamera single-exposure system of Muybridge. In 1885 Marey, in his version of the **photographic gun**, describes the use of a chamber containing 12 pieces of photographic emulsion, which when triggered rotated at high speed with intermediate full stops, thus making serial exposures within 1 s with an aperture time of 1/720 s.
Using three such cameras and proper triggering, for instance three perpendicular projections were obtained of ten phases of a seagull in free flight. Marey (1885) was aware of stroboscopy, as used already by Savart in the optical subsampling of periodic phenomena by exploiting the eye's image retention, and he extended the method to photography with what he called **photochronography**. Here, the rotary disk shutter with one or more slits was incorporated with the single-plate camera.

With this instrument he recorded human movement with subjects dressed in white against dark backgrounds, thus obtaining a time decomposition of for instance pole-vaulting as in his 1894 book. To obtain less crowded pictures, not shunning the more abstract representations of complex progressive motion, he dressed his subjects in black, limbs and head brightly marked by lines and buttons shining in the sun. Thus photochronography yielded the first so-called **stickdiagrams**, fig. 1.2, reported in the 1885 and 1894 books.

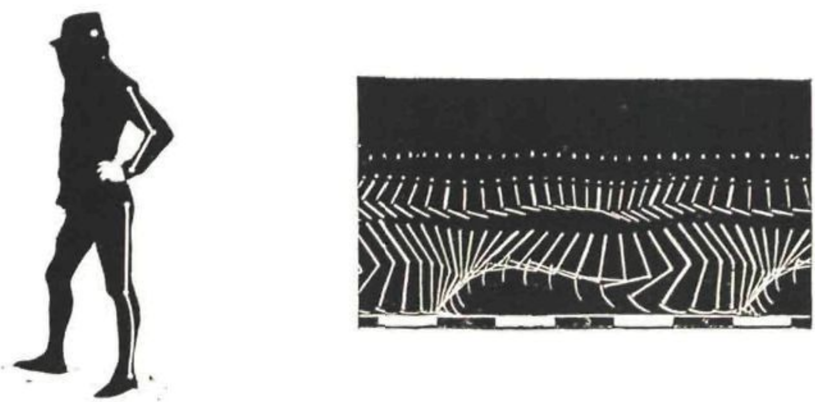

Fig. 1.2. Black dressed subject with markers, stick diagram (Marey).

Observing that the pictures, taken at successive time instants, tended to crowd if the subject did not move enough, Marey first installed a moving mirror inside the camera to spread out the images across the sensitive surface, and then thought of moving the plate itself.

When he finally exchanged the still plate enclosure for his chronophotographic box, the film camera was born as described above.

The use of a single flash for photographic exposure dates back to 1851 and is due to the Briton W.H.F. Talbot, who between 1835 and 1840 photographed on paper prepared with silverchloride and invented processes like developing, after short exposures, and fixation. For his flashlight Talbot used a 10 μs spark-gap discharge from parallel Leyden jars. His demonstration was to "freeze" with an open-lens camera a newspaper glued to a rapidly rotating disk.
Marey proves well aware of the possibilities when he mentions periodic illumination by spark discharges, while discussing stroboscopy for the *dissociation of rapid phenomena, as reviewed above.*

For indoor experiments, Marey's successors replaced the passively contrasting tapes with incandescent light bulbs or flashing gas-discharge tubes. Now the active-markers or **interrupted-light** methods were coined **cyclography**. These extensions, and others like incorporating reference grids, were partly pioneered by the German physiologists Fischer and Braune, to whom also one of the first mathematic elaborations is due.

Not satisfied with visual inspection of the new cyclogram recordings, Fischer and Braune (1895-1904) performed exhaustive calculations, with 3-D reconstruction from central projections with four cameras, in a monumental and extensively documented analysis of human gait. This study included double differentiation and the consideration of forces acting on estimated centres of gravity of body segments. Fischer's work is basic to all subsequent biomechanics, results also conditioned the design of external prostheses for the first half of the century.

Though, contrary to (Tichauer 1966), the interrupted-light method with point sources cannot be attributed to Gilbreth (1919) who called it **chronocyclography**, few contemporary research teams were as outstanding and far-seeing as the F.B. and L.M. Gilbreth couple. Their analysis as from 1911 has concerned motions inventory, time performance, shape and extent of motion pathways of the US industrial worker. The study aimed at improvements of tooling, seating, posture and prevention of fatigue and occupational disease. This work, the basis for ergonomy and human factors engineering, has (in conjunction with F.W. Taylor's principles of organisation, 1911) been vital to the second industrial revolution.

In the Netherlands, it was Godefroy (1917, 1921) who described the use of interrupted-light photography with blinking point sources, in hand motions of normals and epileptics. Not only was the subject instructed to add a slow vertical component to the main horizontal fast movement cycles, to avoid superposition of records. Also, the trace of the successive light dots shows the sense of motion by the trailing ends of individual spots. This predates by six decades the modulation patterns used for direction and timing in 3-D LED **motography** by Baum (1978).

Other improvements to cyclography were introduced by Bernstein and coworkers at the Moscow school of Biometrics, such as the introduction of **mirror cyclography** (cf. Bernstein 1930). This was by placing an overhead mirror, oblique to the optical axis, in the field of view of a single camera, in order to record on each common exposure two split projections to be used in 3-D reconstruction.
Even the speed adjustment reported for Bernstein's rotary shutters marks an early application of stroboscopy in a control loop. He used a tuning-fork as electromagnetic contactor for a neon lamp, shining on a circle of asterisks imprinted on the shutter, and adjusted speed till apparent standstill. This begot countless, even domestic applications.

High-speed flashing however, powerful enough for stroboscopic lighting in photography (Früngel 1956) or with TV recordings (Glew 1963), took longer to emerge, being largely geared to the development of the Xenon tube. Early work is due to Edgerton (1954, 1961) of EG&G Inc USA. As a weaker source, the Kodatron speed lamp had been used by Bresler (1950) to identify details of a subject otherwise wearing light bulb markers. Stroboscopic scene illumination, instead of using rotary shutters for cyclography, was introduced to human motion studies by Murray (1964). The low rate of 20 flashes per s permitted separation of the stick-diagrams. To obtain sufficient contrast, she used Scotchlite retro-reflective tape for anatomical marking, and for maximum capture placed the flash unit close to the camera lens. Using an open-shutter camera configuration restricted these experiments to semi-darkness.

Cinematography, as originated by Marey to succeed Muybridge's serial photography, has, while rapidly maturing in other directions, impacted less on early stages of motion analysis. Beyond doubt, cine film was used extensively to record all types of fast and ultrafast processes in research and industry.

Slow-motion or single-frame playback allowed visual scrutiny. Perhaps because of the wealth of data, it took longer to realize the numerical extraction of coordinates and express these as functions of time.
As to applications in gait analysis, Elftman (1938) recorded by cine-camera the positions of the foot, together with the spring deflections of his mechanical force plate, which measured components of ground to foot reaction forces. In 1939 he studied the planar kinetics of the human leg with cine methods, by measuring from each frame the displacements as well as force plate readings. By the way, forceplates with pneumatic transmission to a kymograph recorder were already described by Marey (1873).

All these tools, in the form of high-speed film recording, contrasting anatomical landmarks, stroboscopy, 3-D algorithms, computer projection of shifted or superimposed stickdiagrams so familiar to medical staff, have survived in today's world-wide research and diagnostic arsenal.

Indicative of the state of the art, some twenty years after the trend-setting studies of normal and amputee locomotion between 1944 and 1947 at the University of California, San Francisco and Berkeley (School of Medicine and Dept.of Mech.Engineering), is the account by Paul (1967a) on the University of Strathclyde, Glasgow, Biomechanics Laboratory.
Now a manually operated 'Spectro' X-Y film analyser was available for numerical coordinate extraction from cine records. These were obtained with two orthogonal Bolex 16 mm cameras synchronously running at 50 frames/s, with aperture times of 8 ms. Under constant illumination, subjects on a walkway wore 6 mm white paper dots as anatomical markers on darkened skin areas. Force plate and electromyography signals were separately recorded, and synchronised by recording pulses fed to flash bulbs in the camera's field of view. Marker coordinates were measured to within approximately 1 mm.
Two operators were occupied for nine hours with transcribing 60-70 film frames into tabular numerical form, which represented about one stride in stereo view. Another five man-hours were spent punching paper tape for computer input.

The digital computer had entered the campus as an analytical tool, and it is from this time-frame of development that our efforts in on-line movement data acquisition will be described in the next chapters.

1.2 Computer processing of photographic data

The nineteensixties and early seventies saw the development of several approaches to computer acquisition of pictorial input data. We will in this section be concerned with input from intermediate storage, which is the essence of the photographic or cine film medium. Relevant only after film developing, such methods are inherently off-line. Likewise, all methods depend on scanning, be it manually or automated, mechanically or by electronics. Even in a frame-by-frame projection analyzer, visual scanning by the human operator is a prerequisite to the fine positioning of crosswires over points of interest. The supplementing of vernier read-out with tape encoding or computer interfacing only replaced the manual tabulations.

Ayoub (1970) used a manually-operated **stereophotogrammetry comparator** to analyze pairs of interrupted-light photographs in human arm motion, and included a discussion of the precision required for individual point estimations in order to obtain the claimed 2 % overall accuracy.

Poulson (1973), describing the labour-saving papertape **X-Y analyser** at Strathclyde Biomechanics Lab, mentions 1.5 to 2 hours to transcribe the film data for a single stride. Where manual positioning with X-Y analysers, such as the commercial NAC line, is still in use (van Ingen Schenau, 1987) it is where reasons of speedy turnover are subordinate to reasons of visual control. This concerns a class of experiments, e.g. in sports, where anatomical landmarks consist of visible detail of the underlying skeleton, rather than clearly contrasting markers. The latter are amenable to automation, but confidence level may suffer from markers being attached to skin surfaces, where shifting cannot always be prevented or taken into consideration. On the other hand, we have with other investigators witnessed instances of biased landmark centre or contour identification. In the case of manual digitizing the standard procedures should include randomisation of film-frame order.

For a review of **automated mechanical XY steppers** with a local electro-optical, e.g. photomultiplier, sensing device, the reader is referred to (Kofsky 1966) on reduction of pictorial data by micro-densitometry, in aerospace applications, and for earlier references to (Krug 1954). Comparable high-precision XY scanners were introduced for analysis of Wilson bubble chamber photographs.

Similar methods have more recently been applied to the (Baum 1986) motography pictures of interrupted-LED tracks. No reference to automatic analysis of stick-diagrams made by cyclography came to the author's attention.

Electro-optical line-scanning devices still depend on one mechanical displacement dimension, which in the case of film frame analysis can obviously be a transport stepper instrumented with a shaft encoder. An early version was reported by Pepoe (1970), who used fibre optic links bundled in three sheets of 1024 fibres in an encoding arrangement to a limited array of phototransistors, which for x-information interfaced the computer, together with y-shaft code. At the time, that solution could only cater for one marker per scanned line. Such methods gained feasibility when 1K and larger linear arrays reached the marketplace.

High-resolution linescanners, with mechanical stepping or mirror-scan, are now widely used input peripherals for pictorial or written records in several areas of research and industry. New consumer development in facsimile transmission belongs to the same category, first-generation fax having depended on two-axis mechanical scan with a single sensor.

In the low-cost brackets of **manual graphic input devices**, mention must be made of the XY-tablet, where a hand-held stylus or a sliding cursor with cross-wires is positioned across the pictorial record. This is referenced to the surface of the platen, instrumented so as mostly to contain a wire grid driven by pulse patterns for electrostatic pickup by the stylus or cursor. For increasing the resolution without undue wiring, van 't Hof (1970) at Delft University of Technology introduced interpolation between adjacent lines by pattern processing. Designed as a transparent tablet, such devices were in a way precursors of the light-pen, for transcribing or editing projected data e.g. from stop-motion videoscreens. XY-tablets now are commonplace computer peripherals for manual graphic input, in applications where massive data or high precision is not emphasized.

The drive towards replacing manual input of large amounts of graphical data, such as cell microscopy or human motion records, by automated configurations, was by the 1960's focusing on the **flying-spot scanner**.

Applied to directional control of an X-ray beam by deflection of the electron beam impinging on the emitting target, Greatorex (1960) used the flying-spot terminology. A scanning X-ray tube had been earlier described by Moon (1950). In these applications it was the real object under study that was placed in the transmission path to the single photomultiplier detector and thus was subject to the low-dose scan.

By contrast, the visible-light flying-spot scanner which uses computer controlled beam deflection in a quality oscilloscope, is necessarily limited to scanning of a transparent record in the form of photograph or film frame. With FIDAC: Film Input to Digital Automatic Computer, (Ledley et al. 1965) report an early automatic digitizer of pictorial data from 35 mm film, scanning 750 lines by 1000 spots per line at a rate of about 500 kbits/s. This system starts a history of chromosome analysis by computer (Ledley, 1966), where follow-up soon proliferates and competing systems emerge, as witnessed e.g. by (Groen 1971) and (Groen et al. 1976) at Delft University of Technology.

Departing from still-picture analysis, Kasvand and Milner (1971) used flying-spot scanning for computer analysis of human gait by film taken at 50 frames/s. The procedure included an operator-controlled phase of acquisition of contrasting marker images in the first three frames, to be followed by an automatic mode. Here extrapolation of trajectories for the acquisition of markers in the next frames is combined with the scanner's hardware control for rough sweeps and spiraling fine search. For anatomical markers, 1 inch circular black dots were used on white backgrounds. For photomultiplier read-out a 50 μs 13 bit A/D converter was used. The system had 14 bit D/A converters for spot positioning. It was reported that each film frame of five markers took typically 15 s to process, if no operator intervention was needed.
Availability of random addressing, inherent to flying spot scanners, had permitted the small computer memory to store only limited data of interest, intelligently derived from the film frames. It was pointed out that each film frame was like a 4000x3000 point read-only memory.

In certain aspects contuinuing along the lines set by the flying-spot scanner, was the application in the early 70's of an image dissector tube in the Optical Data Digitizer by EMR Photoelectric/Schlumberger Inc. This random access system was an adressable computer input medium that will be met again in section 3.4.

The flying spot method is quite in contrast with contemporary **TV image grabbers** which use standard video cameras. In a PC age with memory galore, these input one or a few complete frames first, and analyze later.
However, the operation of frame grabbers [2] is not restricted to film pictures or transparencies, as video cameras can be viewing the real world of artefacts and live creatures.

Mention of **video cameras** has brought us within sight of the main tool for implementing our real-time, TV-based coordinate data acquisition system, to which the chapters after this introduction will be devoted. There we will also review other opto-electronic sensor solutions.

But, as our efforts in motion analysis instrumentation were initially part of a research project in prosthetics control, we will now briefly survey the relevant topics in human limb substitution before embarking on the principal substance of the thesis work.

note
2 *TV frame grabbing will be revisited in section 3.3 and chapter 7.*

1.3 Prosthetics control and human motion analysis

The use of tools for extending manipulative control of the daily life environment has been observed (Goodall 1964) with chimpanzees in their natural habitat. It may be by association that mankind has designated these as high primates. In many respects, human society has evolved beyond this, provision of the handicapped with anthropomorphic tools being just one example, which is documented since antiquity and was to re-emerge with the iron hand of the medieval warrior knight Goetz von Berlichingen. Indeed the painful cycle has never been long, from tools to warfare, inflicting limb trauma, amputation, in its turn necessitating evermore prosthetic care and specialized manipulative tools. This rehabilitation and health care is in modern times partly delivered or sponsored by the national veterans administrations.
Accidentally or not, it is a German military doctor (Reiter 1948) who was first to publish on an externally-powered hand, controlled by EMG, or electromyographic signals which consist of action potentials picked up from remaining muscles.

We will not digress on preceding developments in body-powered limb prostheses, except to note that human movement analysis (with methods pioneered by Fischer and perfected as outlined in section 1.1) was a primary expedient in their design, fitting protocols and evaluation.
Also, cooperation of engineers in the development of artificial limbs was advocated by Schlesinger (1917), who by the way concluded that the ancient Goetz articulating hand prosthesis already provided the hook, lateral and cylindrical types of grasp (fig. 1.3).

Reiter's contribution of **EMG-control** has long passed unnoticed. Of limited impact was also (Berger and Huppert 1952) on the use of electrical and mechanical muscular forces for controlling an electrical prosthesis, made at IBM. A greater stir was caused by the actual prototype of an EMG-operated handprosthesis, reported by Battye and Nightingale (1955), soon to be followed by pneumatic and electric hands with proportional EMG-control (Bottomley 1962, 1964). Much attention was also enjoyed by (Kobrinski et al. 1960), reporting the USSR version of an EMG-controlled hand prosthesis, fig. 1.4. Their patent brief (Yakobson 1958) holds an early mention of gripping-force feedback, to be transmitted by a hearing-aid type of bone vibrator, though this sensory-feedback design has failed further to materialize.

Commercial electro-hands providing EMG control of a single degree of freedom (open/close) have since been introduced (Viennatone 1967). These hands reduced but did not eliminate the requirements of patient training and adjustment programs. At some institutes, patient sessions routinely involved some early notions of biofeedback (Soerjanto 1971).

It was in the early 1960's, with an undercurrent of optimism spurred by treatises like Wiener's Cybernetics (1961) and by extrapolations on processing power by integrated circuit electronics, that engineering teams began to focus on biomedical subjects like prosthetics control.

The pharmacological epidemic of congenital malformations caused by the Thalidomide sleeping drug had in many countries initiated new research into externally-powered childrens' prostheses. Progress in some areas, such as pneumatic control with tiny body-operated valves was reported (Marquardt 1959) and control concepts were proposed and demonstrated, like extended physiological proprioception (Simpson 1965, 1971). This featured position servos in 3 spherical coordinates, with force-demand valves operated by the shoulder girdle or by phocomelic digits.

We do not propose here to dwell at length upon ensuing or related work at the Prosthetics Control Group, which was established in 1963 at the Delft University of Technology [3], staffed by M.J. Wijnschenk [4] and the author. Rather, we have sketched circumstances and motivation for the University's wish to contribute [5]. We now intend to retrace the rationale for designing our own on-line, non-contacting movement data acquisition system which is the subject of this thesis. It is relevant to outline some early concepts of automatic control in upper extremity prostheses and orthoses.

note

3 *till 1981: within the framework of the interfacultary Cooperation Centre for Measurement and Control, director B.P.T. Veltman.*
from 1981: within the Signal Processing Department (Prof Veltman) of the Faculty of Applied Physics; to reflect Faculty policy the name changed from Prosthetics to Motion Studies Group.

4 *mr Wijnschenk left the field in 1969.*

5 *Parallel efforts were started at the Faculty of Mechanical Engineering (Prof. Boiten) to develop lightweight orthotic and prosthetic modules, with passive positioning or pneumatic power.*

Fig. 1.3. Medieval hand prosthesis.

Fig. 1.4. Russian EMG-hand.

Tomovic (1960) discusses the **automatic closing** of a prototype hand, on sensing an object applying pressure in the palm. Elaborating on the assumption that a basic requirement for a succesful artificial hand is that it demands a minimum of effort from the man who carries it, a new adaptive artificial hand was reported in (Tomovic and Boni 1962).

The main proposition was that the principle of minimum mental effort does apply to the control signals and thus calls for a high degree of automatism. This should relieve the human user of providing control signals other than those of initiating or interrupting the prosthesis' operation. Where different prosthetic modes are provided, the initiating also involved selection, as in this Tomovic/Boni hand. For this purpose it had a disposition of tactile sensors, activated by the individual deliberately touching the object.

Sensor pads in the fingertips evoked pinch grip when the object was contacted there. When the user directed the hand so that first contact was made at the palm, a cylindrical type of grasp ensued by sensors at the palmar location. Adaptive weight control by sensors at the wrist joint was added to govern the gripping force. Release was again under human control, by volar sensors not normally contacting any objects. Having been first implemented as a cooperative effort at Lyman's UCLA Biotechnology Lab, the Belgrade hand demonstrated an exciting route in rehabilitation engineering. As a sobering reflection on market forces, we see currently fitted hand prostheses still devoid of any notions of sensory feedback, either to internal servo-loops or to the individual. By contrast, tactile feed-in features in all respects similar to those preceding, are cropping up in present-day robotics.

Turning to **total arm** research projects which were to generate advanced concepts for automation, we mention such seven-degrees-of-freedom arm aids or orthoses, including active handsplints as reported by Bahniuk and Wijnschenk (1964) and in (Allen et al. 1966). Both devices were operated by cervical-lesion patients confined to the wheelchair, thus no problem was presented by bulk and power consumption. The Rancho arm was controlled by an array of seven tongue-operated three-position switches located near the mouth. Sequential control was on a one-to-one basis for each degree of freedom, confined to on-off-reverse. By contrast, the Case arm-aid provided a near maximum of automation. Here the patient controlled the selection of a movement out of a library of pre-programmed motion trajectories, generally involving all degrees of freedom. Pre-dating by some decades the principles of playback-robots, the programming was effected by a healthy subject, strapped to the arm aid, going through the motions of a limited repertory of Activities of Daily Living. The system now stored the output of servo-transducers at each of the seven degrees of freedom.
Patients signalled their choice of motion, including a repeat option and override, by means of eyebrow switches or a light beam pointer on a spectacle-frame, by puffing code into a membrane switch, or whatever could be used for voluntary expression.

Emerging confidence in the future availability of multiple body sites amenable to separate or separable multi-degree-of-freedom voluntary control, such as patterns of EMG activity (Finley 1965, Finley and Wirta 1967) inspired authors like Tomovic (1965) and Reswick (1965) to propose concepts of **endpoint control**, which implied an intermediate level of automation in orthotics and prosthetics.

In this context endpoint control goes beyond those simplifications one already envisaged by the voluntary control of just the terminal device (hand, hook or splint). Automation would take care of the intervening degrees of freedom for its positioning and orientation, much like the mechanical linkages of Simpson (loc.cit.). The notion of endpoint control became to imply signalling only at intermittent time instants. While relieving the individual of continuous signals for his control of the (terminal device) trajectory, the control would be more flexible than just a choice from preprogrammed motions. Control vectors, signalled only at discrete times, would be taken to indicate goals in working space, automatically to be reached by trajectory synthesis.

Thus endpoint control used the double sense of the word, it concerns the end of a mechanical chain, at the end of a time interval.

Synthesis of artificial arm movement, especially the time pattern of coordinated segmental motions, was seen to require the formulation or selection of control paradigms, criteria and algoritms. Criteria were to be derived not only from mechanical consideration. The individual's psychological need for both functional and dynamic resemblance to the unimpaired biological system, in other words his craving for social cosmesis which had been observed by rehabilitation services, would be met by mimicking natural arm movement during the semi-automatic phase of the activity.

Among the control concepts, whose applicability for prosthetics was to be verified by analysis of natural, unobstructed arm movement, were the findings of Denier van der Gon (1962, 1965) in human handwriting recording and simulations.
Fast goal-directed hand movement was understood to be controlled by on-off patterns of opposing muscle activitation, leading to positive and negative accelerations, in two perpendicular directions. In this apparently open-loop control, timing relations were demonstrated as being crucial in determining the hand's trajectories.

Considerations like the above for automatic control of arm aids and replacements were summed up by Lyman (1965) while on sabbatical leave at the Prosthetics Control Lab. and elaborated by Wijnschenk (1967a,b) as part of the research program.
The need for **analysis of natural arm movements** was implied as one of the tools to contribute to prosthetic motion synthesis. The same epoch saw the recognition that the analysis of arm movement patterns should contribute to functional design progress from the existing level of externally-powered prostheses (Engen 1967).

By then we had (Furnée 1967) our first motion analysis system ready.

CHAPTER 2. TV-BASED MOTION ANALYSIS SYSTEM, MARK I

2.1 Introduction

The original motion analysis system, presented in (Furnée 1967) and more fully reported as BSc and MSc thesis work in (Steilberg 1967, 1968), already displayed many of the features retained or refined in later developments. Then as now, basic constituents of the system are:

- contrasting markers, as anatomical landmarks on the subject
- TV-camera(s), viewing the subject with the markers
- processor, extracting marker image coordinates from the video signal
- on-line host computer, for data acquisition and analysis.

Fig. 2.1. main components of TV-based motion analysis system
(Steilberg with 1967 system)

Characteristic elements in the first and subsequent systems were:

hardware

- use of commercial, monochrome, closed-circuit TV-camera's
- video-to-digital coordinate-conversion, essentially based on readout of electronic binary counters to immediately provide X and Y words
- synchronization of the counters and the camera(s)
- providing a TV-image field identifier or separator word
- real-time reduction of marker contour data: to limit the converter output to a minimum of relevant coordinates, and so to economize on the host computer resources
- converter independence from host computer; straightforward, standard interfacing.

software

- primary data acquisition, file and record organisation
- marker identification: allocation of the successive coordinate pairs to the moving markers, within each TV-field
- linearization: correction of electrontube camera non-linearities
- marker coordinate processing: smoothing, estimation of derivatives, angles, etc.
- application-dependent motion analysis and display programs.

It is within this framework, that the present chapter will highlight the main features of prototype and early subsequent systems, spanning a decade further represented by (Furnée 1969, 1970, Furnée et al 1974) and by numerous MSc theses from the author's Prosthetics Control Lab.

Chapter 3 will review a derived version of the system, worked out in concord with the author (Paul, Jarrett and Andrews 1974, Jarrett 1976, Andrews 1982), other video-based systems of a derived or independent origin, and alternative opto-electronic systems based on other sensor principles. Section 2.10 will be concerned with primordial TV-oriented position measuring systems, involving applications along different lines, prior to 1967. There we will review a list of authors, largely due to Andrews (1982), only a few of which seem to address our main subject of digital coordinate extraction.

Chapter 4 will be devoted to our current precision motion analysis system PRIMAS. As a preview, we summarize the main extensions and differences from the systems to be discussed in the present chapter:

- substitution of contour suppressor schemes by dedicated hardware for the estimation in real time of marker image centroid coordinates:
  . data reduction
  . interfacing to desktop and personal computers
  (Furnée 1984)
- application of solid-state matrix image sensors:
  . development of dedicated, electronically-shuttered, CCD cameras
  . improvement of marker contrast
  . providing system/camera synchronization down to pixelclock level
  (Furnée 1986)
- system integration with commercial measurement-quality CCD cameras (Furnée 1988).

2.2 Structure of the TV scan

As follows from the introductory section, the main building block of the movement data acquisition system (fig. 2.1) is the **video-digital coordinate-converter** (fig. 2.2). This consists essentially of 2 binary counters, one for the horizontal X-count and one for the vertical Y, the X-counter being provided with a parallel read-out register. The counters are locked to the TV sync pulses, which are standard for the horizontal and vertical camera synchronization [1]. The X-register serves, when triggered, an instantaneous read-out of the running X count. The Y-counter changes only when video is suppressed and thus, within proper timing limits for read-out, no separate register is required. Where a Y-register is mentioned, its inclusion serves mainly conceptual purposes.

For those familiar with the principles of TV image scanning, the concept of video-digital coordinate-conversion is readily introduced by the observation that the position of any image point, selected e.g on the basis of brightness level, is digitized in a straightforward binary code just by triggering of the X-register followed by read-out of this register and the Y-count. The triggering occurs whenever and whereever the selection criterion is satisfied.

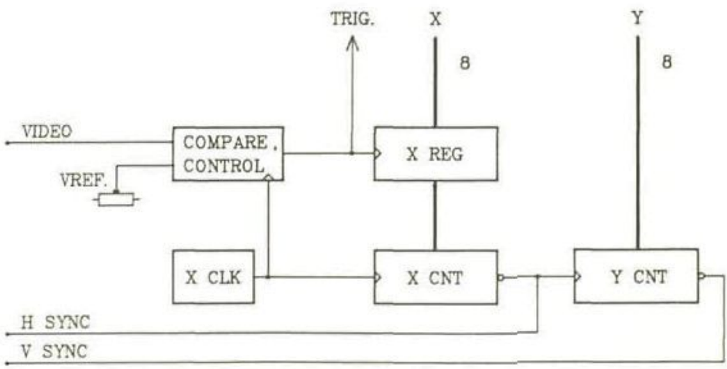

Fig. 2.2. Video-digital coordinate converter, block diagram

note
1 *The free-running clock for the X-counter was exchanged for the pixel clock in the CCD camera systems as described in chapter 4.*

To gain further insight in the operation of this coordinate-converter, we proceed to outline the **structure of the TV scan**.

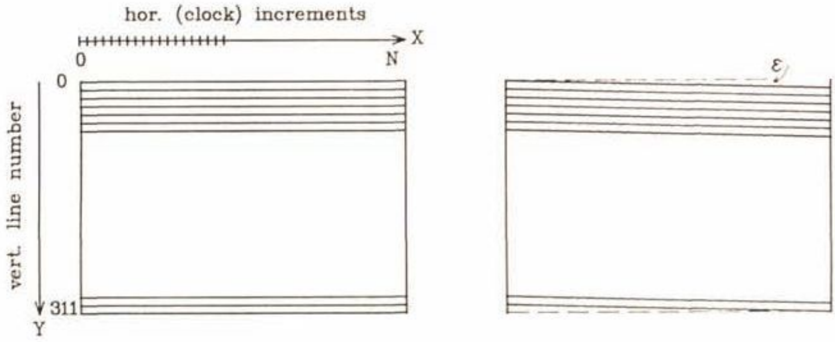

Fig. 2.3a. idealized TV scan structure   b. actual electrontube scan.

Using, for clarity's sake, only the European CCIR norm, the field rate is 50 Hz and each field consists of 312 TV-lines if the non-interlaced mode is selected (fig. 2.3a). In the interlaced (broadcast) mode each of the alternating fields consists of 312.5 lines for a total line number of 625 per image frame and a rate of 25 frames/s (fig. 2.4).

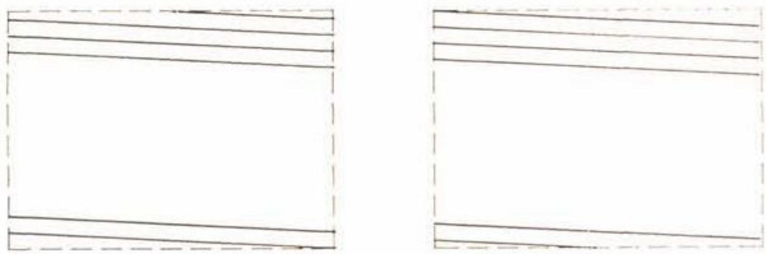

Fig. 2.4 a. interlaced TV scan: even fields   b. odd fields

Of the 312 (+.5) lines, 18 are blanked by a suppression of the video during field fly-back (this old terminology is still applicable to the electronbeam picturetube in TV receivers, less so to modern sensors). Field fly-back is started by the vertical synchronization pulse, which is slightly later and shorter than the blanking pulse. In other words, a vertical sync pulse initiates the vertical scan.

In the 1967 coordinate converter prototype it was decided to use only 256 of the 294 non-blanked lines, to allow a representation by 8-bit binary code. The other 38 lines, more than in usual fly-back, were suppressed by a prolonged vertical blanking pulse.

The interlaced scan mode has only been used in the 1967 prototype. In all subsequent systems **externally synchronized cameras** have been used, with sync pulses derived from the system. By making no difference for odd and even image fields, the non-interlaced mode was implemented. This was considered the best option from a sampling point of view, as the use of interlacing would imply that successive samples are subject to an alternating shift, over half a line distance, for the origin of the vertical coordinate grid on which the markers are imaged.

We will return to the vertical scan, and vertical coordinate encoding, but first direct some attention to the **horizontal scan**. Each TV-line is scanned in the horizontal sense, within a period of 20 ms divided by 312, or about 64 μs, including a standard 12 μs for the horizontal fly-back. During the fly-back, video is suppressed by the horizontal blanking pulse. Each horizontal scan (TV-line) is initiated by a horizontal synchronization pulse, occurring within the blanking pulse.

Until the advent of solid-state image sensors of CCD or other types, the notion of a pixel (smallest discernible picture element) in the horizontal sense was not inherently defined by the camera's imaging or scanning structure. From the above, it is clear that with electrontube cameras the horizontal position (coordinate) of any image element of interest is a continuum value, which is defined by the value of the deflection voltage or current. This, generally a sawtooth function, is in turn defined by the time elapsed after the horizontal sync pulse. It should be noted, by the way, that the use of this relation supposes the linearity of the horizontal scan profile as a function of time, or else the calibration of any non-linearities, and this for all values of the vertical coordinate: across the whole image.

Before our development of a dedicated, electronically-shuttered solid-state matrix camera (section 4.4), the system used commercial **electron tube cameras**. An expedient such as digital control of the horizontal scan by staircase functions has never been incorporated. One notes that the assumption of linearity, or the calibration of non-linearity, would be required in a comparable fashion if digitally coded control of the horizontal deflection voltage or current had been attempted.

Summarizing, to obtain the **horizontal** position coordinate, the system had to rely on the relation of horizontal position of the scanning beam to elapsed time from sync. Consequently, real time encoding of horizontal coordinates boiled down to implementing some form of time measurement. Our purpose of digital coordinate conversion imposed that the time continuum was to be measured in discrete steps.

In the 1967 prototype we decided to use 256 horizontal increments to make full use of an 8-bit code, to complement the 8-bit vertical code mentioned above. Thus the time measurement came to be implemented by using a 4 MHz system clock and the appropriate 8-bit binary counter to subdivide the 64 μs line time. Of these 256 horizontal increments, 32 were blanked (corresponding to 8 μs), so effective subdivision of the imaged line was by 224. The horizontal sync pulse provides reset for the X-counter, so that each TV-line is subdivided in equal increments.

If one considers the standard TV image aspect ratio of 4:3, it is seen that the width/height ratio of the imaginary pixels, defined as above by a 224 * 256 grid, differs from unity. The 1967 prototype provided software correction, as has become customary in our later systems with increasing primary counter resolutions.

In the **vertical sense**, position measurement is, at first sight, more straightforward by its direct correspondence to the line number. And line number is easily obtained by counting the horizontal sync pulses from an initial reset by the vertical sync.

Here again, the method implies that the vertical deflection provided by the camera manufacturer be linear, so that all new lines start at equal vertical increments from the preceding. If not so, then any non-linearities should be sufficiently corrected, or remaining deviations systematically calibrated.

In this preliminary discussion of adverse effects of the electrontube camera scanning properties, the observations should be mentioned that both horizontal and vertical nonlinearities of the swept electron beam proved temperature dependent, thus requiring warming-up in terms of an hour to settle for the stable calibrated system performance.

It should be noted moreover, that in standard electrontube cameras the vertical beam deflection is derived from a continuous control voltage (sawtooth) made up of two ramp functions. So during horizontal sweep the scanning beam is also linearly deflected over a small distance in the vertical sense. This effect, illustrated in fig. 2.3b entails that the coordinate system, defined by the vertical line number and the horizontal increment number is slightly **skew**. The error angle from the orthogonal is $\epsilon \approx 10'$. By consequence, the vertical coordinate as derived from line number should be corrected, in software, by a fixed factor multiplied by the horizontal coordinate, according to:

$$Y_c = Y + X \tan \epsilon$$

If uncorrected, this vertical error was obviously less than one least significant bit, as $X_{max} \tan \epsilon < \Delta Y$, with ΔY the line distance. The software correction required by this phenomenon could be explicit (as indicated above) or it was implicitly effected along with a linearity calibration in which camera and system are confronted with a precision planar distribution of control points.

This phenomenon of skew X,Y scanning is absent in the case where the vertical deflection driving function is stepwise incrementing rather than linear. Such staircase functions, derived by D/A conversion from a two-section, dual-clocked Y-counter, have been used in some of our experimental systems. This modification was aimed at providing **fine scanning** *zones across the markers, in a* ***tracking mode***, *with a rapid* coarser scanning inbetween. The build-up of charge in the coarse-scan regions, even with control of defocus and beam current of the electron beam, was one cause for abandoning this approach.

However all previous restrictive observations no longer apply with the *modern* ***solid-state image sensors***, *where the deposited matrix of lines* and columns implies an inherently high geometric linearity of a stable nature, fixed pixel dimensions, an exactly rectangular X,Y coordinate grid, and the direct determination of horizontal position by counting clocked columns (pixels), not time.
It is the advent of the solid-state matrix sensor with these and other exploitable properties, that with a manifest impact on performance has clinched the TV-based motion analysis systems as the viable concept. The more reason for giving our account of a sustained line of developments, including the stroboscopic CCD camera coming up in chapter 4.

2.3 Video-digital coordinate-conversion

The video-digital coordinate-convertor, with ancillary circuitry, was the main innovative component in the on-line motion data acquisition system, and the principle has carried over in all subsequent designs from this author's and other institutes, and later commercial vendors.

In the preceding section on the basic structure of TV-scan, we have in two instances and in fig. 2.2 anticipated and explained the principles of **binary counting** to establish in direct digital code the coordinates of image points of interest. Vertical coordinates are expressed by the TV-line number. Horizontal coordinates are expressed by the number of time intervals of the horizontal sweep in the case of electrontube cameras, or as the column or pixel number with the recent solid-state matrix cameras. The binary coordinates thus obtained are in a format for immediate transmission to the system's host computer.
Only some provisions, to be discussed in section 2.4 and later ones in chapter 4, will be seen to intervene between the counter/registers of the coordinate converter and the computer.

No originality is claimed for digital counting of elapsed time, as an expression of displacement or other transit phenomena. The original application to the TV scan conversion may in part be attributed to an earlier radar involvement, where dependable instant readout methods of running counters were realised in 15 MHz discrete ECL (Furnée 1961).

With the 1967 chip technology of RTL gates and flipflops it was state-of-the-art to design the 4 MHz 8-bit **X-counter** with an 8-bit parallel register, where read-out of the running count was free of transients by synchronizing the transfer pulses to the system clock (fig. 2.5).
For minimizing the transient errors, the synchronizing of the transfer pulses was preferred to using univariant codes, as the counter content is more profitably fed to the computer if coding is straight binary.

The further concept is readily understood, that the X-counter, clocked at 4 MHz, was reset by the horizontal sync pulse. The X-counter thus expresses the running number of horizontal time (position) increments. Furthermore one also conceives that the **Y-counter** (equally 8-bit) was clocked by the horizontal sync pulse and was reset by a pulse derived from vertical sync, so as to represent the running line number.

The 1967 prototype was the only one to employ a free-running TV camera and thus to use the sync pulses coming from the camera, mixed with the video signal according to CCIR norms. After separation, the vertical sync pulse had to be stretched by a univibrator to prolong the reset state of the Y-counter to the above-mentioned 56 blanked line periods. As from the 1968 system with a new set of cameras, **external synchronization** was employed (fig. 2.6). Sync and blanking pulses were provided by the system through decoding of the appropriate states of the X and Y counters. Now there was a 9 bit, modulo-312 Y-counter, with an 8 bit Y-output. Still, the X-counter incremented by a free-running clock.

Now having a set of X,Y counters running in synchrony to the scanning of the cameras, and so defining a binary number grid across the image area, mechanisms were at our disposal to directly digitize the coordinates of any point of interest simply by triggering **parallel readout** of the counter contents.

Being concerned, in the intended movement analysis applications, only with **markers** (section 2.7) having sufficient contrast to the subject's body and to background, points of interest for coordinate conversion were limited to those small bright spots that were the marker images.

At the outset it was decided, first, to use monochrome video, second, to use no more than a one-bit **binary** representation of **video** signal amplitudes. This obvious reminiscence to contemporary one-bit signal processing methods (Veltman 1961) has carried the day, up to our and other vendors' present systems. A single analog comparator with manual control of the threshold setting provides the one-bit video amplitude conversion. The coordinate converter operates only on this single-bit binary video, in the sense that this brightness signal is basically the signal used to trigger the instant read-out of the running X, Y counter contents.

The 1967 prototype has used only the black-to-white transitions of the binary video to trigger the counter read-out. Later systems, as from 1970, had the options to use both the black-white and/or white-black transitions (edges or semi-contours) of the binary marker images. To obtain the edges or contours of the brightness signal, univibrators or clocked digital differentiators delivered the counter read-out pulses. Outputs were available to monitor video brightness or contour signals.

As a marker image usually occupied two or more succeeding TV lines, a conversion on the black-white edge would lead to multiple coordinate pairs, corresponding to that marker's left half contour. But already here a further mechanism, called **contour suppression**, was incorporated whereby the read-out pulses on subsequent lines, following a first one were inhibited within a certain zone around the previous X-value. The width of the rejection zone was adjusted to allow neighbouring markers to be detected. These were to be processed with the same mechanism. Section 2.4 has the details.

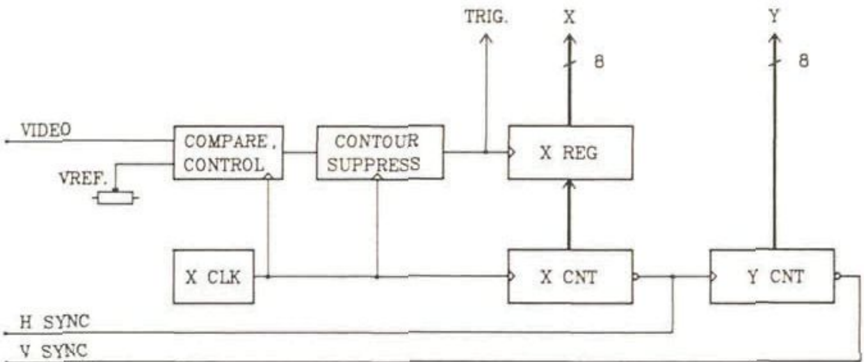

Fig. 2.5. video-digital coordinate converter, with contour suppression free-running camera (1967 prototype)

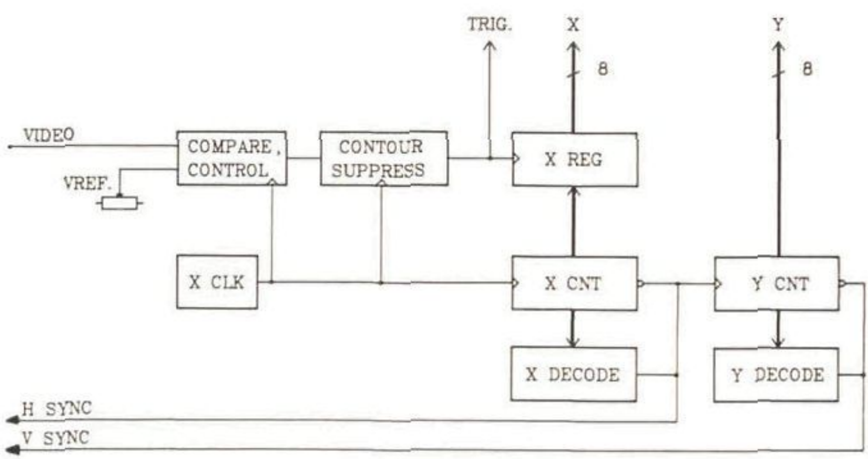

Fig. 2.6. same, with externally synchronized camera (1968)

2.4 Marker contour suppression

The earliest contour suppressor or local blank circuit of our 1967 and 1968 prototypes was equipped with a cascade of univibrators to provide inhibition pulses of proper width τ and delayed by $T-\tau$, with T the TV-line period (fig. 2.7a). This inhibited coordinate conversion of all points except the upper point on any continuous edge or semicontour. By extending its automatic analog reset timing, this filter [2] could if desired cater for small breaks in a marker semicontour. Resuming the local inhibition thus prevented the splitting of an imperfect marker image. This circuit could accommodate any number of markers, if separated in the vertical sense. But to allow contour suppression of (then) two markers occupying a same TV-line, it had to be incorporated in duplicate.

One of our next motion analysis systems (Furnée 1970, Bijlsma 1970) featured a digital contour suppressor. This involved a shift register configuration, the general idea is shown in fig. 2.7b. This solution allowed a larger number of horizontally adjacent markers, as each one was represented by one or a few bits travelling in a 256-bit register.

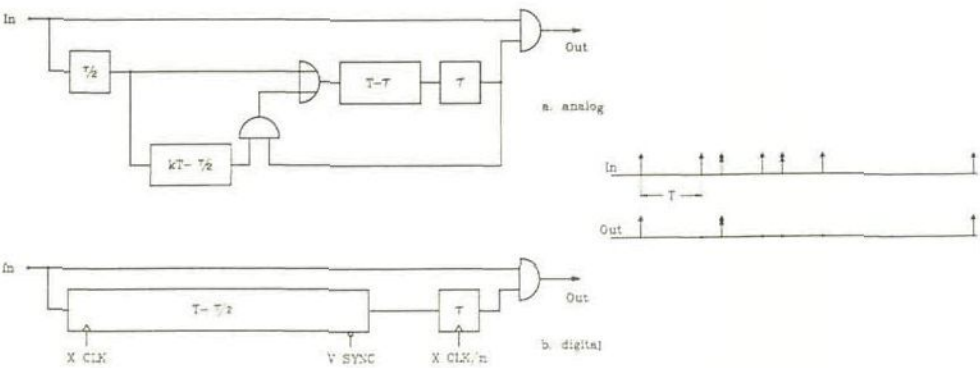

Fig. 2.7. marker contour suppression

note

2 *The contour suppressor design bore some resemblance to the self-resetting contour filter, which was used to the opposite purpose in a tv-based analog contour tracker, built by Houtkooper (1968). This was at the Pattern Recognition Group within the affiliated Instrumentation Dept. That tracker continued their early work on an analog sampler for a single semi-contour as a time-function (Boekhorst 1966). Groen (1969) reports multiple contour tracking in a potato shape recognizer and in a dice tester, which counted the number of eye contours in random throws.*

This latter system had the option of using not only the black-to-white transition (left semi-contour), but alternatively the white-to-black edge (right semi-contour), or both (full contour). The **full-contour mode** did not offer the contour suppression option of the semi-contour.

So here we had the capability of coordinate conversion for complete marker contours. Its potential for determining marker positions with higher precision had been recognized by Steilberg (1968) [3]. But risk of computer overflow decided for data reduction as the default option. Save for visual monitoring, and in applications as a graphic input device of still pictures, cf. section 2.6, our option of coordinate conversion of the full marker contours was not used before the experiments of van Antwerpen (1983) with centroid processing software.

The limitations of a single-point representation of the markers, only the upper point on each semi-contour being converted, were recognized at an early stage. The marker image radius proved dependent on image intensity, which was related to distance and transverse speed. These factors were liable to introduce measurement errors, as observed by Steilberg (1968).

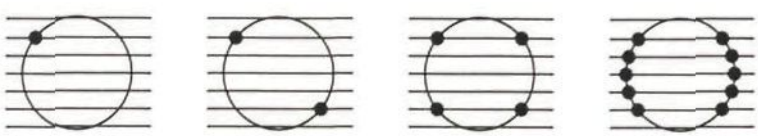

Fig. 2.8. contour suppressor options

In later systems (Klunder 1976, de Bie 1980), **options** were implemented to suppress all but 2 diametral points, or all but 4 quadrilateral points, lying on the markers left and right semi-contour as shown in fig. 2.8. Both solutions, in the providing of more data points, relied on special post-acquisition software in the host computer to estimate the centre coordinates of the marker images, independent of the marker size. This resulted in a **virtual enhancement of resolution**.

note

3 *Only in (Winter et al. 1972) were large markers used, albeit with off-line conversion of tv-recordings, and their centers estimated by averaging of all contour and interior coordinates (sect. 3.4). Not before (Taylor 1982) was the geometric centroid estimation implemented, in software, from full marker contours (sect. 3.5).*

That is why noise performance of estimates acquired by these options was compared by de Bie (1980) and van Antwerpen (1983). The latter also investigated the estimation by software of marker centroid points making our first use of all coordinates from the full marker contour. By that time the system was interfaced to the Faculty's central HP1000 computer, which could take care of the higher data rate, incurred in bypassing the contour suppressor. Results are reviewed in section 4.1.

It has remained a hallmark of all generations of our motion analysis systems to provide the facility of **real-time data reduction** on the marker contour coordinates. To this end the contour suppression option was used till 1983. The prime consideration for data reduction was the initial limitation, and later the economy aspects of the host computer resources. Notably we aspired to minimize the requirements of data transfer speed, buffering and disk storage as reviewed in section 2.5.

The final incorporation of a real-time centroid coordinate processor (Furnée 1984) is one of the subjects of chapter 4. While remaining true to the main feature of data reduction in preceding systems, this added the high-resolution capability which was otherwise attempted in post-acquisition software by our earlier and other vendors' systems.

Having discussed the contour suppressors of the 1967 and subsequent systems, with their varied options of data reduction, some attention is due to the host computer and its interfacing.

2.5 Host computer and Interfacing

From the 1967 prototype to the configuration used by Andriesse (1977), our host computer has been the **IBM-1130** of the Signal Processing Group (Prof. Veltman) of the Instrumentation Dept. This remarkable desksize minicomputer had a 16 kbyte magnetic core memory, organised in 16-bit words, with a read cycle time of 3.6 μs, and it boasted beside a fixed hard disk a 512 kbyte removable disk cartridge. Storage Access Channel provided a bus facility to connect a user interface, which was however not marketed by IBM.

An experimental **cycle-stealing interface** with an address and word count generator for Direct Memory Access had been built in the Signal Processing Group (Angad Gaur), with I/O routines written in Assembler.

It sufficed to hook up the system's 8+8 bit coordinate output to the 16-bit data input of the interface, and to provide for each word just the cycle-steal request pulse as a delayed version of the X-register read command. In the cycle-stealing mode, is was possible to use the computer core memory as a buffer, for subsequent DMA dumps to disk.
This allowed long runs of uninterrupted data acquisition, as storage requirements of our video-digital coordinate conversion systems were modest: An exemplary 50 Hz 6 marker (8+8 bit) application would take an approximate 17 s to fill the (max.) 6 kWord DMA buffer. Disk space would allow some 80 cycles, totalling some 24 minutes. The absence of contour suppression would imply one order of magnitude runtime loss.

However, with the computer's transfer cycle time of those days, the prototype and other early systems, which had no internal buffering, suffered the restriction that marker points on the same TV-line were not allowed to be closer than 3.6 μs. Line time being 64 μs, this amounted to a minimum horizontal clearance of some 1/16 of the image width. For the envisaged application to arm motion studies with a limited amount of markers, the disadvantage was at that time not too discouraging.

Moreover, this transfer speed limitation permitted only semi-contour operation (section 2.4) as in full-contour left and right edges would, with the common marker sizes, occur with less separation than 3.6 μs.

Therefore the feature of full-contour conversion, through by-passing the contour suppressor as mentioned in section 2.4, remained idle till the introduction of fast data buffering.

The 1972 system as used by Hendriks (1972) featured a modest **buffer** of 16 words. Filled with coordinate data and the field separator word during scan conversion, the buffer was read out during field flyback. This eliminated the restrictions on marker separation, and has allowed the full-contour conversion of single markers for test purposes.

A simpler, albeit multi-channel, computer interface had meantime been built for general use within the Signal Processing Group. Straight-forward and more dependable, but requiring more cycles per transmitted data word, this interface was developed for **programmed I/O** along the XIO protocol of the IBM-1130 (Furnée 1969). After this we built a new *four-channel cycle-stealing interface (Gombert* 1970).

For the acquisition of motion data outside the Faculty, a **digital tape recorder**, initially an 8-bit Kennedy 3110 interfaced by Klunder, was used by Hendriks (1972) and van Ingen Schenau (1973) in pilot experiments. These concerned human gait at the Biomechanics Laboratory of the Free University Amsterdam and cat locomotion at the Anatomy Dept. of the Rotterdam University.

The 25 ips 800 bpi recorder was first used in the synchronous mode, the above mentioned 16-words buffer being also used to pad the tape with zeroes between the field data. Padded zeroes were suppressed by the output circuitry while writing tape to the IBM-1130 XIO interface.

As from 1974, the digital tape recorder was used in the asynchronous *(start/stop) mode. To this end, a 2*1280 byte buffer made by Nagtegaal* complemented the modified tape unit controller (cf. Halbertsma 1975). In this ping-pong buffer one section was written to by the coordinate-converter, while the other section was either writing to the recorder or idle. As no padding was used, the tape was used more effectively. The choice of 1.6" tape blocks of 1280 bytes was a compromise with the 0.6" start/stop blanks. The same dual buffer was used for dumping data from the tape unit to the computer.

An automatic tape positioner to a selected record within a selected file, made by Nagtegaal, and a set of d/a converters completed our facility for off-line recording and checking (cf. Halbertsma 1975) and for the new HP 7970B tape unit a stand-alone interface was built.

Especially the digital recorder application for off-line experiments, but also bandwidth requirements for on-line host computer interfacing, or the interposition of on-line buffering, have stressed the advantage of a one-way traffic: output-only of the coordinate data. All systems that have evolved from the 1967 prototype, remained independent of any real-time control from host computers. Accordingly, in the most recent system the host computer is only used for menu-oriented initialization of system and camera options, to obviate switches and threshold knobs.

Extending the primary 16-words buffer, some later coordinate converter systems (Klunder 1975) featured a large FIFO output **buffer** and also a multiplex subsystem. The **multiplexer/serializer** allowed digital data from external instruments to be dumped to tape or to the on-line computer in a synchronous way, together with the motion coordinate data.

Examples of such external data sources were digitized **EMG** signals from subjects' musculature or digitized output from **force platforms**. Multichannel throughput was possible, the channel number being reflected in the label bits (see below). As the buffer was mainly dedicated to the marker coordinates, prevention of overflow was a main consideration for the external signal sampling rates. In an 8-channel application in locomotion studies of the cat, the sampling rate per channel was fixed at 4 samples/TV-field, or 240 Hz with a 60 Hz TV system (section 2.7). Additionally, the occurrence of **external events**, such as the states or transitions of foot contact switches in gait analysis, or contact with distributed objects in arm motion studies, could be exactly timed with reference to TV-based motion data. The expedient here was to output an extra word containing the instant Y-value, and padded with appropriate values of the newly introduced event and label bits.

This configuration also brought the change of representing X and Y in separate words, the 1973 system using 9 bits each for X and Y, padding the rest with partly undesignated label bits. The **9+9 bit definition** reflected the increased resolution of the newly used system with high quality closed-circuit TV cameras at 875:2 lines 50 Hz (section 2.7).

The use of label bits in the 16 bit output words also permitted the tagging of coordinate data with the camera number, necessary in a **dual camera** multiplexed implementation (Klunder 1976) for 3-D applications.

From 1973 the IBM-1130 minicomputer was superseded by HP-2100, later HP-1000 configurations. These became the central and more powerful faculty facilities, equipped not only with distributed terminals but also with an optically isolated star net for remote I/O of 16-bit data words, which was realized by the Signal Processing Group (Bakker). This hooked up to local lab. peripherals, with transmission rates up to 1 Mbyte/s.

With little modification, our motion analysis system has profited from this new on-line connection to the powerful HP-1000 minis. Later, as described in chapter 4, the system as from (Serlé 1983) used a desktop computer host, then a PC or portable. As a versatile concept, which can be a turnkey operation, the system has grown transportable to the site of experiments, independent of local or central minicomputers.

2.6 Video-digital coordinate converter as a graphic input device

An early application as a graphic input device for detailed stationary images has been in computer chromosome analysis, which was pursued by the Pattern Recognition Group. This subject area was and has remained in clear distinction to our main research interest of nonstationary images with little detail, pertaining to moving markers and optimizing their contrast to background. Fruitful collaboration has thereby never been excluded [4]. Computer input of this multiplicity of binary image contour coordinates was only possible with repeated scanning of the picture. As explained in the preceding section, the 3.6 μs DMA cycle time of the IBM-1130 minicomputer precluded the input of coordinates from contour points lying within horizontal separations of about 1/16 of line width.

The expedient (Furnée 1969, 1970) was to by-pass contour suppression, but to incorporate a **data inhibition mode**, which allowed coordinates to be output only at 1 out of every 16 steps of the 4 MHz horizontal or X-counter of the original converter. This ensured a minimum of 4 μs separation. With each TV-field the starting point or first step was incremented by 1. As the X-counter remained modulo-256 (section 2.3), the binary picture was completely transcribed in 16 scans.
The implementation of this scanning mode, seeing as it were through a shifting grating (fig. 2.9), required no more than the following:

A 4-bit shift counter incremented by the vertical field sync, a start-stop device, and a comparator for the decoding of the 4 lower bits of the X-counter by comparison with the shift counter.
Except on coincidence, realized 16 times per line, output requests of any possible contour coordinates to the computer were inhibited.

Grating number Δ_{ij} of X-increments in coincidence obeys the formula:

$$\Delta_{ij} = i + 16\,j, \quad \text{with } i=0,15 \text{ the field number and } j=0,15.$$

note

4 *The Pattern Recognition Group contributed markedly to our other topic of EMG classification for prosthetic control (section 1.3), reflected e.g. in (Duin, de Vos, Bakker, de Boer & Furnée 1977).*

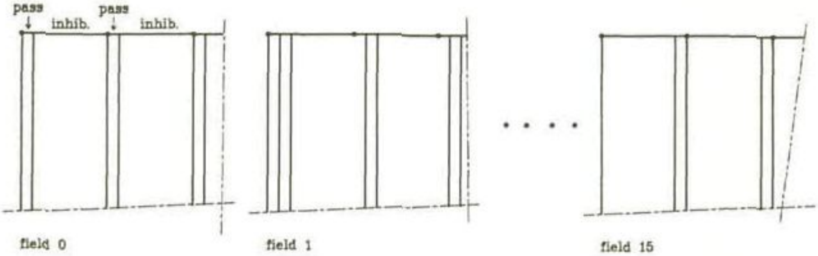

Fig. 2.9 a. Shifted-grating scan, principle

This simple extension to our coordinate-converter has demonstrated the feasibility of standard TV for computer input of stationary pictorial data by a digital device. It signalled an early application of TV in automated chromosome analysis (Aalderink 1970, Groen 1971) [5 6].

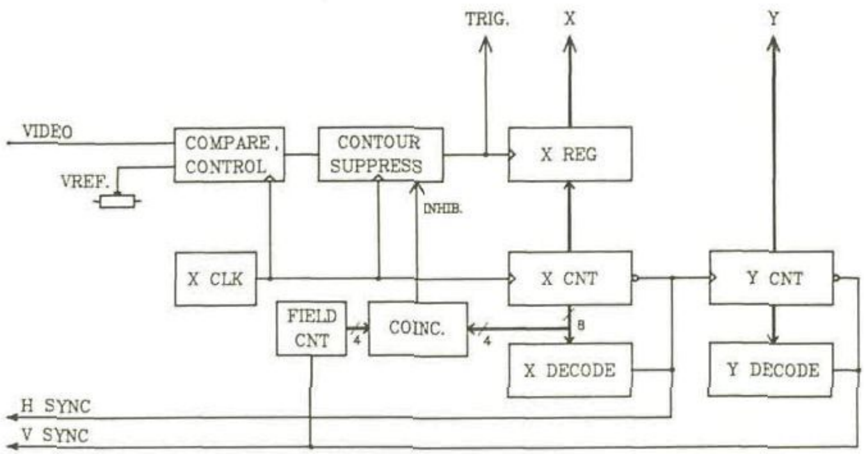

Fig. 2.9 b. Shifted-grating scan coordinate converter, block diagram

note

5 *At that instant of developments, efforts had turned full circle, the Pattern Recognition Group within the Instrumentation Dept. (Prof. Verhagen) having been such an inspiring environment with their use of TV in analog contour trackers (cf. note 2).*

6 *The Pattern Recognition Group has partially pursued this line with their initial development of a 4-level video frame grabber (Gemmink 1971). The video now was quantized in 2 bit binary and the data of alternating strips of 8 adjacent horizontal points were, as 16-bit words, dumped on 5376 words of IBM-1130 memory, using two passes of the scan frame of 192 lines and 224 points.*

2.7 Cameras and rotary shutter, markers and illuminators

For a **TV-camera**, the 1967 prototype system used a Philips surveillance type closed-circuit TV, equipped with a 3/4" Vidicon, with 625:2 lines at 50 Hz. This was a free-running camera, using interlaced scan and providing composite video with sync and blank according to CCIR norms.

As noted in section 2.2, this was replaced by externally-synchronized cameras in the 1968 and later systems. First was a Philips CCTV chain (type LDH 0151/0160/00), equipped with a 1¼" Plumbicon® tube, with the same definition of 625:2 lines at 50 Hz. Used in the non-interlaced mode it provided 312 lines. The sync and blanking pulses were derived from the system by decoding of the X and Y counters (section 2.3).

By 1973, the system used a Philips high-quality CCTV chain (LDH 0151/0160/10), again with a 1¼" Plumbicon but offering 875:2 lines at 50 Hz or a US equivalent of 735:2 lines at 60 Hz. The non-interlaced mode at 60 fields/s would result in 367 lines. But raising the line frequency by 5 % we ran the system at 384 lines, and suppressed 44 for field flyback. Over the earlier 50 Hz systems with 312 lines, of which 256 were used, the sampling rate was now improved by 20 %, and vertical resolution of 340 was up 33 %. Now for the line number we had a 9-bit Y-counter. Concomitantly, a 9-bit X-counter was used, which ran modulo 577, now at a clock frequency of 13,3 MHz. Leaving some 20% for line flyback, the effective horizontal resolution was 454 increments. Compared to the original 224 (section 2.2), the increase is by roughly 100 %. In the system so defined (Klunder 1975, Halbertsma 1975) we had square picture elements (pixels), because the quotient of horizontal and vertical resolutions 454/340 equals the TV aspect ratio of 4:3.

The Plumbicon camera tube was selected for its low-lag properties: low build-up and low decay lag. Figures like 95 % decay over 3 field times are acceptable for broadcast TV, as the smearing or "comet-tailing" of moving highlights is greatly reduced with respect to Vidicon tubes. However, in the coordinate converter system with its inherent sampling of above-threshold video in each field, it is the much inferior values of the one-field time build-up or decay percentages that are decisive. Using all left semi-contour coordinates of a vertically moving marker, at speeds between 300 and 900 TV-lines/s, Bijlsma (1970) found a (nearly linear) twofold increase of the apparent marker size.

The asymmetry of this effect did not improve affairs: it mattered a great deal if head or tail of the distorted moving marker image was encountered first by the downward, rightward scannning beam.
With the, in view of later developments, admittedly primitive method of coordinate conversion, which predominantly used contour suppression of all but the upper left marker image point, this lag or smear effect was liable to introduce speed-dependent position errors. Therefore, as from 1971, the systems incorporated a **rotary slit shutter** made by Nagtegaal, synchronized to the TV field rate and with an aperture time of 2 ms, coincident with the field fly-back (van Ingen Schenau 1972).

The rotary shutter, placed close to the camera lens, performed yet another function, that of providing **equidistant simultaneous sampling**.

Already with the system described by Steilberg (1968) the effect of physical scanning by an electron beam in camera tubes was discussed: Markers with high values of the Y-coordinate are scanned at a later instant of time t_Y within the field period T, than those nearer the scan origin. If the field number is N, the following formula holds:

$t_{N,Y} = (N + Y/Y_{max}) T$, while equidistant sampling would have $t_N = NT$.

The effect on a vertically moving, even perfectly imaged, marker is that of non-equidistant sampling in time. Moreover with more moving markers at different vertical positions, sampling is not simultaneous. So, far from being overlooked as claimed by Greaves (1986) when introducing his misnomer of TV-Doppler shift, this scan effect had been recognized and was accounted for in early software. Using the above formula, *data was interpolated to a set of virtual common sampling* points of time (Steilberg 1968). Even accounting for the time spent in horizontal X scan, Bijlsma (1970) suggested to refine this software, according to the extended formula

$$t_{N,XY} = (N + Y (1 + X/X_{max}) / Y_{max}) T.$$

However, the ill effects of physical electron-beam scanning, which are to some extent masked by the non-negligible Plumbicon lag and smearing effects, were by 1971 removed as a consequence of the rotary shutter. Now equidistant and simultaneous imaging of all markers was assured at the systems sensor front-end.

This obviated the post-acquisition data interpolation, mentioned above which in a sense was unattractive, as it changed measured data values to estimates, in a stage earlier than the 3-D reconstruction.

Lenses for the 1½" cameratubes, with their 21.4 mm faceplate diagonal, were selected from the range of 35 mm photographic camera lenses. The 43.3 mm diagonal of this picture format has two consequences. Firstly, a "normal" camera lens of 50 mm focal distance has a twofold telelens effect with the Plumbicon camera. So for the bulk of applications the choice was for 35 mm "wide-angle" lenses.
The second most welcome effect is for the Plumbicon faceplate to be firmly within these lenses' quality imaging zone. For a Leitz Summilux 1.4/35 mm lens, Halbertsma (unpublished, 1981) has, with a microscope and Kodak Pan-X photo of a grating, measured a non-linear geometric distorsion of maximum 0.14 % across the 29 mm diagonal zone.
Non-linearity of the electrontube TV-camera deflection processes was more serious (section 2.2), and was dealt with by calibrations and software corrections (section 2.8). Only with the recent solid-state image sensors, due to their inherently high geometric linearity and stability, are aspects of lens quality shifting to the foreground. Now with CCD sensors lenses are selected from the 16 mm cine category.

Apart from introductory remarks (sections 2.1, 2.3), little attention yet was paid to the **markers**. As the contrasting anatomical landmarks, strategically disposed on the moving subject under study, markers are the most important elements in the automated measurement chain. It is the marker position and motion in space that all the hi-tech fuss is about.
First markers, in demonstrating the prototype system and running some early experiments in arm motion and gait, were small electric bulbs. Up to 10 small lamps were applied by Bijlsma (1970) with 7 in a ring around the wrist, to obtain independence of pronation/supination of the forearm. Miniature 2*2 mm lamps embedded in a plastic base were used by van Ingen Schenau (1973). Under a short anaesthesia 8 of these had been stuck to the animal's skin in the pilot experiment with cat locomotion (Anatomy Dept. of the Rotterdam University).
However, passive reflecting markers in the shape of 4 mm dia. white paper disks, laid out in a 5 * 6 matrix on a black background, were already used by Steilberg (1968) in the first system linearity test.
They must have resembled those reported by Paul (1967a) for cine work.

The disadvantages of anaesthesia, and of the wiring incurred with the active markers in the cat locomotion experiments, have revived the use of passive reflecting markers by the end of 1973 (Nieukerke 1974).
Not only were 5.5 mm dia. white paper disks used, disposed on cat skin with little drops of glue, their **illumination** had more novelty value, as this was by a set of UV TL or luminescence tubes mounted inside the treadmill cage. The "black light" irradiation gave the characteristic contrast enhancement of the pulp material. Markers stood out clearly even on white animals (Halbertsma 1974). Even in cat experiments with simultaneous recording of EMG, the absence of (extra) wiring favored the use of passive markers.

Moreover, this configuration with passive markers saw the introduction *of **stroboscopic illumination** in TV-based motion analysis*. The UV-tubes were used in a synchronous 325 V pulse mode, with adjustable durations up to 4 ms and in coincidence with the TV vertical field flyback. The controller was due to Halbertsma (1974). The system and results in the collaborative cat locomotion project were reported in (Nieukerke 1974, Furnée et al. 1974, and Halbertsma 1975).

Unsurprisingly, this and similar systems went to replace the previous rotary shutter while retaining its advantages: first the reduction of the camera lag effects (comet-tailing), and second the equidistant and simultaneous sampling of marker positions.

Already in 1972, Winter and coworkers had applied low-inertia passive markers in human gait analysis, with their CINTEL videotape converter (Dinn et al. 1970), cf. section 3.3. They used halfcut ping-pong balls covered *with reflective* tape, and *illumination was conventional*.
To enhance contrast, **retro-reflective tape** (Scotch 3M®) was used by Jarrett, under constant illumination by 500 W halogen lamps, placed as close as possible to each camera side (Paul, Jarrett & Andrews 1974). Their paper concerned the Strathclyde TV-based motion analysis system, derived from ours in a collaboration to be described in section 3.1.

Having adopted the retro-reflective markers, we saw fit to pursue the stroboscopic illumination that had replaced the rotary shutters. Using a Xenon flashtube of a tenscore W, its efficiency was greatly enhanced by placing it virtually on the optical axis of the camera lens.

The camera and stroboscope assembly (made by Klunder 1979, cf. de Bie 1980) featured a semi-transparent mirror in front of the lens at 45° to the axis, with the Xenon lamp flashing from below. In an earlier arrangement (1978) a normal mirror had been used with a hole for the camera lens (fig. 2.10). Brief high-energy pulses were synchronized to the TV field flyback.
One drawback of the Xenon flash tubes was the slight acoustic noise.

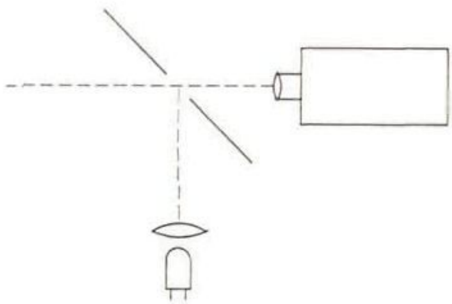

Fig. 2.10. Xenon tube illuminator

Fig. 2.11. LED ring illuminator

Proximity of the light source to the (optical axis of the) camera lens is a must for an optimal imaging efficiency from the retro-reflective material. This requirement derives from the retro-reflector divergence diagram which has a half-value half-width of approximately 25' of arc. This initially fostered our cumbersome mirror-illuminator arrangement.

Not waiting for expensive doughnut-shaped Xenon flash tubes to fit around the lens, we were more inclined to take advantage of the then emerging high efficiency LED types to make dedicated **stroboscopic LED illuminators**, as did (Andrews et al. 1981) who followed a non-strobed surveillance camera design (Texas Instr. 1972). By arranging LED's in concentric rings, fig. 2.11, the illuminator left the lens free.
This assembly also allowed the insertion of optical filters for an extra contrast enhancement of the irradiated markers. The LED's were operated at near-maximum pulse peak currents, with duty cycles of initially O(0.1) and presently O(0.01). With the latter illuminators, average electric power consumption has come down to the order of 5 W.

It fell to Serlé (1983) to improve the LED ring assembly by **optimizing for constant intensity** across the field of view, perpendicular to the camera optical axis. The device was to compensate for the narrow-beam pattern of some high-efficiency LED's, exemplified by fig. 2.12.

In each of the concentric rings, LED's were oriented at a proper angle to the optical axis, <u>fig. 2.13</u>, instead of pointing all in parallel. The angles were determined for a specific LED type's radiation pattern and for coverage of a desired field of view, determined by the lens.

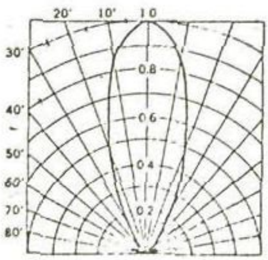

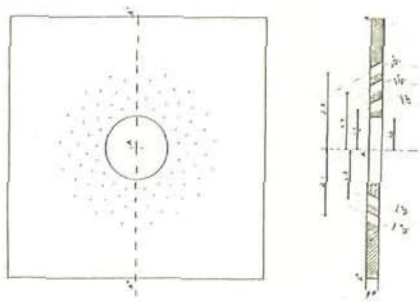

Fig. 2.12. LED ESPY-5501 polar diagram   Fig. 2.13. slanted-LED ring

Later implementations (Furnée 1984) include the scatter diagram of the retro-reflector, shown in <u>fig. 2.14</u>. This utilises the effect that, with greater distance, the relative luminance of the reflector will increase, by the decreasing divergence angle between the lens aperture and the LED-rings. And not only across the field of view but also over a range of distances along the optical axis, the reflective efficiency behaviour of the markers tends to offset the square-law distance rule. <u>Fig. 2.15</u> shows the marker image intensity (relative video amplitude) as a function of percentual off-axis displacement in a perpendicular plane, located at various distances from the camera.

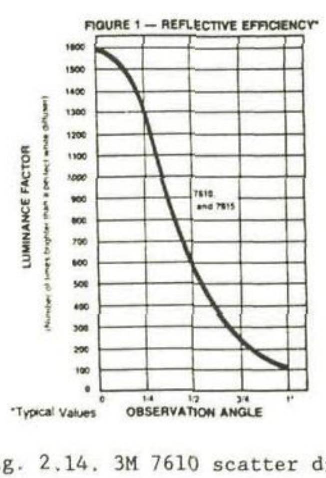

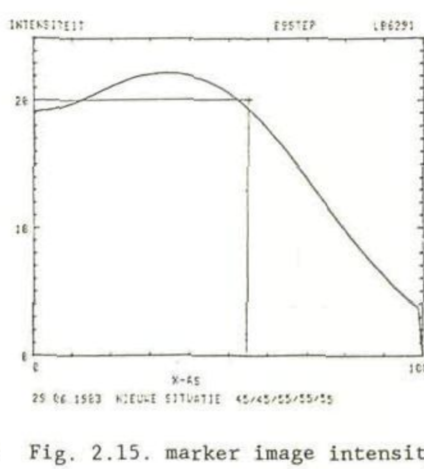

Fig. 2.14. 3M 7610 scatter diagram   Fig. 2.15. marker image intensity

As the first high efficiency LED's were IR types, imaging efficiency could be further improved by applying them with the more IR-sensitive Silicon Target Vidicon. This had by 1974 replaced the Plumbicon camera tube in one of the CCTV chains. Using invisible irradiation of the markers was considered of psychological advantage in some co-operative projects with handicaped and neurologically impaired subjects.

Near-infrared LED's emitting at 830 nm can be used as a trade-off with residual sensitivity of the presently employed solid-state sensors.

2.8 Software: marker identification, linearization

As the originator of real-time TV based hardware for motion analysis, we had to develop the first basic software. Section 2.5 has already indicated a progression of interfacing techniques, each requiring the appropriate data acquisition software. This was for the most part written in Fortran and utilized various native or specifically written assembler routines or I/O drivers for the particular host computer.

The major need for further data processing before entering the actual movement analysis software is, it should be mentioned, also the single *major drawback of the class of TV based motion acquisition systems*, and this concerns the **identification of the markers**.

As recognised with our first prototype (Steilberg 1968), the regular TV format by its nature of a vertical progression of the image scan, introduces a definite ordering of the marker image coordinates as the output of the converter system. To be more specific: whatever the marker disposition is, the (X,Y) coordinate pairs are produced in ascending order of the vertical coordinate Y, and for equal Y the order is in ascending horizontal value X.
It is in this order that the coordinate pairs get sequentially stored in the primary input array of the host computer memory. By consequence and as indicated in the example of fig. 2.16, coordinates of markers 1 and 2 will change places in memory for consecutive image fields n and n+1, if the projection of marker 1 moves from above that of marker 2 to a position below marker 2 between fields n and n+1. The example is an illustration from arm motion, where the hand H with marker 1 may be initially above the shoulder S with marker 2 and then dropped below shoulder level.

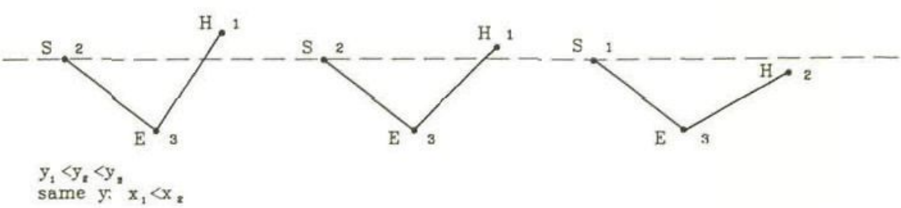

Fig. 2.16. changeover in the ordering of marker coordinates.

Clearly, a special software routine is required to shuffle, field by field, the primary array of input data, and produce a secondary data array in which the coordinate pairs for each successive field are consistently ordered in the sequence:
$(XY)_m = (XY)_1, \ldots\ldots, (XY)_M$, with m the marker index, $m = 1, \ldots, M$.

Because of the dynamic nature of the primary data ordering, the marker identification software involved cannot be one of the regular feature sorting algorithms. It should be understood that in each new field the coordinate pairs have no features or attributes linking them immediately to the respective markers. Only by considering consecutive fields does a pattern for classification emerge: the common feature of the coordinates for any marker is that they constitute a trajectory in time, which is hopefully unambiguous and uninterrupted. The mechanism for coordinate sorting or marker identification is as follows.

In the initial stage of the routine each of the coordinate pairs from $(XY)_{j1}$ in the first field is automatically tagged as belonging to one of the markers m, so to obtain the first ordered sequence of marker coordinates $(XY)_{m1}$. The tagging order may be changed by the operator at the display terminal of the host computer. The input ordering index j is 1, .. , M (in fields with no missing or spurious coordinates).

The marker identification routine then proceeds to each successive n-th field by allocating new coordinates from $(XY)_{jn}$ to the original m markers. This gives newly ordered sequences $(XY)_{mn}$ in what becomes the routine's output array for sorted marker coordinates.
To accomplish this in situations of any generality, no other method has emerged than that of extrapolation of the marker trajectories. This was basically implemented as early as in (Steilberg 1968) running our first system. The procedure is as follows.

Same as in the first field, also for the second field each coordinate pair from $(XY)_{j2}$ is tagged as belonging to one of the markers m. So a second ordered sequence of marker coordinates $(XY)_{m2}$ is obtained. Here again, the operator may intervene to change this assignment if between first and second field a marker crossover was observed.
After this initialization, so for $n \geq 3$, the routine proceeds by linear extrapolation from two previous fields, notably $(XY)_{mn-2}$ and $(XY)_{mn-1}$, to **predict** the n-th field marker coordinate set $(\tilde{X}\tilde{Y})_{mn}$.

Actual coordinates $(XY)_{jn}$ from the primary array are then **assigned** to markers m on account of their distance to the predicted coordinates $(\widetilde{XY})_{mn}$. Thus rearranged, the actual coordinates are ordered as $(XY)_{mn}$. The predicted coordinates $(\widetilde{XY})_{nm}$ are then discarded, and the algorithm is resumed for the next field. Now the $(XY)_{mn-1}$ and the newly assigned $(XY)_{mn}$ are used for the next prediction.

In the original version, as reported by Steilberg (1968), the distance criterion for assigning actual coordinates to markers by their predicted positions was implemented as a rectangular **prediction box** centered at each of the predicted marker positions. The assignment was made, if an actual coordinate pair from the primary array satisfied the prediction box for a particular marker. Optimum size of the box was adjusted by the operator. However, it was already recognized that box size for best results was dependent upon marker acceleration and this was used as a guideline for box size selection by the operator.
A major rewrite for more application generality by van Ingen Schenau (1973) retained and refined the above principles of the marker identification routine. The automatic adaptation of the prediction box size to instantaneous marker speed was introduced by Nieukerke (1974) in his program series for the cat locomotion studies (fig. 2.17).

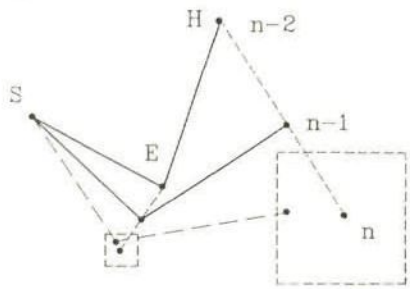

Fig. 2.17. marker extrapolation and prediction box.

In rewriting the program package for the new hook-up to the central HP-1000 faculty computer, cf. section 2.5, de Bie (1980) departed from the prediction box concept. Now the distance criterion for assigning actual coordinates to markers on account of their predicted positions was implemented by selecting the coordinates with the **minimum distance** to any of the predicted marker positions. This same principle, where for each n-th field a distance matrix is construed between all actual coordinates $(XY)_{jn}$ and all predicted marker positions $(\widetilde{XY})_{mn}$, was used by van Antwerpen (1983) who however changed the extrapolation method.

Quadratic extrapolation was introduced for marker position prediction, this now uses the marker coordinates from three previous fields. This means operator involvement in identifying the markers for the first three fields. There are also thresholds for minimum distance, which if violated call for operator intervention. This method has carried over to the versions written in HP-Basic (Demper 1985) for HP-9000 series desktop hosts, and in ASYST (Zuidhof 1989) for IBM-AT compatibles.
These two latter algorithms contain automatic short-cuts for simple marker configurations, where there is little change in the relative positions. They retained provisions for missing or spurious markers.

For non-general cases, Bijlsma (1970) and Hendriks (1972) enriched the identification routines with **a-priori knowledge**, like geometric marker disposition. This preceded (Ferrigno et al. 1988) on geometry-aided classification, one of few papers published on this kind of software.

We have elaborated on the marker identification software because the need for coordinate-to-marker assignment distinguishes the video based coordinate data acquisition systems from other opto-electronic motion analysis systems. This might appear as a disadvantage.
Of those **alternative commercial systems** which are (with their peculiar limitations) reviewed in sections 3.5/7, SELSPOT uses time-multiplexed active LED markers. Marker identification is **inherent** as only one LED fires at any one time. And the CODA-3 system, which uses mirror-swept rotating white light beams and passive retro-reflective prism markers, identifies an albeit limited number of markers by colour.

Nevertheless, we emphasize that the marker identification algorithm is nothing but a re-ordering of measured data, and that the assignment of coordinate data to individual markers implies no change whatsoever to the actual data values. This part of the software, typical of TV based systems, bears no analogy to routines for interpolating between actual data as required by non-simultaneous marker sampling in other systems.

Subsequent operations which do indeed alter the data values, such as linearization, smoothing or other filtering operations, are part and parcel of the motion analysis software for all of the contemporary systems. So are the basic analytical routines and most application routines, of which planar angular calculations and estimation of speed or higher derivatives are just a first example.

Then the more involved routines are concerned with 3-D calibration and reconstruction, ending up with 3-D linked segmental motion analysis. We should add that, with exception of the marker identification, most of the methods, mechanized in this software arsenal, already belonged to the heritage of cinefilm motion analysis, and little originality is claimed for a lot of work done in this area.

Of the above-mentioned routines, **calibration and linearization**, though meeting common optic problems, have some specificity indeed for the various sensor systems, and deserve some attention with our TV system.

Non-linearities of the TV scan, notably in the deflection of the beam with electron-tube cameras, and non-linear lens distorsion, discussed in sections 2.2 and 2.7 respectively, were noted as error sources and investigated in (Steilberg 1968). His result, that non-linearity error was within ±1 %, was only consistent with the random noise errors having the same order of magnitude in this prototype hardware system.

Only when the resolution or random error performance was improved, by adopting better cameras and 9-bit X- and Y counters as reviewed in section 2.7, was renewed attention paid to camera non-linearities. First correction routines were written by van Ingen Schenau (1973) and correction software has remained part of the program package till the advent of solid-state sensors with their linear and fixed geometry.

This early linearization software consisted of polynomial correction applied to the measured X, Y coordinates. This had to be preceded by a calibration routine, where the polynomial coefficients were derived from actual observations of a known planar distribution of control points. Most of the applied distributions consisted of a rectangular grid of 20*25, 10*12 or similar numbers of markers. The coefficient array could be recalled for successive sessions, and recalibration for changed camera settings belonged to standard procedure.
The first calibration experiments seem in retrospect to have suffered from a difficulty of assuring the reference plane to be perpendicular to the optical axis of the cameralens. In this case big and linearly increasing errors in adjacent marker image distances, dependent on one of the coordinates only, invited quadratic correction polynomials in X and Y respectively. More refined methods showed smaller non-linearity errors, which however were no longer dependent on one coordinate only.

In (Andriesse 1977), additive correction matrices were established for X and Y, where each element was the correction value to be applied at the corresponding point of the calibration grid. With some subsequent improvements by (de Bie 1980), this matrix scheme reduced the errors resulting from camera non-linearity to within ± 1 pixel size. Now for each camera, by type and setting, two matrices of 120 elements had to be stored and utilized, instead of a few polynomial coefficients.

This and the disadvantage of the inherent granularity of the matrix correction scheme led van Antwerpen (1983) to return to the polynomial correction method for camera non-linearities. The discontinuities that were caused by the piecewise fixed corrections over each of the meshes of the calibration grid, were liable to be reflected as jumps in the time history of coordinate data when markers crossed grid boundaries. Polynomial correction is better behaved in this respect.

Now for X and Y correction, polynomials in both variables X and Y were used and their coefficients were established by a linear least squares approximation across a 10x11 calibration grid. The polynomials obeyed:

$$X = \Sigma_{i=0}^{M} \Sigma_{j=0}^{i} C_{Xj,i-j} X_0^j Y_0^{i-j} \quad \text{and} \quad Y = \Sigma_{i=0}^{M} \Sigma_{j=0}^{i} C_{Yj,i-j} X_0^j Y_0^{i-j}$$

Here (X_0Y_0) are the measured coordinates. In calibration, (XY) are the grid point coordinates, and with linearization (XY) are the corrected coordinates. M is the order of these polynomials, in the sense that no terms are allowed where the sum of powers of X_0 and Y_0 exceeds M. This conveniently limited the number of coefficients, together with other advantages in numerical calculation.

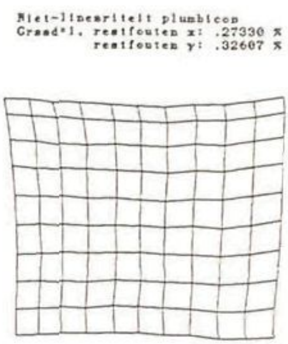

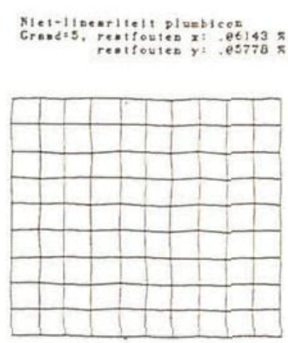

Fig. 2.18. Residual error distribution example (10-fold error blow up)

Fig. 2.18 shows the effect of linearization with M=5 compared to the raw data (M=1) with a Plumbicon tube camera from section 2.7. Residual error (standard deviation) at the grid points, from the least squares coefficient determination, reduced from .3 % to .05 % in this example. The choice of M=5 already generated 21 polynomial coefficient pairs.

Before we leave this account of calibration and linearization efforts, where some significant contributions (as by Woltring or other authors) will be left alone, some consideration of **adverse temporal effects** should not be omitted.

Though any system utilizing some form of A/D conversion, albeit just 1 bit as in our video-digital coordinate converter, must be critically *screened for e.g. threshold drift, the electrontube cameras proved the* prime source of time dependent bias error.
Observing a planar distribution of 9 markers along the two image diagonals, Zandbergen (1984) has investigated the warming-up behaviour for several 4 hours series. Every 5 minutes a 2 seconds record was taken at 60 Hz and averaged. The full contour option was used, with software estimation of all marker image centroid coordinates (section 2.4). Results are shown in fig. 2.19 for the central marker #5 and the 4 corner markers, where DX drift is relative to the X range of 450, and time t is in minutes. The traces show the averages plus and minus standard deviations. Cameras were the Philips 1973 CCTV chains from section 2.7, with SiT Vidicon and Plumbicon respectively, and a solid-state camera General Electric TN 2505 borrowed for the occasion.
The conclusion as to the validity of linearization is only too clear. It shows the way to our development with CCD cameras, cf. section 4.4.

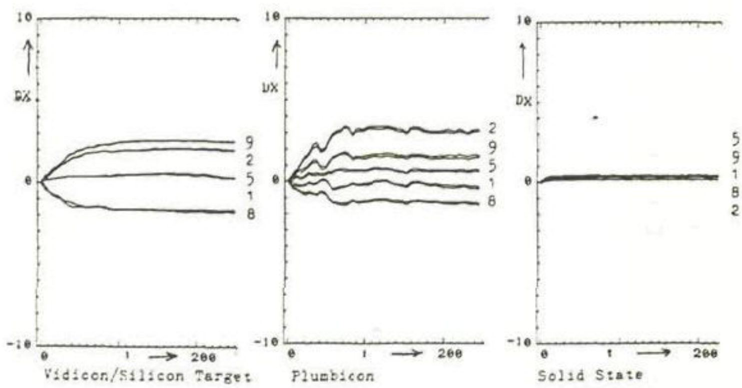

Fig. 2.19. Thermal coordinate drift with tube and solid-state cameras

2.9 Synopsis

The chapter was concerned with the Mark I family of TV-based motion analysis systems, which was developed in a 1967-1982 period and is summarized below.

The original 8+8 bit 50 Hz version used a 625:2 lines/field TV-camera and 256 horizontal pixels were defined by a 4 Mhz central clock.
The principle of video-digital coordinate conversion was that video signal transitions across a threshold translate to trigger pulses, which cause an instantly latched read-out of the running count of X and Y counters. These are simply binary counters of the pixel number, derived from the central clock, and the line number, derived from the line sync. The latched counter states reflect the image coordinates of rising and/or falling edges of bright markers in monochrome video.
Due to horizontal and vertical fly-back loss, the basic X,Y resolution was 224 pixels by 256 lines. As from the 1968 implementation, cameras were used in the non-interlaced mode and for reasons of stability they were externally synchronized from the system.

The video-digital coordinate converter hardware had by 1973 progressed to 9+9 bit systems which used quality cameras of 768:2 lines/field at the US 60 Hz rate. A 13.3 MHz clock defined 577 pixels per line. Subtracting fly-back, this meant a basic camera resolution of 454 by 340. Square pixels were now implied by the 4:3 resolution and aspect ratio.

One of the configurations was a two-camera system, with multiplexing, buffering and labeling of the coordinate outputs. Main effort in this phase of developments has however not been with 3-D systems or 3-D reconstruction software, as was rightly observed by (Jarrett 1976).

The first systems were hooked up to an IBM-1130 minicomputer by a DMA channel. This allowed the transfer of an ample 16 markers per line, though minimum marker separation was by 16 pixels.
By 1972, buffering of the output data with contemporary modest FIFO's removed the marker distance restrictions. It also allowed interfacing to newly designed, simpler XIO-channels with the IBM-1130.
For remote application, first a synchronous, and later an asynchronous digital tape recorder was applied. For the latter unit, a twin-section read-write buffer was introduced to accumulate 1280-byte tape records.

As from 1974, some of the configurations carried a larger FIFO buffer and 16-bit multiplexers, to allow the synchronous data acquisition of motion coordinates and digitized electrophysiology signals like EMG.

With the advent of the HP-1000 series central faculty minicomputer, the system was interfaced to the 16-bit laboratory data network. Soon after its introduction in 1979, the extensive transmission and storage capacity of this facility was to allow the input of complete contour coordinates of any practical number of markers, with run time only limited by the multi-megabyte disk space allotment.

However, all of our original and other early systems, as well as the PRIMAS system to come up in chapter 4, are characterized by real-time coordinate data reduction.
Distinct from PRIMAS, with all systems reviewed here we implemented a more or less sophisticated marker contour suppressor.

This logic subsystem featured one or two one-linetime delays, which since 1970 were implemented by clocked shift registers. Its original function was to inhibit the read-out pulse responding to any but the upper- and firstmost point on the marker image contour. Later versions had the additional option of converting two contour points, upper- and lowermost, respectively, diagonal on the rising and falling edge of the marker image. The alternative option was to take four upper- and lower points on the front and aft contour. A 1980 software addition allowed the estimation of marker centre coordinates from these two or four diagonal points on the marker contour.

Apart from the first 1967 version, camera tubes were of the low-lag Plumbicon type, and for IR sensitivity the Silicon Target Vidicon was used. A CCD camera of an appropriate resolution was only used in 1984.

As early as 1968, the effect of position-dependent sampling of the marker coordinates in the TV image was recognized and a first software correction was attempted. However, the problem of non-simultaneous sampling was eliminated with a rotary shutter (1971), or with strobed illumination (1974 onward) of passive reflective markers.
Replacing the early paper disk reflectors, the use of retro-reflective tape was adopted from (Paul et al. 1974), like our use of a multi-LED illuminator was preceded by Andrews (1981).

An improved LED-ring was to take account of the spatial patterns of LED radiation, as well as of the retro-reflective marker sheeting, in optimizing the intensity response across the camera field of view.

Unprecedented as the coordinate converter motion recording system was, so was at least one part of the software: from the earliest hardware prototype throughout the ensuing complexity of later applications, a progression of marker identification routines had to be pioneered.

The need for a dynamic assignment of coordinate data to moving marker images is due to the characteristic of TV to scan the field of view in fixed directions. By consequence the marker data from each image field are ordered in ascending vertical coordinate values. This means that with moving markers transpositions may occur. Reordering of coordinate data, according to a sequence of individually designated markers, is required before further analysis with any kind of software. Part of the marker identification algorithm relies on the prediction of moving marker coordinates, which is based upon extrapolation from a number of previous fields. Based upon distance considerations to the predicted positions, newly acquired data are assigned to corresponding markers. The actual values of acquired or assigned coordinates are not changed.

Software for the automatic marker identification, with initialization and supervision by the human operator, has been written and extended for the variety of host computers having interfaced the system.

Another software topic with some specificity towards TV-based systems was the correction of non-linearities in vertical and horizontal scan with electron-beam camera tubes. Calibration grids with some 10 by 10 markers in assumedly known positions have been used to estimate the coefficients of X and Y correction polynomials in X,Y. Residual (s.d.) non-linearity error in a 1983 application was 1:1700, down from 1:333.

If the non-linearity correction was one way of improving accuracy, the use of two or more diagonal marker contour points was another, as this tended to reduce bias from markersize otherwise incurred. As to repeatability, precision or (loosely equivalent for this discussion) the overused term of resolution, this is affected by camera and converter noise as well as by the system's line and pixel resolution. The 1980 system with 4-point detection had a 1:4300 X and 1:1500 Y noise s.d.

2.10 Primordial TV-based instrumentation

Chapter 3 will review derived and alternative motion analysis systems, which emerged after our first developments described in the preceding sections. For the completion of our picture we shall now focus to some of the earlier attempts to harness TV in scientific instrumentation.

Already note 5, section 2.6, witnessed precocious efforts at the then closely linked Dept. of Instrumentation to make use of TV in analog circuitry for feature extraction, such as contours, from stationary images.
But only in retrospect, such as compiled in (Andrews 1982) and supplementing (Sydenham 1968), does one recognize familiar trends in the early worldwide applications of TV in such areas as non-contacting monitoring and measurement of dimension, position or displacement.

In the context of this account on our development of motion analysis systems, based on video-digital coordinate conversion from TV images, we attach less relevance to the fully **analog processing** methods which have been realised or propounded in the earliest video applications to provide analog output values for measurement or control.

Examples are (Bryant 1962, Pasecki 1967, Saprykin 1968) for linear dimension measurements, while (Sorensen 1966) was concerned with area measurement and (Hooper et al. 1968) with spun yarn cross dimensions. Bryant (op.cit.) did introduce an option of manual digitization by adding a pulse counter to the adjusting knop for positioning a visual crosswire over the TV screen. Some note is deserved for the industrial environment, manifest in these early TV applications.

In **(d'Ombrain et al. 1966)** we find a first attempt at **digitizing**, but in an awkward hybrid way where a simple stationary picture, consisting of a single-valued graph on plotting paper, was viewed by slow scan TV at 9 s/frame. The video output was graded in 3 levels for straight recording on binary tape, which allowed 250 byte spaces per TV line. The extraction of digital coordinates was only by off-line computer processing of the tape. In the sense of storing quantized video from every pixel, the system belongs to the early frame grabber category.
By contrast, real-time data reduction and discarding blank pixels is of the essence in video-digital coordinate conversion.

The earliest known reference on TV instrumentation (**Wisnieff 1961**) is also the one most concerned with our subject of extracting position information. His **automatic tracker** concerned an analog video processor for 2D coordinates, albeit of a single object. This used a pair of gated integrators to produce voltages proportional to the X,Y position of a small bright target, to which the system had been previously locked by manual windowing. This target was e.g. the contrasting image of a missile or aircraft drone at the ordnance range.
A continuation to this work was by **Kruse (1964)**, who is only cited for his last words, reading "variations on the basic track-while-scan system are limited only by engineering imagination and ingenuity".

This was not lost on **Schuck (1966)**, where the first reference is found to on-line digital video coordinate extraction, once more limited to a single object. The application now was in **star tracking**, the system performance was improved by a reduced TV scanrate of 3 frames/s and by an option of averaging a number of successive coordinate pairs. Only a crude blockdiagram and a summary description were given, to the extent that the digital processing circuitry "derived the coordinates of the star by comparing the time base of the pulse (derived from the video threshold crossing) with the position of the vidicon's electron scanning beam as determined by the horizontal and vertical sweep voltages" and it then read out or stored the X,Y coordinates.
No clue was given as to whether the vidicon beam position was monitored by two digital counters, to be read out on occurrence of the video pulse, like in our video-digital coordinate converter system (Furnée 1967). Or by the A/D conversion of X,Y position voltages obtained from the sweep voltages or from gated analog integrators like in (Wisnieff op.cit.) or other tracking systems. The unclassified literature has yielded no further reference to this intriguing project.

It's an interesting speculation that the on-line extraction of digital coordinates from a TV image in an astronomic application, though just for a single point object, may by a margin of one year have preceded our video-digital multi-point coordinate converter, independently arrived at.
This is reminiscent of the early use of the "photographic gun" by the Paris astronomer Janssen (1876) to record on a single plate the successive phases of a Venus solar passage, some years before Marey's use of such an instrument to record animal movement (cf. section 1.1).

There again, the astronomers' application concerned a single object and slow motion, in fact Janssen introduced time-lapse photography, as opposed to Marey's physiological studies in time-dissection at high rates and with a minimal aperture times[7].

Another, much more developed TV-based system, though once again aimed at feature extraction from still pictures (and as such a successor of the flying spot scanners mentioned in section 1.2), was to be found in the **Quantimet Image Analysing Computer** (Fisher 1967). Upgraded over the years, it is still marketed by Cambridge Instruments Ltd. UK.
Originally developed for metallurgical research, but applicable for cytometry and related biomedical analysis, the Quantimet was basically a particle counting and mensuration device. First, using an adjustable threshold, the video was quantized to a binary black/white pattern and subsequent operations were on the binary valued video signal, which remained analog as to the duration of the on-off phases.
Pulse duration being equivalent to the width of a white segment intersected by the TV line, the determination of the sum of particle areas was by straight gated integration of these chord length pulses. The determination of total horizontally projected feature length was even simpler by counting the number of chord pulses. The system also had a size elimination control by an adjustable pulse width discriminator, this allowed the operator to disregard certain of the smaller particles or to obtain distribution functions of the chord length of particle intersections. Finally, this early Quantimet included a one TV-line memory system, for the optional rejection of repetitive intersects from the same object by an anti-coincidence circuit. This mode allowed the straight counting of the imaged particles. The description of this last feature was very much like the principles of our contour suppressors reviewed in section 2.4.

Nevertheless, nothing suggested the use of a pixel-frequency master clock, chord pulse integration may have been analog, and counting was restricted to events. In the manual version of this selfcontained instrument, readouts were presented on a front panel meter. With the

note

7 *And as we saw, Marey did not stop there, but invented what was to become the filmcamera, in fact the first sampled-data system. This we note, is where the analogy ends, as the invention of such a formidable scientific instrument -giving birth to a consumer industry of global consequence- beats comparison with what was done in interfacing existing video sensors to digital computers.*

automatic option, the parameters were dumped to tape or printer. Apart from its speed of max. one image/s, Quantimet's main difference with our video-digital coordinate converter is that, being an overall mensuration device across a particle distribution, it is not concerned with positional information proper. Though using some digital logic or counting circuitry, the purpose of Quantimet (winning a Queen's Award in Industry, 1967) differed radically from the real-time coordinate digitizer, even for the processing of a limited number of objects.

After touching upon certain common aspects of Quantimet and the video-digital coordinate converter, while being aware of the differences, this section on early TV-based devices cannot overlook the closest, though least well documented, approach to real-time marker position digitizing. This concerns a reference in (Murphy et al. 1966) to the prospective use in body motion measurement of a **Metro-camera** developed by those authors's **General Electric** company. As briefly stated there, the function of the instrument, consisting of a TV camera and a block of logic circuitry, was to track an optical point object and provide the X,Y coordinates of the point in electrical form, at 60/s and with a basic accuracy of 1:250. Taking the restriction to a single point for granted, one speculates if this implied that coordinates were derived by correspondence to the X,Y sweep voltages or by the A/D conversion from gated integrators, as in some of the earlier trackers. Such a camera system might be used in a multi-point mode if provided with active switched markers on the body. No more information materi-alized from writing to GE and no references were found in literature, not even by later US authors reviewed in section 3.3. It seems safe to conclude that the unpublicized Metro-camera was an abortive, perhaps a military, project from one of the backyard recesses of big industry.

Summarizing this retrospect, literature offers insufficient detail to ascertain if our video-digital coordinate converter was the very first in the real-time extraction of digital coordinates from TV images. But (Furnée 1967), cf. also (Woltring et al. 1980, Andrews 1982) certainly contained the first unequivocal description of the straightforward use of 8-bit digital counters, one incrementing at the TV line frequency and the other at a pixel frequency 256 times that high, relating time intervals to position along the horizontal line. Coordinate conversion was documented as the instant read-out of the running counter content. Multi-marker 50 Hz operation was equally explicit.

2.11 Conclusion

This chapter has described a period of some fifteen years, in which a new category emerged of on-line 2-D or spatial position measurement systems. This first member of the opto-electronic motion recording family, with fully documented real-time digital processing of video signals, originated from a small University laboratory, as a research tool dedicated to human arm motion in a prosthetics control project.
The potential for a wide range of motion analysis applications was soon realised and indeed some spin-off activities in co-operative projects were already noted in the mainstream of our account.

The main hardware feature of this video-digital coordinate converter system, distinguishing it from later opto-electronic solutions, has been shown to be the reliance on TV as the standard commercial image sensor. All innovations and improvements in the cost/performance of this mass produced technical and consumer product can be reflected with a minimum lead time in the TV-based motion analysis systems. Not without reason did this chapter end with the first utilization of a solid-state matrix camera.
This beneficial aspect of technology push has a counterpart in our early decisions for real-time data reduction from marker image contour coordinates. This has enabled us to hook up to one of the first small-sized IBM minicomuters, to dump data for temporary storage on digital tape units in outside locations and later, discarding tape units, make an early use of all the desktop, and portable PC hosts that technology push provides. This again demands new interfaces or software rewrites.

What one may also glean from preceding sections, is the realization how long it takes from the quantum leap of a working prototype, with its first appropriate software and computer interface, to the more fully developed, but still not finalized, versions of a going concern. And this not only in a University environment, as is seen in chapter 3 where we will trace the adoption and adaptation of a similar movement analysis system by the UK firm of Oxford Metrics, who first marketed their VICON product in 1981.

The final, and perhaps prime moving factor may be recognized as the curiosity or performance pull, as this chapter has reviewed a procession of major as well as incremental improvements upon one basic idea.

CHAPTER 3. DERIVED AND ALTERNATIVE MOTION ANALYSIS SYSTEMS

3.1 Strathclyde University TV/computer system

The demonstration at the 7th ICMBE of our prototype system, extracting digital coordinates from TV marker images (Furnée 1967), met with a prompt request for details from the Bioengineering Unit of Strathclyde University, Glasgow. Concurrently, Paul (1967b) had suggested that TV techniques be investigated as a potential on-line method for acquiring 3-D coordinate data. Actual work on a Strathclyde system, and detailed transfer of information, only got well under way with the recruitment of Andrews (PhD 1982) and Jarrett (PhD 1976). Our earliest exchanges in this fruitful endeavour are not on record. Andrews' prolonged stay in the Netherlands only materialized when the Strathclyde system was in the early stage of development and a first paper had been presented (Paul et al. 1974). This paper was much concerned with the hardware side of the coordinate converter, though already the markers had been implemented in the form of Scotch 3M retro-reflective disks.

The **dedicated interfacing** to a DEC PDP-12 host computer, by means of a DMA controller included in the system, appeared as one of the main departures from our approach. An 16-word buffer register was included, which permitted DMA transfer during line fly-back, when there would be no video-derived coordinate inputs. This technique however, restricted to 5 the number of markers allowed on any single line, as during the 12 μs fly-back just 7 words could be transmitted: 5 horizontal coordinates, 1 common vertical coordinate and 1 additional status and code word. In the case of more than 1 marker on a line, this scheme implied a reduction of vertical coordinates to be transmitted and stored. An advantage of this method of buffering is that markers may be closely together, whereas the unbuffered DMA transfer as in our prototypes imposed a minimum distance of 1/16 of line width because of transfer cycle time (section 2.5). However, our unbuffered DMA proceeded during the line scan and allowed 16 markers per line. And our FIFO-buffered 1974 system did not restrict the number of markers at all.

Utilizing one set of X,Y counters and the buffer register, the system could accommodate **up to 6 cameras** by adding 2 code bits to the output coordinate words, and an additional bit in the line status word.
A priority scheme selected one of the cameras in case of coincidence of marker detections. But there seems to have been no encoding of the other cameras, with ensuing data loss in such, admittedly rare, cases of coincidence.

This Strathclyde prototype featured **no marker contour suppression**. As described in (Jarrett 1976), the marker size was chosen small, so as to cover two lines at most. Averaging software was used to cater for the case of multiple coordinate pairs on the same marker.
Only one marker detection pulse, causing readout of the X-counter, was generated per TV-line intersection with the marker image. This pulse occurred at the positive-going threshold crossing of the video signal and thus corresponded to the black-white or leading edge of the marker image. Marker image width, or the white-black or trailing edge, was in this design not taken into account.
As a distinguishing feature, the **adaptive video threshold level** was derived from the peak value of previous video pulses. One may comment, that this automatic threshold setting can introduce one more degree of unpredictability, if not all markers are imaged with adequately equal or constant video amplitudes, as might be the case in non-planar work.

Cameras were used in the interlaced mode, a 10-bit Y counter being used which ran up to 625 lines and was reset only at alternate fields. However, no software was described to deal with the peculiar ½ line, 1 LSB offset in Y values, incurred between even and odd fields.
The vertical resolution in each field, excluding field fly-back, was 292 lines. Horizontal resolution, in this context equalling the number of horizontal counter increments, was 1000. There is no mention how the figure matched the actual camera resolution or modulation transfer function. The 20 MHz horizontal counter clock is a RC generator with start/stop derived from the line sync pulse. Vertical and horizontal field and line sync pulses are extracted from camera composite video.

Anyhow, system stability and repeatability tests were described, using a KGM Vidiads (UK) model 113 TV-camera and a 0.2 Hz sampling rate as described below. This indicated good results, with random errors not exceeding 1 LSB on stationary markers.

As in our systems at that time, event label bits were additional to the marker data to provide a means of synchronizing external data.

The Strathclyde system had the **additional facility** of providing pulses to external equipment, which were derived from the line counter by coincidence with an auxiliary register, loaded from the host computer. This gave more flexibility than the fixed rates, also derived from the line counter, in for example our 1974 subsystem of a multiplexer/EMG-serializer (section 2.5).

In another mode, the coincidence of the auxiliary register and line-counter could provide patterns of simulated video pulses on a selected line. On that line however, the pattern location was derived from a chain of monostables, subject to a less secure definition.

A second register preloaded from the host was, in coincidence with an additional field counter, used to inhibit the coordinate converter so that coordinates were only generated on every 2nd, 3rd, etc. TV-field, down to every 256th field. In this way it was possible to lower the system's sampling rate from 50 Hz down to 0.2 Hz.

Finally, it was realized that the restriction to 5 markers horizontally on a line forbade the calibration by anything better than a 5 * N rectangular marker grid (unless this was positioned at a skew orientation with respect to the TV image rectangle). So another auxiliary register, in coincidence with the horizontal or X counter, provided a calibration mode in which coordinate generation was suppressed outside a window of preset width. With each alternate TV field, this window moved from a left to a right margin across the image field of view, these margins being preloaded from the host computer. Such measures were not necessary in our systems, which allowed up to 16 markers on a line. The solution is however not dissimilar from our 1969 principle of shifted-grating scan for still more detailed images (section 2.6).

Only some first-stage **programming**, after the data acquisition phase, was described for this handwired 1976 prototype. The scheme adopted for marker identification was that by linear extrapolation (Steilberg 1968, van Ingen Schenau 1973).

More first-stage software, such as smoothing, derivative estimation and higher-order extrapolation for the marker identification routines, was described in (Andrews 1982). This ensuing work on the Strathclyde system was also more concerned with error and performance analysis.

Moreover, **hardware improvements** were described on some accounts.

A marker **contour coordinate suppressor** was implemented in this newer configuration. However, still only leading edges of marker images were detected and converted. And the contour suppressor lacked our option of providing both upper and lower contour points (cf. section 2.4), and thus generated no more than one coordinate pair per marker.

A **stroboscopic illuminator** was developed, with an annular Xenon flash tube and later with IR LED-rings, to prevent Vidicon image streaking and to provide equidistant simultaneous sampling (cf. section 2.7). With strobed illumination, because of residual partial images, the use of a non-interlaced scan format was advocated but apparently not yet implemented.

In 1980, the PDP-12 was replaced by the PDP 11/34 and a **new interface** was developed for hooking up to the DR11-B DMA channel. DMA transfer was now asynchronous with the TV coordinate generator and the amount of local buffering, employing FIFO's, was increased. This allowed the detection of typically up to 64 markers on any one TV line. Now the drastically simplified system catered for up to 4 cameras, and had got rid of the auxiliary preset registers and the corresponding functions of marker video simulation, moving window and scan rate reduction.

A subsystem, consisting of a 16-channel 12-bit A/D converter and its associated control, was incorporated to accept for each TV-field one scan of analog data from external transducers, such as forceplate or EMG signals. This obsoleted the provision of external synchronization pulses, as described above.

As data flow now was unidirectional, from a handshake buffer straight to an external computer interface, this version of the Strathclyde system bore considerably more resemblance to what had evolved at this side of the Northsea.

Though not containing tests of measurement noise of stationary markers (Andrews 1982) described a quasi-stationary **test** with two markers on a disc rotating at 0.4 rev/s, parallel to the camera faceplate. Low-pass filtering techniques and relations between input and output noise led to an estimate of the standard deviations of coordinates. Related to the range, these turned out as 1:3000 horizontal and 1:900 vertical. These trials were with a marker image size of 10 TV-lines, employing no contour suppression, and averaging of only the leading edge contour coordinates. Curiously enough, the random error performance estimate on the basis of this test was appreciably better for the small marker of 5 TV-lines, to wit 1:3300 hor. and 1:1200 vert.
Basic resolution of each coordinate pair, as dictated by the system's counters, remained the original 1:1000 horizontal and 1:292 vertical per field, 2 fields/frame, 50 interlaced fields/s.

Much the same system had been set up at the Dundee Limb Fitting Centre by Jarrett, who had also been engaged in the redesign simplifications for interfacing to the PDP-11 (pers.comm. 1977). It was at this centre that, under a visiting scientist grant, Woltring (1981) implemented a TV oriented version of his **3-D utility software** for Simultaneous Multiframe Analytical Calibration, which applied ideas of (Brown 1969) for calibration by 3 different views of a planar control distribution.

3.2 VICON [1] TV/computer system

The commercial potential of the Strathclyde/Dundee measurement system had been recognized for some time and a medical instrumentation firm approached the development parties with proposals for collaboration early in the project. An agreement was reached in consultation with the Scottish Home and Health Department in 1980 which gave Oxford Medical Systems access to details of the system design and the basic 2-D analysis and display software. And indeed, for the first few years after entering the market, VICON commercial literature has maintained an acknowledgement: based on Strathclyde/Dundee TV-computer system[2].

With redesigned hardware, interfacing by DMA to the PDP-11 family of host computers, and with basic 3-D software the video-converter VICON system was marketed by the beginning of 1981.
The **first technical descriptions** (1980, 1981) indicate a system with features inbetween the Strathclyde prototype and the 1980 Strathclyde PDP-11 version mentioned by Jarrett (personal comm. 1977) and reviewed in (Andrews 1982). Like the latter it had a 16-bit 64-word FIFO buffer and all 3 coding bits for camera number were in the data words, which used 10 bit for coordinates and 3 bit for external event marking. The A/D conversion subsystem had been left out however.
Like both Strathclyde systems, only the leading edges of marker images were detected. And like the first system, VICON had no hardware marker contour suppression, any multiple images detected for each marker were resolved by software into a single coordinate value. Also, the VICON scheme retained a separate 16 bit input data register for controlling the system sampling rate as submultiples of 50 fields/s, as well as the simulated video test pulse generator.
The system, which again could cope with up to 7 cameras, featured a central generation of 2:1 interlaced TV sync and of strobe control for the IR-LED ring illuminators.
The automatic threshold setting depending on video peak pulse history (section 3.1) was abandoned for manual control of detection level.

note

1 *VIdeo CONverter. Trademark of Oxford Medical Instruments (Oxford Medical Computers 1981, Oxford Metrics 1985), UK.*

2 *On a personal basis, which dates back from exhibiting at a 1981 Dundee Workshop, those responsible for VICON at Oxford Medical Systems and offspring companies are well aware of the earlier Delft ancestry.*

The first cameras were again KGM model 113 and linearity was specified as ± 1% horizontal and ± .5 % vertical.

The resolution specification was better than 0.1% hor. and 0.17% vert. at 25 samples/s or 0.34% vert. at 50 samples/s, a quotation clearly in terms of the basic 10-bit horizontal counter increments and the number of 292 lines per field. Apparently no use was made of averaging on any multiple marker coordinates. Random error specifications, such as the precision estimates in (Andrews 1982) were absent until the 1983 sales brochure. This and subsequent commercial literature quoted precision figures (standard deviation) in 3-D reconstruction of better than 0.1% depending on calibration and experimental conditions. The same figures are given for 3-D reconstruction accuracy (after the 1986 brochure, no precision or repeatability figures are given and the specifications of accuracy remained the same, for 50 or 60 Hz 3-D systems).
Cotron cameras were used as of 1983, with Ultricon 4532 silicon target vidicons and a linearity of 0.2% typical, 0.5 % worst case.

The **turnkey VICON system** with a PDP-11/23 host computer using two RL01 hard discs, included a Tektronix 4006 graphics storage terminal.
Later additions were the provision of DEC input modules under software timing and control, for analog signals such as forceplate or EMG's.

The first **software** with the VICON system came in two packages, called engineering software and analytical software. The former contained the data acquisition module, by DMA to memory and hence to disc, and the miscellaneous control modules for cameras, sample rate or simulations.

The analytical software package included the former and added modules for data decoding, calibration of camera constants and orientation, 2-D marker trajectory identification, 3-D reconstruction and graphic output, including 3-D projection transformations and stick diagrams.

The **3-D reconstruction** routines used the techniques of close-range photogrammetry and required the preliminary calibration by a number of markers set up in known positions as an object space frame. Contrary to marker identification, which was much along the lines reviewed in section 2.8, this subject was hardly covered in the Strathclyde papers mentioned heretofore.

Only (Andrews 1982) contains a discussion of an orthogonal 2-camera system, and a reference to an in-house implementation of the Direct Linear Transformation (Abdel-Aziz and Karara 1971) in a 3-D study of hand motion by Philippens (1980).

Having adopted neither the SMAC nor DLT techniques, referred to in the preceding section, there is little doubt as to the extent of the VICON people's own contributions to the 3-D part of the analytical software.

A march 1986 sales leaflet enumerated 30 VICON installations worldwide in clinical and gait research environments, with a few exceptions in ergonomics and sports biomechanics. This is a notoriously difficult market where potential customers having a lot of expertise in either a clinical or engineering field may not easily agree on the questions to be demanded from the system and on the extent of in-house support.
Like with other system investments, there is an emphasis on the most user-friendly and most general-purpose and highest-definition software on some of which points even VICON did not always satisfy as well as some other sources.

The new VICON VX system (section 4.8), one decade after VICON's first model, offers improved primary software AMASS from ADTech Inc. Adelphi MD, USA and analytical software from the Newington clinic, CT, USA.

3.3 Other TV/computer motion analysis systems, 1969-1977

A PhD thesis by **Waas (1969)** describes a fairly complex system, with an even for those days seemingly outdated technology, to interface two TV cameras to a pulse-modulated instrumentation recorder, which had to be played back into an apparently too slow IBM-format digital tape unit. The cameras were however high-resolution COHU 3200 models, with 945:2 lines/field (440 unblanked), 2:1 interlaced at 60 fields/s.
The unblanked horizontal line duration, 28 μs of the 35 μs line period was divided in 1000 pixel increments by a 3 stage BCD counter clocked with 36 MHz. Similarly, vertical count was by 3 stage BCD. The markers were small incandescent lamps and the system could not cope with more than 4 markers. Another constraint on marker disposition was that of a minimum vertical separation of 10 TV lines. There was apparently no latch for intermediate storage of the running counter contents, so the horizontal counter and the least significant decade of the vertical counter were stopped altogether for readout on each threshold crossing by marker video, skipping the next 10 lines. From the second of the two orthogonally disposed cameras only the horizontal coordinate was read out and this added the Z value to the X and Y values from camera number one. The analog instrumentation tape recorder accepted already forceplate signals, at the same time that coordinates were recorded in a bit-serial pulse-pattern mode on some of the remaining tracks. The report contains no reference whatsoever to previous TV oriented work by other authors. It is understood that the project was discontinued.

In **(Arzbaecher et al. 1970)** a digital **eye-spot processor** for corneal reflection is described. Monocular tracking and recording of voluntary human eye movement was conceived as a 2-D location problem of a single light spot. The by now familiar principle of X and Y counters, with a read out at the light spot video spike occurrence, is like a single-marker application of the motion analysis system. The coordinate grid definition was however very coarse in that a 0.5 MHz clock and a 5-bit counter provided the horizontal sync and divided TV lines in 32 increments. Moreover an adjustable delay held the actual 4-bit X-counter for a left margin of up to 8 increments which preceded the X-window of 16 pixels. A similar arrangement provided a vertical division into 23 zones of 11 lines each, equally with an adjustable top margin which preceded the 16 Y-zones counted off by a 4-bit Y counter.

By consequence of these counter subdivisions the camera was externally synchronized in the non-interlaced US format of 525:2 lines/field at 60 fields/s. But the resolution of the windowed system was no better than 1:16 in both horizontal and vertical senses, and digital coordinate output was in one byte of 4+4 bit at 60 samples/s for the single spot of corneal reflection.

A system described in (**Winter, Malcolm and Trenholm 1968**) was more of an **early TV frame grabber** in that it accomplished, albeit partially, a video image conversion in real time and with a 4-bit resolution in the gray-scale amplitude. In this system a 20*20 sample window had medium spatial resolution (every 5th TV-line). Every TV field was sampled with the window in a predetermined position to cover the desired area (about 20% of the screen dimensions). Data input was to an IBM-1800, whose built-in DMA channel distinguishes it from its family member our first IBM-1130. Applications were aimed at the automated analysis of dynamic video X-ray or fluoroscopic images of morphology or physiological events. It was to lead to more significant developments.

CINTEL, reported in (**Dinn, Winter and Trenholm 1969, 1970**) was a next step in the Winnipeg group's <u>C</u>omputer <u>In</u>terface for <u>Tel</u>evision. Much like a final step too, in that after (Winter et al. 1972) an abundance of reports ensued on motion study applications but no more on hardware development. And admittedly, many later papers from Winter's group at Waterloo University again use cine film analysis.
The CINTEL interface front-end contained an adjustable low-pass video filter and a max. 6 MHz 5-bit flash A/D converter. Any number of bits up to 5 could be selected for the final input to the computer. Horizontal and vertical sync pulses were extracted from the internally synchronized camera and were used to affect control of the viewing and conversion window. The window height and width permitted independent adjustment, from a 1*1 to a 256*256 window. The window could be positioned horizontally and vertically over the desired area to be sampled and within the window the spatial resolution could be preset to 1, 2, 3, 5, 8 or 12 pixels. To this end the horizontal clock was adjusted to 6, 3, 2, 1.2, 0.75 and 0.5 MHz to provide the basic A/D sample pulses. Concomitantly, to get the same resolution in the vertical sense, the vertical counter, clocked by the hor. sync pulses, was organised as a presettable divider so that every 1, 2, 3, 5, 8 or 12 -th submultiple of lines could be used to gate the A/D sampling pulses just mentioned.

Finally the overall sample rate was adjustable in that a vertical sync counter/divider provided every TV field, or every second, fourth, down to every 64th field to be sampled.
A 4kbyte buffer was used for data output to the computer, a selectable interface could accommodate 12, 16, 20, 24 or 32 bit wide datapaths for computer independence. As the window position and other parameters were known, output consisted only of the sample point amplitude data.
It is easily seen that data throughput to internal memory and hence to mass storage was a major limiting factor with contemporary computers, and that only restricted use could be made of all CINTEL degrees of freedom in temporal, spatial and amplitude resolution and window size.

An **application** of CINTEL in human gait analysis is first mentioned in (Winter et al. 1970) and more fully reported in (Winter et al. 1972a). Reflective markers are attached on anatomical landmarks of the subject who is tracked for up to 5 strides by a television camera, on a moving trolley and feeding video into a tape recorder. One 60 Hz camera views the sagittal plane down from the pelvic region while a series of large background markers is used for encoding the progression of the camera along the walkway. On replay in real time CINTEL converts the taped video into a CDC-1700 computer. The appropriately positioned window is set to 192*192, while the spatial sampling resolution is set at every 2nd pixel for a 96*96 matrix. The selected amplitude resolution is one bit, just like with our and all other presently reviewed systems.
In line with (Winter et al. 1972b), relatively large body markers were used, having a diameter of some 4 points in the sampling matrix, which corresponded to 8 TV-lines. Note that adult pelvic height down to the floor was imaged on 192 TV-lines and we arrive at markers of some 5 cm dia. For both X and Y marker coordinates, an unweighted average was taken of each marker's edge and interior points on the sampling matrix so as to obtain an **estimate** of the **center of the marker**. This procedure yielded a numerical resolution that was significantly improved over the basic spatial sampling matrix resolution.
Software had been developed to reduce the converter data, cluster the marker points, calculate their geometric centre and determine their absolute coordinates with respect to the plane of progression on the walkway, take account of parallax to the background with the reference markers, and present results in stick diagrams. Analyses of derived quantities followed in later papers on human locomotion.

An (Anonymous 1973) paper describes another solution for the vidicon to minicomputer converter. This again had more in common with digital image frame grabbers, in that a just 1-bit video quantizer was run at a 2 MHz horizontal clock that was gated during every n-th TV-line. The quantizer output was accumulated in a buffer memory that was unloaded to the computer during the n-1 subsequent lines. Clearly in the system of 525:2 lines/field a modest 128*1 bit line data buffer sufficed.
The line inhibitor consisted of a register, incremented from the mini, arranged in coincidence with the vertical counter that was clocked by line sync. The lower limit selected for the divisor n depended on the minicomputer or main storage transfer speeds and on the width of the input data path.
A sample 12-bit 2μs cycletime machine would cope with n=5 and it would take 5 field passes to grab the complete image (no provision was noted for selecting of either odd or even fields, and this was overlooked as an error source, with the apparently used interlaced TV). Noting the difference in some computer parameters, and the direction in which the scanning was inhibited, such a system is similar to those described in section 2.6 (Furnée 1970, Gemmink 1971). Apart from an image scanning example, no mention is made of any application, least of all in marker motion analysis.

This is different with the system of (Cheng 1974, Cheng et al. 1975), which incidentally is the first system to bear a maximum resemblance to our earliest prototype (Furnée 1967). The Cheng system has been applied with human locomotion modelling and recording (McGhee et al. 1976, Morecki et al. 1978) but no improved or commercial version has been seen to materialize. Markers were active in the form of pinlights and the host computer was a PDB-11/10. The internally synchronized 60 Hz camera operated in the interlaced mode, with the effect that the coordinate data could vary by 1 LSB. The scanned image was 240 lines by 237 pixels, so 8-bit counters were used for both X and Y, and for each marker detection spike a 16-bit word was latched into a register and presented to the host's Unibus. Data transfer was under program control and real-time software evaluated the data as spurious (caused by imperfect horizontal blanking) or as belonging to a marker detected on a previous line, and only new coordinates were stored. This process inhibited all data transfer for the duration of 2/3 of TV line width.

This imposed a severe restriction upon the marker disposition and the movement pattern, in that such a large value of minimum horizontal separation of markers on one same line was mandatory. Even our first systems described in chapter 2 had hardware provisions, such as the marker contour suppressor, which eliminated these limitations.

In **(Merchant et al. 1974)** the **oculometry** application is taken a great step forward from the (Arzbaecher 1970) system, in that the location of the corneal reflection is measured within and with respect to the bright pupil image. The bright pupil arises in imaging backscattered light from the retina. By monitoring these two elements of eye detail, where, cf. <u>fig. 3.1</u>, the corneal reflection is arranged to be the brighter one, the system allows the separation of actual eye rotation and spurious translational head movement.
Essentially this is a dual-level single-spot version of the by now familiar video coordinate converter. Note the difference of scale as the pupil image covers a substantial part of the camera viewing area. Separate sets of X-registers were latched with X-counter contents upon the leading and trailing edges of the bright pupil image with the lower threshold crossing, and of the corneal reflection at the higher threshold setting. The minicomputer took care of real-time processing of both the center of the pupil and of the corneal reflection, and of using their relative positions to calculate 2-D eye viewing angles. More functions provided by the computer were the control of a moving mirror tracking system for expanding the eye observation region from a still limited cubic in to one cubic foot of space. This team [3] was the initiator of the commercial Honeywell Oculometer. The applications were eye movement monitoring in perception psychophysics, ergonomics, NASA and the military, which hoped for benefits of the low eyeball inertia in ocular targeting and aerospace control.
This non-contacting method compared favorably with the (Robinson 1963) method of an eye-borne scleral coil in a magnetic field, which however as improved e.g. by (Collewijn et al. 1975) can resolve down to 0.1'.

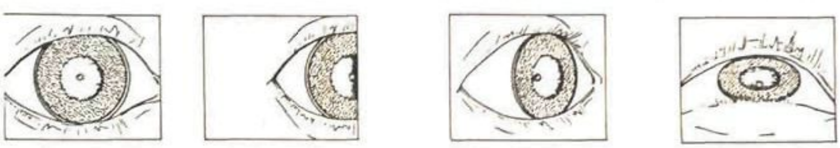

Fig. 3.1. Bright pupil image and corneal reflection

note
3 *Honeywell Radiation Centre and Wright-Patterson Air Force Base.*

In (**Lappalainen et al. 1975**) we are confronted with yet another marker oriented system for body motion analysis, which is once more composed of a set of horizontal and vertical counters and buffers. The buffers hold the coordinate data, plus the field number for timing purposes. These are transferred to the HP-2116 minicomputer on the basis of an interrupt during field fly-back. The reported limitation to 4 markers was apparently due to the data transfer routine. Two cameras are used, in a perpendicular or parallel orientation, camera number two providing one horizontal coordinate only, much like the system by Waas. Though the cameras were synchronized from the system, the scanning mode was 2:1 interlaced, and the recommended mode of data acquisition was to use every second field which implied a 25 Hz sample rate. The system featured a high-pass filter (100 kHz corner freq.) in the video input circuit, as well as hardware contour suppression. This allowed detection only on the first leading edge point of any marker. Apart from an example in jumping there is no history of further application.

We do not intend a further review of alternative TV/computer systems either for motion analysis by marker coordinates or for digital acquisition of other image features, except for the next section where we will highlight a few items, that were influential or of retrospective significance for some developments which are the subject of chapter 4.

The **conclusion** up to this point in time would appear to be that, with respect to work started in 1967 and discussed in chapter 2, hardly any noteworthy advances were reported with the exception of the intriguing but abortive design of CINTEL, which was a precocious real-time frame grabber at that time not taken up by industry (Winter, pers.comm. nov. 1988). *The Honeywell Oculometer was in its TV conversion and processor* part more like an advanced system for tracking one single image spot at two amplitude levels. Realistic contributions towards multi-marker movement analysis only came from the Strathclyde Bioengineering Unit which had creatively used, and acknowledged, their access to thesis reports of the period, referenced in chapter 2. It was this project in the UK which led to VICON, the first commercial TV based multi-marker movement analysis system, appearing in 1981.
A further aspect, which comes to mind when reviewing some of the other systems' limitations, is how fortunate we were in having access to the versatile IBM-1130 minicomputer, with an in-house prototype DMA interface as early as 1968.

3.4 Other TV/computer systems, 1978-1983

In (**Brügger and Milner 1978**) the flying-spot scanner for film analysis (Kasvand, Milner and Rapley 1971) was abandoned for the design of a TV based on-line motion analysis system. Partly motivated by (pers.comm. Milner, sept.1971) and citing much of the relevant literature, this paper describes a system configured along well-trodden lines.
Nevertheless, it seems to be the first to propose and implement one of the new solid-state image sensors, in this case a 190*244 CCD array. Absence of deflection nonlinearities like in camera tubes was already mentioned as one of the advantages. The basic resolution was certainly modest as the array was operated in the interlaced mode at 190:2 lines per field. The 8-bit Y counter used just 7 bit for line number and the MSB was used for passing the field number.
The second innovation consisted of a first step towards the hardware determination of the marker's centre coordinates. Thus there was no contour suppression, and on each TV line segment of each marker image the hardware took the average of the leading and trailing edge X coordinates, so as to produce one X_i midpoint value per line i per marker. Software collected the adjacent Y coordinates having similar X_i values as well as these X_i values proper, for producing the final average $\tilde{X},\tilde{Y}$ marker centre coordinates. Larger markers as in (Winter et al. 1972) led to an, unspecified, increase of resolution over that of the basic sensor array, which we have seen to be still inferior to camera tubes. The combination held promises indeed but was used only as a prototype.

By (**Mesqui et al. 1981, 1984**), a computer controlled **film analysis system** was developed on the basis of a video dissector and image RAM. The computer controlled sensor was a random-access dissector camera by EMR Photoelectric/Schlumberger Inc. which, cf. section 1.2, was available as early as 1973. This ODD 658 optical data digitizer provided 4096*4096 addressable data points, though its resolving power was specified lower, as 2048*2048 for the Image Dissector tube, and down to 512*512 for a range of Vidicons. Static addressing accuracy in these early models was 3 %, repeatability 0.1 %.
First data reduction item in this film analysis application was the use of passive illuminated markers which we have grown used to by now. Frame by frame, the system could zoom in to the smallest rectangle holding all projected markers. Then a search algorithm was executed and on each marker detected, a fine scan was performed.

The fine scan was to confirm the marker and establish the marker coordinates. Markers were identified by extrapolation from the previous frames, like described in section 2.8.
No further reports on this system or on the EMR/Schlumberger random access camera came to our attention [4].

In (Charlier and Hache 1982) we see the (Merchant et al 1974) oculometer system stripped not only of its dedicated minicomputer, but also of the moving mirror system which had expanded the freedom of head movement from its initial cubic in. As an innovative and cost-reducing feature we signal that built-in intelligence, using a Motorola 6802 microprocessor, took care of processing the bright pupil and corneal reflection coordinates to obtain centroid estimates, their differences and the eye viewing angles. Like the original, this single-spot dual-level system worked in real time, albeit only at alternate TV fields or a sample rate of 25 Hz.
It was overlooked that as the averaging was unweighted, this was a poor substitute for the geometric centroid estimation, in this application where the bright pupil image is not necessarily circular, and depends upon gaze angle. However, firmware corrections should have been easy, the more so as the difference between trailing and leading edge X-coordinates was calculated anyhow, and totalized to obtain a size estimate of the bright pupil.

With (Taylor et al. 1982) we are back to multi-marker body/limb motion analyzers with the description of another 2-D single camera system. A Hamamatsu C-1000 measurement-type camera is run at 60 Hz, 256 lines per field (non-interlaced). Markers are 17.5 mm flat squares or 28 mm spheres covered with Scotchlite 7610 retro-reflective tape and they are illuminated by strobed IR LED's mounted around the lens. A remote PDP-11/70 is hooked up by means of a MST link (for multi-wire serial terminal) as the data rate was said to prohibit the use of DMA.
This system therefore adds a 128kbyte buffer memory to store all coordinate data of a single experiment, for a subsequent dump to the host. The arrangement limited the run time to e.g. 8 s for 10 markers sized 4 TV-lines.

note
4 *The comparable Hamamatsu C1181 random access camera (1974), using an N1070 image dissector tube will be seen in section 4.8, teamed up with a dedicated high-speed multi-marker tracking system.*

This buffer cannot be considered a useful contribution, though it was also proposed to retain buffering with an on-site PDP-11/44 mini [5].

A more interesting feature of the (Taylor et al.) system was a slight reduction of the primary coordinate data. This is obtained by hardware determination of the marker **line segment width** δ_i between the trailing and leading edges. This width value, being less than 8 bit, was stored together with the trailing edge coordinate X_{2i}. This introduced an auxiliary width counter running between leading and trailing marker edges. Not quite doubling the Hamamatsu C-1000 cameras video bandwidth of 15 MHz, the system used a 25 MHz clock, specifying some 1580 X-increments per line, which required an 11 bit X-counter.
Marker width δ_i may therefore have been limited to 5 bit to fill a 16 bit word, together with the X_{2i} value. Like in the Strathclyde system, the Y-coordinate is only stored at the end of a line containing marker segments. Clearly the Y-counter is 8-bit.

But the most distinguishing feature of this system is that for each marker, the **geometric centroid** (not just the average) of the marker coordinates is estimated by the subsequent **software** in the host computer. If we now omit the marker index, for each marker the procedure implements the following formulas:

$$\tilde{X} = [\ \Sigma_i (X_{2i} - \delta_i/2)\ \delta_i\ ] / \Sigma_i\ \delta_i \quad ; \quad \tilde{Y} = [\ \Sigma_i\ Y_i\ \delta_i\ ] / \Sigma_i\ \delta_i \qquad (3.1)$$

This conforms to the standard formulas by noting:

$$X_{2i} - \delta_i/2 = (X_{1i} + X_{2i})/2 = \tilde{X}_i .$$

The calculation of the marker's geometric centroid is reminiscent of (Winter et al. 1972a) with the averaging of edge and interior points on the marker image line segments. But it can be simply shown that the Winter method yields slightly erroneous results compared to geometric centroid, the more significant with the not exceedingly big markers.

If the centroid calculation as by Taylor bore any conformity to VICON methods prior to 1982 as claimed by Jarrett (1983), this was not borne out by VICON datasheets or scientific literature (cf. section 3.2).

note

5 *The buffer idea was taken up in the new VICON VX system, with its 1 or 4 Mbyte buffer, where the fast but dedicated DMA connection has been replaced by a slower but versatile Ethernet link. Also the ExpertVision system, cf. section 4.8, has to buffer the data.*

But resolution and long-term stability figures of 1:2000 and 1:1000, respectively, were no great advance on the VICON 1983 specifications anyhow (cf. section 3.2). It was not sufficiently clarified if all quotations referred equally to vertical as to horizontal coordinates, given the big difference in camera line count and range of X-counter. The effect of marker size on attaining the high resolution figures could not be judged, as either the field of view dimensions or marker size were omitted in the description of experimental conditions.

This paper from an industrial group [6], one of the relatively few in the field, which had moreover used an extensive literature retrieval, was a first journal publication to contain an elaborate account of the marker identification algorithms. Unsurprisingly however, no substantial departures were seen from the methods reviewed in section 2.8. Again, except for one 3-D system installed in the Newington CT clinic, there is no record of later developments or a commercial offspring.

Finally the acceptance of (**Aylor et al. 1984**) which, apart from noting a mask technique for associating marker image coordinates within each image's data flow, offered nothing of novelty value, and which for TV methods only cited (Lappalainen et al. 1975) from the same journal, speaks only for the insularity of reviewers for one of the particular societies within the prestigious institute concerned.

Section 4.8 will review the VICON upgrades and, with ELITE and Expert-Vision, two late arrivals on the commercial scene of TV-based systems, as well as the new image dissector based system mentioned in note 4.

note
6 *United Technologies Research Center, East Hartford, CT USA*

3.5 Alternative opto-electronic systems, the SELSPOT system

A digression is warranted from the mainstream of TV-system development toward a decade of emerging alternative position sensing devices. To the exclusion of systems with sensors located on the moving body, such as Polgon (Grieve 1969) and the (Güth et al. 1973) rotating light-beam devices, we will pay attention only to commercially impacting systems, like SELSPOT, the derived WATSMART, CoSTEL and OPTOTRAK, and CODA-3.

In contrast with TV and any other position sensing methods proposed or implemented, the **SELSPOT** [7] optoelectronic system depends essentially on a non-scanned 2-D sensor. The planar homogeneous sensor having no discontinuities (and supposedly no defects), used in SELSPOT and some derived systems, implies an in principle infinite resolution in both horizontal and vertical senses, if it were not for noise contamination of the sensor and ancillary signals.

The non-addressing lightspot position sensor, or **Position Sensitive Device** (PSD) depends on the lateral photoeffect across the extent of a planar biased semiconductor junction. As a position sensor for locally incident radiation it was first described by Wallmark (1957). It was later pointed out that the lateral photoeffect was first reported by Schottky (1930), as a matter of theoretical importance. The Wallmark PSD was a 2-D device with a 1 mm separation between point contacts, a far cry from the 2-D 25 mm square PSD's which evolved first in nuclear physics instrumentation and later in the domain of optoelectronics[8]. Among the 2-D particle physics sensors was the dual-axis duo-lateral PSD by (Owen et al. 1968), which on each of the opposing faces of the planar diode, separated by the junction, had a pair of lateral ohmic contacts along the sensor boundaries (fig. 3.2b). The earliest optical dual-axis PSD had tetralateral contacts on one sensor face (fig.3.2a).

Extending both the steady-state analysis of (LaBaw 1970) for dual-axis lateral contact PSD's and the single-axis (1-D) transient analysis by (Connors 1971), Woltring (1975) in a unified investigation considered several configurations of a square sensor having either Wallmark-type pointcontacts or the above-mentioned lateral contact configurations.

note

7 *Trademark of SELCOM AB (Selective ELectronic COMpany), Partille S*

8 *e.g. SC-25 by United Detector Technology Inc., Santa Monica CA.*

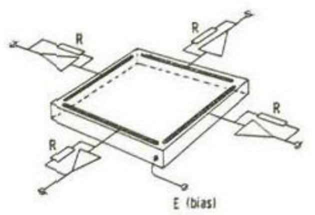

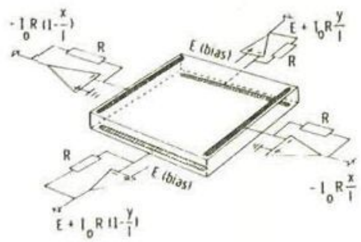

Fig. 3.2 a. dual-axis tetralateral PSD   b. dual-axis duo-lateral PSD
(courtesy Woltring 1975)

Woltring concluded that the duo-lateral PSD type held most promise for position sensing because, in the fully reverse-biased mode, distribution of current from each of the two contact pairs bears an inherently linear relation to the position of a single light spot, impinging on the sensor surface. He ascertained the exact relations of the form:

$$I_{x0} = I_x(1 - X/L) \quad \text{and} \quad I_{xL} = I_x\, X/L, \quad \text{whereby} \quad I_x = I_{x0} + I_{xL} \qquad (3.2)$$

with I_{x0}, I_{xL} the electrode currents at X=0, X=L, respectively, and X,Y the coordinates of the incident light spot of intensity αI_x.

$$\text{So} \quad X/L = I_{xL} \,/\, (I_{x0} + I_{xL}) \quad \text{and} \quad Y/L = I_{yL} \,/\, (I_{y0} + I_{yL}) \qquad (3.3)$$

independently express the coordinates in terms of electrode currents.

By contrast, Woltring showed that the tetra-lateral PSD, which he had been using experimentally, exhibits an approximately linear relation only between light spot position and the log ratio of output currents, while outputs for X- and Y-direction are not mutually independent.

Small wonder, that at Wallmark's laboratory at Chalmers University of Technology, Gothenburg, Sweden an early duo-lateral dual-axis optical PSD was constructed, exhibiting position linearity to within 0.2 % of full scale over a 24*24 mm active area (Lindholm and Petersson 1976). Indeed this pointed the way to replace commercial tetra-lateral PSD's in the SELSPOT system which, based upon such sensors, had originated with some Chalmers' graduates (Lindholm and Oeberg 1974). The newly founded SELCOM AB drew heavily upon the selfsame intellectual pool.

It is readily understood that, whereas the above theory is expressed for a single light spot (as in the original PSD-camera by UDT Inc), it applies to any incident light distribution where the X,Y coordinates denominate the intensity-weighted centroid.

This at once focuses us to the main feature of the SELSPOT motion monitoring system, in that the moving body markers are represented by light spots imaged on the PSD in such a way that the weighted centroid of incident light intensity delivers a meaningful set of coordinates. As markers are by preference not restricted to a single one, some form of marker encoding is a matter of principle for PSD-based systems. The immediate consequence is that active, modulated markers are required, with concomitant and disadvantageous wiring at the body.
SELSPOT has opted for a **time-division multiplex** system with the LED markers sequentially and periodically switched on and off [9].
As shown in fig. 3.3, only one marker is active at any one time, so that in principle the X,Y values of the centroid of impinging light do correspond to that marker's proper coordinates, projected on the PSD.

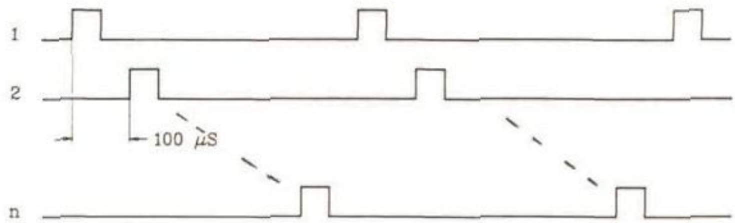

Fig. 3.3. LED switching sequence (time-multiplex) with SELSPOT system.

As a favourable item, note that the intensity-weighted centroid is to some extent insensitive to the defocusing of the LED light spot image. This allows uncommonly-large-aperture lenses to be used for increasing the otherwise not too favourable signal-to-noise ratio of PSD sensor and preamplifiers, within the usual bracket of LED power for markers.

note
9 *The SELSPOT patent brief summarily covered the alternative option of frequency-multiplex, in which the marker LED's would be continuously emitting, each with a distinct frequency of a sinusoidal intensity modulation. In this case marker coordinates were to be retrieved by having filter banks in each of the 4 PSD electrode channels. For a laboratory realization, cf. section 5.4 (MARIN).*
In Chapter 5 we describe an alternative multifrequency PSD system based on synchronous detection. It features a very small equivalent noise bandwidth, and it has zero or near-zero sensitivity for steady-state or electric ambient light, resp. (Furnée 1984b).

It is also patently clear that the SELSPOT system is one, where the **identification of marker coordinates is inherent**. This advantage over TV-based systems is due to the unambiguous timing of the switching sequence of the individually active marker LED's.

As indicated by the timescale of fig 3.2, the marker LED's are "on" for some 100 μs, including switching time and separation of previous and next ones, which points to the **speed advantage** of the SELSPOT system: with a nominal configuration of 30 LED's (128 is maximum), the maximum cycle or sampling rate is at 312 Hz. A reduced number of LED's can be fired more than once per cycle, so as to further increase the sampling rate, while retaining the basic 10 KHz per marker.

However, it has not in all quarters been realized that **sampling** of the moving markers, though equidistant in time, is inherently **not simultaneous** for all markers. Multi-marker configurations being used for the estimation of angles and other quantities derived from more than one marker's coordinates, it is a source of error if these coordinates do not represent the same instants of time for the position of all points of the segment(s) involved.
As a numerical example, skew between the mid-cycle marker and either the first or the last one is 0.4 ms with 8 markers. For sinusoidal motion, maximum amplitude errors are easily derived as tabulated:

		skew error (± %)		
frequency (Hz)	markers:	8	15	30
1		0.25	0.5	1
8		2	4	8
64		16	30	57

Though the 64 Hz frequency is well below half the 312 Hz sampling rate dictated by the Whittaker-Shannon theorem, it is the highest frequency to obey a practical recommendation that the sampling rate be 5 times the highest signal frequency (Baumann et al. 1983) [10]. Clearly, error due to marker skew is considerable and if uncorrected, it defeats all resolution and accuracy accomplishments of this or derived systems[11].

Not mentioned in the trade literature however, **software** may be used for **de-skewing**, by interpolating the coordinates of all but one marker back to common instants, as virtually simultaneous samples, fig. 3.4.

note
10 *more discussion on sampling rates and noise in section 4.9.*

11 *Our frequency-multiplex system (note 7) has simultaneous sampling*

A methodological drawback of this approach is that further analysis, even in 2-D, is not with observed but with reconstructed coordinates.

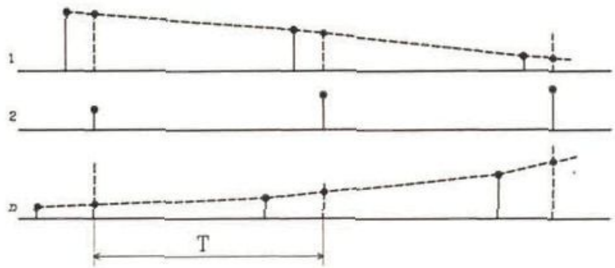

Fig. 3.4. Skew correction by interpolation

A more important drawback would appear to be that practical methods of interpolation either lack the desired accuracy or, for total accuracy, require all samples of the complete record for any interpolated point. The accuracy goal would aspire to match the SELSPOT 0.025 % resolution performance. This however would seem to prohibit real-time processing. This is because an exact interpolation involves, for each of the m-1 markers, either of two methods. First method is the general discrete-time interpolation, effected by

a. padding the marker coordinate samples with m-1 zeroes, followed by
b. passing the padded signal through an ideal low-pass digital filter, having the sampling period T/m and the cut-off frequency $|\omega_c| = \pi/T$, where T is the original sampling period.

As per period T, only one additional interpolated sample x_{int} is needed at the intermediate instant ΔT, the method is for that single point equivalent to continuous-time interpolation. This is by convolution of the original samples with the sinc kernel, or

$$x_{int}[(k+\Delta)T] = \sum_{n=-\infty}^{\infty} x[nT]\ \mathrm{sinc}(k-n+\Delta) \quad \text{, any integer } k.$$

Clearly, both ways, for each of the m-1 skewed markers, extensive calculations are due, to correct for the adversities of SELSPOT's time-multiplexed marker sampling.

As the ideal rectangular low-pass filter has neither a physical or a digital realization, and in practice one will not extend convolution across all past and present samples in any one run, both interpolation procedures will only yield approximated results. The non-ideal interpolation is equivalent to low-pass filtering on the one hand, which tends to offset the system's advantage of high-speed sampling.

On the other hand, the non-ideal interpolation introduces attenuated high-frequency components, which derive from the shifted replicas of the original signal spectrum, generated by the sampling process [12].

Similar considerations apply to the other time-multiplexed, active marker systems like WATSMART, CoSTEL, OPTOTRAK. As to non-simultaneous sampling of the moving markers, still more serious flaws have to be discussed with respect to the real-time passive-marker system CODA-3.

Now to return to SELSPOT (and derived **WATSMART** or **Hamamatsu**) systems, among the most serious drawbacks of the PSD as used therein, is its susceptibility for spurious light impinging from ambient or background luminosities, and from reflections of the high-intensity LED markers themselves. These spurious sources may induce a considerable offset in coordinate values, because the electrode signals at any time represent the coordinates of just one intensity-weighted centroid:
the PSD is an integrator of photocurrent over all of its active area.

To combat **spurious light interference**, the first category of these error sources, the SELSPOT PSD camera uses infrared filters to limit the response to within 800 and 1100 nm radiation wavelengths, and 950 nm IR-LED markers are used. Still, interference must be avoided from ambient or background light which contributes in this near infrared range, such as sunlight and incandescent artificial light.

The later SELSPOT-2 system offers one solution in that a feedback system is employed, to the effect of raising each individual LED intensity such that the sensor outputs I_x, I_y reach a prescribed, sufficiently high level to dominate the ambient light contribution (which can be monitored between LED pulses). Only then are the PSD signals sampled. The high-intensity mode can however be run only for some seconds, and needs cooling pauses for the LED's.

As originally suggested by Woltring (pers.comm.) the derived WATSMART system [13] takes additional reference measurements between the LED pulses, and calculates coordinates on the basis of the difference of "on" and "off" signals.

note
12 *cf. (Oppenheim, Willsky, Young 1983, v.d. Enden, Verhoeckx 1989).*
13 *for WATerloo Spatial Motion Analysis and Retrieval Technique, trademark of Northern Digital Inc., Waterloo Ontario, 1986.*

The method is optimized only for fluorescent light and appears to fail for daylight's large IR content, cf. Watsmart trade literature.

The use of IR-LED's however tends to aggravate the second category of PSD errors, as the **spurious reflections** from IR emitters are with most materials more intense and anyhow less tractable than visible-light reflections. The reflection error is visualized in fig. 3.5.

In one of the first documented SELSPOT applications, Gustafsson and Lanshammar (1977) described, quantified and attempted to compensate reflection errors. Their approach was limited to marker reflections in the floor, which cause an upward shift of the image centroid. By calibrating over angles of incidence corresponding to the full vertical field of view, initial errors of 3.4 cm s.d. over a height range from 0 to 160 cm could be reduced, but by no more than a factor 2.5.
As the PSD image centroid coordinates are intensity-weighted, a more substantial measure was to reduce reflectivities in all possible ghost pathways in the camera's view, and even on the moving subject proper.

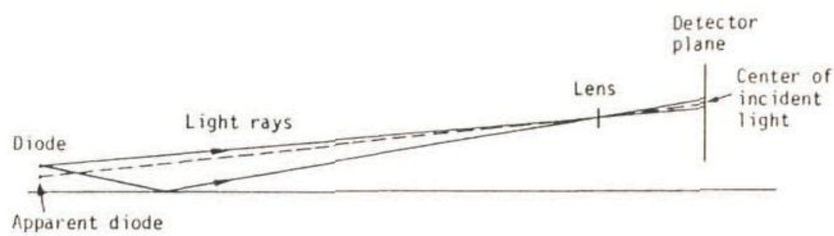

Fig. 3.5. Reflections in the floor
(courtesy Gustafsson & Lanshammar loc.cit.)

In (Halbertsma 1983) elaborate precautions are described for a SELSPOT system viewing cats at Karolinska Institutet, Stockholm. This involved a dedicated floor carpet to reduce reflections by 99.7 % and a camera baffle of 1*1 m PVC to intercept pathways from the walls and ceiling, while preventing internal lens reflections.
In (Röhrle et al. 1984) the SELSPOT cameras for human gait analysis at Dornier, Friedrichshafen, were arranged very low by the floor to keep reflections out, and with tilted optical axes intersecting at half the subject's height. But as other reflecting surfaces could not be fully eliminated, the method was reported as only partly successful.

Noise is another subject of concern with any position sensing system.

Halbertsma (op.cit.) reports on noise level of detected positions with stationary markers. By increasing the acceptance threshold for LED/PSD signal amplitude, low intensity images were avoided and noise standard deviation improved to between 0.05 % and 0.1 % of the field of view for high and low-intensity marker signals, respectively. After this modification, these figures tally well enough with the system's 10-bit resolution. However the modification changed the intensity range from the original 64:1 to 7:1, which now allowed a 2.65:1 range of marker distances, or corresponding tilt angles for individual LED's.
With Selspot-2 (1981) the 10-bit resolution was enhanced to 12 bit or 1:4.000 of field of view, and inaccuracy and non-linearity specifications are only within 0.5 % of FOV when using the 0.1 % SELCOM lens.

On the balance of performance merits and liabilities, as reviewed above, SELSPOT systems have since 1975 found an appreciable acceptance in the motion monitoring and analysis field. Turnkey packages include the elaborate MULTILab software and optional 3-D calibration objects. Their SELSPINE branch has entered the industrial area, e.g. of robot certifying.
Not only Northern Digital (Waterloo Canada) with WATSMART, but also Hamamatsu with a full copy C-1373 has invested in PSD systems.
Improved sensors are a commercial product of SiTek Inc.
Noorlag and Middelhoek (1979) describe PSD's made in silicon epitaxial technology, one of their aims being to have on-chip preamplifier and processing electronics.

3.6 CODA-3, a mechano-optoelectronic system

The first CODA [14] prototype, described by Mitchelson (1975), featured sequentially-switched active IR LaserLED markers and three dedicated 1-D cameras, which used cylindrical optics and a purpose-designed uni-axial photosensor with an axially coded optical mask. Impact in the motion analysis field was very limited and in 1981 the unflinching author presented a radically alternative system with CODA-3 [15].

CODA-3 held on only to the stereometric camera arrangement, which now consisted of one solid oblong box, holding two 1-D transverse scanners at a 1 m base distance, for the triangulation of X,Z coordinates. With a third 1-D scanner inbetween, and turned by 90°, a vertical angle was determined which, with the others, triangulated to the Y coordinate.
The system principle is shown in fig. 3.6a.
The markers are passive, high gain retroreflectors, specially composed of 4 bonded glass prisms to attain a wide acceptance angle of ± 100°. They have a scatter of reflected intensity within 1′ of arc, and mass is 3.5 g. The markers have coated colour filters, as identification of a maximum of 12 markers is by colour. The restriction is that 2 sets of 6 different colours must remain separated, each in its half-height compartment of the field of view.

The guiding feature of each of the 3 **proprietary 1-D scanners** is that they combine light source and sensor, much in the following manner.
A mirror drum with 8 facets rotates at 37.5 rps and is illuminated from a collimated slit source to produce a planar sheet of light which sweeps the observation space at a 300/s rate. When incident upon a marker, a pencil ray of light is reflected back unto the mirror. By a beam splitter this return bundle is projected on an axial detector element. The detector pulse triggers the instant readout of the drum angle. The same principles apply to all 3 scanners, to yield the 3 basic angular readings for any marker reflector. Proprietary solutions are contained for marker identification by a colour classification scheme. A 1986 improvement, by replacing the axial detector by a sheet of fibers bonded to 128 independent photodiodes, allows a multiplicity of markers in any instant direction of the scanning planes.

note
14 *CODA for Cartesian Optoelectronic Dynamic Antropometer*

15 *CODA-3, trademark of Movement Techniques Ltd, Loughborough UK.*

CODA-3, with its 1 m stereobase, is contained in a box of appreciable dimensions and weight. The solid construction required by the high-precision triple rotary mirror, illuminator and detector assemblies explains its 65 kg mass. By being inherently a fixed-base 3-D system, CODA-3 is factory-calibrated and should need no on-site adjustment. The mirror optics are devoid of the common lens non-linearities.

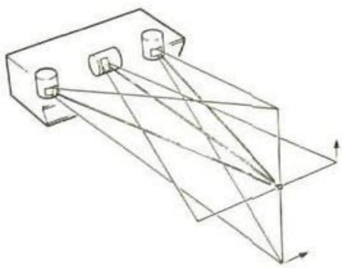

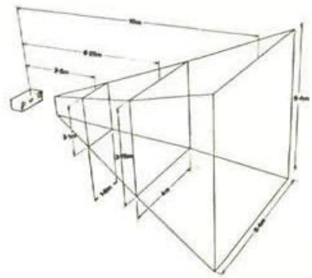

Fig. 3.6a. CODA-3 system *(trade lit.)*   b. CODA-3 field of view

Though the mirror and ancillary optics mediate a ± 20° viewing angle, marker coordinates are only generated when in the reach of both outer scanning beams. The common field of view (FOV) width is expressed by

field width $= \begin{cases} 0.8\ Z - 1\ \text{m}, & 1.25 < Z \leq 6\ \text{m} \\ 0.64\ Z\ \ \text{m}, & Z > 6\ \text{m} \end{cases}$, cf. fig. 3.6b.

For field height, the ± 20° viewing angle of the Y-scanner obtains.

Limitations of the 1 m fixed stereobase are rapidly felt at increasing distances. **Transverse resolution** is specified as 0.1 Z mm, with the longitudinal distance Z in m (for Z > 1.25 m). This proportionality is the usual behaviour for normal cameras.
However, **longitudinal** (depth) **resolution** is specified as $0.1\ Z^2$ mm. So at 3 m distance it is some 0.9 mm, which is already 3 times worse than the transverse resolution, while at 10 m, depth resolution of 9 mm is 10 times worse than the 0.9 mm transverse.

The formulas suggest that at distances Z > 6 m, transverse resolution amounts to 1:6400 of FOV. At Z ≤ 6 m this relative performance is seen to decrease somewhat, and at close quarters e.g. Z = 2.5 m it derates to 1:4000 FOV, which equals the SELSPOT-2 performance.
The absolute depth resolution of CODA-3 is inferior to the transverse values, but to quote the relative performance is less straightforward. With any system, the depth or longitudinal range might be assumed from the origin of the field of view to the outer limit of detectability.

It is more realistic though to assume a longitudinal range of interest equal to the transverse field of view dimensions, and so to define an approximately cubic envelope of observation. It is this dimension which we will relate to the depth resolution, and we will quote only two extreme performance values:
From the above FOV equations and the 0.1 Z^2 relation (for $Z > 1.25$ m), it follows that at a 2.5 m distance the relative depth resolution is 1:1600, better than that at 10 m, which derates to just some 1:640.

The difference of CODA-3 with SELSPOT and TV-based systems is that the latter have the advantage of locating and orienting separate cameras, for the optimal covering of the observation space without jeopardizing the resolution in one of the three coordinates. But never without a penalty, which consists of having to resort to a calibration procedure and 3-D reconstruction software.

It is indicative of the random character of the errors affecting the specified resolution, that CODA-3 has an enhanced resolution option, which is effected by digital smoothing, apparently of the scanners' $\tan\alpha_i$ data, before the rest of nonlinear triangulation operations.
Transverse and depth resolution are improved twofold and fourfold, respectively, at the expense of the sampling rate being down to 50 Hz.

Comparable to SELSPOT, but to a more dramatic extent, CODA-3 suffers the inherent property of **non-simultaneous** marker position **sampling**. But worse than with SELSPOT, the rotating scanner beams hit individual markers at position-dependent time instants. So the sampling by CODA-3 is also **non-equidistant** in time, in the case of moving markers, which for all systems concerned is the intended application.
With devices boasting a high sampling rate, there is little justification for neglecting these effects or assuming negligible values of the within-cycle marker shifts.
The only correction, implemented on 16-bit microprocessors, of which there are seven on-board CODA-3, is for the time-shift between the two outer transverse scan beams hitting the same marker. But even here, between scans, a constant (transverse) marker velocity is assumed. And for the correction algorithm this velocity value is apparently derived from preceding samples.
The algorithm assumes that incremental (transverse) position change ΔA within a sample period τ is $\Delta A = \tau\ dA/dt$.

If this assumption is tested on single sinusoidal motion at some tabulated frequencies, the following simple equations are involved:

exact $A(t+\tau) = \sin \omega(t+\tau) = \cos \omega\tau \sin \omega t + \sin \omega\tau \cos \omega t$

assumed $\tilde{A}(t+\tau) = A(t) + \Delta A = \sin \omega t + \omega\tau \cos \omega t$, with $\tau = 1/300$ s.

frequency (Hz)	cos $\omega\tau$	% off 1.0000	sin $\omega\tau$	$\omega\tau$	% difference
8	0.9860	1.4	0.1668	0.1676	0.5
16	0.9444	5.6	0.3289	0.3351	2.8
32	0.7837	21.6	0.6211	0.6702	7.6
64	0.2284	77.2	0.9736	1.3404	37.7

Clearly, the coefficients in the exact expression are systematically below those assumed. So for e.g. all $0 < \omega t \pm 2n\pi < \pi/2$, the true $A(t)$ is systematically less than the assumed $A(t+\tau)$ by percentages between the tabulated values for any of the test frequencies. The actual error percentage between those bounds depends on the weight of the $\cos(\omega t)$ and $\sin(\omega t)$ terms, which changes with the t value.

Now we have shown that the delay of the left outer transverse scanner has been corrected with assumptions which bear the risk of gross error relative to the stationary marker resolution claims.
But CODA-3 left apparently uncorrected the characteristic that also its height scanner hits the marker at a time instant that is generally unrelated to the sampling instant by any of the transverse scanners.
Time skew of the X and Y samples of one marker at (X_{mid}, Y_{min} or Y_{max}) will amount to $\pm \tau/2$ or $\pm$ 1/600 s, for instance. Referring to section 3.5 on SELSPOT skew, maximum error with sinusoidal vertical marker motion amounts to ± 1, ± 8 and ± 33 % at frequencies of 1, 8 and 32 Hz respectively. If CODA-3, other than suggested in the user manual, does include an Y-correction, the above shows the magnitude of the Y-skew errors. These would then be subjected to the correction routine, which is far from error-free as discussed for the transverse case.
Fidelity of the samples of the Y-coordinate is moreover put in doubt by triangulation with those outer scanner data. The real-time CODA-3 output of X,Y,Z and marker number provides no clues, moreover, for a reliable post-acquisition correction of single marker coordinates.

Whereas the above observations concern the sampling deficiencies on any one marker, we have already remarked that in the case of more markers, CODA-3 samples these non-simultaneously. But even this time skew is not constant, as with SELSPOT, but position-dependent.

With moving markers this has the effect that sampling is also not equidistant. This latter phenomenon should not be left uncompensated, if at any stage of the further analysis digital filtering, derivative estimation etc. are attempted. As discussed in section 3.5, the non-simultaneous marker sampling should be compensated by interpolating to one set of common sampling instants, if the usual planar angular or 3-D segmental calculations are to be performed on any combination of multiple marker coordinates.
Here again, it should be noted that sample skew between a mid-field marker and one near the FOV edge will amount to ± 1/2 sample period. Interpolation methods to address such compound problems as position-dependent sample skew, belong to a still more demanding algorithmic level than the example for equidistant fixed-skew markers. The more so if results are to balance the high resolution performance of CODA-3, at the elevated frequencies compatible with its high sample rate. Such software has not been provided nor even mentioned by the manufacturer.

Despite the attractive properties of
- a stable stereobase with immediate 3-D coordinate output (albeit at a limited depth resolution)
- the inherent identification of up to 12 markers
- the basically high sample rate and
- the relatively low noise properties, reflected in the good transverse resolution,

CODA-3 was shown to suffer serious accuracy problems introduced by the asynchronous, position-dependent sampling of the marker coordinates. From this point of view, CODA-3 is a shade too much an approximator, where applications call for a more straightforward measurement device.

Other vantage points, such as cost, should also not be neglected.
Already the handcrafted marker prisms are expensive at £ 200 apiece, while the dedicated electromechanic and optoelectronic scan assemblies have no future of mass production, comparable to contemporary quality CCD TV-sensors or even PSD's. The investment in clever ideas and good workmanship seems to have met with limited commercial success. Latest tidings confirm that manufacture of CODA-3 has met with difficulties and that marketing was temporarily discontinued.

3.7 Uni-axial camera systems (CoSTEL, OPTOTRAK)

Uni-axial PSD's, the original lateral photodiode form of the Position Sensitive Device, were already reported in the system by (Saito 1974), where three of these sensors were used for X,Y,Z sensing of a single miniature lamp.
Each of the uni-axial cameras consisted of such a longitudinal PSD, axially aligned perpendicular to the generatrix of a planocylindrical lens. The marker light source gets projected as a line image across the uni-axial sensor, and output signal is proportional to the image position. It was already pointed out by Andrews (1982), that the non-standard cylindrical lens is a costly solution not only in cash terms but also as to light, in comparison with a spherically focused light spot. For any light source position, at right angles to the sensed direction, the line image spills over one or both sides of the oblong uni-axial sensor. This has adverse effects either on the required marker power, or on admissible distances, or on system noise.
These were not specified in the Saito prototype, where probably the marker was a continuous light source.

The **IROS** system by one of the former SELSPOT executives has arrived at solving the light efficiency problem with the uni-axial PSD. Instead of a standard longitudinal PSD, each of the four 1-D cameras features a PSD with a square active surface, similar to fig. 3.2 but with the use of only one pair of electrodes. This PSD collects a much larger fraction of the line image, projected by the cylindrical lens.
Four cameras mounted on a fixed stereobase cross structure serve a dedicated VME microprocessor board for 3-D operation. Using PSD's and active LED markers in time-multiplex, IROS is open to similar critical considerations as its SELSPOT forerunner. The problem of spurious LED reflections, with any non-addressable sensor, appears to have clinched the decision to discontinue IROS in its infant commercial stage.

Back to oblong uni-axial sensors, the use of a linear photodiode array was suggested in (Fuchs et al. 1977) and implemented with 1728*1 pixel arrays by (Leo and Macellari 1979). Perfected by Macellari (1983), the **CoSTEL** system [16] featured multiple uni-axial cameras each made of a toroidal lens with a 2048*1 linear CCD array on the first focal plane.

note
16 *for Coordinate Spaziali mediante Transduttori Elettrici Lineari.*

Here again, even in the uni-axial addressable sensor, there is no way of distinguishing between projected multiple marker images, so the active LED markers are used in time-multiplex. The system, as recently marketed by LOG.IN srl, Roma Italy, features 0.4 ms marker "on" times to partly compensate for the loss of light from the anamorphic lens as mentioned above, and a system scanning rate of 1 kHz. Also, this lens type has some focusing action in the plane transverse to the sensor axis, being +5 dioptres compared to +20 dioptres in the sensor plane. This improves the projected intensity on the sensor elements. At the same time, the anamorphic lens introduces optical distorsion errors in the uni-axial sensor, and a light source position dependence in the transverse plane. This requires calibration of any pair of uni-axial cameras to provide accurate coordinate pairs. The lens field of view is ± 15° off-axis, equivalent to a 30° degree pyramid.
Spurious light signals are abated by special filtering and digital conversion techniques, and the system is claimed to be insensitive to illumination conditions in the measurement field.
The LED markers allow a great latitude in rotational subject motion, by having a ± 85° off-axis mainlobe radiation pattern.
CoSTEL supports up to six uni-axial cameras, the system is interfaced to the IBM-PC, XT, AT or compatibles.

The actual sample rate R of marker coordinates may be preset for a range of marker numbers M, such that $R*M = 1000/s$, with $R_{max}=200/s$.
Maximum distance is specified at 20 m, depending on LED marker power.
Per camera, resolution is specified at 1:4000, precision at 1:1350 and accuracy at .4 mm over a 2.3 m measurement field, amounting to 1:5750. These figures are not too remarkable, as the use of three cameras to obtain one set of 3-D coordinates would appear to imply more than the usual degradation.

Though (like with its WaTSMART kinship to the SELSPOT system) Northern Digital Inc. of Waterloo, Ontario, Canada, is not inhibited to appear the company of original adaptations, in a time where original concepts are hard to get by, its newly released **OPTOTRAK** system is not unworthy of mention by bringing some competitive upgrades to the CoSTEL system.

OPTOTRAK (1988) has the same 30° degree FOV per camera, but the higher speed system, which hooks up to the IBM-AT and compatibles, can handle up to 24 of the special OPTOTRAK cameras and up to 256 LED markers.

Each camera delivers two orthogonal coordinates, by having a dual assembly of a 2048*1 CCD sensor and an anamorphic or plano-cylindrical lens. The acquisition of two coordinates within one unit is a fitting idea, as we saw above that distorsion by the non-spherical lens is one of the critical determinants for the uni-axial sensor performance. Not without reason the OPTOTRAK camera carries a 40 Mpixel 2-D correction CPU board. Apparently, this performs a fixed and optimized calibration of lens distorsions, on the basis of the 3" fixed geometrical offset and alignment of the lens/sensor assemblies in the camera housing. The pixel number for 2-D correction being 10 times the actual number of sensor pixels is suggestive of a parallax calibration algorithm at 10 distances, which would need range information in an unclarified way.
Anyhow, this calibration, and subpixel processing, is understood to be responsible for the excellent figures of 1:10000 worst case accuracy across the FOV of each camera, with 1:20000 under optimal conditions.
The specification of expected 3-D accuracy ranges from 4 mil at a 3 ft distance (or 19" FOV) to 25 mil at 16 ft and a rather unexpected dip of 14 mil at 6 ft. So these figures imply somewhat more modest spatial accuracies of 1:4800, 1:4100 and 1:2800 of FOV, respectively.

With OPTOTRAK there are no specifications of resolution and precision. A 2-D position accuracy and repeatability plot is given as better than 0.25 mm, but without a FOV dimension.
Giving only accuracy figures would be entirely satisfying, if these pertain to any single measurement or, equivalently, if random errors, expressed by precision, are (up to a certain confidence level) less than the remaining systematic error or bias which is expressed by accuracy. More often however, stated accuracy figures pertain to the difference of the mean value of repeated measurements with the real value, which is known a priori or precalibrated to a greater accuracy standard (Walton 1986, Sydenham 1982). In this sense a low-precision noisy system may yet be highly accurate.

The camera system sampling rate is 2.5 kHz, with an announced upgrade to 5 kHz. Again, actual marker sampling rate depends on the number of markers, which again are active time-multiplexed infrared diodes.

One interesting novelty with OPTOTRAK is the **optional real-time board**, which will at 100 Hz deliver the six degrees of freedom of position and attitude of a solid object, specified by three or more markers.

To track more solid objects or segments, multiple boards may be added. This real-time option is however a less remarkable contribution if it is considered that, as in any time-multiplexed system, the markers are inherently identified. So with all respect, the tracking board boils down to a dedicated accelerator of 3-D photogrammetric algorithms, which in other systems are run by host computer software.

A precalibrated short-range OPTOTRAK 3D system is available, which features three single-axis versions of the camera assembly, mounted on a 0.9 m fixed stereobase (cf. CODA-3) and with a very satisfactory system accuracy, specified at 0.1 mm within a 0.8 m FOV volume.

Both CoSTEL and OPTOTRAK systems come with multichannel analog signal data acquisition facilities, and both offer the appropriate basic and analytical software.

There is little doubt, that these systems have a brighter future than the electromechanical-electronoptical CODA-3 system, and have got what it takes to outdo the SELSPOT system on spurious LED reflection errors though not in speed.
CoSTEL and OPTOTRAK do no better where, in parts of the application field, especially with animal and human subjects, the need for active wired LED markers is a disadvantage.
The implications of non-simultaneous sampling of the markers remain worthy of the considerations in section 3.5, in particular with the lower sampling rates than SELSPOT, and with a view to fully exploit the higher positional accuracy per marker attained with OPTOTRAK. If the skew problem was pooh-poohed in the WATSMART trade literature, it is not even mentioned with the recent systems. One would look forward to see the problem addressed, perhaps by implication, in the software supplied or in the real-time tracker option.

Now this discussion of recently announced systems in the non-TV based category has led us far afield in the historic progression. We will in chapter 4 take some steps backwards, picking up from chapter 2, for an account of our further developments in TV-based motion monitoring.

3.8 Conclusion

Though the Strathclyde TV-based system of section 3.1, developed in a collaborative effort to add more muscle to our first prototypes, is still intermittently used (Andrews, pers.comm.) and has spawned the commercially succesful VICON system, section 3.2, this chapter has in sections 3.3 and 3.4 reviewed many abortive prototypes, some of which were involved in reinventing the wheel.

Only the CINTEL system of Winter and associates was notably different and original, in that it was in many respects more like an early frame grabber with its 5-bit gray scale converter, and selectable line and column resolution over windows of adjustable size and position.
The Honeywell Oculometer was most noteworthy because of its two-level detection of the corneal reflection location superimposed upon the bright pupil image. From another point of view this system was limited to the processing, at each of the threshold levels, of no more than a single image contour.
The paper by Brügger and Milner (1978) introduced a 190*244 CCD sensor and a real-time hardware step providing midpoint X-segment values for further software averaging toward marker centre coordinates.
By Charlier and Hache (1982) an 8-bit microprocessor was put on board a single-spot dual-level oculometer for the estimation of centres of corneal reflection and bright pupil images.
The (Taylor et al. 1982) system is a first encounter with geometric centroid estimation, albeit implemented in off-line software. Moreover some additional real-time hardware provides the width δX of marker segments, which is required in the weighted average centroid software.

A review of the commercial SELSPOT, WATSMART and CODA-3 systems, which are based on alternative sensors or scan assemblies, has in sections 3.5 and 3.6 emphasized some of their strong points and some of their inherent weaknesses.
Finally section 3.7 reviewed the 1989 systems of CoSTEL and OPTOTRAK, which both use multiple cameras consisting of a linear photodiode CCD array and an anamorpic lens. OPTOTRAK with its dual-axis sensor/lens assembly and CPU correcting board, features the highest accuracy by an optimum calibration of anamorphic lens distorsion.

Some general conclusions may be drawn in a basic systems comparison.

TV sensors and linear CCD arrays, as opposed to the PSD of SELSPOT and WATSMART systems, are not offset by ambient light or LED reflections.

Non-TV systems have a much higher overall sample rate [17], the actual sample rate per marker being dependent on the number of markers.

Contrary to all alternative systems, TV sampling is simultaneous for stroboscopically illuminated markers or by using shuttered cameras. The other systems, that use LED markers activated in time-multiplex, would require the interpolating of data values to counter the ill effects of sampling skew.
With CODA-3, the non-simultaneous sampling of separate coordinates per moving marker is even position dependent and not equidistant in time, which defeats all but the crudest correction.

SELSPOT, CoSTEL and OPTOTRAK use active wired LED markers, while the TV-systems and CODA-3 have passive retro-reflective markers.

The alternative systems feature inherent marker identification by the time-multiplex switching of marker LED's. CODA-3 has identification of up to 12 markers by colour. TV-systems must identify the markers by software, though this involves only the reordering of coordinate data without in any way changing data values.

One application category, where real-time marker identification is a bonus, are those feedback or monitoring experiments where some of the observed coordinate values, preset position or speed should affect the experimental conditions, control an intermediate stimulus etc.

After presenting developments of our PRIMAS TV-system (including first attempts at real-time marker identification for control purposes) its performance will be discussed in section 4.10. With an occasion to put the various systems in the perspective of spatio-temporal resolution.

Finally, in chapter 5 we will account for an endeavour in synchronous detection with a SELSPOT-type PSD camera, using the active LED markers in frequency-multiplex. Some advantages are the suppression of ambient light interference and the inherently simultaneous marker sampling.

note
17 *Section 4.8 will review some recent high-speed TV alternatives.*

CHAPTER 4. 'PRIMAS' PRECISION MOTION ANALYSIS SYSTEM

4.1 Estimation of marker centroids

The early development of a marker contour suppressor, which had the option of passing the coordinates of two or four diagonal upper and lower points on the contour, was reported in section 2.4. This feature was used by 1980, with software to average the coordinates as an estimator of the marker image centre. A complete by-passing of the contour suppressor seemed at variance with the real-time datareduction philosophy of our Mark I systems family. But in 1982 the first experiments by van Antwerpen (1983) benefited from the availability of a powerful faculty computer with a high-speed parallel datanet.

Meanwhile, as reviewed in sections 3.4 and 3.5, off-line software had been applied as early as by (Winter et al. 1972) in averaging the coordinates of large markers acquired by the CINTEL system, whereas geometric marker centroids had been estimated in (Taylor et al. 1982).

This proved a timely challenge for an investigation of measurement noise with stationary markers, under a variety of centroid estimators.

Van Antwerpen (loc.cit.) reports on 2 markers, with image sizes of some 10 and 24 TV-lines, and at 6 locations after displacements of about 1 pixel. Standard deviations over 200 samples each are averaged over the 6 locations. Table 4.1 includes the s.d. % from the mean s.d. Precision is noise s.d. divided by the range. The 60 Hz system used the SiT camera tube, the image definition was 344 lines by 454 pixels.
Method 1 used the 4 diagonal upper- and lower points on the contour.
Method 2 used all contourpoints and unweighted averaging.
Method 3 used all contourpoints and geometric centroid estimation.

marker size:		method	1		2		3	
10-lines	X	precision	1: 3 900	±20%	8 700	±16%	8 800	±9%
	Y	"	1: 2 700	±26%	2 900	±30%	4 600	±22%
24-lines	X	"	1: 3 200	±16%	10 200	±19%	11 100	±30%
	Y	"	1: 3 800	±39%	4 100	±45%	8 400	±24%

Table 4.1. Precisions of centroid estimators, cf. text.

Method 2, using all contour points, proved superior to method 1 in the horizontal precision.
Method 3, the geometric centroid estimation, was clearly superior to method 2 in the vertical precision and was the best method overall.

In this experiment, the 30% standard deviation from the best average X result corresponded to precision values between the extremes of 6 042 and 80 000. More consistent results are to be preferred, extending to smaller markers, but already these figures for the centroid estimation method compared favourably to the specifications in (Taylor loc.cit.) and they were better than any other system cited in chapter 3.

In experiments by Serlé (1983) the relatively poor noise performance for the Y coordinates was traced by FFT to a 20 Hz frequency component in the 60 Hz sampled data coordinate sequences. This was attributed to the aliasing of a 100 Hz ripple voltage in the power supply, related to the rectified 50 Hz mains. As a battery supply eliminated the error phenomenon, this stresses the need for an excellent power regulation and smoothing in the video, threshold and comparator circuitry.

A measurement series by Serlé (loc.cit.) used 18 runs of 200 samples with stationary markers. The following are the averaged results:

markersize:		mean noise s.d. (%)	s.d. from mean (% of mean s.d.)	mean precision 1:
10 TV-lines	X	0.0142	10	7 100
	Y	0.0078	20	12 800

The vertical precision average shows a marked improvement. Although here again there is a considerable spread, the minimum Y-precision of 3401 is not too much below the average 4558 tabulated above, and above the corresponding minimum value implied in the (van Antwerpen) result.

In another experiment by Serlé (loc.cit.) geometric centroid calculus was used for the 2-D estimation of fixed distances between 3 collinear markers on a bar, fig. 4.1, where the 25 or 60 cm distance between the outer markers was used for scaling.

The averaged standard deviation for inter-marker distance estimates is represented in table 4.2.

marker spacing:	camera distance (cm)	FOV cm	av.standard dev. mm	% FOV	precision 1:
25 cm	100	35	0.065	0.0182	5 500
	150	52	0.057	0.0109	9 200
	370	130	0.247	0.0190	5 300
60 cm	370	130	0.207	0.0159	6 300

Table 4.2. Precision of inter-marker distance estimates, cf. fig. 4.1.

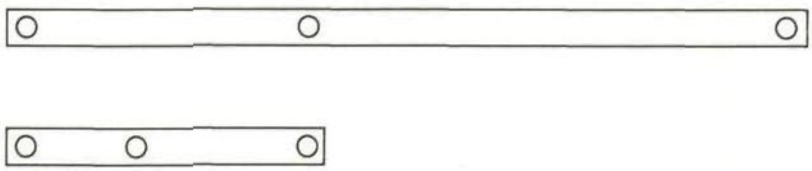

Fig. 4.1. Test bars for inter-marker distance estimation, cf. text.

These values, which encompass horizontal as well as vertical positions of the marker bar, and various sites in the field of view, compare favourably with experiments on a 60 cm bar with 2 markers reported by Jarrett and Woltring (1982). With the Dundee system as in section 3.1, they found a reconstruction standard deviation of the inter-marker distance ranging between 1 and 2.5 mm, with the bar held horizontally in the centre of the observation field, twice as bad when moving out of centre, and also about 2 to 5 mm with the bar held vertically. This experiment however involved two cameras plus the 3-D calibration and reconstruction routine which was the subject of their paper. Allowing for a certain degradation in 3-D, the planar results reviewed above clearly testify in favour of geometric centroid estimation from full marker contour coordinates.

4.2 Real-time estimation of marker centroids

In order to secure the advantages of marker centroid estimation and to recover the main feature of real-time data reduction, it was decided to abandon the marker contour suppressor and in its place to design and incorporate a **centroid processor subsystem**. Obviously the centroid processor was to operate in real time, in pace with video field rate.

In considering marker sizes of 10 TV-lines, exceeding a minimum width, the substition of 20 coordinate pairs by 1 pair of centroid values is indicative of the relief gained for the host computer system.

The new prototype by (Furnée 1984a, Serlé 1984) remained hosted by the faculty's HP-1000 system. But full benefit of real-time data reduction was soon realized with (Demper 1985a) in a first hookup to the HP9816, as a modest member of an emerging line of desktops, portables and PCs. This allowed application in cooperative projects outside the faculty.

Expanding upon the video-digital coordinate conversion system, which consists of a master clock, X, Y counters and registers, as reviewed in section 2.3, and which also synchronized the cameras, the centroid processor has to mechanize an algorithm like (3.1) in section 3.4:

$$\tilde{X}_m = [\, \Sigma_i \, PX_{mi} \,] \,/\, 2\, \Sigma_i \, dX_{mi} \qquad \tilde{Y}_m = [\, \Sigma_i \, PY_{mi} \,] \,/\, \Sigma_i \, dX_{mi} \qquad (4.1)$$

with $\quad PX_{mi} = SX_{mi}\, dX_{mi} \quad$ and $\quad PY_{mi} = Y_{mi}\, dX_{mi} \quad (4.2)$

$\quad SX_{mi} = (\, X_{1mi} + X_{2mi}) \quad$ and $\quad dX_{mi} = X_{2mi} - X_{1mi} \quad (4.3)$

where, cf. fig. 4.2, m is the marker index, i the marker segment line index; X_1 , X_2 are the X-coordinate of the rising and falling edges of the marker image.
The breakdown of the equations in 3 steps relates to hardware design.

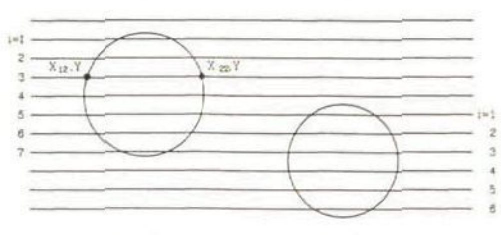

Fig. 4.2. Indices and coordinates of 2 markers on the line/pixel grid.

To suppress any speckle noise, a digital pulsewidth discriminator only allows the processing of marker segments with $dX_{mi} \geq$ say 4 pixels.

Successive centroid processor implementations, up to and including the one by (Demper 1987), have relied on a division of labour by dedicated **arithmetic hardware** and a general-purpose microprocessor board.

On the fly, at the occurrence of each video pulse which gave rise to the primary X_{1mi} and X_{2mi}, formulas (4.3) and (4.2) were mechanized by an adder and subtractor and two multipliers, cf. figs. 4.3 and 4.4. Results were stored in an intermediate, dual-ported memory which was to hold the data for a maximum of 512 marker image line segments. This was equivalent to say 20 above-average markers, sized 25 TV-lines.

The microprocessor board was dedicated to the clustering of the data prior to mechanizing the formulas (4.1) for output of the centroids.

The main reason for the division into two functional blocks was one of speed. Execution times for integer multiplication were some 70 clock cycles or nearly 9 μs at 8 MHz with the first 16-bit microprocessor selected from the Motorola 68000 family. The maximum of 512 marker segments would waste more than half of the available TV-field cycle time (16.7 ms at 60 Hz) before the processor could even tackle equations (4.1) and associated data clustering. Hardware multipliers were some 30 times as fast, and were operated simultaneously for PX and PY.

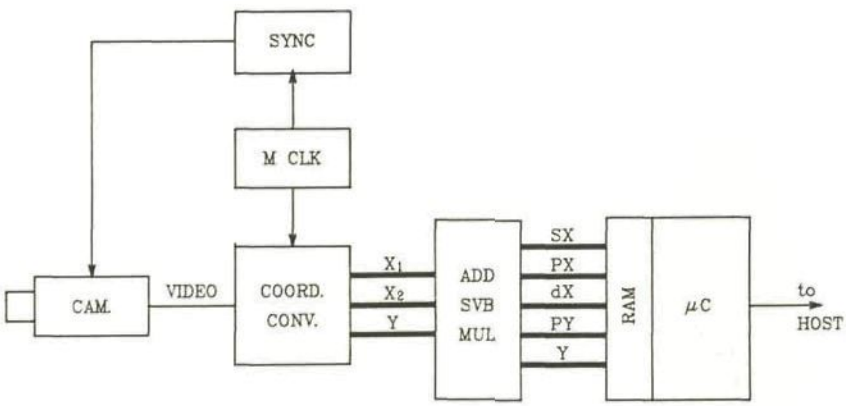

Fig. 4.3. Blockdiagram of centroid processing coordinate converter.

The SX_{mi} and Y_{mi} values were passed to the microprocessor as auxiliary data, for the purpose of clustering the dX_{mi}, PX_{mi} and PY_{mi} data which belong to the distinct markers m. Only then could the main arithmetic data $(dX_i, PX_i \text{ and } PY_i)_m$ be involved in equations (4.1) to obtain the centroid coordinates per marker m. The clustering algorithm is reviewed further below.

The coordinate converter block, much like the previous system with the full contour processor, contained an X and a Y counter for pixel and line number, plus X_1, X_2 registers to hold the instant coordinates of rising and falling video edges respectively. Its controls included the video pulse width discriminator. The 16-bit Y word could convey up to 7 bit external label information, some of which have been used e.g. in recording on-off signals from in-sole footcontacts in gait analysis. A later design added an X_1 pipeline latch to hold X_1 at X_2 latch time.

This pipeline of X_1 and X_2 registers, adder/subtractor, multiplier and RAM, in conjunction with the minimum 4 pixel marker segment width, once more met the requirement of a minimum separation of 1 pixel for adjacent markers on any line. Just like the earlier systems with the contour processor and a modest FIFO buffer. The situation of closely approaching markers may arise in perspective with certain movements.

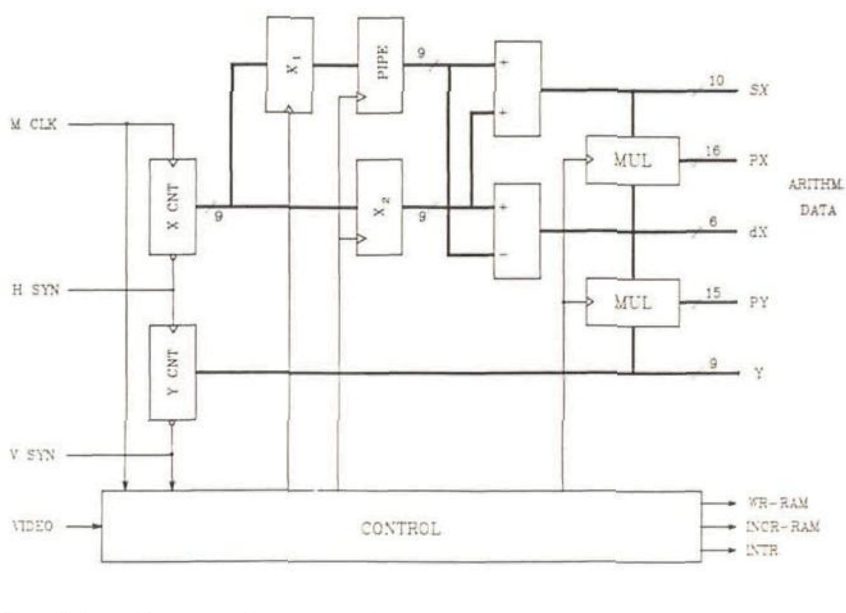

Fig. 4.4. Diagram of coordinate converter and arithmetic blocks.

The arithmetic hardware block featured a 9-bit adder and subtractor implemented as two triads of 4-bit 381-type ALU's with 182-type carry-look-aheads, resulting in below 30 ns delays. The SX output was 10 bit and from the dX output only 6 bit was used. This sufficed for markers of a maximum 64 pixel width, more than 1/8 of effective field width. Thus even large markers were allowed to approach the camera closely. The 12-bit multipliers were 240 ns ADSP-1012 CMOS types. Obviously, the products PX and PY were 16 and 15 bit, respectively.

In the first systems, dual-port RAM chips were not yet available for the **dual-ported memory**. So this was implemented, cf. fig. 4.5, as a two-stage memory pipe, which used isolating gates and bidirectional switching on and off the processor bus. This design was completed by a multiplexing scheme, where for input and transfer both memory banks were addressed by a sequential counter, whereas bank two could also be addressed from the processor bus.
Memory bank number 1 was organised as 512 quads of 64 bit, and during field scan it was filled with the video arithmetic data SX, dX, Y, PX and PY in parallel from each marker segment. Its contents were dumped to bank number 2 during field fly-back. Only this second RAM bank, now addressed in a 2k by 16-bit organisation, was accessed from the bus for data processing. These data were those of the previous field.

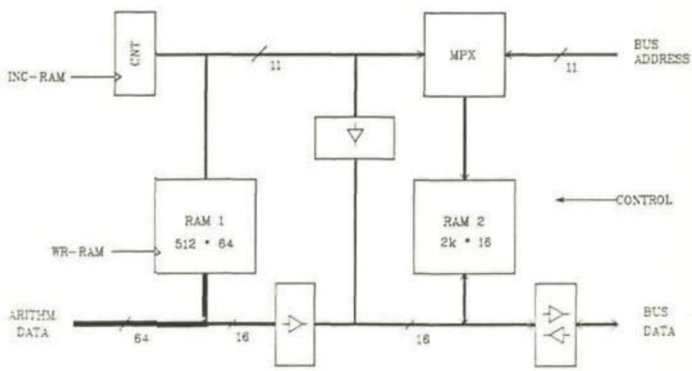

Fig. 4.5. Blockdiagram of dual-ported (dual-RAM) workspace memory.

The memory controls included a read-out gate to the processor bus of the primary data count, being the final value, after each field, of the address counter of the first memory bank. This counter also served a DMA function in copying the data to the second RAM bank. The dump operation was under the control of vertical sync and blanking pulses.

Moreover, vertical sync provided interrupt to the microprocessor for the signalling of every new field. Upon interrupt, the processor left a wait loop to reenter its clustering, algorithmic and output loop.

Obviously, the real-time centroid processing implies a one field-time delay with this and subsequent designs.

Output of the estimated marker centroids was by a 16-bit latch gate on an additional **RAM and I/O board** on the common bus. The HP-1000 hookup used the Control/Flag handshaking protocol of the remote HP-12566 interface, while the microprocessor used a Run/Halt sequence. The signalling of each new field was, as before, by insertion of a coded data pair preceding the marker coordinates.

The RAM board had a write protect option to operate as a ROM simulator for program development. This mode used the download facility provided by the Monitor firmware and serial port on the microprocessor board. Program development was by a dual-ported CIT-102 terminal hooked up to the faculty's Tektronix 8540/50 microprocessor development station. Later, the same MEM I/O board could carry the final program in EPROM.

The **microcomputer board** applied in this centroid-estimator prototype was the MPU4A from the Swiss GESPAC SA. A single-height Euroboard, it carried the 8 MHz Motorola 68000 microprocessor with its 16-bit data and 24-bit address buses (the 68000 has an internal 32-bit register organisation, only fully exploited in later 68020/68030 types). Also on board were EPROM with the GESBUG Monitor system, 16 kbyte user RAM, a programmable counter-timer and an RS-232 serial communication port. The 64-pin GESPAC bus was to become one of the single-board industry standards, with the mechanical advantage (like VME) of a pin connector rather than the prevailing card edge connectors. With the advent of the 68020 and other 32-bitters, the GESBUS was enhanced to 96 pins, but by then we had switched to full VME boards.

Fig. 4.6 shows the two dedicated boards described above, on the GESBUS with the MPU4A general-purpose microcomputer board. Use of the CRT/KB terminal was restricted to operator supervision like program start and such error messages as may arise. The HP-1000 link had a separate data acquisition program running, with only modest demands on disk storage and transfer rate, as an advantage of the real-time data reduction.

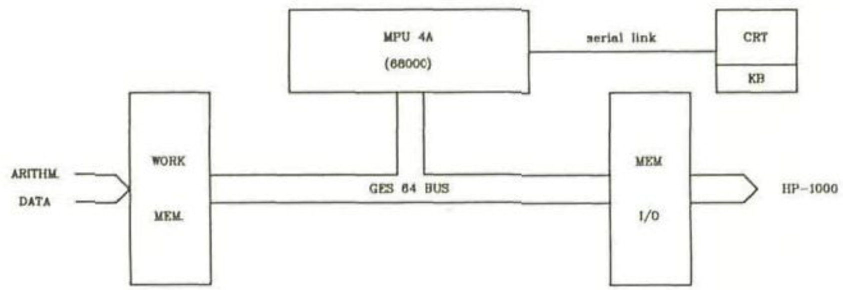

Fig. 4.6. Outline of the microcomputer centroid processing subsystem.

The **clustering program** was hinted at previously. In its final firmware form it was stored in EPROM. Its task was to collect, for each marker index m, the arithmetic data (dX_i, PX_i and $PY_i)_m$ for all marker segments i belonging to the same marker m. Only clustered data for each m could be used in the sum and quotient calculations of equations (4.1).

Some of the clustering algorithm could be borrowed from the earlier routines developed by van Antwerpen (1983) for the software centroid estimation from full marker contours, cf. section 4.1, method 3. If that software used the X_1, X_2 and Y data for clustering as well as for arithmetics on these data values, the present algorithm only uses the SX_{mi} and Y_{mi} for clustering purposes.

Two routines have emerged, the first one most like the early clustering program. This was serial or linear in this respect, that the whole workspace array was scanned for data pertaining to any one marker, a loop which ended with the centroid calculation along equation (4.1). The routine then returned to the array origin for a next marker.

A closer description of the clustering algorithm will be given with a second version, which is a parallel one in the sense that workspace is scanned only once, till the end of marker segment data. This, we remember, was defined by the data count and is read as the final value of the workspace RAM address counter. The program details are due to Serlé (1984), the description includes improvements by Demper (1985a).

During the workspace scan, a new 5 * m dimensional array is built in the user RAM area, where m is incremented for each distinct marker encountered. In this so-called marker array, for each m, the first 2 elements store the last Y and SX values, characterized by the highest index i. These only serve the clustering algorithm, as we shall see.

In the other 3 elements, for each m, the running sums are formed of dX_i, PX_i and PY_i. The elements sum PX_m and sum PY_m are long words of 32 bit. From this marker array finally, the centroid coordinates for each marker m are easily established by the division of sum PX_m and sum PY_m by the sum dX_m, respectively. For the purpose of scaling, the PX and PY sums are premultiplied such as to make full use of a 15-bit positive-sign output representation. This implies centroid coordinates in a range of 0-32768.

Also the marker count can be output as the final value of the index m. Distinguished by the sign bit, the marker count may serve as the field separator between the marker coordinates.

The actual clustering routine, which only uses the Y_{mi} and SX_{mi} data, starts by reading the first Y, SX, dX, PX and PY workspace values and storing them all as the first 5 elements, m=1, in the marker array.

The next Y is read and if it equals the preceding Y, as checked from the stored value in the marker array, this can only be from another marker on the same TV-line, cf. fig. 4.7 a. In that case, SX and subsequent values are read, m is incremented and the new Y, SX, dX, PX and PY are stored as new elements in the marker array.

If the newly read Y has equalled the previous Y plus 1, it may belong to the previous marker. This is decided by checking the new SX value against any of the previous SX, by reading back from the marker array. As SX is (twice) the average X location of the segment, the case of the SX difference being within a preset limit decides for the same marker. Otherwise a new marker is opened with the procedure described above.

A practical limit for the SX difference is a fixed one, the algorithm uses (twice) the minimum accepted segment width of say 4 pixels. As an alternative, the criterium might be derived as a fixed fraction of the actual dX value. We have not deemed this worthwile.

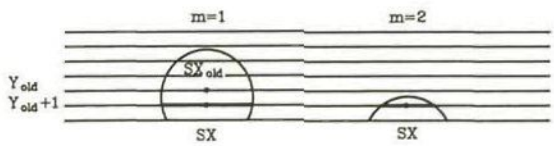

Fig. 4.7a. Continuing on previous marker or opening a new one.

If the new Y and SX test decides for a marker previously encountered and stored in existing index-m elements of the marker array, then the new Y and SX replace the older values, and subsequently the new dX, PX and PY are read from workspace and added to the older values, to form the respective sums at the index-m elements.

If the newly read Y has neither equalled any previous Y, nor Y plus 1, this means that the new marker segment is unconnected to any of the previous markers. Now the marker array up to the present index m is considered closed, cf. fig. 4.7 b. By consequence, for this and any subsequent Y and SX values no checking is done for matches against array elements below this value of marker index m. This is effected by incrementing the current start address of the marker search array.

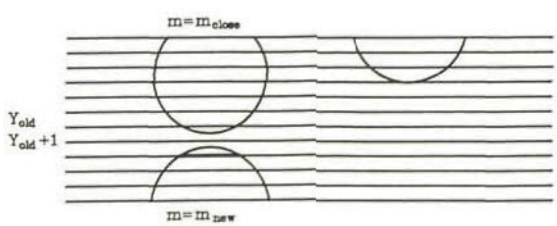

Fig. 4.7b. Opening a new marker and closing the previous marker array.

The clustering loops finish when the end is reached of the arithmetic data workspace. Then the final processing and output loop is entered.

Equipped with this real-time centroid preprocessor, the coordinate converter has joined the ranks of "intelligent measurement devices". The system performed fully as expected.

The cameras and basic pixel definition not having changed, the noise and resolution performance as checked by Serlé (1984) were in the order of magnitude as reviewed in section 4.1.

Indicative figures of processing speed were given by Serlé (loc. cit.) for the serial loop algorithm and by Demper (1985a) for the improved one-pass parallel routine.
Using markers of 12 TV-lines, the serial routine processed 6 markers in 6 ms. In a comparable optimum marker configuration the parallel routine coped with 10 markers in 6 ms, and 25 in 16 ms, outdoing the serial method and showing linear behavior of the number of markers and processing time. The optimum configuration for the parallel clustering algorithm is with no markers occupying the same TV-lines.
Some more realistic marker situations will be met with the performance review of later system versions, in section 4.10.

4.3 A desktop-compatible system

A first modification of the new real-time centroid processing system concerned the dependence upon the real-time HP-1000 central faculty computer link. The 16-bit parallel data connection was scrapped and this was exchanged for a local connection to an HP-9816 desktop host computer with the **HP-IB interface bus**. This byte-wide multipurpose computer and instrumentation bus was pioneered by HP with its series 9000 desktop computers and later solidified in the IEEE-488 standard. The *MEM I/O* board on the *GES-64* microcomputer bus, mentioned in the preceding section, was adapted to hook up to an HP-IB interface board of the talker/listener type produced by the faculty's Electronic Service Dept.

The HP-9816 desktop computer, also designated the HP 200 model 16, was an early specimen of the successful line of 680X0-based workstations by Hewlett Packard. This link-up brought the asset of portability to our motion analysis system, which has enabled a variety of cooperative projects outside the laboratory. With its modest 14Mbyte hard disk and the limited data acquisition speed, using the TRANSFER statement on the HP-IB bus, the combination was only feasible as a result of the real-time date reduction inherent to the marker centroid processing.

Much of the **software packages**, developed over the years first for the IBM-1130 and then for the HP-1000 minicomputers, was overhauled and rewritten for the HP desktop. Though adhering to most of the earlier principles, complete rewrites were dictated as our machine came with the BASIC and PASCAL languages. Most of the work by Demper (1985a) was dedicated to this area, notably with new routines for data acquisition and interactive marker identification, along the lines discussed in section 2.8. Also for subsequent data file management and analysis new software was generated. These included a file transfer option by the newly featured HP-IB net to the HP-1000 faculty computer, for backups or for analysis by our resident Fortran package. The main application of post-processing with the earlier Fortran programs on the HP-1000 minicomputer was in dual-camera 3-D calibration and reconstruction.
New BASIC software on the desktop computer featured missing marker interpolation, elaborate graphics including design of stick-diagrams, trajectory generation and time-plots.

Additional test software was directed to statistical analysis of the noise performance, as a tool in further system improvement.

There were only slight additions to the **hardware**, which for the time being featured only a single subsystem for marker centroid processing. For the purpose of camera calibration, aided by a known distribution of a multitude of markers, the system had a simple reduced-rate option. This was a 1:16 divider, converting vertical sync pulses as the sync interrupts to the microprocessor subsystem. This left the camera scan rate and the other video definitions unchanged.

For **dual-camera** applications, the system sampling rate was temporarily reduced to 30 Hz, with both cameras operating at 60 Hz.
For one of the cameras a newly developed solid-state system was used (Furnée 1986). To be discussed in the next section, this dedicated camera featured a frame-transfer CCD sensor, and we had stroboscopic camera operation by electronic shuttering.

In this 3-D configuration, the read-out of an image field was deferred by one field time, during which no new image was integrated. In the same time, the normal video from the other Plumbicon-type camera was read in for processing. At both cameras, the LED's, illuminating the retro-reflective markers, were strobed simultaneously at the reduced rate of 30 Hz. Essentially the video was processed at the normal 60 Hz but alternating between cameras.

A number of cooperative pilot projects were run with this portable, high-resolution 3-D system, albeit at one of the lowest samples-rates contemplated in modern gait analysis (Winter 1982). We soon had two of the new stroboscopic solid-state cameras, running at 100 Hz, and the dual-system sample rate was improved to 50 Hz. Inadvertently, both delicate sensors were blown up while checking supply voltage and, to the disappointment not only of our gait analysis partners, it took quite a time for delivery of the sensors to have the system up again.

A major new hardware design was started shortly afterwards, with the decision to hook up to the AT-line of IBM-compatible PC's, which was poised to become an industry standard and small laboratory workhorse. This funded project, based on our new camera, aimed at raising speed of centroid processing, to cope with more markers in 3-D applications.

4.4 PRIMAS electronically-shuttered CCD camera

Section 2.7 recalled our pioneering both of the stroboscopic TV-camera by inserting a synchronous, rotating shutter (1971), and stroboscopic illumination of reflective markers (1974). These measures reduced the image streaking, provided simultaneous marker sampling and enhanced marker contrast against background or scene luminosity. Now, adopting solid-state image sensors for our motion analysis system, we set out to develop a stroboscopic TV-camera. This was to be a CCD-camera with reduced integration time, at the normal field repetition rate. The rotating shutter was to be substituted by electronic means.

The rationale for **solid-state sensors** was partly presaged in section 2.8 with the experiments of warming-up and linearization. Contrary to the camera tube, the pixel grid is not defined, with all its deficiencies, by a scanning electron beam and associated electronics, but is laid out as a fixed-geometry pattern in silicon. Deposited with high linearity and precision during manufacture, with solid-state imagers the pixel definition is also a highly stable one. Thus the camera calibration for non-linearity mainly involves alignment and properties of the lens. These may depend on the setting of distance or aperture, but calibration is otherwise independent of the course of time.

Furthermore, if the Plumbicon or SiT camera tubes were selected for their properties of low lag, reasonable cost and adequate sensitivity, the solid-state sensor of the MOS-switching or CCD variety improves the performance by its negligible lag in build-up or after-images.

The GE 2505 TN solid-state camera, mentioned in section 2.8, had the not uncommon option of variable integration time. This meant that for low light level operation the integration time, and field repetition period, was extended beyond the ordinary value of 1/50 (or US 1/60) s. We were not cognizant of cameras with the reverse option of a reduced integration time, while maintaining normal TV field rates and formats.

Yet the idea was that the **stroboscopic TV camera**, by further enhancing the contrast of stroboscopically illuminated retro-reflective markers, against arbitrary scene highlights under strong ambient or background flux, should greatly enhance the performance and applicability of our motion analysis systems.

As far as we were aware, the **frame transfer CCD sensor** offered optimum opportunity for storage and normal read-out of briefly exposed images.

Without proposing a detailed review [1], a brief digression is in order (Feddern et al. 1984, Collet 1985, 1986).
The frame transfer sensor, <u>cf. fig. 4.8</u>, comprises two main areas of a similar layout, comprising 288*604 pixels in the actual sensor used. The first is the imaging area where a photon-induced charge pattern is accumulated during the integration period. The other area, adjacent to the first one, is the storage area into which the image charge pattern is shifted during the so-called frame-transfer.
Shifting of individual charge packets is by the CCD mechanism, and frame transfer takes only a small fraction of field repetition time, normally during the field blanking time.
Across the image and storage areas, the frame-transfer sensor has as many vertical CCD structures as there are columns (or pixels per line) separated by vertical stop isolators. By a deposition of horizontal isolating gate electrodes, connected and repeated in quads, and to which a four-phase clock Φ_A can be applied, the CCD contents in the image section are shifted simultaneously for all columns. A separate but similar set of quad electrode gates serves all CCD's in the storage section with an independent four-phase clock Φ_B. During frame transfer both section shift concurrently, as visualized in <u>fig. 4.9 a</u>.

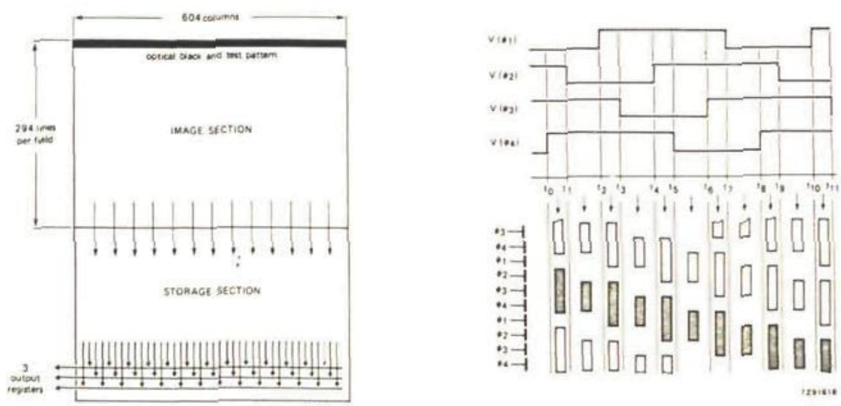

Fig. 4.8. Schematic layout of the frame-transfer image sensor.

note
1 *Actually, CCD sensors derive from the Bucket Brigade analog shift register invented at Philips Research Lab. (Sangster & Teer 1969)*

In the standard frame-transfer sensor the storage area is shielded from incident light and it is from the storage section that the charge pattern is read out on a line-by-line basis to produce a video signal. This read-out is mechanized by a horizontally oriented CCD structure which is, separated by transfer gates, adjacent to the lowermost elements of the storage CCD columns. All elements of the output CCD are charged in parallel by dumping the lowermost line from the storage section. Normally, at the beginning of each line, this involves one transfer gate sequence and just one cycle of the storage section clock Φ_B (the image section clock Φ_A is not involved). Then, as a serial representation of individual pixel charges, from this output CCD the line content is shifted out by a video-frequency pixel clock Φ_C.

To implement a **reduced-integration time** or stroboscopic camera with an otherwise normal read-out sequence, the frame-transfer sensor allowed us to be concerned only with the imaging section. Without affecting normal operation by tampering with substrate voltages, we saw no means to really inhibit the accumulation of photon-induced charge, the way a mechanical or electron-optical shutter operates. So the only realistic way of effecting a reduced integration time was to allow integration for a nearly standard time, then to clear the image area and integrate anew for the desired image, and shift this into the storage section.
All this within a single field period of the normal operation cycle. In this way, the problem reduced to the clearing of the image section.

On the sept. 1984 development samples of the Philips NXA 1010 sensor, our first experiments were aimed at reverse clocking the image section CCD's with a modified Φ_A pattern. This should flush the charge into the upper few lines reserved for test pattern purposes. This only met with partial success, as this area could only hold a limited amount of charge before spilling over into upper lines of unblanked video [2].

note

2 *It turned out not so much later that this was exactly how the EEV (UK) type P 4320 variable-integration camera (down to 1 ms) had capitalized on their otherwise lower-resolution P 8602 frame-transfer sensor: this had an actual test electrode at the top of its imaging area, which could be used as a drain to dump charge accumulated by reverse clocking.*

Much more scene illumination was allowed, when we succeeded to clear the image area by a specially designed **charge flush sequence**, which however involved all three sections of the frame-transfer sensor. This new TV-camera with reduced integration time featured prominently in the high performance motion analysis system reported in (Furnée 1986).

The new flush transfer operates by not only dumping the image section into the storage section as in the normal operation but, with open transfer gates and an active pixel clock, by shifting all charge on to and through the output CCD registers. This requires an early start of the frame blanking pulse to suppress spurious video output.
Shifting the flush charge out of the storage section is continued while already the image section takes no longer part in shifting but is integrating the new image, for the desired short period of time.

This intermediate phase, visualized in fig. 4.9 b, is followed by a normal frame transfer of the 288 image lines into the storage section. From this point on, the normal cycle ensues, of shifting out line by line through the regular pattern of transfer gating into the video CCD register and shifting out by the 604 cycles of the pixel clock.

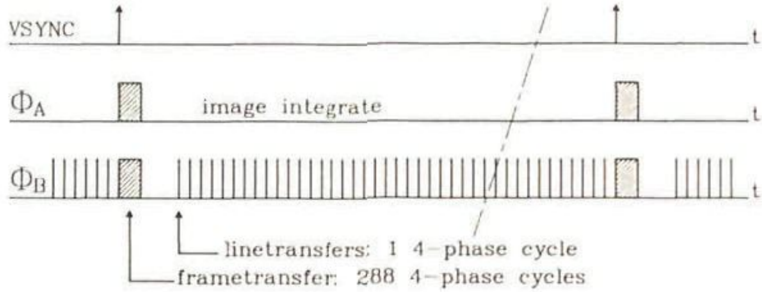

Fig. 4.9 a. Timing of normal frame transfer operation.

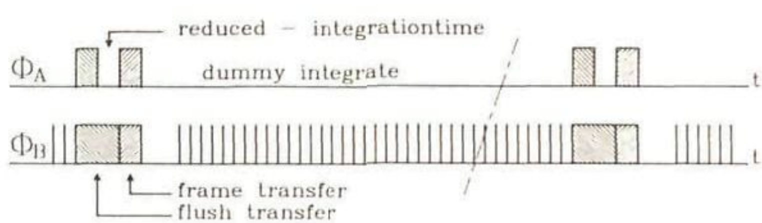

Fig. 4.9 b. Timing of washout and normal frame transfers.

Implicit in this review is our adoption of the Philips NXA-1010/1011 sensor with its 288 line by 604 pixel definition, where it should be understood that the vertical microstructure is four times as dense. Each TV-line comprises four vertically adjacent elements with a quad gate electrode deposition in order to operate the four-phase Φ_A and Φ_B peristaltic shift clocks. Interlacing may be realised by a half-cycle offset of the four-phase clocks, applied at alternate fields. But our systems, as outlined before, do not use interlaced TV. A three-phase clock Φ_c suffices for shifting the horizontal or video output CCD.

As a further peculiarity, the Philips frame-transfer sensor is organised not with 1 but with 3 **video output** CCD registers. Their layout and that of the associated transfer gates is such, that alternatingly, any one of three adjacent column CCD's in the storage section delivers its charge to one of the three output CCD's. This configuration allows an increased length of each output shift register element, to improve the handling of individual pixel charge. Moreover, with the additional deposition of a simple vertical structure of coloured filter stripes in repeated triplets, the basic silicon sensor turns into a colour imaging variety, where each of the three output CCD's corresponds to one of the colour constituants. The colour sensor is, however, not used in our present systems.

By consequence of this layout, the basic monochrome sensor version requires the reconstitution of three intermittent CCD pixel outputs into a single video signal. As a minor drawback of the Philips chip, this involves a dedicated video amplifier input stage, where a triple input sampling adder, driven synchronously with the pixel clocks, is the recommended solution [3]. No such device being offered with the Philips auxiliary chip set, a less elegant but adjustable video adder featured in our first electronically-shuttered camera's (Furnée 1986).

Yet another all-important feature was incorporated when integrating the new camera with our coordinate-converter and processing system.

note

3 *The 1987 measurement-quality MX-type camera by High Technology Holland (Eindhoven), using the same Philips sensors, implements a selective feedback scheme to adjust weight factors in the triple sampling adder. So as to permanently minimize monochrome video signal discontinuities or spikes at the pixelclock frequency. More on the HTH cameras, and their adoption with the PRIMAS system, by the end of section 4.5 and in section 4.6.*

This was the availability of the camera pixel clock as a system input to master both the X-counter and associated controls for reading out the running count. This **tight coupling**, by using the pixel clock as a system clock, makes for a better repeatability of the process of video to digital coordinate-conversion. This is an improvement over the tube-camera systems where the horizontal scan is only synchronized to the X-counter at the level of line reset intervals (cf sections 2.2, 2.3). We had already explored this advantage, possible only with clocked solid-state sensors, when hooking up the GE TN-2505 camera for the stability and linearity experiments mentioned in section 2.8.

As a clarification to the timing diagrams in fig. 4.9 we note normal frame transfer to take some 7.4 line times, out of a total of 24 lines suppressed or used for test and blacklevel purposes during a normal vertical blank, which leaves 288 lines out of a 312 CCIR noninterlaced format. The Philips Pulse Pattern Generator SAD-1019, and predecessors from the auxiliary chip set, did not permit our use of the 10.6 lines wait state. By consequence, as shown in the timing diagrams, the extra flush transfer, of some 10 lines duration, and the reduced-duration integration time are at the expense of the available 288 TV-lines. The slightly prolonged flush transfer is a compromise between loss of useful lines and scene or highlight luminosity: the amount of charge to be gotten rid of.

As an additional feature it was found that using 50 Hz sensors and the auxiliary chip set, and adapting our proprietary PAL designs for the reduced-integration time, the **field rate** could be **doubled** to 100 Hz. So we obtained a relatively high-speed system without apparent loss of quality (Furnée 1986).

As to **integration time**, our published 1986 prototypes featured a short integration of 15 line times, equivalent to a 1:20 ambient light suppresion. The later PRIMAS cameras have a flash integration of no more than 3 line times or 0.1 ms at the field rate of 100 Hz (Furnée 1988). Correspondingly, the latter leave more useful lines. More reduction of the integration time does not contribute much to useful lines, and is not feasible with the present LED illuminators, as below a 1:100 duty cycle one may no more increase the peak values of LED current, and LED efficiency is already derated near maximum peak currents.

Our **implementation** of the flush transfer and reduced integration time was, as shown in fig. 4.10, with digital multiplexers which selected between the standard Philips chip set for normal operation, and the dedicated Sync and Flush pulse pattern generator. This was a counter-controlled and PAL-decoded subsystem, from which all clocks derived.

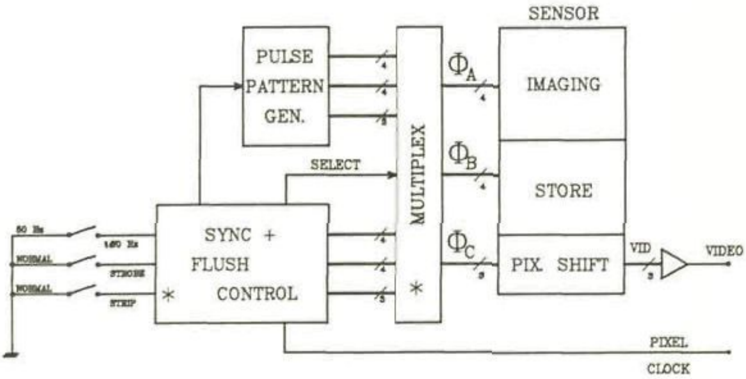

Fig. 4.10. Block diagram of stroboscopic frame-transfer camera.

Since then, we have extended the options with a new **200 Hz mode** of operation. Running at the same doubled pixel rate, equivalent to the 100 Hz upgrade, the 200 Hz mode is a compromise between scan rate and number of lines per field, for a constant number of lines/s. While for instance the commercial NAC electrontube-camera sacrifices resolution by skipping alternate lines at 200 Hz, with our reduced-integration time frame transfer camera in CCD technology we have opted to maintain resolution by scanning half-height images at 200 Hz.
The application philosophy is that of rapid phenomena, where trajectories of the points of interest can be captured within an oblong area, not necessarily meeting the 4:3 TV aspect ratio, such as heelstrike in gait biomechanics, or the binocular recording of eyelid wink (fastest human ballistic motion except eye rotation).

The 200 Hz half-height or **strip-scan** feature (Furnée 1988) is implemented by performing a new frame transfer beginning from line 156, instead of waiting for the full field cycle of line transfers from the storage section to have finished at line 312.

Fig. 4.11 shows some effects with a prototype stroboscopic TV-camera.

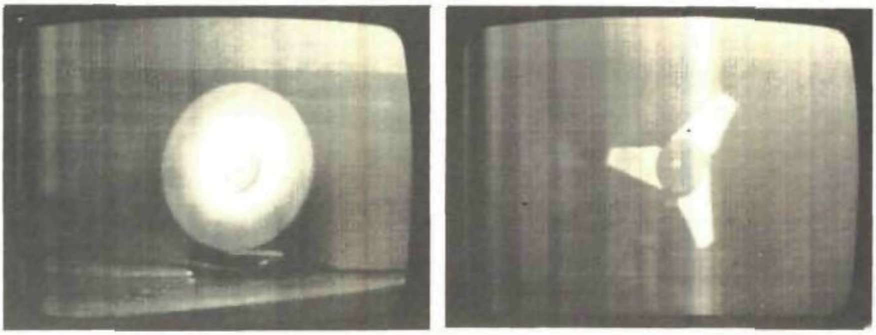

Fig. 4.11a. Rotating fan, under constant (daylight) illumination:
normal vs. stroboscopic TV-camera operation.

By the option of also performing a frame reset or flush phase shortly before the mid-image frame transfer, the strip-scan mode also features the reduced integration time at 200 Hz. It should be clear from some of the above discussions, that the modes of strip-scan and reduced integration time are at the expense of some more TV-lines. This may be evident as a narrow black band separating the even and odd half-height fields, if these are imaged on an otherwise normal 100 Hz TV monitor.

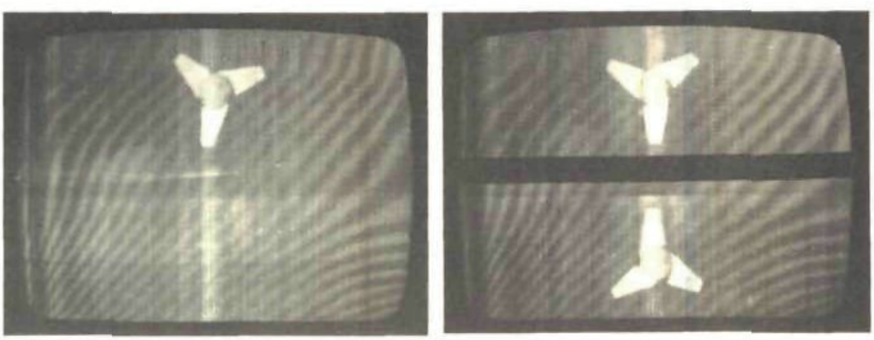

Fig. 4.11b. Same rotating fan, viewed in the stroboscopic TV mode:
normal scan vs. strip scan at double rate (note antiphase)

The reduction of integration time by a factor of 20 (Furnée 1986), and presently 100 as mentioned above, is equivalent to a reduction of the sensitivity for steady-state ambient or background illumination by the same factors, as compared to the sensitivity for the stroboscopically illuminated reflective markers. This amounts to a **contrast enhancement** of markers to ambient by more than 4 and 6 lens stops, respectively.

These novel camera features have, while retaining the low-power LED illuminators, opened up new possibilities as to the applicability of TV-based systems outside the specialized laboratory into the open daylight, for motion recording in sports, industry and ergonomics.
In an outdoors experiment with the early 1:20 ratio, markers at 30 m, viewed with a telelens, stood out clearly under 2000 Lux of overhead illumination.
At the TNO Delft indoor facility for vehicle crash research, markers at 5 m contrasted well under 10000 Lux overhead light, necessary for conventional high-speed film sessions in parallel to any new method.

Supplanting the bulky mechanical, rotating slit shutter, still evident with e.g. the renowned NAC camera [4], we deem the "all-electronic shuttering" of our reduced-integrationtime PRIMAS CCD-camera (or such devices as the EEV camera mentioned in note 4.2) to be preferable to the following **industry solutions**.
These are characterized by the insertion of special units into the optical pathway, like an image intensifier operated in switched mode.
This is an expensive solution with considerable overkill, though it is capable of (unnecessary) sub-microsecond exposures. Image intensifiers should be matched to the high pixel resolution of the basic sensor, at the risk of introducing patterned sampling errors.
From the class of variable-opacity "optical shutters", the Kerr cell with its high switching voltage is unattractive, but a different element has surfaced in recent consumer video-camcorders. Some doubt remains on the optical qualities such as plan-parallelism and homogeneity of this electron-optic switching medium, as compared with our more conservative method of direct imaging by a high-quality lens on the high-resolution sensor face, followed by creative electronics.

note
4 *The 200 Hz colour camera HSV-200 (Holzapfel 1981) features three Plumbicon tubes, 220 effective scanning lines and a 210 lines horizontal resolution. The HSV-400 (1987) scans 103 lines/field.*

4.5 PRIMAS [5] real-time system

Winning a competition, the project got funded by SPIN [6] from early 1987. The grant application was inspired by pilot experiments with the Dept. of Fundamental Mechanics, Eindhoven University of Technology, on strain and vibration dynamics in metallurgy (cf. section 6.7).

The emphasis on patterns of small deformations, to be measured with high definition by a large array of small markers, if possible on a rapid timescale, led to formulate the requirements for an upgraded high-resolution system, which would accommodate an order of magnitude more markers, without loss of real-time speed for the estimation of marker centroids. At the same time, the project aimed to interface the system to the newly emerged industry standard of the IBM-AT personal computers and its growing array of compatible competitors.

From section 4.2 we recall that, after the coordinate conversion, the marker centroid estimation was implemented in two stages, the first consisting of dedicated DSP hardware in the form of adder, subtractor and two multipliers. The second stage was clustering and concentrating the arithmetic data in a microcomputer board (μCB or CPU). Transfer of these data to the CPU was by dual-ported workspace memory (fig. 4.12).

One straightforward way of increasing the processing speed was to opt for one of the new μCB's which used the Motorola 68020 microprocessor (μP), then running at 16.7 MHz. This doubled the basic clock rate, and added performance as compared to the 68000 μP by its more pipelined, 32 bit architecture and the provision of 256 byte on-chip instruction cache. The nucleus or most frequently used loop of the cluster program could be made to fit within this cache range. As measured by Demper (1987), this chipped off some 30 % from total processing time.

Our selection was a CPU-21 board by FORCE Computers Gmbh, a full VME board which moreover provided a local memory extension bus for hooking up external memory directly to the CPU. This bus, called FLME, we used to connect the dual-ported workspace memory, referred to before.

note

5 *PRIMAS for Precision Motion Analysis System.*

6 *SPIN for Stimulatie Programma Informatica, sponsored by the Dutch Ministry of Economic Affairs; project number is PKO 710-48.*

However, the new design of the **workspace memory** could be simplified by making full use of the new truly dual-port RAM chips, 2 kbyte 90 ns devices equipped with dual separate address and data ports.

As reviewed in section 4.2, the workspace memory can only be organised in two sections, one being written by new arithmetic marker data while the other section's contents, the data of the previous TV field, are being accessed by the μP for final centroid calculations.
With the new dual-port RAM's, we accommodated these two workspace sections within the same chips, as distinct address spaces of 1 kbyte each. This ping-pong arrangement requires just one flipflop with its direct and complement output to control the most significant address bits of the write and read ports, respectively. This flipflop, simply controlled by the microprocessor, changes states at each TV field.

The dual-port workspace RAM was laid out as 32 bit wide at both input and output, and thus two 32-bit long words are used to hold each of the 64-bit arithmetic data SX, dX, Y, PX and PY per marker image line. So, as in the previous design, this workspace RAM may accommodate up to 512 marker image lines. This may increase to 1024, enough for an array of say 10 * 10 markers of a 10 line size (realistic numbers for calibration or deformation experiments) as soon as the newest 4 kbyte chips become available.

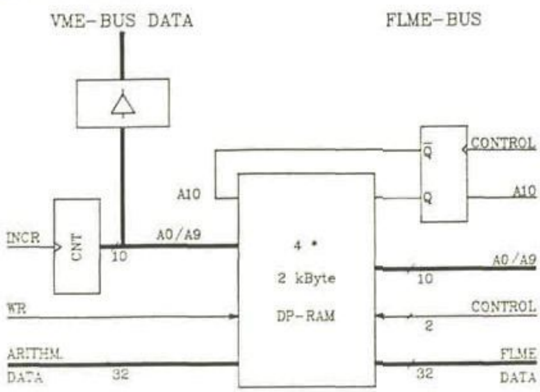

Fig. 4.12. Blockdiagram of dual-port (twin section) workspace memory.

Replacing the IEEE-488 interface to the HP desktop computer (section 4.2), in our new system the concept of **dual-port RAM linkage** was also used to transfer the output data from the CPU to the family of IBM-AT compatible host computers.

By virtue of the inherent data reduction by the centroid estimation process, the 2 kbyte DP-RAMs are too big for the purpose of output of marker data, but they got used all the same. Also, the same subsystem may handle the multiple output in a later multi-camera development.

Organised in a similar ping-pong fashion as the marker workspace, the output dual-port RAM's are written to from the microcomputer's FLME bus and at their second port they are accessed by the Expansion Bus of the IBM-AT. At this side, by chip selects, the quad byte DP-RAM array is accessed by single bytes only. The hookup is by 37-wire flat cable carrying 8 bit data, 10 bit address, and controls. This connects to a simple dedicated PRIMAS interface board of the short-slot variety on the IBM-AT Expansion Bus. Thus, as far as output data is concerned, the complete PRIMAS system is seen by the AT host as part of its fast non-resident address space.

Now concerning the **timing** between the miscellaneous subsystems, the only synchronisation between the coordinate-converter hardware and the μP board is effected by the vertical sync pulse. Generated at each TV field, it serves as the level-6 interrupt to the CPU. This signals the start of a complete iteration of the data clustering, centroid processing and output program.

The completion of centroid processing and the availability of output data is signalled by the microcomputer subsystem as an interrupt to the AT-type host computer. This is passed on thru the PRIMAS interface board as a level-9 interrupt on the AT Expansion Bus.
For its part, notably for start, test and control purposes, also the host computer can generate an interrupt (level-2) to the microcomputer subsystem.
This is effected by writing to a certain location in the address space monitored by the PRIMAS interface board on the AT Expansion Bus.

The **communication** between the AT host and the microcomputer subsystem is augmented by a one-byte mailbox register which resides on the 8-bit AT data connection. It connects to the VME Bus at the μC side.
The mailbox register can be written or read by either of the two sides and it is used to transmit extra code bits to specify the interrupt by messages like "normal end", "time-up error", "too-much-input error", "start-command", "reset-command", "option-control", etc.

Detailed by Demper (1987) and the author, the afore-mentioned modules of dual-port RAM's for input and output, mailbox register and interrupt structures have been put together on a **dedicated PRIMAS board**, fig. 4.13. It is shown in fig.4.14, how this board connects to the CPU both by the FLME local memory bus and by the general-purpose VME bus.

Of course, this board also contains a 9-bit address generator, plus an overflow detect, for the input side of the input DP-RAM's. Moreover, as a fill counter, this is read and reset through the VME Bus by the CPU, first thing after receiving the field sync interrupt.

Finally, this densely populated board also contains two EPROM's to store the complete CLUST program. Originating from Serlé (1984) and reviewed in section 4.2, CLUST was rewritten with major adaptations by Demper (1987). New control modules in CLUST serve the interrupt and mailbox functions for interfacing to the new READ program, which runs on the host computer, as reviewed below.

As the available EPROM's were slower than the microcomputer's on-board RAM, the CLUST **program starts** by dumping itself via the VME connection to that faster RAM. It continues from there in the quad byte, no wait state mode (with further speeding by the use of instruction cache).

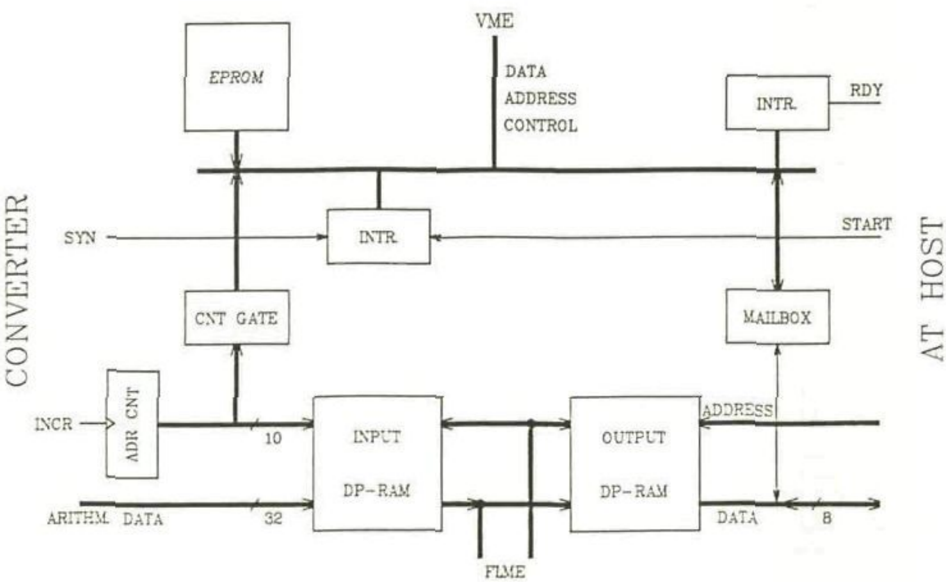

Fig. 4.13. Block diagram of PRIMAS VME / FLME-board

We had no wish nor courage to tamper with the FORCEBUG Monitor system program, resident in proprietary EPROM on the CPU board, for instance to insert a dedicated interrupt vector or routine on a semi-permanent basis. This might have handled an interrupt, such as the level-2 which originated from the AT-host, when the CLUST program was not activated yet. This would be a way to get this very program started.

Therefore, for starting and otherwise supervising the CLUST program, another secure but slightly encumbering way was selected. This depends on the normal use of FORCEBUG to change the Program Counter contents, so to point at the first executable statement of the CLUST program.

For the implementation, the standard serial RS-232 connection is used as a link between the microcomputer and the host computer, which in this phase serves as an RS-232 terminal. A minor drawback of this approach is that of using a second (albeit standard) link, next to the flat cable, reviewed before for the data and mailbox communication.
Both connections are shown in fig. 4.14, referred to before.
This solution, moreover, required the incorporation of standard serial communication software, such as KERMIT which was chosen at the time.

As an advantage of the chosen route, the direct serial hookup to the FORCEBUG monitor, apart from starting the CLUST program, may also be used for testing and supervision purposes, by the facility of access to all FORCEBUG commands and responses from within the READ program running on the AT host.

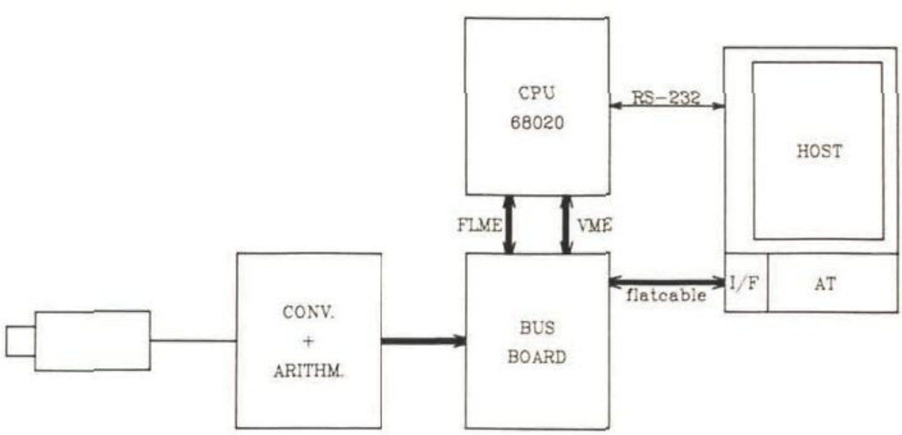

Fig. 4.14. Block diagram of the PRIMAS real-time system.

The **READ program**, mostly written in C but containing parts in Intel 80286 Assembler to access certain BIOS and interrupt functions of the IBM-AT, is a most notable contribution by Demper (1987). READ is the host program for the data acquisition of marker centroid coordinates and for the control of the PRIMAS system. As a software implementation of features reviewed above, the READ program has access to the system by means of the AT-compatible PRIMAS interfaceboard and flat cable (for the data, mailbox code and interrupts), as well as by the serial link to the FORCEBUG monitor (mainly to start the CLUST program).

Because of the data reduction, inherent in the marker centroid estimation, and the speed of byte-parallel data transmission from the output DP-RAM's, the READ program running on the AT host has ample time to perform another function besides data acquisition. This is to provide a running 2-D display of the incoming marker position data, annotated with the running field count and number of markers per field. Other TV-based systems (e.g. those reviewed in chapter 3) without real-time processing are lacking in this desirable on-line checking facility, which competing systems like SELSPOT may easily provide.

The final function of READ, part of its data acquisition task, is to name, organise and file the data to hard disk, in a standard format, with an interactively written descriptor (like van Antwerpen 1983) and further header information. Here, the format chosen for the data files follows the definition of ASYST, the Scientific System software by McMillan Software Inc, now Asyst Software Technologies Inc.

With the current PRIMAS systems, we have adopted ASYST for the rewrite of the **marker identification software** (Zuidhof 1989, cf. section 2.8) as well as for the **3-D camera calibration and marker reconstruction** programs (Sabel 1989) and all subsequent analytical programs in collaborative projects. Also the author's test programs for statistics on stationary and incrementally moving markers (section 4.10) are written in ASYST.

The modular structure of the READ program may be considered to easily admit rewrites for any data filing format, to adapt to future choices of post-processing language systems other than ASYST. For instance, a software interface was feasible to the attractive, marketplace SELSPOT MultiLAB motion analysis package: until its sudden price raise.

To return to the **READ program**, running on the AT-type host, some error conditions were removed and some refinements added by Sikkenk (unpublished), while some optional functions were added by the author. These and the next one will be revisited in the application chapter 6.

Written on the basis of an outdated Aztek compiler, the READ program was adapted by Klunder and Bak (unpublished) to the latest Microsoft C 5.1 compiler. This involved a major rewrite for new functionality and maintainability.

For the case of relatively stable marker configurations, e.g. affixed to a rigid moving object, the trainee Le Gal in 1988 implemented a first software version of real-time marker identification. This had the purpose of real-time object tracking as to location and attitude, cf. section 6.6.

As a recent activity, general-purpose **real-time marker identification** is being explored as a module to be implemented into the READ program to run simultaneously with coordinate data acquisition.

Routines for marker identification, along the principles described in section 2.8 with the extensions by Zuidhof (1989), were written by Schilt (1989) as a sequel to his work on transputer-based processing (cf. section 4.10). Rewritten in C and ported to the 25 MHz 80386-based host PC, this identification routine performs on-the-fly during data acquisition. Testing on some 10 markers, with not overly complex trajectories, real-time coordinate assignment took a mere 1 ms per incoming TV-field.

Section 4.10 will review some of the performance tests and figures for this satisfactory stage of development of the PRIMAS real-time system, with redesigned hardware and software for marker centroid processing and interfacing to AT-compatible host computers. With these tests, and with some recent collaborative projects, the system uses the reduced-integration time PRIMAS cameras of the previous section 4.4 as well as the measurement-quality MX-type cameras by High Technology Holland bv, which follow in section 4.6.

This stage of development of the PRIMAS system and the PRIMAS strobed CCD-cameras was the basis for considerably extended funding from SPIN, granted by mid-1988, and for strengthening the collaboration with High Technology Holland.

4.6 HTH commercial electronically-shuttered CCD cameras

The MX measurement-quality camera by High Technology Holland bv has been introduced in note 3 with section 4.4 and in the last paragraphs of section 4.5, with mention of the co-operation effort as a corollary of our renewed SPIN funding.
The SPIN organisation is sponsored by the Economic Affairs Ministry, so its requirements, next to those of technological development, are for the prospect of a new dutch commercial product, and at this stage a public enterprise has to commit its share in future development.
After the initial fruitful contacts on the HTH MX camera, this engendered the institutional collaboration with High Technology Holland bv, of which some current results are reflected in the following section.

The HTH company has fruitful relations with the Philips divisions responsible for the NXA-1011 series of frame-transfer sensors and is in a prime position to utilize the sensor and its successors under present development (HDTV) to its utmost advantage, to produce a first-class range of professional cameras for research and industry. Closely knit to its camera activities HTH exercises an expanding interest in Vision Systems. Here, next to frame grabbing and picture processing they are, by adopting the PRIMAS approach to specially marked objects, entering the sector of biomedical and industrial motion analysis.

The MX-range of frame-transfer cameras boasts a superb video amplifier stage, cf. the note referred to above, a stable black level reference and other features which designate it as a measurement-quality device. Like the original PRIMAS camera, the MX has the pixel clock available as an output signal to provide, next to horizontal and vertical sync, the tightest synchronous coupling to any video sampling and processing system. Alternatively, the MX camera can be run from a master clock of twice the pixel clock frequency, provided by such measurement systems and supplemented by a vertical or field reset sequence.

The MX-camera proved capable of running at 100 fields/s, and by its better video signal definition the camera has been shown to improve, also with a range of small marker sizes, the noise performance of the PRIMAS system to which it was easily interfaced (Furnée 1988).

Based upon our discussions and demonstration of the PRIMAS cameras, HTH made available their prototype of a **reduced-integrationtime** camera as recently as april 1989. With their intricate knowledge of the chip, they went their own happy ways and did experiments with substrate and electrode voltages which we had not envisaged, for fear of damaging sensors and incurring long delivery times. Anyhow, the HTH proprietary methods for obtaining a stable, high-quality reduced-integrationtime camera are different from ours and do not entail the loss of TV lines.

The striking result of this first HTH MX-based prototype, with its factor of 1:100 reduced-integration-time, equal to the PRIMAS spec's, has led to the optimization of this camera also for 100 Hz operation.

Sales considerations will decide if the PRIMAS option of double-rate, half-height scanning is to be featured in the new HTH camera, which HTH intends to be offering to a wider market than the complete PRIMAS motion analysis systems.

Concomitant with the adoption of the small-sized HTH cameras, the LED illuminators are being further developed, with Nagtegaal shrinking the mechanical design, having halved the supply voltage with controlled-current switching. Fig. 4.15 gives an impression of size and finish of the camera and illuminator assembly, while also showing a 1988 PRIMAS system enclosure.

Fig. 4.15. The PRIMAS system, with LED illuminator and HTH camera.

4.7 PRIMAS simplified converter, multi-camera systems, communication

Simplification of proprietary hardware being a major consideration, not only for primary pricing but also for serviceability and cost of maintenance, the relations with HTH as the future commercial producer (according to the SPIN grant intentions) are beneficial to some solid rethinking on some of the PRIMAS system components.

But it was also revisiting the literature, reviewed in section 3.4 and notably (Taylor et al. 1982), that brought home the fact that we had not changed the coordinate converter and arithmetic hardware section since the (Furnée 1984a, Serlé 1984) system reported in section 4.2.

In a new design, with reference to fig. 4.4 (section 4.2) we dismissed the ALU's for SX and dX. Also, same figure, the X_i and pipe registers were left out and, like in (Taylor op.cit.), for dX a 6-bit counter and register were implemented. New circuitry is shown fig. 4.16. Control is by a single PAL, which now includes a downloadable video pulse width discriminator.

A further hardware saving was by dumping the multipliers for PX and PY (cf. same fig. 4.4, and fig. 4.17). Deletion of these arithmetic chips in *favour of all-CPU processing has become feasible in the context of* the fast 68020 μP on the CPU-21 board. This runs at 16.7 MHz and takes only 28 clockcycles or 1.7 μs for an integer multiply.

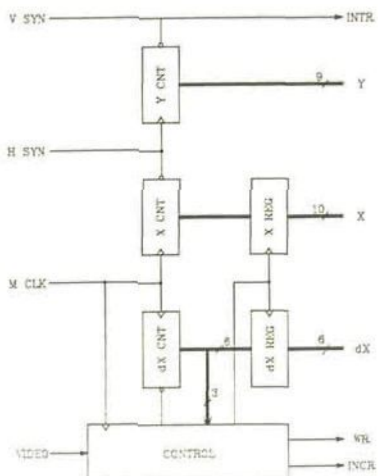

Fig. 4.16. Blockdiagram of simplified coordinate converter.

The processor time spent in the two multiplications proved halfway balanced by not having to fetch and disentangle the 17 and 15 bit hardware products from workspace memory.
Moreover, adapting and streamlining of the CLUST program with a new cross-assembler for the 32-bit series of Motorola μP's has actually resulted in some additional time gain. A main finding is mentioned below, and will be put in perspective in the performance section 4.10.

Testing an array of 35 markers, average size some 14 lines, we found the centroid processing time to be within 10 ms per field, with our FORCE CPU-21 board. By the number of marker data, this is equivalent to 50 markers of the more realistic size of 10 lines. Apparently, this marker number and size can be processed at 100 Hz.

This simplified hardware design, however, anticipates the refurbishing of the system with the presently acquired Motorola MVME-141 CPU board. It boasts the even more powerful 68030 μP running at 25 MHz, and using only 1.1 μs per integer multiply at the same 28 cycles. So, additional time gains may be expected, also from the elaborate on-board caching, which supplements the new 256 byte data cache on the 68030 chip.

However, in the CLUST algorithm (section 4.2) caching is only relevant to the intermediate marker array, as all raw arithmetic data is only accessed once.

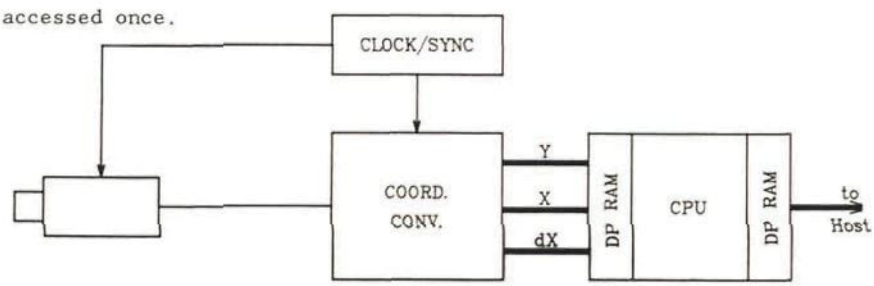

Fig. 4.17. Blockdiagram of simplified centroid-processing system.

Summarizing, in the new PRIMAS design the only proprietary front-end hardware is the video-digital coordinate converter proper. Output is a single 32-bit word, holding X_2, dX, Y plus eventual label information, such as a dX Overflow bit or external event code. The dual-ported RAM workspace can now hold twice as many marker data. The marker centroid estimation became an exclusive software task run on the microcomputer.

This simplified coordinate converter hardware is eminently suited for duplication in a **dual-camera system.**

Curiously enough, apart from an early dual-camera multiplexed system referred to in section 2.5, and the single-converter, alternating-camera configuration mentioned in section 4.3, the observation of (Jarrett 1976) remains to the point, in that we have until recently less concentrated on 3-D and multi-camera systems than on improvements of basic system and on front-end (hardware and firmware) performance.

Based on the speed performance of the new converter, mentioned above, one dual-camera converter board can be serviced by a single processor system of the CPU-21 type for centroid estimation of up to 25 markers sized 10 lines, and more with the new MVME-141 Motorola (68030) board.

Such a new dual-camera converter board has been designed and put to work, with the addition of one more set of dual-ported RAM workspace for the second camera channel. This board hooks up to the FLME and VME buses of the CPU-21 (68020) board in the present PRIMAS system, and for the first camera channel it connects to the input side of the DP-RAM on the existing PRIMAS VME-board, described in section 4.5.

This dual-camera configuration in shown in fig. 4.18.

As one of the new features, this board carries a dual D/A converter for the control, from the AT-host across the VME bus, of the threshold settings of the front-end video comparators.

Inherent in this dual-camera design is that each of the coordinate converters connects to its own dual-port workspace RAM for the write operation. At the read side, these workspaces are bused to the common FLME/CPU connection. Though demanding more real estate, this solution is free of any write contention from the randomly occurring coordinate data, which would otherwise require some form of priority arbitration between camera channels. Moreover, this solution is the easiest way to permit linear addressing in distinct workspace sections for each of the camera/converter channels.

Finally, in a **major overhaul** of the **PRIMAS system** as a prototype for the marketplace HTH product, it was decided to drop the FORCE Gmbh VME boards for the new line of 68030 boards products such as the MVME-141, already mentioned above and released by Motorola Inc. itself.

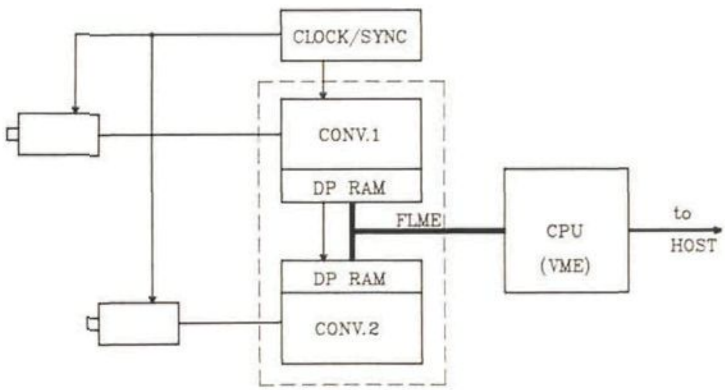

Fig. 4.18. Block diagram of dual-camera CPU-21 based PRIMAS system.

For the connection of multi-camera converter boards, present redesign focuses on the VSB local subsystem bus (IEC 821 bus standard), while dismissing the non-standard buses like the FLME or Radstone's PEX.

Anyhow, the continued use of a local bus for the contention of one or possibly even more dual-camera boards, leaves the VME bus free for the output and control communication with the host computer. This should simplify the overall software.
Also, keeping abundant front-end data on the local bus is in line with use of the VME-bus for interprocessor traffic, in any future multi-CPU configurations as may become feasible in heavily extended multi-camera applications, where marker numbers may exceed those indicated above.

Concerning the software, it should be understood that this is planned as an extension to the PROM-resident CLUST program (section 4.5), with reliance on the CPU's MVME BUG firmware or, say, an OS-9 PROM kernel. Adoption of disk storage with a full-blown realtime operating system is outside our philosophy of portable intelligent measurement devices.

Returning to the VSB-bus connection, the new converter board will use today's high-speed 2 kbyte FIFO's, which consist of DP-RAM and on-chip address pointers for separate I/O. Within a 28-pin package, these are space savers as compared to the presently used DP-RAM workspace chips.

The block diagrams below outline the new designs, where the mid-1989 effort is focusing on the single-processor configuration of fig. 4.19.

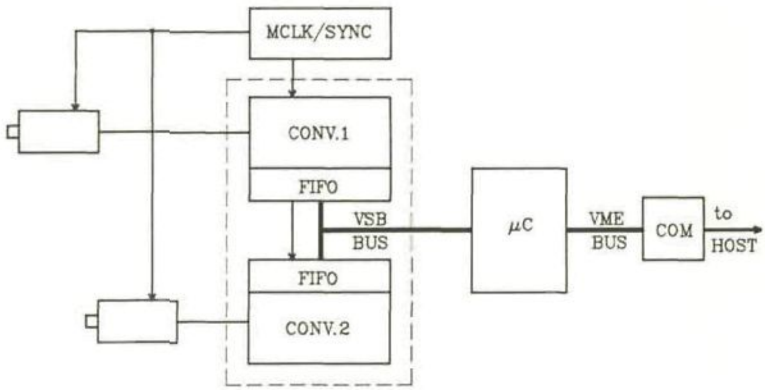

Fig. 4.19. Block diagram of VSB-bus based multi-camera design.

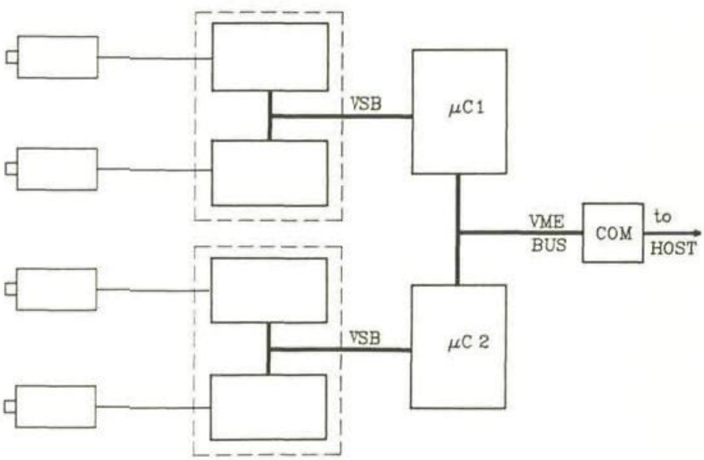

Fig. 4.20. Block diagram of multi-camera, multiprocessor design, for future high-speed, high marker number applications.

At the same time with the new boards we are investigating alternatives for the (multi-)processor to host communication.

For the data transmision we have used sub-MHz word-parallel DMA to the IBM-1130 and HP-1000 minicomputers (section 2.5). Having realised our data reduction by marker centroid processing, we went to byte-parallel IEEE-488 for the HP-9000 series desktopcomputer which was considerably slower because of the un-compiled BASIC statements (section 4.3). And in interfacing PRIMAS to the IBM-AT compatibles with dual-port RAM we have in section 4.5 discussed the unhindered bus-rate transmission by the Block Move instruction. But with the flatcable connection we incur the penalty of length restrictions to within some 50 cm, impractical in a transportable or laboratory system.

Of late, faster but still sub-Mbyte/s IEEE-488 interfaces have hit the market for VME as well as AT applications. In the framework of the HTH and SPIN project, we are looking into the on-board intelligence of the new offerings, versus the overhead time of the software protocol. This consideration must include ASYST, which supports the IEEE-488 bus. As ASYST is already used with the PRIMAS marker identification routines and analytical software (section 4.5), the combination if fast enough, would be an attractive choice of a marketplace hardware/software link.

However, this investigation will also be concerned with the facility, which we want to retain, of a running graphic display of the incoming position data. In the present PRIMAS system this is organised by the READ program, written in C. Replacing such a handcrafted program will mean a hard look into the ASYST data acquisition and graphics routines as well as real-time capabilities and pointer and array organisation.

Though READ also takes care of the system control from the AT host, as reviewed in section 4.5, there is little reason why full control could not be exercised by ASYST across the IEEE-488 bus, if only overhead is low and bus protocols are fast enough.

Another aspect of this investigation into host to PRIMAS communication is to get rid of the second, though slight, umbilical chord which is the RS-232 serial link. For the advantages, hesitations and drawbacks, we refer to discussions in section 4.5. Any new solution should also implement the passing of error messages from the CPU's BUG/Monitor.

As an alternative to multiwire parallel data transmission, where also SCSI [7] has to be considered, a range of protocols, chips and boards have emerged for high and very **high-speed serial** communication. Most protocols *(cf Tanenbaum 1981) have organised this as (packets of) bit-*serial bytes, representing ASCII or numerical data, and separated by start- and/or stop bits. The data packets are separated by sometimes elaborate headers, containing addresses, checksums etc. which all have to be taken care of by the pertaining protocol at both the sending and receiving end. If for the PRIMAS to host hook-up we consider only the point to point link, or the small local area network, the high speed transmission medium is single-ended or differential coax or twinax.

Among the manifold offerings of intelligent communication boards in the Mbyte/s speed range for VME and AT systems, the marketplace LAN of the **Ethernet** variety is under consideration. Here again we are looking for standard solutions with a minimum of software overhead as to speed and complexity. At the PRIMAS side the VME communication board should not require another stored operating system than the resident firmware of VMEBUG/Monitor, or the board should provide its own EPROM kernel. Summarizing, the intention is that an Ethernet link be incorporated in a straightforward way for data transmission and system control, with only some modular rewrite in the CLUST or READ programs on VME and AT.

In the last resort, we are ready to take up the new **TAXI-chips** [8] by AMD Inc. These provide a transparent bus-oriented parallel interface for data bytes and/or control nibbles, while actual transmission is bit-serial, and formatted for in-line integrity checking. A prototype interface for the AT Expansion Bus was built by a trainee (Lok 1988), using a FIFO buffer at the receiving end, as shown in fig. 4.21.
We had satisfactory tests, up to the rated clock frequency of 70 Mhz for a speed of 7 Mbyte/s, by coax connecting the sending and receiving ends, and some lines of C. We already used the nibble format for status, control and interrupt.
Writing and inserting the appropriate subroutines for the VME-CLUST or AT-READ programs, taking care of both data communication and system control looks like a less formidable task, than inserting the Ethernet software with its considerable networking overkill and CPU overhead.

note

7 *SCSI for Small Computer Systems Interface (ANSI X3T9.2 specs.)*

8 *TAXI for Transparent Asynchronous Transmit/Receive Interface.*

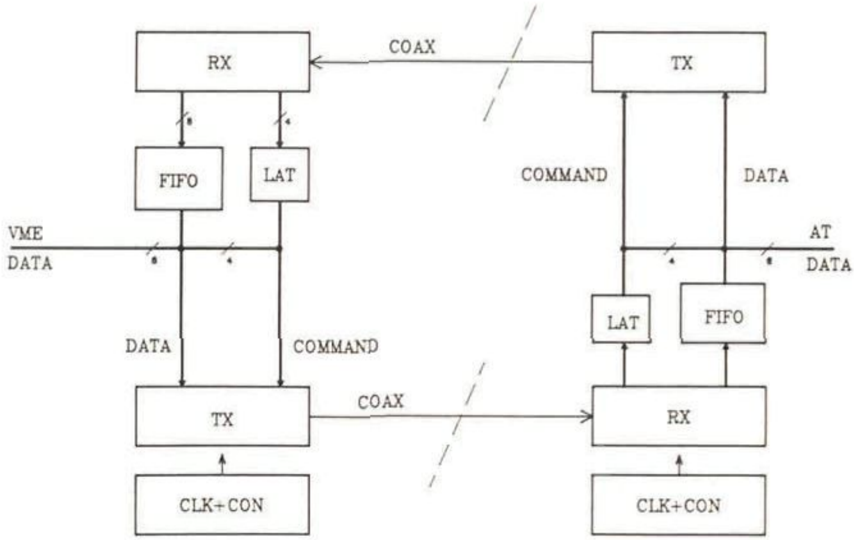

Fig. 4.21. Block diagram of TAXI-chip duplex communication interface.

As to the design strategy of a PRIMAS market prototype, a disadvantage of the TAXI approach is that, though an AT-compatible evaluation board was announced, this would (like the dual-port RAM's) be a non-standard solution, and thát in a computer market with communications galore.

Finally, we are engaged in the **interfacing** of the host computer to **external sources** of analog or digital measurement signals, such as EMG or forceplate signals. Contrary to our early versions as from 1974 (section 2.5), where the externally digitized data was buffered and multiplexed with the coordinate data and fed through the system's data link to the host computer, it is now preferred to input the external data through standard digitizing interfaces on the AT Expansion Bus.

The external data sources can be synchronized by pulses, and if need arise by line plus field count bytes, from the PRIMAS central clocking module. Moreover, the incoming data synchronization is a task of the data acquisition program, at least at the field rate of the PRIMAS coordinate data, such as is signalled by interrupt (section 4.5). This feature of field rate scanning of a buffered external data interface is to be added to the READ or its successor programs.

4.8 Commercial TV-based systems (VICON, ELITE, ExpertVision etc.)

We have seen in chapter 3 that the Strathclyde University / Dundee Limb Fitting system, derived from our prototpes in a co-operative way, gave birth to the commercial VICON system by Oxford Instruments UK, which by 1989 has sold some 100 units worldwide. This section will review contemporary TV-based systems, joined by new brands of e.g. ELITE (Italy), ExpertVision (USA) and SIGHT (Japan), before continuing with section 4.9 on PRIMAS performance and making some comparisons.

The **VICON** system, discussed in section 3.2, saw some further development. As from the 1983 sales brochures there is a mention of marker centroid calculation by software on the basis of the acquired marker contour coordinates. Clearly, in contrast to previous versions, the trailing edge coordinates were now also taken into account. The option had remained however of restricting the data to leading edge detection (Bradstock VICON pers.comm. oct.1983). Anyhow the centroid estimation does not show up in improved resolution performances, compared to the earlier 1:1000 standard error in 3-D reconstruction.
This may be affected by the relatively small size of the 19 mm conical or 14 mm cylindrical retro-reflective markers specified and used in gait, ergonomic and sports applications equally with grown-ups as with children. Bigger (semi-) spherical markers, like with CINTEL (section 3.3) or PRIMAS, have only been seen since the 1987 ISB exhibit.

A 1986 VICON brochure introduced the option of a 200 Hz mechanically-shuttered NAC camera featuring a 244(V)*320(H) MOS image sensor. With this one, 3-D reconstruction accuracy was specified at 1:400 of field of view. Later brochures show a 60 Hz mechanically-shuttered colour camera and a powerful light source, coaxial to the lens with a mirror arrangement like our fig. 2.10 (section 2.7). However, no mention is made of colour applications in on-line video motion analysis, and the colour system is apparently intended for VCR tape archiving.
As a rigourous precaution, with the non-shuttered Cotron camera and an IR-LED strobe illuminator, the 1986 VICON ambient specification prohibited daylight and incandescent light, while fluorescent light tubes should be kept out of the cameras' field of view.
As a final point on VICON cameras, when discussing the VICON interest in our PRIMAS electronically-shuttered CCD camera, we suggested a new commercial EEV (UK) camera (Morris VICON pers.comm. dec. 1986).

Though this has no 100 Hz and does not provide for control or output of the pixel clock, the EEV camera (cf. section 4.4 note 2) was indeed seen in the VICON booth at the 1987 ISB Amsterdam exhibit. Shuttered cameras at 0.8 ms are included in the recently announced 1989 VICON VX system, to relax much of the ambient light constraints.

Clearly, having been involved in many biomechanical research projects, VICON have strengthened their position in application software. Also, we understand from ADTECH Inc. Bethesda MD USA, that they have contributed commercial AMASS software, including a marker centroid algorithm that would provide an overdue upgrade of resolution. However, the 1989 VICON VX brochure adheres to the 1:1000 resolution specification.

Meanwhile, no scientific literature detailing VICON system definition or performance has come forward, except by third parties on either applications, such as (Whittle 1982), or feasibility (Kepple 1988).

With (Ferrigno et al. 1985), at least one journal paper was devoted to introduce the new **ELITE** [9] system. This has sought to obviate one of the main shortcomings of VICON which at the time was the poor contrast of markers, even under strobed IR-LED illumination, except under tight ambient and background light conditions. By dedicated processing of the video signal, ELITE allows a greater latitude of luminous conditions and of arbitrary background or scene luminosity distributions.

The expedient is real-time pattern recognition by 2-D crosscorrelation of the video signal with the predetermined intensity distribution of a template marker image of a specified size and shape. For this purpose, video is quantized to 4 bit, and a 6 * 6 pixel template is used over the 256 * 256 camera pixelgrid. Only if and where the crosscorrelation value exceeds a predetermined threshold, the pixel coordinates are digitized in the by now familiar way. Video threshold crossings, not corresponding to a marker match, such as local background clutter, small or extended scene highlights, are by this mechanism rejected.
At the time of visiting ELITE early 1986, the real-time computation of marker centroids, claimed in (Ferrigno op.cit.) had not been realized, and all coordinates of the accepted pixels were dumped to the host computer, together with their associated crosscorrelation values.

note
9 *ELITE stands for Elaboratore di immagini televisive. Marketed by BTS, Milano Italy.*

The same state of affairs was reported in (Ferrigno et al. 1988) on the ELITE marker identification software. Nor had the reported feature of on-line adjustment of the marker template parameters been realized.

Already it had been recognized that the shape classification was less useful in the general case, where there should be no restrictions on the orientation of the markers attached to the body in motion.
So the template matching boiled down to a size and intensity profile of generally circular marker images, and to the elimination of non-circular or wrong-sized lightspots.
As an objection, such a system is essentially critical of the imaged marker size, which means that ELITE can tolerate only limited marker motion along the camera's line of sight. This would appear to restrict ELITE applications to roughly planar movement, such as gait (including running and cross-country skiing) viewed in the sagittal plane.

The acceptance, according to the sales brochure, of small markers with dimensions hardly exceeding 1:256 of the field of view, so projecting to sub-template size, relies on an intentional over-exposure, blooming or defocus of such marker images in order to cover a desirable number of pixels (Ferrigno, pers.comm. 1986). This seems a less dependable way of obtaining the sub-pixel resolution which centroid estimation can deliver.

Unlike the geometric centroids, cf. sections 3.4 (Taylor et al. 1982) and 4.2, the ELITE algorithm estimates a form of intensity-weighted marker image centroid. But instead of the pixel intensities associated with the pixels (x_i, y_j), the values R_{ij} of the bi-dimensional cross-*correlation with respect to the 6 * 6 marker template are used in the* following formulas for the centroid coordinates (x_c, y_c):

$$x_c = \Sigma_i (x_i \Sigma_j R_{ij}) / \Sigma_{ij} R_{ij} \; ; \; y_c = \Sigma_j (y_j \Sigma_i R_{ij}) / \Sigma_{ij} R_{ij}$$

In (Ferrigno et al. 1985) a resolution test is described on the basis of minimum discernible linear marker displacement. Standard deviation of the residual from a linear regression line is reported as σ = 0.06 pixels or some 1:4000 of the field of view. This corresponds to a 90 % confidence bound of 1:2500 quoted in the sales brochure. The rewarding result was obtained with the characteristic small markers, matching the 6 * 6 pixel template under the circumstances discussed above.

The noise performance with stationary markers is however not specified and no precision or repeatability figures are given for ELITE.

The use of local crosscorrelation values in the centroid calculations is a bonus from this system's concept of marker template matching for the suppression of ambient, background or scene highlights other than the stroboscopically illuminated retroreflective markers.
However, the central concept of elaborate signal processing applied to the video, like the A/D conversion and crosscorrelation with a bank of dedicated VLSI chips (where the 5 Mhz real-time clock limits the pixel count to a mere 256 * 256 at 50 Hz), though an original departure from our Mark I and VICON systems, is at variance with the PRIMAS concept developed by the same time. Our effort, after implementing a geometric centroid estimation in real time (sections 4.2, 4.3), has concentrated at the front or sensor end, in developing an electronically-shuttered camera, which is able to discriminate strobed markers against ambient and scene highlights already at the system's input (section 4.4).

The benefits, in this respect, of a stroboscopic camera in conjunction with strobed marker illumination have curiously enough not appeared to the ELITE engineers, though (Ferrigno 1985) reports on the option of a rotary mechanical shutter to avoid image shape distorsions with rapid marker motion, which else might obfuscate the template matching.
The recommendation in the ELITE sales brochure of a rotary-shuttered camera (albeit at no less than 1.5 ms aperture time), when analyzing fast movements in very critical environmental conditions, would appear to prove our point. The failure with IR-LED illuminators at the indoor 1987 ISB exhibit sheds a particular light on the critical conditions referred to.

The **ExpertVision** system by Motion Analysis Corp., Santa Rosa CA USA, is unlike ELITE in its global conventionality. Only one hardware feature deserves of any mention. This constitutes an adjustable mask for selecting a window of interest outside of which, to eliminate unwanted background or highlights, no video contours are digitized. In the same vein, an unspecified coarse and fine background filter is part of the proprietary circuits, but may remind of the pulse width discriminators as from our Mark I prototypes. No more information is given in company literature such as (Greaves 1986). However, (Walton 1986) has a clear account of accuracy and precision assessment and results.

These results, though, are less than impressive, averaging some 1:3000 for precision with 60 Hz commercial RS-170 CCTV cameras, and just some 1:1000 for the playback from VCR tape of 200 Hz NAC camera recordings. Accuracy has been shown to exceed 1:1500.

We note here, with reference also to VICON, that in our PRIMAS and earlier systems we have always refrained from digitizing marker coordinates taken from recorded video, comparatively easy as that would be in providing playback from high-speed facilities. Abandoning the close synchronization, down to the pixelclock level, by severing the tight coupling of camera and system, was contrary to our main engagement in low noise or jitter and high resolution performance.
Again, as a commercial system, and hooked up to a powerful Sun Microsystems SPARC computer, ExpertVision boasts simplicity of operation and extensive software packages. Latest software option is Orthotrak, a full-body gait analysis package, which was developed in cooperation with the Cleveland Clinic Foundation and the Human Motion Laboratory, University of Florida, USA.

The Japanese tele-visual motion analysis systems **SIGHT 2D/3D**, marketed by Sakai Inc. Tokyo, look too uncomfortably like copies on the basis of earlier systems and older literature (with a sample output graph of prehistoric noisiness) that no more attention is deserved in a review of scientifically-based worldwide efforts at further development.

Certainly worth of mention is the **Kodak EKTAPRO 1000** high-speed motion analysis system, outlined in fig. 4.23. Though not a real-time coordinate digitizing system, this is a medium which may have a role to play as an off-line sensor / on-line tape device, when really high speeds of 1 kframes/s are at a premium.

EKTAPRO is a parallel recording system of 16 parallel strip images subdividing the normal frame height. It derives from the 2 kfields/s SP2000 system from Spin Physics (an Eastman Technology Inc. company), which boasts a 16-track microgap videorecorder, in conjunction with a 16-output CCD sensor developed by Eastman Kodak. This dedicated CCD camera provides 16 parallel outputs from 16 sections of 12 lines * 240 pixels. Each of these strip images is produced at 16 times the normal 60 Hz rate, totalling 1000 fps. But for any strip image the pixel rate is below 3 MHz, or clearly within the limits of standard technology.

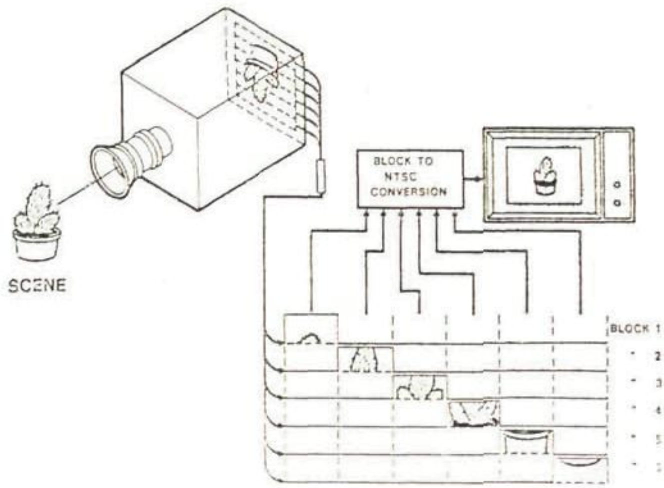

Fig. 4.22. Outline of Ektapro 1000 high-speed camerasystem. (courtesy *Hyzer 1981*).

Presently, EKTAPRO offers a manual crosswire digitizer and other more automated analytical options in the videorecorder replay mode.
But the quantum leap in attainable speed, though at the sacrifice of basic resolution being no more than 192*240, is a challenge to go for real-time hook-up of the EKTAPRO camera to an extended PRIMAS system.

The **HENTSCHEL** on-line high speed high accuracy random access tracking system (Zamzow 1988) [10] is a recent addition to the motion analysis toolshop. The basic idea is less recent, being clearly reminiscent of the 1981 system by Mesqui, discussed in section 3.4. That system used a computer controlled EMR/Schlumberger optical data digitizer, which had an EMR image dissector. The commercial Hentschel system features Hamamatsu's C1181 random access camera, cf. note 3.4, and a dedicated interface to effect the local marker search and tracking algorithms, determine marker centroid coordinates, and pass them to the host PC.

The image dissector tube being a non-storing device, it has the advantage that there is no need of a total scan of the target surface. With vidicon/plumbicon camera tubes this is a necessity, to prevent charge build-up from ambient illumination, the reason why selective tracking, as mentioned in section 2.2, was discontinued in our developments.

note
10 *Trademark of Hentschel System GmbH, Hannover FRG.*

The disadvantage of a non-storing imaging device is, that stroboscopic illumination of reflective markers is not within the possibilities. This means that this attractive method of enhancing marker contrast, especially with some form of shuttered camera, is unavailable.

Moreover it implies that although this is a TV-based method, marker sampling is inherently not simultaneous. Consequences have been discussed in section 3.5, for systems having a comparable sample rate.

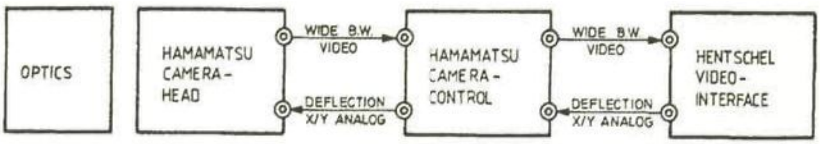

Fig. 4.23 a. Block diagram of HENTSCHEL video marker tracking system. *(trade literature).*

System configuration is shown in <u>figs. 4.23 a,b</u>, where the differences with systems using standard TV sensors are apparent. System operation is in two distinct phases.

First phase is marker search and set-up, where the scan pattern is the usual line and pixel sequence across the total target area or FOV, and where up to 100 markers (and any other above-threshold luminosities) are stored in tracker memory. In this phase the assignment of a marker number can be automatic, as encountered, or adjusted by the operator (who probably may intervene to discard unwanted objects [11]).

The tracking phase is the actual data acquisition mode, and this may proceed at high rates, as around each of the stored marker positions only a small area is scanned. The local scanning area is preset to cover between 1 % and 5 % of the imager's FOV dimensions. Local scan control is by 8+8 bit X and Y, out of a total of 13+13 bit controlling the scan beam position in total FOV, equivalent to 8192*8192 pixels. Evidently, the small area of local scanning, multiplied by the number of markers or scan zones, is a fraction of the total image FOV area and it is this feature which determines the high rate of marker data acquisition.

note
11 *for as long as these remain isolated and not accidentally covered in subseqent fine scan tracking frames.*

HENTSCHEL system sampling rate for one marker is at 15 kHz maximum. Even at the stated average 100 KHz pixel scan rate (Hamamatsu camera access time for any one pixel being below 15 μs), this implies just some 6 pixels scanned per field, in this single marker 1 % local mode. Anyhow, this 15 kHz sampling rate outdoes SELSPOT by 50 % and ups the current OPTOTRAK rate by a factor 6. For accuracy, HENTSCHEL advocates a 7.5 kHz sampling rate, so markers are sampled at 7.5 kHz/marker. Evidently (like with SELSPOT, OPTOTRAK etc.) system sampling frequency derates linearly with the number of markers.

Moreover, with the HENTSCHEL system sampling frequency would appear to derate quadratically with the increase of local scan area dimension, from 1 % to the maximum of 5 % of FOV (unless pixels will be skipped). One should consider that a compromise is necessary, where for the case of markers moving at high speed the local scan area should be maximum, at penalty of losing track, while an increased scan size contradicts the sampling rate requirement.

System description has the previous marker position, not a prediction for next frame's marker position, as the means for centering the local scan. So next frame's marker should be within 0.5 % to 2.5 % of its previous position.
Assuming sinusoidal motion with an 0.8 FOV amplitude and frequency f_0, this means that the sampling rate f_s should be $f_s = 1000\ f_0$ to $200\ f_0$, respectively. This may explain why examples in (Zamzow 1988) feature only small-amplitude motion at the indeed elevated $f_0 = 500$ Hz.

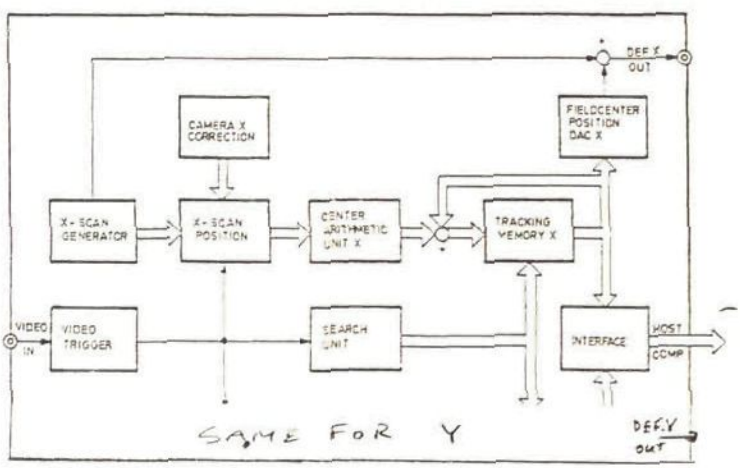

Fig. 4.23 b. Block diagram of marker-tracking HENTSCHEL interface.

Also, the system can evidently not support any loss of a moving marker due to temporary obscuring by intervening parts of subject. Except perhaps, though this is not mentioned, by setting up (time permitting) *a coarse local search centered at the latest marker position.*

The Hamamatsu random-access camera is an analog-deflection device, basic distorsion is only better than ± 2 %. However, camera stability and repeatability figures are better at ± 0.1 % and ± 0.05 %, respectively. Even if calibrated, as shown in fig. 4.23 b, accuracy can be no better than that, in line with the HENTSCHEL specification of a better accuracy than 1:1000 FOV, and 1:2000 at a reduced 7.5 kHz sample rate.

With these already modest figures, with respect e.g. to OPTOTRAK, no resolution or precision is specified for this interestingly conceived, but expensive system around the equally costly random-access cameras.

Applicability of this system, outside of some small-amplitude, high-frequency niches, remains to be seen.

4.9 Sampling rate and precision in noisy sampled-data systems

In biomechanics applications, for which the clear majority of systems described in this thesis were originally designed, the **sampling rate** requirements are subject of debate, if not a bone of contention. But the sampling rate rat race is not limited to optoelectronic systems, rather, it has carried over from the cine film era. With cine, the development track has been from the 20 fps Marey chronophotographic box to commercial high-speed cameras of say 500 fps, the ultra-high-speed machines not having proliferated in biomechanics as in some industrial areas. Incidentally, the Marey camera (1888), which allowed acquisition and storage of a sizeable number of consecutive picture frames, must be considered science's first sampled-data system.

For this and all ensuing cine and electron-optical sampling systems, the Whittaker-Shannon theorem obtains. Many authors have been engaged in assessing the frequency content of the movement phenomenon under study with respect to the Nyquist frequency of their instrument. This is a point of great interest, as in cine and electron-optics there is no option of designing an anti-aliasing filter between scene or lens and the sampling sensor device. Such an unimaginable filter should have a low-pass transfer characteristic with respect to the frequency of projected motion [12].

Among the authoritative investigators, Winter (cf. section 3.3) has contributed to assessing the **frequency content of gait**, one of those quasi periodic movements, which proved most rewarding to decades of biomechanical recording and analysis. In (Winter et al. 1974), using a 60 fps CINTEL TV system, with the Y-coordinate of the toe marker, the normalized amplitude spectrum at harmonics of the step frequency rolls off to "a fairly constant low level above the 7th harmonic". It was calculated that 99,7 % of the power was contained in the harmonics up to this frequency. The noise level, ascertained in the stance phase, was of approximately the same magnitude as the data spectrum above the 7th harmonic. We note though, that the 7th harmonic amplitude level is still shown at some 10 % and the 1 % level is only reached at the 13th harmonic of the step frequency.

note

12 *An unintentional and badly controlled low-pass effect is to be found with the undesirable lag phenomenon in cameratubes.*

These findings led the Winter group to use digital data filtering, zero-phase and with cut-off at 4.8 Hz, standardly in subsequent work.

In (Winter 1982) the case for a sampling rate of 4 to 5 times the highest frequency "present in the movement" was argued, and referring to the above-mentioned results, sampling rates of no more than 24 or 30 fps for cine or TV, respectively, were deemed sufficient. In what was claimed as "additional conclusive analytical evidence", that these standard cine film frame rates are "adequate for the assessment of normal and pathological gait", the results were compared of recordings with a 25 and a 50 fps sampling rate. The lower sampling rate records were extracted by using alternate samples from the 50 fps record.
Finding no differences, even in the second derivatives (rightly deemed sensitive to the higher frequencies) was to clinch the decision.

However, the flaw in the propounded evidence must be obvious from the account of the experiment: after the sampling, the displacement coordinates were subjected to the 5 Hz cut-off low-pass filter which had become standard practice in the Waterloo group. By consequence, in the 25 fps sampling rate experiment, any frequency components between 12.5 and 20 Hz were aliased into the filter cut-off band. Their presence in the original movement signal cannot have been disproved. In the 50 fps sampling case, the same frequencies, if present in the signal, were straightforwardly filtered out and no comparison of the 25 and 50 fps results could yield the claimed evidence (Furnée 1986e, 1988d).

Biomechanics was well served, that this strongly worded advice from the respected investigator, against the use of higher-speed and more costly equipment has not deterred manufacturers and system developers in providing sampling rates upwards from 100 Hz.

Cases in point are sinusoidal oscillations at 16.7 or 22.2 Hz in knee varus/valgus instability with ligamentous injury or spastic diplesia, respectively, observed by (Baumann et al. 1983) in frontal cine film recordings at 100 fps, reported at Waterloo (ISB) of all places.
A much more marked and clearcut phenomenon (being proportional to the second derivative of position) concerned the vertical force peak at heelstrike, presented in (Antonsson et al. 1985). Recorded at 2 kHz force-plates and well below the resonant frequency, a near 60 Hz triphasic component stands out in the 0.8 s stance record of fig. 4.24 a.

If undersampled, this peak was bound to have been missed and to have contributed to aliasing error. But an intriguing observation is, that judging by the power spectrum of fig. 4.24 b, a low sampling rate of, say 50 Hz, would not have been unreasonable. The composite power spectrum of 30 stance phase force records has 99 % contained below 15 Hz. The composite amplitude spectrum only shows a minor ripple near 50 Hz, superimposed on the 1.5 % to 0.5 % trend between 50 and 100 Hz.

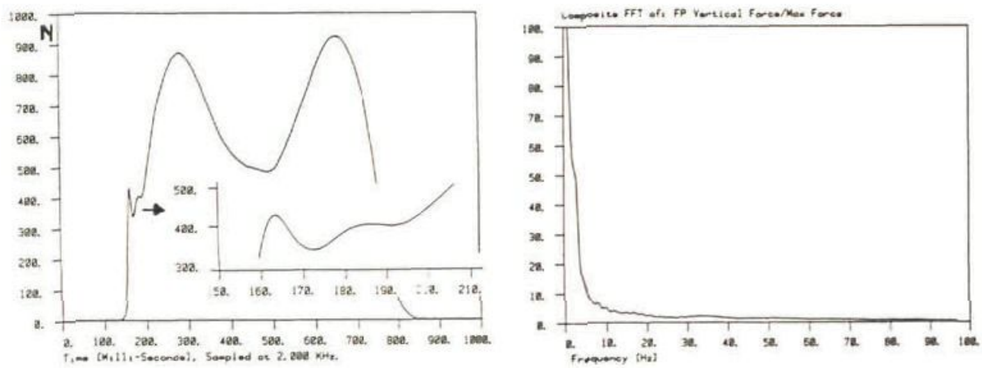

Fig. 4.24 a. Vertical force gait pattern b. Power spectrum of same
(*courtesy Antonsson & Mann loc.cit.*)

This boils down to the argument, which relative power spectrum levels constitute near enough zero to minimise aliasing error when one is, in the strict sense, violating the sampling theorem?
Even when there is no more than a rule of thumb, as cited above, the pitfall in (Winter 1982) must be avoided that a lower sampling rate will do, if one is not setting out "to capture the higher frequencies associated with jerky pathological movement". Interested or not, in the presence of high-frequency movements, even if due to marker shift, one is obliged to take these into account for fear of aliasing errors.

Now if there is no hard and fast rule covering the gamut of movement phenomena that are not strictly bandlimited, cf. (Slepian 1976), we will not pursue the matter further from this viewpoint, and now focus on other instrumentation criteria.
In the arena of movement recording equipment a figure of merit has emerged, which relates the **sampling rate** to **system noise performance**.
This is of particular significance in those common applications, where the interest of analysis resides with the **estimates of derivatives**, e.g. in considering accelerations to estimate unaccessible torques.

An early account of the increase of the noise power by differentiation of a signal contaminated by additive white noise, with power spectral density K, was given by (Andrews et al. 1976), who have

output noise power $= K\ \omega_b^{2k+1}/(2k+1)$ (4.4)

for k=0,1,2,... where k is the order of the derivative, and ω_b is the measurement system cut-off frequency.

A more elaborate discussion is found in (Gustafsson & Lanshammar 1977) where it is proven that

$$\sigma_k^2 \geq \sigma_{k,min}^2 = \sigma^2\ (2/\omega_s)\ \omega_0^{2k+1}/(2k+1) \qquad (4.5a)$$

where ω_s is the system sampling frequency, σ^2 the variance of the additive white noise, the input signal being strictly bandlimited, with a cut-off frequency $\omega_0 \leq \frac{1}{2}\ \omega_s$.

In (4.5a), σ_k^2 is the variance of the estimate of the derivative of the k-th order and $\sigma_{k,min}^2$ is the minimal value of this variance.
The equation holds for any undistorted linear estimate of the k-th order derivative. The transfer function H(z) of the k-th derivative estimator then has to obey $|H(\exp j\omega)| = \omega^{2k}$ for $0 \leq \omega \leq \omega_0$.

The equality $\sigma_k^2 = \sigma_{k,min}^2$ holds only for the additional assumption that
$|H(\exp j\omega)| = 0$ for $\omega_0 \leq \omega \leq \frac{1}{2}\ \omega_s$ (4.5b)
This represents the "boxcar" or "brickwall" differentiator, adapted to the bandwidth limit of the input signal.

One of the consequences of (4.5a) is that noise variance may already be reduced for the non-differentiated case by increasing the sampling rate $\omega_s >> 2\omega_0$, while obeying (4.5b).
Obviously, for the Nyquist frequency $\frac{1}{2}\ \omega_s = \omega_0$, equation (4.5a) degenerates to $\sigma_k^2 = \sigma_{k,min}^2 = \sigma^2$ in the non-differentiated case.

Also in the case k≠0, for the k-th derivative estimation, oversampling is seen to be beneficial for counteracting the amplification of noise.

Already (loc.cit.) introduced a **figure of merit** for the noisy sampled-data system, which they coined the information retrieval capacity IRC, defined by

$$IRC \equiv 1\ /\ \sigma^2 T \qquad (T = 2\pi/\omega_s = 1/f_s) \qquad (4.6a)$$

So that in $\sigma^2_{k,min} = (1/IRC)\ \omega_0^{2k+1}/\pi(2k+1)$ (4.6b)

the system performance indicator is separated from the signal and differentiation process variables.

In (Lanshammar 1982) equation (4.5a) was repeated with some of its consequences.

In (Woltring 1984) the factor $\sigma \surd(T/\pi) = 1 / \surd(\pi.IRC)$ was introduced as a figure of merit for spatio-temporal resolution. This yielded an expression similar to (4.6b).

In (Furnée 1988d) is was seen fit to adapt the figure of merit to a relative one. This used the precision p, defined by noise standard deviation divided by the measurement range r of the position variable (in practice, the precision p is 1, divided by a large number).
The **relative spatio-temporal resolution quality factor** Q is defined by

$$Q = (\surd f_s) / p \qquad (4.7a)$$

where f_s is the sampling rate and p the system precision.

Now in terms of precision, (4.5a) becomes

$$p_k^2 \ge p^2_{k,min} = (1/Q^2)\ \omega_0^{2k+1} / \pi(2k+1) \qquad (4.7b)$$

Obviously, high values of Q are desirable to minimize relative output noise variance in k-th order derivatives, k=0,1,2... of strictly bandlimited signals.
These high values of Q are attained by high sampling rate and high 1/p figures, equivalent to low relative system noise.

It should be noted from (4.7a), that system noise abatement is quadratically more effective than raising the sampling rate.

Aided by this spatio-temporal resolution quality factor Q, we will in the next section assess the PRIMAS system performance. This will be put in perspective with some contemporary commercial systems.

4.10 Performance, systems comparison

Some indications as to performance of the earlier PRIMAS systems have been given in sections 4.2, and 4.7, pertaining to the marker centroid processing speed and in section 4.4, with respect to the ambient light tolerance of the strobed 100 Hz cameras.

The **processing speed** story, which determines how many markers can be handled at the 100 Hz camera rate, is best told by fig. 4.25 taken from (Demper 1987).

This shows processing time in ms vs. number of markers. Increments are by a horizontal row of four markers. Marker size averaged 9 TV lines. Processing time was shown to be proportional to marker size.
Centroid processing time is mostly spent in clustering, cf. fig. 4.7.
Full curves join the measurements for the following implementations:

hatched	8 MHz 68000		section 4.2 system
open	16.6 MHz 68020,	cache disabled	section 4.5 system
full	same	cache enabled	" "

Single symbols represent processing time for a pattern of 35 markers, same 9 TV lines size in "tilted, portrait and landscape" orientations. The landscape pattern, 7 markers in a row, takes most processing time.

Open symbols represent the non-cached, closed symbols the cache case. For the landscape (slowest) configuration the fastest (cached) processing was at 7.7 ms.

With the simplified hardware and streamlined firmware of section 4.7, the comparable time, as inferred from measurement, has come down to 6.3 ms. Measured time for 35 markers, sized 14 lines, was at 9.8 ms. Equivalently, 50 markers, sized 10 TV lines, can be handled in 10 ms, or at 100 Hz camera rates.

The prognosis with the 25 MHz Motorola 68030 board is an improvement by a factor 2.25 [13], so some 100 markers of 11 TV lines may be accommodated, or 50 for a dual-camera, single CPU option, cf. fig. 4.19.

note

13 *Breakdown is a 1.5* higher clockrate and an estimated 1.5* higher throughput with respect to the 68020, which is conservative as to Motorola trade literature.*

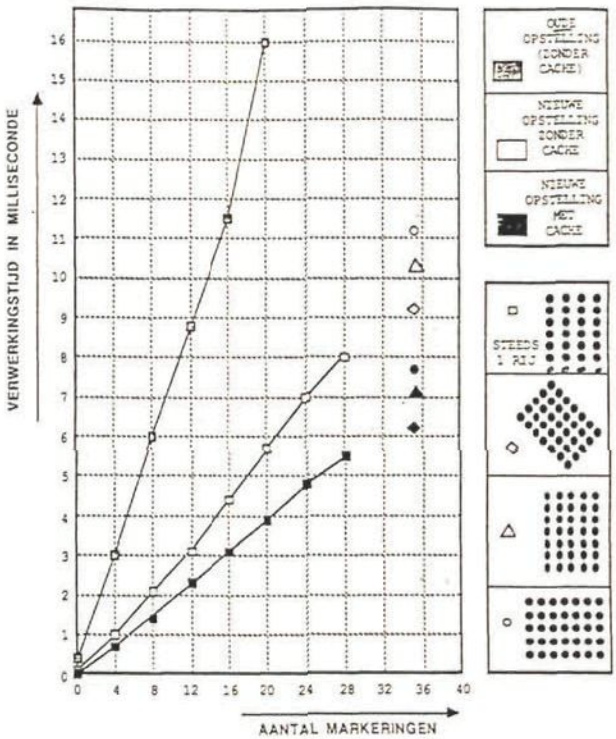

Fig. 4.25. Centroid processing speeds vs. number of markers, cf. text

Meanwhile, concerning processing speed or marker handling performance, preliminary experiments were performed with simulated raw marker data X_2, dX and Y (cf. section 4.7 on the simplified converter hardware) presented to a transputer system [14]. The Occam program by Schilt (1989) implemented the CLUST routine reviewed in section 4.2.

Surprisingly, the single transputer, though running at a 20 % higher clockrate, took 15.6 ms for a simulated 35 markers, 15 TV lines landscape configuration. So it proved to usurp 50 % more time than the cached Motorola 68020 microprocessor.
However, a parallel program using two transputers was shown to effectively halve the CLUST processing time as expected, not counting some set-up overhead. Comparable speeds as expected with the Motorola 68030 appear, nevertheless, to demand a foursome transputer board.

note
14 *The MTM-2 dual 20 MHz Inmos T-800 transputer board from Parsytek GmbH, Aachen, FRG, hosted by an IBM-AT compatible PC.*

By the way, the CLUST-type routine proved easily amenable to any degree of parallelism. The raw data may be partitioned as it comes in an ascending order of Y-values, cf. section 2.8. Subsets of raw data may be clustered to obtain marker vectors, cf. once more section 4.2. The problem of joining any marker projections across subset boundaries can be solved in a straightforward way, by reconsidering the mechanism of opening and closing the pertaining marker vectors.
The parallel approach is being considered for interfacing the Ektapro camera, section 4.8, as a proper extension to PRIMAS system concepts.

The **resolution** is a sometimes misleading term, if in a measurement system with binary coded output it is only used to specify the number of bits provided, without the additional assurance that these are meaningful to the least significant bit.
Resolution, though the word is not included in the BSI English translation PD 6461 of the OIML fundamental terms document (Sydenham 1982), is taken to mean **discrimination**, being the descriptor of "the quality which characterises the ability of the measuring instrument to react to small changes of the quantity measured".

It has become clear in preceding chapters, that PRIMAS hardware offers a 15+15 bit output for the projected marker X,Y centroid coordinates, and that centroid estimation (in software with other TV based systems) *achieves a sub-pixel "resolution" compared to the basic sensor layout.*

Resolution, in the sense of discrimination of marker position changes, has been tested with markers attached to the bed of a Swiss Micron WF-21 numerically controlled milling machine.
Marker size was 14 TV lines, and the prototype camera of section 4.4 was used.
Horizontal marker position was incremented in 20 steps of 0.5 mm, centrally in the 700 mm FOV. In each position the mean value was taken of 500 consecutive samples, as shown in fig. 4.26. Standard deviation within each position was, averaged over all positions just 0.0348 mm (or 1:20100 of FOV).
Fig. 4.26 also shows the least-squares linear fit, with manifest small deviations of the mean positions from the regression line.
As an expression of the just noticeable difference or discrimination or positional resolution of the system, the root-mean-square value of these least-square residuals equalled 0.1142 mm or 1:6100 FOV.

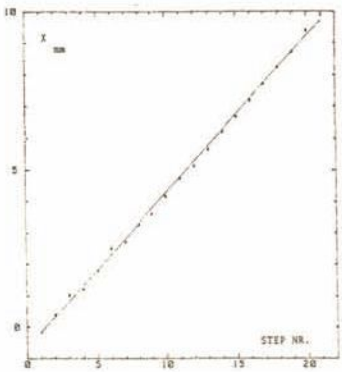

Fig. 4.26. PRIMAS incremental marker displacement test results.

As to the dependence of positional discrimination upon marker size, a not unexpected phenomenon with a binary image encoded on a quantized pixel grid, an early simulation series by Demper (1985b) yielded first incomplete results. The routine displaced a circular marker, in a size range of 4 to 14 TV-lines, over a fine test grid across one elementary pixel, and the simulated input centre coordinates were compared to the estimated centroids. Average error was near to nil, root-mean-square error ranged between 0.02 and 0.08 pixel dimensions.
Translated to the 288*604 Philips frame transfer sensor (cf. sections 4.4, 4.6), worst and best case discriminations would range from 1:3600 to 1:30000.
This subject, as meaningful for PRIMAS as for any competitive TV based system (where marker centroids are estimated in software) warrants an in-depth investigation and experimental validation.

Assuming a uniform distribution in the continuum of (moving) marker positions (not necessarily across the FOV but over successive pixels), it is textbook material, that resolution in the sense of the relative discrimination step δ entails a relative quantization noise component or precision of

$$p_q = \delta / \sqrt{12}.$$

The contributions to imprecision by the positional grid quantization would with the above figures roughly range from 1:12000 to 1:100000, which compare well enough with the the PRIMAS precision obtained with stationary markers.

The **precision** of the system, equivalent to the term repeatability used in the OIML [15] document (Sydenham 1982), may once more be circumscribed as the degree of mutual agreement among repeated observations made under identical conditions. It is a measure of random error, whereas the accuracy is a measure of systematic error. Precision is expressed as the standard deviation of the system's measurement noise divided by the range. In a position sensing system both accuracy and precision are estimated by using stationary markers. The measurement range is taken as the relevant transverse field of view dimension.

The **accuracy**, being expressed (cf. Walton 1986) as the r.m.s.deviation of the average measured coordinates from the true coordinates across a test marker distribution, divided by the measurement range, has been less of a concern with CCD-sensor based TV-systems. As the optics, and the lens alignment with respect to the sensor image plane, are the only significant sources of non-linear distorsion, the appropriate calibration for lens correction potentially increases the accuracy much beyond the basic value.

As a corollary to a 3-D PRIMAS application by Sabel (1989), relative accuracy, being concerned with the rendering of inter-marker distances was found to be some 1:2000, without lens correction.

More attention was devoted to specifying the **precision**. This involved a series of 2-D measurements, using stationary distributions of 20 markers, runs of on the average 260 observations, at a selection of marker image sizes of 12 to 4 TV-lines.
The 12 to 7 TV-line sizes were obtained by viewing the same pattern of 4*5 markers at the appropriate distances, the larger sized pattern covering the FOV. The 20 markers sized 4 TV-lines were smaller ones, on a diagonal across the FOV. Results, expressed in noise s.d., are represented in table 4.3 as averages over the 20 marker distribution.

marker size	(TV-lines)	12	12	8	8	7	4	4	Avg.
σ_X	(units)	1.3	1.3	2.6	1.6	2.1	1.0	1.4	1.61
σ_Y	(units)	1.6	1.4	2.6	1.4	5.4	.9	2.0	2.17

Table 4.3. PRIMAS noise s.d. with stationary markers, cf. text.

note
15 *OIML for Organisation Internationale de Métrologie Légale.*

The measurement range in X,Y being 29500, 29300 units across the FOV, the average precision amounts to $p_X \approx 1{:}18000$, $p_Y \approx 1{:}13500$.

The ratio of X and Y precisions tallies well with the 4:3 aspect ratio of the standard TV image. Though it may be fortuitous (cf. the less good σ_Y result with the 7 TV-line marker run) it is suggestive of an imaginary subpixel confidence unit of square dimensions.

The observed spread in the noise s.d. results for individual markers, within the test series of table 4.3, may be expressed as the r.m.s. differences of individual marker standard deviations with the average of the 20 marker pattern.
Averaged over all runs, all marker sizes, the r.m.s. spread amounted to 0.96 units in σ_X and to 2.46 in σ_Y.
The distribution of individual marker s.d.'s was asymmetric.
Zero s.d. or infinite precision was observed in 11 % for the X and in 14 % for the Y coordinates.
It would appear that, contrary to the resolution, the precision does not depend on marker size.

Similar precision as the figures from this experiment was manifest with the resolution experiment, quoted above.

The remarkable precision figures of the PRIMAS system are partly due to the absolute coupling, down to pixelclock level, of the coordinate converter hardware, first to the proprietary camera of section 4.4 and presently to the HTH camera (Furnée 1986e, 1988c). For the other part, these figures reflect the low-noise, no-glitch properties of the HTH quality camera video stage, cf. section 4.6 and section 4.4 note 3.

The pulse width discriminator which, cf. section 4.2, only accepts image segments above an adjustable pixel width and thus is liable to reject the upper or/and lower chords of the circular markers, accounts specifically for some of the Y standard deviation. This leaves room for improving the Y precision to the X precision level.
Clamping the camera blacklevel to the threshold voltage of the video comparator has the potential for still further improvement.

PRIMAS' high precision and the, for TV-based systems, relatively high sampling rate make for an exceptional spatio-temporal resolution, the Q factor as defined in the previous section, equation (4.7a).

Table 4.4 puts this in perspective with current commercial systems, where we have used company literature and system specifications. Where no precision was specified, the resolution figure, and otherwise, the accuracy was used instead.

system	sampling rate (Hz)	bits	resolution	precision p	remarks	spatio-temp. resolution quality Q
PRIMAS	100	15	1:6000	1:18000	X	180 000
				1:13500	Y	135 000
VICON	50		1:1000 X	1: 1000	3-D precis.	7 000
	200		same?	same?	NAC camera	14 000
ELITE	100	16	1:2800 3-D acc.	better	(unspecified)	28 000
ExpVision	60		1:3000	same?	2-D	23 000
	200		1:1000	same?	NAC, taped	14 000
CODA-3	300	14	1:6000 max.	same?	X,Y only	104 000 [16]
			1:1000 max.	same?	Z	17 000
SELSPOT	500	12	1:4000	same?	20 markers	89 000 [17]
	1250				8 markers	200 000
OPTOTRAK	125		1:10000 2-D acc.	same?	20 markers	112 000 [18]
	313				8 markers	176 000
HENTSCHEL	375	16	1:2000 2-D acc.	same?	20 markers	39 000 [19]
	938				8 markers	61 000

Table 4.4. Spatio-temporal resolution performance of current systems, cf. footnotes and text (for VICON, ELITE, ExpertVision and HENTSCHEL section 4.8).

note

16 *non-equidistant, non-simultaneous marker sampling, cf. sect. 3-6.*

17 *non-simultaneous marker sampling, 10 kHz/marker, cf. sect. 3-5.*

17 *non-simultaneous sampling, 2.5 kHz/marker, only accuracy specs., cf. section 3.7.*

19 *non-simultaneous sampling, 7.5 kHz/marker, 2-D accuracy specs.*

4.11 Conclusion

This chapter has described the continuation of developments, as from the prototype TV-based coordinate converter systems reviewed in chapter 2, towards the present PRIMAS TV/computer motion analysis system. This features high resolution, high marker contrast and high speed.

Little further attention has been devoted to describing the analytical software part, or the 3-D camera calibration and 3-D reconstruction. The latter involves either the 3-D marker coordinates or the location and attitude of multi-marker clusters, characterizing solid objects or articulating segments.
Rather than actively contributing to this field (which has moreover much in common for all categories of motion analysis systems and has evolved from cinephotogrammetry) our students' efforts have been mainly at implementing existing theory into software, for some of the applications to be reviewed in chapter 6.
However, to match the present level of system precision with the utmost in 3-D calibration and accuracy, the closer interaction with the Photogrammetry Department, Faculty of Geodesy offers rewarding prospects. Also the exploitation of more of Woltring's recent work (1989) would appear beneficial to the PRIMAS and SPIN projects.

To summarize some main features of the present system, the subpixel resolution with respect to the basic sensor definition was obtained by estimating the geometric centroids of each of the marker images. As before, the marker projections covered several TV-lines, but the contour suppressor of section 2.4 was eliminated. Instead, a real-time microprocessor-based subsystem was incorporated (Furnée 1984a), to mechanize the same equations as used by (Taylor et al. 1982) in early off-line software. The real-time prototypes used dedicated arithmetic hardware to supplement the Motorola 68000 microprocessorboard. Present simplified systems, using only a faster 68020/30 board, permit single or dual-camera centroid estimation of up to 50 markers at 100 Hz.

Supplementing the estimated marker centroid coordinates, in 15 + 15 bit, the system optionally generates height and width bytes. These may be used in the subsequent marker identification software, to help in resolving pathological cases, such as the loss of separation by the apparent contacting or merging of projected markers.

The data reduction, inherent in the real-time centroid estimation, as it was with our earlier contour suppressors, is beneficial as to the modest transfer speed and storage requirements of the host computer. It obviates the intermediate data buffering to resolve the speed differential, typical of contemporary commercial systems. Also, the data reduction feature allows some 10 to 20 times longer runs of experimental data to be stored to disk before further off-line analysis. As an option, centroid processing may be bypassed for analyzing full contour data in special applications.
Interfacing of PRIMAS systems is to the industry workhorse of IBM-AT and compatibles. Reduction of data to centroid coordinates has allowed a running display of the incoming markers on a quasi-realtime basis. Frames may be skipped, depending on the number of markers, but viewing incoming data is an asset anyhow.

Contrast of the stroboscopically illuminated retro-reflective markers has been greatly enhanced, allowing even outdoor daylight operation, by introducing electronically-shuttered TV-cameras (Furnée 1986).
This effort at the sensor front-end of the measurement chain obviates the dedicated real-time crosscorreleation processing such as in the ELITE system, which has to rely on marker template matching for the separation of markers from ambient light or background clutter.

Reduced-integrationtime or stroboscopic TV cameras have since been adopted in competing commercial systems.
To complement the PRIMAS system, in a cooperative project, funded by the SPIN agency, the High Technology Holland (Eindhoven) company have adapted their MX measurement camera to a reduced-integrationtime MX-E.

Other advantages of the CCD frame-transfer sensor of our prototype camera and the HTH MX camera are, that it proved amenable to raising the image field frequency to 100 Hz, and that it has an inherently stable and highly linearly deposited pixel geometry. Potentially this leads to calibration, mainly for lens distorsion, being a one-time effort with beneficial consequences for a high system accuracy.

Lastly, the CCD-based camera has allowed the absolute coupling of the pixelclock to the coordinate converter hardware. This was not possible with tube cameras or with taped video. The pixelclock is not provided with the RS-170 standard cameras used with most commercial systems.

To a large extent, the synchronization at all clock levels makes for the high repeatability, low noise performance that is (Furnée 1986e) one of the PRIMAS hallmarks.

Though the spatio-temporal resolution is a kind of misnomer (spatial precision rather than resolution is involved), as reviewed in section 4.9, it has in the motion analysis literature become a major indicator of system performance.
It is an apt conclusion of this chapter, having reviewed in section 4.8 some state-of-the-art entries in the field, and discussed PRIMAS speed, resolution and precision performance in section 4.10, to draw up a systems comparison (Furnée 1988c) based on this spatio-temporal figure of merit.

As noted, alternative systems, scoring high only with a limited number of markers, have the drawback of non-simultaneous marker sampling, but their advantage over TV systems is the inherent marker identification. On all other counts, PRIMAS appears the best performer.

As a late addition, we have been making inroads on the real-time identification of the markers by enriching the data acquisition software with an on-the-fly coordinate assignment module. This is only feasible by the preceding data reduction, which is one of the features of the PRIMAS real-time marker centroid estimation.

Some remaining desiderata and future prospects will be addressed in the final chapter 7.

CHAPTER 5. A PSD SYSTEM WITH SYNCHRONOUS DETECTION

5.1 Introduction

In section 3.5 we have discussed the SELSPOT system, which features a Position Sensitive Device (PSD) sensor and the use of active markers, switched in **time-multiplex**. Some attention was devoted to the effects of non-simultaneous or skewed sampling of the individual marker positions. This, if left alone, tends to offset the advantages of a high samplerate for which the SELSPOT system was widely commercialized.

Next to the disadvantages, such as the requisite wiring, of the active markers, we noted one other advantage, in that an active marker system is inherently self-identifying.
This is in contrast to TV-based systems, where marker identification software is needed. We have noted however, that the marker assignment entails no more than rearranging the data in the coordinate array, and that this software does not in any way change the actual data values.

In section 3.5 we also noted the susceptibility of SELSPOT systems to spurious, ambient or scene highlights other than emitted from the LED markers. This is due to the non-addressing PSD sensor performing an intensity-weighted surface integration of all impinging photons.
To combat the ambient or background light, SELSPOT relies on IR LED power, together with optical filters. This solution however tends to aggravate the problem of spurious reflections from the markers.

In order to get the best of both worlds, *and as a sideline activity* from our TV-based passive-marker systems, we embarked upon a different scheme of coding the individual active markers. Rather than the time-multiplexing of SELSPOT LED's, we opted for **frequency-multiplex** for the identification of LED markers. LED emissions, at a same optical wavelength, were intensity modulated at distinct frequencies. The amplitudes of the individual marker signals were retrieved by a periodic synchronous detection system (Furnée 1984b). This had the advantage of simultaneous sampling of marker positions. Other advantages were an improved noise performance and ambient light suppression.

5.2 Periodic synchronous detection in deterministic PSD systems

Synchronous detection is particularly appropriate in those measurement systems where the testsignal $s_{in}(t)$ to the object, which gives rise to the measurement signal s(t) received from the transducer, is generated in the system itself. In this case $s_{in}(t)$ may be used to advantage to form the product $s(t)s_{in}(t)$ as the basis for averaging procedures like integration or summation across the repetitive measurement interval.

By contrast, in communication systems like single-sideband radio, the additional problem is encountered of locking to the carrier frequency.

The **main components** in the block diagram of fig. 5.1 are the central generator G, the individual marker LED's M_i, the PSD sensor S and the synchronous detection processor module P. This consists essentially of multipliers and low pass filters or, with discrete-time systems, of a set of accumulators.
These system parts are described below, together with some theoretical considerations.
The **host computer** carries out the divisions implied by equations (3.2) of section 3.5.

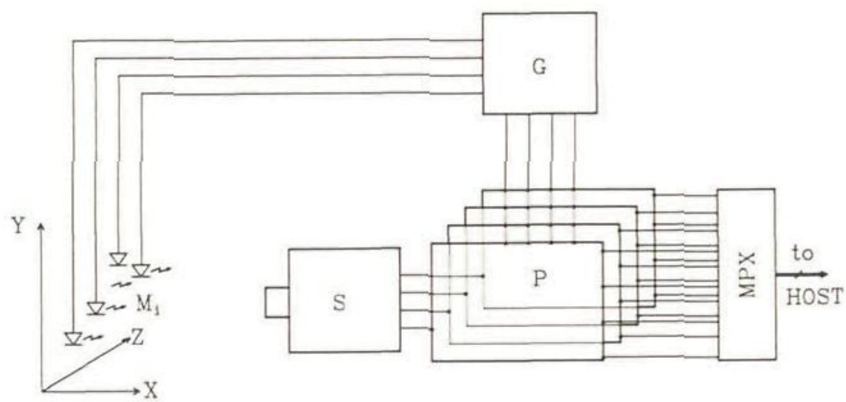

Fig. 5.1. Multi-marker synchronous detection PSD system block diagram.

The **central generator** provides LED signals $s_{LED,\ell}[n] = \cos(2\pi p_\ell n/N-\psi_\ell)$ as well as the quadrature detection signals

$$c_{d\ell}[n] = \cos 2\pi p_\ell n/N \text{ and } q_{d\ell}[n] = \sin 2\pi p_\ell n/N, \quad \ell=1,2,\ldots,L \qquad (5.1a)$$

Within any single measurement cycle we have $n = 0,1,\ldots,N-1$ [1] (5.1b)

The periodic nature of the synchronous detection measurement system is emphasized by writing $n = (0,1,\ldots,N-1) \bmod N$, and where useful, time dependence is explicit by $n = (0,1,\ldots,N) + mN$, $m = 0,1,\ldots$. (5.1c)
For the present discussion we stick to (5.1b).

The **marker arrangement** is that all LED's ℓ are continuously emitting at one certain radiation wavelength, but each at a different intensity

$$s_{in,\ell}[n] = 1/\mu + s_{LED,\ell}[n]$$

Here $\mu<1$ is the intensity modulation depth. The constant term will be dismissed as it does not contribute to $C_{i\ell}$ or $Q_{i\ell}$ results, cf. (5.5a). The case of higher harmonics, multiples of p_ℓ, by nonlinearities in the current-controlled LED emission, will be discussed in section 5.4.

The **PSD sensor** has, cf. section 3.5, four electrodes, $j=1,2,3,4$, each of which delivers an in principle composite signal. Each channel has a bandlimited preamplifier. After sampling, each signal is written as

$$s_j[n] = \epsilon_j[n] + \Sigma_i\, s_{ij}[n], \text{ where } i=1,2,..,L,L+1,\ldots, L' \tag{5.2}$$

Possible indices $i>L$ represent spurious signals at other frequencies than the LED marker signals.
For a, presently, deterministic sensor signal any component may be written as

$$s_{ij}[n] = A_{ij}\cos(2\pi r_i n/N + \phi_{ij}) \tag{5.3a}$$

With reference to equations (3.2), section 3.5, the amplitude values A_{ij} carry the x,y position information of marker i.

note
1 *The link between discrete-time signals and continuous-time signal notation is the sampling interval τ.*
N is the number of samples on the measurement interval.
The synchronous detector measurement frequency is $\omega_0 = 2\pi/N\tau$.
For any frequency ω, p denotes the harmonic index so that $\omega = p\omega_0$
The Whittaker-Shannon theorem requires $|r|$, $|p| \le \text{int}(N-1)/2$.

If, for simplicity's sake, we consider one sensor channel, fixed j, we aim by synchronous detection to retrieve the A_i values from each of the generic signals $s_i[n] = A_i \cos(2\pi r_i n/N + \phi_i)$. (5.3b)

Defined for the general signal s[n], the outputs of the quadrature **synchronous detector** are products summed over the measurement interval

$$C_\ell \equiv \sum_{n=<N>} s[n]\ c_{d\ell}[n] = \sum_{n=<N>} s[n] \cos 2\pi p_\ell n/N$$

$$Q_\ell \equiv - \sum_{n=<N>} s[n]\ q_{d\ell}[n] = - \sum_{n=<N>} s[n] \sin 2\pi p_\ell n/n \quad (5.4a)$$ [2].

With real signals s[n] and for integer $p_\ell = 0,1,\ldots,N-1$, synchronous detection is equivalent to the discrete Fourier transform S[p] in that

$$C_\ell = \mathrm{Re}\ S[p_\ell] \text{ and } Q_\ell = \mathrm{Im}\ S[p_\ell]. \quad (5.4b)$$

However, synchronous detection systems generally are concerned with only a fraction of the N coefficients of the DFT.
As to implementation (section 5.4), a future synchronous detection PSD system could well be equipped with a dedicated FFT chip. Focusing on the present system specifications, the requirement of 4 FFT's of about 1200 points within some 4 ms is well within the state-of-the-art.

Applied to the generic signal $s_i[n]$ of (5.3b), the definitions of $C_{i\ell}$ and $Q_{i\ell}$ in analogy to (5.4) are straightforward.

We recollect, that with integer $p_\ell \neq 0$, specific results are [3]

. $C_{0\ell} = Q_{0\ell} = 0$ for $r_i = 0$, the DC case (5.5a)

. $C_{\ell\ell} = (A_\ell N/2)\cos\phi_\ell$
$Q_{\ell\ell} = (A_\ell N/2)\sin\phi_\ell$) for $r_i = p_\ell$, the coherent case (5.5b)

. $C_{i\ell} = Q_{i\ell} = 0$ for integer $r_i \neq p_\ell$. (5.5c)

note
2 *In this chapter* $\sum_{n=<N>} \alpha(n)$ *denotes* $\sum_{n=0}^{N-1} \alpha(n)$.

3 *The simple proof is by the orthogonality relations.*

The consequence of (5.5a) is the elimination of constant-valued background or ambient light, such as daylight (except for saturation of the sensor). This is a major advantage over SELSPOT systems.

The consequence of (5.5c) is the selectivity of synchronous detection against non-coherent frequency components. This feature, which should lead to individual detection of the distinct markers as well as to the suppression of low-frequency components, like from electric sources of ambient light, must be further explored for non-integer r_i values.

The influence of ambient electric light would be totally suppressed if the mains frequency corresponds to an integer frequency index r_m. However, the low value of the measurement frequency, implied hereby, is unacceptable in the PSD system applications. So, the case of non-integer r is relevant to the suppression of ambient electric light.

Now still considering, from a multifrequency signal $\Sigma_i\ s_i[n]$, a single generic component with index i as in (5.3b), then in the **general case**, for r_i (and p_ℓ) not necessarily integer, one derives from (5.4) [4]

$$C_{i\ell} = \pi A_i [\cos(M\theta_{1i}+\phi_i)\ D_M(\theta_{1i}) + \cos(M\theta_{2i}+\phi_i)\ D_M(\theta_{2i})] \qquad (5.6a)$$

and $$Q_{i\ell} = \pi A_i [\sin(M\theta_{1i}+\phi_i)\ D_M(\theta_{1i}) - \sin(M\theta_{2i}+\phi_i)\ D_M(\theta_{2i})] \qquad (5.6b)$$

with $$M = (N-1)/2 \text{ and } \theta_{1i} = 2\pi(r_i-p_\ell)/N, \quad \theta_{2i} = 2\pi(r_i+p_\ell)/N \qquad (5.6c)$$

This particular set of expressions, exemplified in <u>fig. 5.2</u>, reflects a behaviour that corresponds to the leakage phenomenon in the discrete Fourier transform.

This becomes apparent if, say, $C_{i\ell} = C_i(p_\ell)$ is interpreted as function of integer p_ℓ. It then denotes the set of DFT coefficients (real part) for a cosine signal at a certain choice of the frequency index r_i.

Indeed, compared with the coherent case of integer r_i where a complex exponential $s[n] = \exp j(\phi+2\pi r_i n/N)$ has a nonzero DFT only at $p = r_i$, the same signal at non-integer r_i has a DFT $= 2\pi \exp j(\phi+M\theta_{2i})\ D_M(\theta_{2i})$.

note

4 *one uses the cosine sum* $\sum_{n=\langle N\rangle} \cos(\phi+n\theta) = 2\pi \cos(\phi+M\theta)\ D_M(\theta/2)$ *and its sine equivalent, with the Dirichlet kernel defined by* $2\pi\ D_M(\theta) \equiv (\sin(2M+1)\theta/2\ ) / \sin(\theta/2)$, *and with* $M = (N-1)/2$.

The function $W_{i\ell} = 2\pi \exp(jM\theta)\ D_M(\theta)$ (5.7)

is recognized as a frequency-domain window. By convolution, this window is invoked in case of signals with non-integer r_i.
This is due to rectangular truncating by the N-sample measurement window or equivalently, by the fact that a signal with non-integer r_i does not equal its periodic extension outside the measurement window. The point of reducing leakage by more appropriate windowing in the time domain is taken up in section 5.5.
The convolution window concept is also invoked when considering noise in section 5.3.

On the other hand, and fit to the synchronous detection application, with integer p_ℓ we interpret $C_{i\ell} = C_\ell(r_i)$ as the p_ℓ-th DFT coefficient (real part), viewed as a function of the frequency index r_i of the object cosine signal. This is illustrated in fig. 5.2.

A similar windowing, and indeed leakage, phenomenon is obvious with respect to noninteger values of r_i.

One implication of the leakage is that in the presence of more than one signal, with different frequency indices r_i, their contributions, multiplied by the local $C_{i\ell}$ value, add to the central value considered at $r_i = p_\ell$. This point is taken up with (5.9 et seq.).

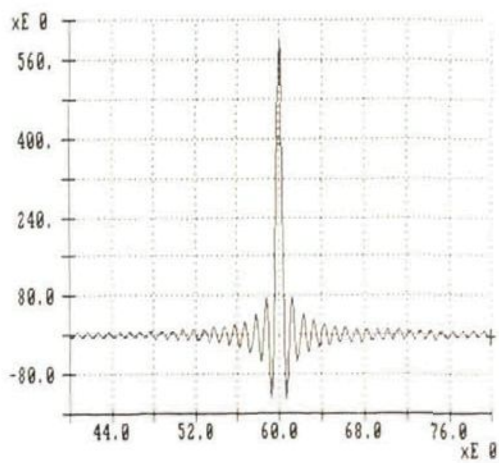

Fig. 5.2. Synchronous detector output $C_\ell(r_i)$, $p_\ell = 60$, $N = 1200$, $\phi_i = 0$

A function, which gets rid of ϕ_ℓ at least at the coherent frequency p_ℓ is

$$S_{i\ell} = (C_{i\ell}^2 + Q_{i\ell}^2)^{\frac{1}{2}} = \tag{5.8a}$$

$$= \pi A_i [D_M^2(\theta_{1i}) + D_M^2(\theta_{2i}) + 2 D_M(\theta_{1i})D_M(\theta_{2i})\cos(4\pi r_i M/N + 2\phi_i)]^{\frac{1}{2}}$$

This results in $S_{\ell\ell} = (A_\ell N/2)$ (5.8b)

With respect to (5.4b) we note that, with integer p_ℓ, $S_{i\ell} = |S_i[p_\ell]|$. Fig. 5.3 illustrates $S_{i\ell} = S_\ell(r_i)$.

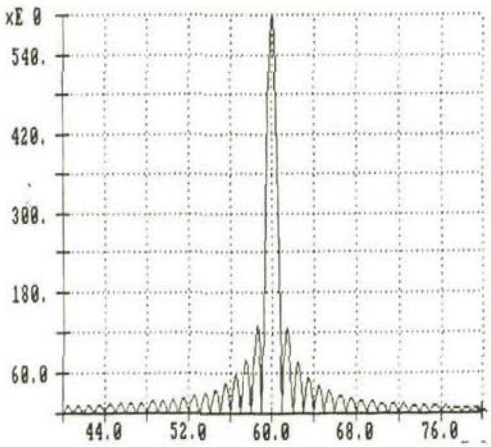

Fig. 5.3. $S_{i\ell}$ as a function of r_i, with $p_\ell = 60$, $N = 1200$ and $\phi = 0$.

To complete this part of the review, we return to the composite or multi-frequency signal $s[n] = \Sigma_i\ s_i[n]$ with $s_i[n]$ as in (5.3b).

Now, for any fixed detection frequency with integer p_ℓ, and among the r_i a certain $r_\ell = p_\ell$, the quadrature synchronous detector outputs are

$$C_\ell = \Sigma_i\ C_{i\ell} = (A_\ell N/2)\cos\phi_\ell + R_{r\neq p} \tag{5.9a}$$

with the rest term, cf. (5.6),

$$R_{r\neq p} = \pi \sum_{i, r_i \neq p_\ell} A_i[\cos(M\theta_{1i}+\phi_i)D_M(\theta_{1i}) + \cos(M\theta_{2i}+\phi_i)D_M(\theta_{2i})] \tag{5.9b}$$

Similarly, $Q_\ell = (A_\ell N/2)\sin\phi_\ell + R'_{r\neq p}$, with (5.9c)

$$R'_{r\neq p} = \pi \sum_{i, r_i \neq p_\ell} A_i [\sin(M\theta_{i1}+\phi_i) D_M(\theta_{i1}) - \sin(M\theta_{2i}+\phi_i) D_M(\theta_{2i})] \quad (5.9d)$$

The rest terms $R_{r\neq p}$ and $R'_{r\neq p}$ are zero (5.5) if all $r_i \neq p_\ell$ are integer.

As already implied by the leakage phenomenon, these equations show the synchronous detector mechanism of scooping up all incoherent frequency terms, and adding these to the single coherent term considered.

In particular, with unknown or uncompensated ϕ, the quadrature outputs may be used to obtain the result

$$S_\ell = ((C_\ell)^2 + (Q_\ell)^2)^{\frac{1}{2}} = ((A_\ell N/2)^2 + R''_{r\neq p})^{\frac{1}{2}} \neq (\Sigma_i S^2_{i\ell})^{\frac{1}{2}} \quad (5.10a)$$

where the rest term

$$R''_{r\neq p} = (R_{r\neq p})^2 + (R'_{r\neq p})^2 + A_\ell N (R_{r\neq p}\cos\phi_\ell - R'_{r\neq p}\sin\phi_\ell) \quad (5.10b)$$

is not easily managed, but is zero if only integer $r_i \neq p_\ell$ are involved.

Our prototype systems did not use quadrature detection for getting rid of the **phases** ϕ, so the detector signals $q_{d\ell}[n]$ were not implemented.

Instead, by choosing appropriate values of ψ_ℓ in the LED-signals from the EPROM-based generator (cf. 5.1), we matched the measured values of the sensor and amplifier phase shifts Φ_{ij} for the points $r_i = p_\ell$.

So by a fair approximation we had $\phi_{\ell j} = \Phi_{\ell j} - \psi_\ell \approx 0$.

Now with the quad-output PSD system, the fact should be appreciated that (using an adapted notation) already the equations (3.2), (3.3) and (5.5b) result in getting rid of nonzero $\phi_{\ell j}$'s, under the condition

$\phi_{\ell 1} = \phi_{\ell 2}$, $\phi_{\ell 3} = \phi_{\ell 4}$. In that case, one has

$$x_\ell/L = C_{\ell 2} / (C_{\ell 1} + C_{\ell 2}) = A_{\ell 2} / (A_{\ell 1} + A_{\ell 2}), \quad (5.11a)$$

and similarly $y_\ell/L = A_{\ell 4} / (A_{\ell 3} + A_{\ell 4})$ (5.11b)

So, if there is pairwise interchannel matching of the phaseshifts Φ_ℓ, there even is no need to correct these with LED phases ψ_ℓ.

But, considering (5.9) this expedient is inaccurate in the presence of contaminating signal components with noninteger frequency indices r_i.

A first case in point is the 50 (or 60) Hz **mains frequency** and its harmonics, unavoidable in electric ambient or background lighting. Anticipating the review of hardware implementations in section 5.4, a few practical values may serve to illustrate the point.

The samplefrequency $f_s = 288$ kHz, the measurement interval is $N = 1200$ samples, so the measurement rate is 240 Hz. A certain marker frequency is 14.4 kHz, $p_\ell = 60$. The mains frequency first harmonic is at 100 Hz, $r_0 = 0.42$.
This means that $\theta_{10} \approx -59.6\ \Delta$, $\theta_{20} \approx 60.4\ \Delta$, where $\Delta = 2\pi/N$ is the *distance between zeroes of the Dirichlet kernels in (5.6, 5.9).*
Thus, spurious contributions from the 100 Hz electric light harmonic are out near the 60th sidelobes of the two $D_M(\theta)$ kernels. Approximated by the $1/\sin(\theta/2)$ or $2/\theta$ envelope (-6dB power/octave), these are down to some $1/30\pi \approx 1$ % (-40dB power) of the mainlobe maximum N/2.
The exact attenuation value depends upon r_i and ϕ_i.

Fig. 5.4 shows the behaviour of $S_{i\ell}(r_i)$ for the small r_i which we have just considered. For reference, the peak value $S_{i\ell}(p_\ell) = N/2 = 600$.

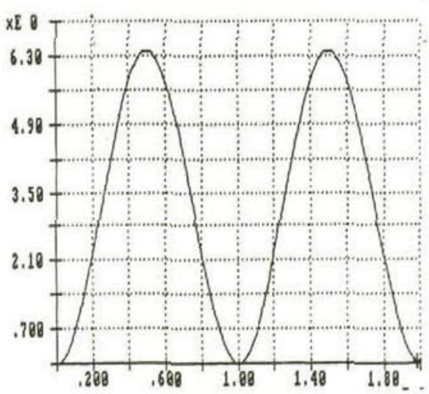

Fig. 5.4. $S_{i\ell}(r_i)$ for small r_i, with $p_\ell = 60$, $N = 1200$ and $\phi = 0$.

A more impressive suppression of contaminating components is obtained by adding some form of tapered windowing, as suggested in section 5.5.

5.3 Sensor noise and discrete-spectrum synchronous detection

The limitations to the attainable accuracy in the extraction of A_ℓ, in the case of discrete contaminating frequencies, have a counterpart in the results in the presence of sensor noise.

The problem can be reformulated, for fixed j, by writing (5.2, 5.3) as

$$s[n] = \epsilon[n] + \Sigma_{i=1}^{L}(a_i \cos 2\pi r_i n/N + b_i \sin 2\pi r_i n/N) \tag{5.12}$$

Here $\{\epsilon[n]\}$ is a random process with $E(\epsilon[n]) = 0$ and $E(\epsilon^2[n]) = \sigma^2$.

The new variables $a_i = A_i \cos\phi_i$ and $b_i = A_i \sin\phi_i$ represent the signal amplitudes and phases, phase not being a random variable within each of signal realisations from the PSD sensor system.

Stated as a **linear least squares** estimation problem, cf. (Priestley 1981), one obtains the set of normal equations (ℓ=1,2,...,L, cf.(5.1))

$$\Sigma_{i=1}^{L} (a_i' c_{i\ell} + b_i' d_{i\ell}) = \Sigma_{n=<N>} s[n] \cos 2\pi p_\ell n/N = C_\ell \tag{5.13a}$$

$$\Sigma_{i=1}^{L} (a_i' d_{i\ell} + b_i' q_{i\ell}) = \Sigma_{n=<N>} s[n] \sin 2\pi p_\ell n/N = -Q_\ell \tag{5.13b}$$

Here a_i' and b_i' are the least squares estimates of a_i and b_i, resp.

Coefficients are $c_{i\ell} = \Sigma_{n=<N>} \cos\alpha \cos\beta$, $s_{i\ell} = \Sigma_{n=<N>} \sin\alpha \sin\beta$ (5.14)

and $d_{i\ell} = \Sigma_{n=<N>} \sin\alpha \cos\beta$, while $\alpha = 2\pi r_i n/N$, $\beta = 2\pi p_\ell n/N$

In (5.13) we have on the right hand side added our earlier notation of C_ℓ, Q_ℓ from (5.4).

This underlines the equivalence of linear least squares estimation with the synchronous detection routine, now applied to noisy signals.

Being concerned with retrieving marker signals from the noisy sensor, we will only consider the case of integer values of r_i and p_ℓ.

Now equations (5.12) simplify by orthogonality in (5.13), so that the estimates follow from the only nonzero values of C_ℓ, Q_ℓ

$$a'_\ell = (2/N)\ C_{\ell\ell} \quad \text{and} \quad b'_\ell = (2/N)\ Q_{\ell\ell} \tag{5.15}$$

Checking these estimates for bias, one has from (5.12) to (5.15)

$$E(a'_\ell) = 2/N \sum_{n=<N>} E(s[n]) \cos 2\pi p_\ell n/N = a_\ell \quad \text{and} \quad E(b'_\ell) = b_\ell \tag{5.16}$$

So these estimates are unbiased.

The variance of these estimates, $\text{var}(a'_\ell) = (2/N)^2 \sum_{n=<N>} \sigma^2 \cos^2 2\pi p_\ell n/N$,

cf. (5.13a), and by orthogonality in (5.14) $\text{var}(a'_\ell) = 2\sigma^2/N$,

similarly
$$\text{var}(b'_\ell) = 2\sigma^2/N \tag{5.17}$$

It can also be proved that $\text{cov}(a'_\ell, b'_\ell) = 0$.

Now to retrieve $A_\ell = (\ a_\ell^2 + b_\ell^2\ )^{½}$ introduces bias in the estimate, as

$$E(A'^2_\ell) = E(a'^2_\ell) + E(b'^2_\ell) = a'^2_\ell + b'^2_\ell + 4\sigma^2/N \tag{5.18}$$

Once more, this indicates that, with a priori knowledge or compensation of ϕ_ℓ as discussed above, it may be advantageous to estimate only $\quad A'_\ell = a'_\ell \cos \phi_\ell$.

We note by the way, that in the case of integer r_i and p_ℓ considered, the deterministic signal part is periodic on the measurement interval of N samples, and equal to its periodic extension, and that the a_i, b_i are its Fourier series coefficients. Now the least squares estimators of the Fourier series coefficients coincide with the corresponding discrete Fourier transforms (van den Bos 1989). And in section 5.2, we saw in which respect the DFT is equivalent to synchronous detection.

Obviously, the interest of synchronous detection, in a multi-marker PSD sensor system affected by noise, is the reduction of output noise variance over the input noise variance by a factor 2/N.

If, for a certain measurement rate ω_0, the time-multiplexed SELSPOT system samples each of the M markers once per cycle $2\pi/\omega_0$, synchronous detection inherently takes N samples, simultaneously on all of the K markers. In both systems, the measurement rate may be raised. But with SELSPOT this is at the expense of the maximum number of markers, which however is about 4 times that of the synchronous detection prototypes.

In another way of looking at the selectivity and noise performance, the synchronous detection system equations (5.6, 5.8) were viewed as the result of **convolution** with the frequency-domain window (5.7), in the basic expressions for the real part, imaginary part and modulus of the DFT with real cosine signals.
The bandpass characteristic of this window is obvious from the equations and illustrations, as are the zeroes for integer frequency index.

In (Harris 1978), time- and frequency domain windows are discussed at length. Of the concepts introduced, we will use the **equivalent noise bandwidth** (ENBW), which derives from the observation (loc.cit.) that the amplitude of the harmonic estimate at a given frequency is biased by the accumulated broadband noise included in the bandwidth of the window. To all intents and purposes, this corresponds with our review of synchronous detection properties.

The ENBW is defined (loc.cit.) as the bandwidth of an ideal rectangle filter, having the same peak power gain as the frequency window under consideration, that would have the same accumulated noise power gain.

It may be easily checked (loc.cit.) that the window of (5.7), a phase-shifted single Dirichlet kernel has an ENBW = 1 bin [5].

This tallies with the preceding review, as

Peak power gain = 1, from (5.16)
Area of the 1 bin wide rectangle filter = 1
Noise power gain = 2/N, from (5.17)
Over the range N/2 of r_i, cf. note 5.1, area or noise powergain = 1.

note
5 *As a bandwidth unit, bin denotes the unit in which we expressed the harmonic frequency indices* r_i *and* p_ℓ.
In frequency terms (cf. note 1) 1 bin denotes the frequency ω_0.

Among the many frequency convolution windows discussed or proposed by Harris (op.cit.) the lowest ENBW value is demonstrated by the rectangular time-domain window. This is the optimum window if low accumulated noise power gain is the only objective.

In (Sikkenk 1988) the noise reduction in the implemented system was verified by injecting a white noise signal of known variance, instead of the already low sensor noise, cf. section 5.4.
The output noise power conformed to the expected ENBW = 0.5, as this synchronous detection prototype only implemented the $C_{\ell\ell}$ output.

In section 5.5, windowing will be revisited for several aspects of the synchronous detection PSD system.

5.4 Prototypes and performance of synchronous detection PSD systems

The **early prototype** (Bakx 1977) used a SC/25 Position Sensitive Device sensor from UDT Inc. (USA) with in-house designed preamplifiers. This was soon replaced by the Mark I version of the SELSPOT PSD camera. Necessitated by the 10 kHz time-multiplex mode of the original SELSPOT system, the camera and preamplifier module featured a .wide bandwidth of 120 kHz. This easily allowed LED signal frequencies in the order of 10 kHz.
Continuous-time signals were used and quad synchronous detection was by **analog** multipliers followed by low-pass filters with a 500 Hz cut-off frequency. The quad channel output of this single-marker prototype was sampled, digitized and presented to the remote HP-2100 faculty minicomputer.
Results with a Monsanto ME 2A SELSPOT-type LED at some 700 mA pp at a 1 m distance, with the SELSPOT/Canon f:0.95 lens, indicated a ± 1 bit or ± 1:4000 precision as the expression of relative noise performance. This already improved some fourfold on the optimum SELSPOT performance discussed in section 3.5, which at that time was met under numerous precautions only. This first result concerned the standard deviation from the averages in a series, which consisted of 15 samples each at 50 incremental positions of a stationary marker.
Interference from overhead fluorescent lighting was prominent in the camera signals and absent in the system output.

A **next prototype** (Oostinjen 1980, 1982) was **all-digital**, in that the LED sinusoids were generated from an EPROM store while the quad sensor signals were sampled and digitized, and were fed to a bank of digital multipliers/accumulators, together with the EPROM-generated detection sinusoids. The available lowcost multipliers were of a serial-parallel type with bit-serial output. So accumulators were implemented by shift registers and a quad single-bit adder.
This multiplier / accumulator subsystem, as well as the EPROM section, was to be replicated for each of the six LED marker frequencies for a pilot system. By multiplexing, a 16-bit read-out was provided to the HP-1000 remote minicomputer.
The A/D converters were 12 bit, and 12 bit were used from the EPROM data, so the dual 8-bit multipliers were not fully occupied. The accumulators held 32 bit, of which the most significant 16 were read out.

The highly **composite number** N=1200 was selected for the accumulation interval. With the basic samplerate of 288 kHz for the A/D conversion, this resulted in a measurement rate of 240 Hz.

The anti-aliasing filter had a passband characteristic of 1-15 kHz. This gave some latitude in the selection of LED signal frequencies. At the same time the bandfilter, with a high-end cut-off well below the Nyquist frequency, contributed to reducing noise as well as the low-frequency electric light interference. At a 4.8 kHz LED frequency, the phase shift was 18^0 or $\cos\phi=0.95$.

With this digital synchronous detection system, more efficient IRLED's (Spektronix SE 3455) were used and, with a quality Summilux f:1.4 lens and an additional 16 * channel amplification, full signal was had at a 3 m distance. In this setting, noise and other performance was similar to the analog prototype. The noise proved to meet the assumption of a normal distribution.

The value chosen for N allowed a fair number of **integer divisors** to be selected as the values for the harmonic frequency index p_ℓ, to accommodate multiple LED markers.

A minor requirement on the p_ℓ values was, that they be not too far apart. Resulting signal frequencies may be contained well within in the passband of a simple bandfilter, so as not to introduce pronounced phase shift differences.

The other main requirement on the p_ℓ values concerns the combating of *nonlinearity error in the LED current/intensity characteristic.* Though the nonlinearity may be compensated by judicious programming of the EPROM voltage source and proper design of the LED control circuitry, one may also profit from the properties of synchronous detection. This approach is to select the p_ℓ values such that **no higher harmonics** of any LED frequency coincide with the fundamental frequency of another. If mutual harmonics coincide, these will be at the zeroes of equations (5.6, 5.8 etc.) and (5.5c) will be met.

At N=1200, typical selections to meet both requirements are quintuples p_ℓ= [15,16,20,24,25], alternatively [16,20,24,25,30], [40,48,50,60,75] which represent a one octave bandwidth.

To prepare the way for the use of more markers, an exhaustive computer search was conducted into more composite numbers N (up to 3000), to yield at least sextets of **mutually anharmonic numbers** having a low bandwidth ratio. At the same time, the focus was at minimization of the crest factor of the summed LED signals (Furnée 1984b).

Within an octave, many more mutually anharmonic sextets were found for N-values of e.g. 840, 1260, 1680, 2160 and 2520. For N=1680, 2 septets exist with a 2.19 bandwidth ratio. The number N=2520 even contains 5 octets within one octave and 16 still more closely spaced septets.
Keeping in mind that the higher N values need faster A/D's to preserve the measurement rate, cf. note 5.1, these findings give scope for multi-marker systems well within the state of the art.
With the same values for N, sets of more widely spaced mutually anharmonic p_ℓ-values may be easily found, if the low bandwidth requirement is relaxed.

The **crest** or peak **factor** of a signal is defined as the ratio of the difference of the maximum and the minimum signal value to the root-mean-square value. With fixed frequencies and amplitudes of spectral components, it is by phase adjustment that the crest factor may be minimized.
In the synchronous detection PSD system, where the LED signals derive from EPROM's, phase is easily controlled.

In this case, as with test signals for parameter estimation (van den Bos 1987), a low crest factor is desirable to maximize signal power within the amplitude range allowed to prevent sensor saturation.
Following the definition in (Schroeder 1970) we calculated the crest factors relative to the $2\sqrt{2}$ crest factor of the single sinusoid.

By a brute-force search program we found the minimum crest factors and associated phases for a large number of mutually anharmonic sextets of p_ℓ values. These minima are not absolute, in that our enumeration procedure (like the computer time) depended on the phase stepsize [6].

note

6 *By the later method of simulated annealing (Lenstra 1987), minimum relative crestfactors of the sextets 3 and 5 (table 5.1) turned out at* 1.36 *and* 1.61, *respectively.*

The examples brought together in table 5.1 show no pattern between the bandwidth ratio and the minimum attainable crestfactor.

#	N	p_ℓ $\ell = 1$	2	3	4	5	6	bandwidth ratio	min. rel.crestfactor
1	1080	24	27	30	36	40	45	1.9	1.55
2	1170	18	26	30	39	45	65	3.6	1.67
3	1260	12	14	15	18	20	21	1.8	1.37
4	1260	60	63	70	84	90	105	1.8	2.09
5	1320	24	30	33	40	44	55	2.3	1.65
6	1365	15	21	35	39	65	91	6.1	1.59

Table 5.1. Minimum crestfactors for a selection of mutually anharmonic unit-amplitude signals, frequency index p_ℓ, N samples/cycle

Fig. 5.5. shows the composite LED-signal of series # 3, table 5.1.

As a cautionary note in the PSD application, maximum and equal amplitudes of the distinct LED-frequency components in the PSD signal will (LED directional patterns being equal) only occur when the markers are all imaged nearest to the field of view boundary, corresponding to the particular sensor electrode. A margin for the crest factor, not only for unequal amplitudes, implies a practical limit to the number of LED markers or to the attainable signal to noise power ratio.

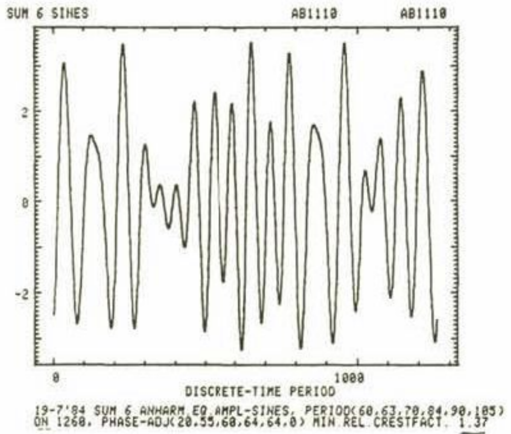

Fig. 5.5. One period of the 6-LED equal amplitude mutually anharmonic minimum crestfactor signal # 3 from table 5.1.

By the time of **extending the** digital synchronous detection PSD **pilot system**, it was no longer practical to replicate the serial-parallel multiplier banks for the accommodation of multiple LED markers and detection frequencies. As from the quad A/D converters, one for each PSD channel, fast 12*12 bit parallel multipliers were incorporated. Within a single A/D cycle, sampling rate being kept at 288 kHz, the multiplier easily handles 16 products for as many LED frequencies.

The values for each of the 16 detection sinusoids are stored in an interlaced way in a single EPROM. Each new cycle has the 16 distinct values consecutively presented to the multiplier to get 16 products.
For each of the four multiplier outputs, there is a 32-bit ALU and a 16-deep RAM with separate I/O, constituting a multi-marker accumulator for the 32-bit product-sums. The multiplexed accumulator read-out port presents 4 * 16 16-bit values to the host computer at the measurement rate of 240 Hz.
Implemented, extended and tested by Sikkenk (1986, 1988), the system shown in <u>fig. 5.6</u> hooks up to an AT-compatible PC by a byte-parallel interface, like the one reviewed in section 4.5 on the PRIMAS system.
The interrupt-driven input program is similar to the PRIMAS one, and likewise, the PC dumps data to file in an ASYST-compatible format for further analysis.
The potential of changing to a quadrature system is obvious. Reprogramming the detection EPROM adapts the present system for up to 8 LEDs.

Noise performance was tested with the Philips CQW 89 IRLED, also used in the PRIMAS illuminator. Now LED signal current was down to 100 mA_{pp} and marker distance was 1.5 m. A mark 2 version SELSPOT camera was used. In order to allow full open iris with the SELSPOT/Canon f:1.0 lens, the *16 channel amplifiers were bypassed for full signal range. Now in runs of 512 readings, with stationary markers at various sites we consistently found per channel precisions of 1:28000.
At an f:4.0 lens stop, equivalently at a 6 m distance, the amplifiers were used to boost the sensor signals to earlier levels, and precision degraded to some 1:7000. This reflected the lower signal/noise ratio, which might have better been raised with different high-current LED's.

Reckoning with a $\sqrt{2}$ downgrade in combining the PSD channel readings to the desired coordinate values, the ultimate precision figures become 1:5000 in the amplified, low signal/noise case and 1:20000 otherwise.

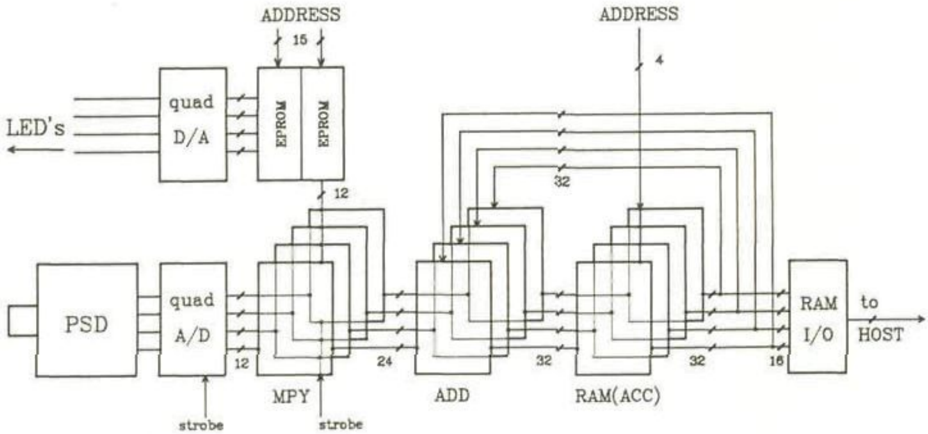

Fig. 5.6. Block diagram of digital synchronous detection PSD system.

The just *4 noise degradation in the case of a *16 amplifier is indicative of quantization error in the digital chain, without which the precision in the no amplifier case might be an extra 2 bit better. Due to hardware constraints this has not been looked into. A first thought is to have the host read out more than 16 bits from the accumulators.

On the other hand there is scope for some simplification, as there was no degradation when only the upper 8 bit (without rounding) were used of the detection sinusoids.

The system is succesful at combating ambient electric light interference, as well as in selectivity with respect to competing LED markers at other integer harmonic frequencies. Down to the least significant bit, the pertaining experiments showed no effects of bias nor upon the standard deviation.

The **insensitivity to ambient electric or daylight** enables the system to operate with visible-light LED markers. To this end, the infrared filter was removed from the mark 1 SELSPOT camera, and Stanley H500 ultrabright red LED's were used. As with visible light the reflections from non-specular surfaces are more tractable and also generally less severe, the red-light PSD synchronous detection system is less prone to spurious reflection errors, described in the SELSPOT section 3.5.

As far as we are aware, the frequency-multiplex concept was taken up in one **alternative** multi-LED PSD system under construction. Though our personal communication (Versmissen, 1984) also stressed the benefits of synchronous detection, the MARIN Maritime Research Institute Netherlands started developing a system utilizing one or a few LED's and analog filters for the LED discrimination, cf. note 3.7, section 3.5. Excursions in the model under study will be small and the LED's can be adequately screened and baffled to prevent spurious reflection paths. For other more complex applications at MARIN, TV-based solutions like the PRIMAS system were recently discussed.

Summarizing, the synchronous detection PSD sensor system has potential and significant advantages over the SELSPOT and derived Watsmart PSD-systems, as to reduced measurement noise, freedom from ambient light interference, and the visible-light option for a better management of spurious reflections. The drawback of active, wired markers is common to all PSD-based systems.

With moving markers however, the essence of any system, some important points remain to be considered.

5.5 Moving markers and windowing in synchronous detection PSD systems

In the previous sections, as from equation (5.3), the amplitude A of the sensor signal was supposed constant. Though adding to complexity, reality demands this condition to be dropped.
All a PSD is about, is that the A_{ij} amplitudes of the LED signals in any electrode channel j reflect the imaged position of marker i. So with moving markers the A_{ij} variables of interest are variable indeed. The **extension to marker movement** proceeds by writing, for any channel or fixed j, an elementary position signal as follows

$$X_{\kappa i}[n] = A_{0i} + A_{\kappa i}\cos(2\pi q_{\kappa i}n/N+\chi_{\kappa i}) \tag{5.19a}$$

So that with (5.3) we have for the generic PSD sensor signal

$$s_{\kappa i}[n] = A_{0i}\cos(2\pi r_i n/N +\phi_i) + \tfrac{1}{2}A_{\kappa i}\cos\{2\pi(r_i+q_{\kappa i})n/N +\phi_i+\chi_{\kappa i})\} +$$

$$+ \tfrac{1}{2}A_{\kappa i}\cos\{2\pi(r_i-q_{\kappa i})n/N +\phi_i-\chi_{\kappa i}\} \tag{5.19b}$$

Denoting n as in (5.1c), for the **periodic synchronous detection** system explicit time across the measurement cycles can be taken into account.

In the case of arbitrary marker movement, we consider (5.19a) as the static or zero-frequency component plus one of the spectral components with frequency index $q_{\kappa i}$, in the Fourier representation. By expansion, equations (5.19a, 5.19b) may represent the full spectrum of the marker number i position and the corresponding sensor signal, respectively.
With respect to note 5.1, we consider the index $q_{\kappa i}$ of marker movement *frequency components limited to* $0 \le |q_{\kappa i}| < 1$.

For the formulation of the **synchronous detection output**, for a real signal, we will once more use the DFT approach, cf. eq. (5.4).

From (5.19b) it is straightforward to derive the DFT (5.20a)

$$S_{\kappa i}[p_\ell] = \pi A_{oi}[\ \exp j(M\theta_{1i}+\phi_i)D_M(\theta_{1i}) + \exp\text{-}j(M\theta_{2i}+\phi_i)D_M(\theta_{2i})\ ] +$$

$$+ \tfrac{1}{2}\pi A_{\kappa i}[\ \exp j(M\eta_{1\kappa i}+\phi_{\kappa i})D_M(\eta_{1\kappa i}) + \exp\text{-}j(M\eta_{2\kappa i}+\phi_{\kappa i})D_M(\eta_{2\kappa i}) +$$

$$+ \exp j(M\zeta_{1\kappa i}+\xi_{\kappa i})D_M(\zeta_{1\kappa i}) + \exp\text{-}j(M\zeta_{2\kappa i}+\xi_{\kappa i})D_M(\zeta_{2\kappa i})\ ]$$

Here M, θ_{1i} and θ_{2i} are as in (5.6c), and additionally we have

$$\eta_{1\kappa i}=2\pi(r_i+q_{\kappa i}-p_\ell)/N, \quad \eta_{2\kappa i}=2\pi(r_i+q_{\kappa i}+p_\ell)/N, \quad \phi_{\kappa i}=\phi_i+\chi_{\kappa i}$$

$$\zeta_{1\kappa i}=2\pi(r_i-q_{\kappa i}-p_\ell)/N, \quad \zeta_{2\kappa i}=2\pi(r_i-q_{\kappa i}+p_\ell)/N, \quad \xi_{\kappa i}=\phi_i-\chi_{\kappa i} \qquad (5.20b)$$

These equations conform basically to (5.6a, 5.6c), but moreover they are duplicated by $r_i \rightarrow r_i \pm q_{\kappa i}$ as a result of the movement component.

In the **coherent detection** case $r_i = p_\ell$, integer p_ℓ, equation (5.20a) holds for the DFT $S_{\kappa\ell}[p_\ell]$ but now with

$$\theta_{1\ell}=0, \qquad \theta_{2\ell}=4\pi p_\ell/N$$

$$\eta_{1\kappa\ell}= 2\pi q_{\kappa\ell}/N \qquad \eta_{2\kappa\ell}= 2\pi(2p_\ell+q_{\kappa\ell})/N,$$

$$\zeta_{1\kappa\ell}= -2\pi q_{\kappa\ell}/N, \qquad \zeta_{2\kappa\ell}= 2\pi(2p_\ell-q_{\kappa\ell})/N, \quad \text{and phases } i \rightarrow \ell \qquad (5.21)$$

Now with (5.21) we can simplify (5.20a) to

$$S_{\kappa\ell}[p_\ell] = \pi[\ A_{0\ell}D_M(0) + A_{\kappa\ell}\cos(2\pi Mq_{\kappa\ell}/N + \chi_{\kappa\ell})D_M(2\pi q_{\kappa\ell}/N)\ ]\ \exp j\phi_\ell +$$

$$+ \pi A_{0\ell}\exp-j(\phi_\ell+M\theta_{2\ell})D_M(\theta_{2\ell}) \ + \pi A_{\kappa\ell}R_{\kappa\ell\ell} \qquad (5.22a)$$

The rest terms involving $A_{0\ell}$ and $A_{\kappa\ell}$, notably

$$R_{\ell\ell} = \ \exp-j(\phi_\ell+M\theta_{2\ell})D_M(\theta_{2\ell}) \text{ and} \qquad (5.22b)$$

$$R_{\kappa\ell\ell}= \tfrac{1}{2}[\exp j(M\eta_{2\kappa\ell}+\phi_{\kappa\ell})D_M(\eta_{2\kappa\ell}) + \exp-j(M\zeta_{2\kappa\ell}+\xi_{\kappa\ell})D_M(\zeta_{2\kappa\ell})] \qquad (5.22c)$$

encompass the far out sidelobe terms, of order $2p_\ell$, of the Dirichlet kernels centered at $-p_\ell$. Small, they are not negligible.

Considering, that $A_{0i} = A_{0i}\cos 2\pi q_{0i}/N$, with $q_{0i} = 0$ (5.23)

we finally write with (5.19b)

$$S_{\kappa\ell}[p_\ell] = \pi\ X_{\kappa\ell}[M]\ \exp j\phi_\ell\ D_M(2\pi q_{\kappa\ell}/N) \ + \pi A_{0\ell}R_{\ell\ell} + \pi A_{\kappa\ell}R_\kappa \qquad (5.24)$$

This exercise teaches two main points about the behaviour at coherent detection.

Firstly and not surprisingly, the estimates involving $X_{\kappa\ell}$, the moving marker position components, pertain to the sample instant $M=(N-1)/2$. This is the midpoint of the N-sample synchronous detection cycle [7].

Clearly, synchronous detection achieves **simultaneous sampling** of all markers within the measurement cycle.
Across the measurement cycles, with (5.1c), sampling of the periodic synchronous detection system pertains to sample instants $n = mN + M$.

Secondly and disturbingly indeed, the estimate of the $X_{\kappa\ell}[M]$ movement component suffers a **frequency-dependent attenuation** by $D_M(2\pi q_{\kappa\ell}/N)$. This transfer function evidently has its first zeroes at $|q_{\kappa\ell}| = 1$.

One recognizes that the synchronous detection algorithm, essentially extending across N sample points, is a low-pass filtering operation with regard to the estimation of moving marker coordinates. The filter characteristic is the main lobe of the Dirichlet kernel. Independent of p_ℓ, this filter transfer function is the same for all markers at coherent detection. It is exact and stable, and for $|q_{\kappa\ell}|<1$ it may be fully compensated in software.

A third and most worrying point is revealed when the selectivity or **leakage** is revisited in the case of moving markers.
With two markers, for simplicity's sake we consider a stationary one at the coherent frequency with index p_ℓ. The moving marker has integer index $r_i \neq p_\ell$. The equation obtaining in this case derives from (5.5b) and (5.20), or with an adapted notation

$$S_{\ell,\kappa i}[p_\ell] = C_{\ell\ell} + S'_{\kappa i}[p_\ell] = \pi A_\ell \cos\phi_\ell \, D_M(0) + S'_{\kappa i}[p_\ell] \qquad (5.25a)$$

where we have (5.25b)

$$S'_{\kappa i}[p_\ell] = \tfrac{1}{2}\pi A_{\kappa i}[\ \exp j(M\eta_{1\kappa i}+\phi_{\kappa i})D_M(\eta_{1\kappa i}) + \exp{-j}(M\eta_{2\kappa i}+\phi_{\kappa i})D_M(\eta_{2\kappa i}) +$$
$$+ \exp j(M\zeta_{1\kappa i}+\xi_{\kappa i})D_M(\zeta_{1\kappa i}) + \exp{-j}(M\zeta_{2\kappa i}+\xi_{\kappa i})D_M(\zeta_{2\kappa i})]$$

note

7 *For even N this represents a virtual point between 2 samples, but for the actual marker movement $t'=M\tau$ is significant all the same.*

Apparently, from a moving marker at integer index i, the contribution $S'_{\kappa i}[p_\ell]$ to the coherent detection output of another stationary marker is nonzero, because all of the $D_M(\eta)$, $D_M(\zeta)$ are nonzero.

With the normalization by $D_M(0)$ already indicated in (5.25), it is clear that the contamination by $S'_{\kappa i}[p_\ell]$ is not necessarily very small.

This depends primarily on r_i-p_ℓ, r_i+p_ℓ which determine the order of the sidelobe of the Dirichlet kernels concerned, cf. fig. 5.2. Within the sidelobe, and symmetrical with respect to the zero at r_i, actual value of $S'_{\kappa i}[p_\ell]$ is determined by the motion frequency index $|q_{\kappa i}|<1$.

It is obvious from the preceding discussion, that the Dirichlet kernel is detrimental, by its relatively high and slowly diminishing sidelobe levels, cf. also (Harris 1978).

At the expense of a slightly inferior noise suppression, cf. (loc.cit) and section 5.3, the synchronous detection PSD system moving marker performance should be dramatically improved by the addition of **tapered windowing**. In the time domain, this can be easily accomplished by the tailoring of the detection sinusoids stored in EPROM.

Tapered windowing in the time domain produces frequency windows, that are generally characterized by a broadening of the main lobe, versus a much lower sidelobe level with the added feature of rapid fall-off.

From the collection presented in (Harris op.cit) we would focus on the well-known von Hann window, modified for an average value of 1,

$$w[n] = 1 - \cos[2\pi n/N],\ n=0,1,\dots,N-1 \quad [8]. \tag{5.26a}$$

The associated DFT frequency window is

$$W[p] = D(\theta) - \tfrac{1}{2}\, D(\theta-2\pi/N) - \tfrac{1}{2}\, D(\theta+2\pi/N), \text{ with} \tag{5.26b}$$

$$D(\theta) = 2\pi \exp jM\theta\, D_M(\theta) \text{ and } \theta = -2\pi p/N,\ M=(N-1)/2 \text{ as before.}$$

note
8 *This adds 1 bit, if implemented with the EPROM coherent sinusoid.*

Noise performance of this window is characterized by the ENBW = 1.5 (Harris op.cit). This would, cf. section 5.3, imply a reduction of precision (increased noise standard deviation) by no more than 1.22. This is greatly outweighed by the benefits which will become apparent.

By the easy calculus implied in (5.26b), the von Hann window is the preferred example for our extension of (5.20) - (5.25).
This involves no more than rewriting (5.20a), while replicating all terms with the appropriate multipliers 1, -½, -½ and with the index r_i common to all arguments θ, η and ζ shifted by 0, +1, -1 in (5.20b).

The same prescription applied to the coherent detection case yields additions to the set (5.21) as follows

$$\begin{aligned}
\theta_{+1\ell} &= 2\pi/N & \theta_{+2\ell} &= 4\pi(p_\ell+1)/N \\
\theta_{-1\ell} &= -2\pi/N & \theta_{-2\ell} &= 4\pi(p_\ell-1)/N \\
\eta_{+1\kappa\ell} &= 2\pi(q_{\kappa\ell}+1)/N & \eta_{+2\kappa\ell} &= 2\pi(2p_\ell+q_{\kappa\ell}+1)/N \\
\eta_{-1\kappa\ell} &= 2\pi(q_{\kappa\ell}-1)/N & \eta_{-2\kappa\ell} &= 2\pi(2p_\ell+q_{\kappa\ell}-1)/N \\
\zeta_{+1\kappa\ell} &= 2\pi(-q_{\kappa\ell}+1)/N & \zeta_{+2\kappa\ell} &= 2\pi(2p_\ell-q_{\kappa\ell}+1)/N \\
\zeta_{-1\kappa\ell} &= 2\pi(-q_{\kappa\ell}-1)/N & \zeta_{-2\kappa\ell} &= 2\pi(2p_\ell-q_{\kappa\ell}-1)/N
\end{aligned} \tag{5.27}$$

Now we write $S_{w\kappa\ell}[p_\ell] = S_{m\kappa\ell}[p_\ell] + R_{f\kappa\ell}[p_\ell]$. (5.28)

By the suffix w we denote the windowed case, by the suffix m the mainlobe terms, and by the suffix f the rest term R due to the far-out lobes of the window kernels centered at $-p_\ell$.

We focus on the mainlobe term by collecting all contributions due to θ, η and ζ with the suffix 1, and derive

$$\begin{aligned}
S_{m\kappa\ell}[p_\ell] = \pi\exp j\phi_\ell A_{0\ell} D_M(0) + \pi\exp j\phi_\ell A_{\kappa\ell}[&\cos(\chi_{\kappa\ell}+2\pi M q_{\kappa\ell}/N) D_M(2\pi q_{\kappa\ell}/N) - \\
&-\tfrac{1}{2}\cos(\chi_{\kappa\ell}+2\pi M(q_{\kappa\ell}+1)/N) D_M(2\pi(q_{\kappa\ell}+1)/N) - \\
&-\tfrac{1}{2}\cos(\chi_{\kappa\ell}+2\pi M(q_{\kappa\ell}-1)/N) D_M(2\pi(q_{\kappa\ell}-1)/N)]
\end{aligned} \tag{5.29}$$

Now with $\cos 2\pi M/N = \cos\pi(N-1)/N \approx 1$ and $\sin 2\pi M/N \approx 0$ this approximates to

$$S_{m\kappa\ell}[p_\ell] = \pi \exp j\phi_\ell A_{0\ell} D_M(0) +$$

$$+ \pi \exp j\phi_\ell A_{\kappa\ell} \cos(\chi_{\kappa\ell} + 2\pi M q_{\kappa\ell}/N)\ D_{WM}(2\pi q_{\kappa\ell}/N) \tag{5.30}$$

where we have defined

$$D_{WM}(\alpha) \equiv D_M(\alpha) + \tfrac{1}{2} D_M(\alpha - 2\pi/N) + \tfrac{1}{2} D_M(\alpha + 2\pi/N) \tag{5.31a}$$

The $D_{WM}(\alpha)$ window resulted from the von Hann frequency window (5.26) applied to the pair of cosine signals in (5.19b). The first zeroes are at $|\alpha| = 4\pi/N$, or $|q_{\kappa\ell}| = 2$ in this application.

Obviously, with $D_{WM}(0) = D_M(0)$, (5.31b)

we may, with (5.19a) and (5.23), rewrite (5.30)

$$S_{m\kappa\ell}[p_\ell] = \pi\ X_{\kappa\ell}[M]\ \exp j\phi_\ell\ D_{WM}(2\pi q_{\kappa\ell}/N) \tag{5.32}$$

The broader mainlobe of $D_{WM}(2\pi q_{\kappa\ell}/N)$ compared to the single Dirichlet kernel in (5.24) bodes good for the low-pass filter characteristic acting on the marker movement frequencies.

In fig. 5.7, illustrating the filter behaviour, the 95 % value at the frequency $\omega = 0.3\ \omega_0$ contrasts favourably with the non windowed case. At the 240 Hz hardware implementation this corresponds to 70 Hz, while at 24 Hz, the 99 % value applies.

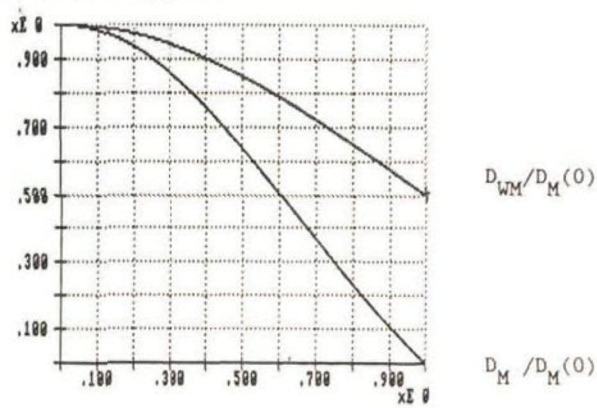

Fig. 5.7. Moving marker frequency transfer functions $D_{WM}(q_{\kappa\ell})$, $D_M(q_{\kappa\ell})$

It should be realised that in run-of-the-mill systems, where like with TV and SELSPOT the measurement frequency ω_0 equals the sampling rate, zero-power must be assumed for components at frequencies $\omega \geq 0.5\ \omega_0$. With the synchronous detection system, there is no aliasing risk with movement components, considering the Nyquist frequency value of $N\omega_0/2$.

Because it is very small, we have not bothered about the rest term $R_{f\kappa\ell}[p_\ell]$ in equation (5.28) for the windowed coherent detection case.

This becomes apparent, when we consider the selectivity or leakage phenomenon from a moving marker at another than the coherent detection frequency. Like in the non-windowed case (5.25) we have integer $r_i \neq p_\ell$. Now if we denote the integer numbers $d = r_i - p_\ell$ and $m = r_i + p_\ell$, while applying (5.26b) to (5.20b) we may write

$$\eta_{1\kappa i} = 2\pi(d+q_{\kappa i})/N \qquad \eta_{2\kappa i} = 2\pi(m+q_{\kappa i})$$

$$\eta_{+1\kappa i} = 2\pi(d+q_{\kappa i}+1)/N \qquad \eta_{+2\kappa i} = 2\pi(m+q_{\kappa i}+1)/N$$

$$\eta_{-1\kappa i} = 2\pi(d+q_{\kappa i}-1)/N \qquad \eta_{-2\kappa i} = 2\pi(m+q_{\kappa i}-1)/N$$

$$\varsigma_{1\kappa i} = 2\pi(d-q_{\kappa i})/N \qquad \varsigma_{2\kappa i} = 2\pi(m-q_{\kappa i})/N$$

$$\varsigma_{+1\kappa i} = 2\pi(d-q_{\kappa i}+1)/N \qquad \varsigma_{+2\kappa i} = 2\pi(m-q_{\kappa i}+1)/N$$

$$\varsigma_{-1\kappa i} = 2\pi(d-q_{\kappa i}-1)/N \qquad \varsigma_{-2\kappa i} = 2\pi(m-q_{\kappa i}-1)/N \tag{5.33}$$

With this notation, we obviously have to expand by another eight terms *the four terms of equation (5.25b) which expresses, in the windowed* case, the crosstalk contribution $S'_{W\kappa i}[p_\ell]$ from the moving marker to the coherent signal of the stationary one.
Clearly this expression is involved, though in no more than elementary mathematics, and computed results are given in <u>fig. 5.8</u>.

Here $|S'_{W\kappa i}[p_\ell]|$, normalized by $\pi A_{\kappa i}/2$, is viewed as a function of marker movement frequency index q_κ at marker indices $r_i = 45$, $p_\ell = 60$. The crosstalk by moving marker leakage is independent of the carrier signal phase ϕ_i, and maximum for phase $\chi_{\kappa i} = 0$ of the movement signal. Even at maximum, the leakage is suppressed by a factor 10000.
This result is some 250 times better than the non-windowed case.

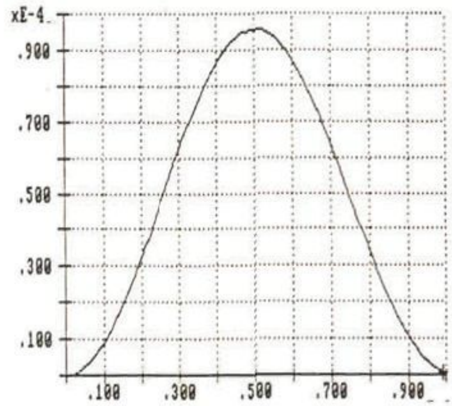

Fig. 5.8. Crosstalk $|S'_{W\kappa i}[p_\ell]|$, normalised, vs. movement frequency $q_{\kappa i}$ of a marker at carrier index r_i=45, coherent index p_ℓ=60.

With $q_{\kappa i}$= 0, and viewed as a function of non-integer r_i, much the same equations may be used to revisit the spurious contribution $S'_{W\kappa i}[p_\ell]$ from background or ambient electric light at low frequencies indexed by, say $|r_i| \leq 2$.
Here the maximum values of interference, at r_i = 0.5, 1.5, still show a suppression by a factor of 340000, or some 3500 times better than the non-windowed case.

This result clinches matters for using time-domain windowing in the synchronous detector PSD system.

For an **improved crosstalk** behaviour at indices r_i nearer to p_ℓ, the index of coherent detection, frequency windows with a lower nearest sidelobe structure are preferred to the von Hann example used in this discussion. In this category, no windows qualify that also have lower ENBW than the von Hann window (Harris 1978).
With just a little higher ENBW at 1.57 (loc.cit.), the Blackman window (the "not very serious proposal" in Blackman & Tukey 1958) is superior in all other aspects.
At $(r_i\ p_\ell)^T$ = $(50\ 60)^T$, the leakage from a moving marker is suppressed 7500 times, some 3 times better than with the von Hann window.

As the Blackman window involves two more terms in the frequency-domain window, it was a less fit example for elaborating the above equations.

5.6 Conclusion

Linearity of the PSD position measurement system can only be as good as the specially manufactured analog sensor and ancillary electronics. This has been discussed by Woltring (1975), as mentioned with respect to equation (3.3). A 0.1 to 0.3 % position-response nonlinearity was judged very good in (Noorlag 1982) in experiments where the sensor was displaced with respect to a focused light spot, so obviating off-axis lens nonlinearities. TV-based systems using mask-deposited CCD sensors which are also sensitive enough to use moderate-aperture high-quality lenses, will remain in a position to claim better linearity.

With this proviso, we have as a sideline activity to attain the higher sampling rates possible with a PSD sensor, developed a system that has several benefits over the original and derived SELSPOT systems.

This periodic synchronous detection PSD system utilizes its active LED markers in frequency-multiplex. For an acronym we coin it $(PSD)^2$, by blending the system and sensor abbreviations.
We note in passing that, like the SELSPOT time-multiplex, this has the advantage of inherent identification of the markers. Apart from speed, this is the one advantage over TV-based systems. Again, the need for active wired markers is a drawback.

The digital-processing synchronous detection PSD system has a 240 Hz sampling rate, accommodating up to 8 markers. Given the bandwidth of the PSD sensor, it is easily within the state of the art to raise the sampling rate upwards of 1 kHz, the SELSPOT rate with this number of markers.
The synchronous detection system has inherently simultaneous sampling of all moving marker coordinates, as opposed to the time-multiplex commercial systems.

Equally inherent is the absolute suppression of daylight interference in the PSD signal.
Interference by mains frequency and harmonics of ambient or background electric lighting is strongly suppressed. This suppression is wellnigh absolute, allowing demanding industrial applications, when windowing is introduced. With the last few pages on time-domain and frequency windowing we outlined the next step in the PSD system development.

The ambient light immunity allows the use of visible-light LED markers and to some extent this alleviates the problem of spurious reflections as a common error source in PSD position sensing.

To prevent untoward effects of harmonic frequencies by remaining LED non-linearity, a set of LED frequencies, which are integer multiples of the measurement frequency, is chosen such that no harmonics equal any other fundamental LED frequency. Being stored in EPROM, as are the coherent detection signals, the LED signals may be programmed by phase adjustment for the minimum crest factor, to prevent sensor saturation.

The well-established fact, that windowing is indispensable to abate the spectral leakage phenomenon, was underscored in the suppression of crosstalk from moving markers.
With moving markers, the consequence of periodic synchronous detection was seen to be a low-pass transfer function, with zero phase shift and with a 90 % attenuation e.g. at 100 Hz in a 240 Hz windowed system.
Inherently with periodic synchronous PSD detection, signal power needs not to be zero up from 120 Hz in the example of the 240 Hz prototype. There is no aliasing risk up to very much higher frequencies than the basic measurement rate.

Finally the sensor noise is markedly reduced by synchronous detection.

As equivalent to the discrete Fourier transform, albeit for a reduced number of coefficients, synchronous detection yields the least squares estimates of LED sinusoid amplitudes, as a measure of marker position.
The concept of equivalent noise bandwidth ENBW of the corresponding convolution window can equally be applied. ENBW was seen to be 1.0 bin or 240 Hz in the prototype, while the time-domain tapered windows that were discussed have an ENBW ≈ 1.5.
Noise performance, expressed in precision, of the non-windowed system was 1:20000 with a standard LED at 1.5 m and an f:1.0 lens stop.

On a number of scores, the periodic synchronous detection PSD system offers improvements over the time-multiplexed originals, even over SELSPOT-2 with its increased ramp LED currents, cf. section 3,5.
For special applications, involving low marker numbers and high speed, a further developed $(PSD)^2$ system may compete with OPTOTRAK and with the TV-based systems, that are the main subject of this thesis.

CHAPTER 6. APPLICATION PROJECTS

6.1 Introduction.

There are few actual recordings left from the earliest applications of the video-digital coordinate conversion system.
Fig. 6.1 presents one stride of a gait experiment at the Biomechanical and Experimental Rehabilitation Lab. (R.H. Rozendal), Free University Amsterdam (Furnée et al. 1972). These records concern 2-D projections in the sagittal plane, at a TV frequency of 50 Hz. The stick diagram is shown, joining the momentary positions, within each TV field, of 7 markers, attached from ear to foot. The angular diagram versus time, over a 2 s interval, shows the angles of the upper leg with vertical and the lower leg with vertical, derived from the marker coordinates, and the knee flexion angle as the difference of the two.

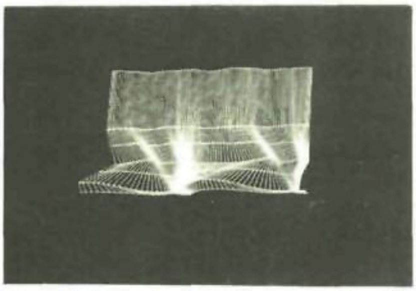

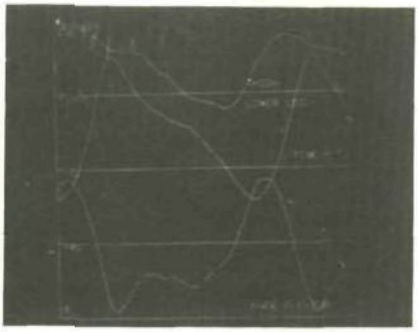

Fig. 6.1 a. Stick diagram of gait: sticks at 20 ms intervals join ear, hip, upper leg, knee, lower leg, ankle, toe. b. angles vs. time, cf. text

From an earlier series on arm movement (Furnée et al. 1972), fig. 6.2 shows wrist motion, viewed in the sagittal plane, while horizontally moving an object in a cyclical way with varying rest periods. Isolated movements gradually merged into continuous motion, with the velocity profile developing into ramp functions and the characteristically timed acceleration pulses merging, to acquire the appearance of block functions.
Fig. 6.3, from the same experimental sessions, is a near example of an on-off acceleration/deceleration pattern with velocity ramps to match.

This record concerned wrist displacement in humeral rotation, with the vertical upper arm supported at the elbow and the forearm moving in the horizontal plane. 2-D Projection is the frontal plane.

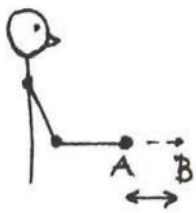

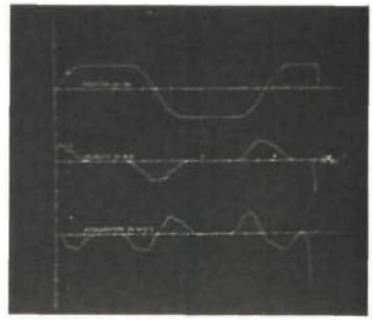

Fig. 6.2 a. Wrist motion, sagittal view b. Slow, X, dX/dt, d^2X/dt^2

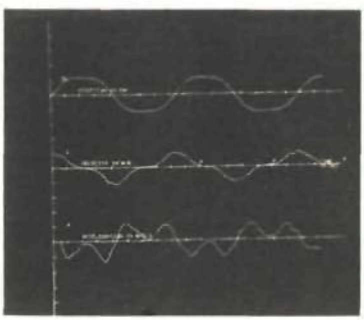

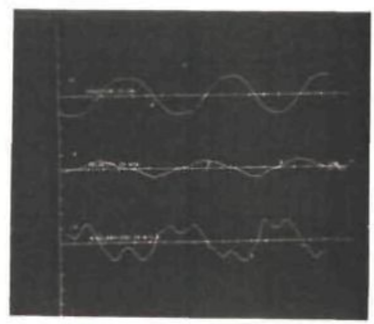

Fig. 6.2 c. same, medium rate d. Fast

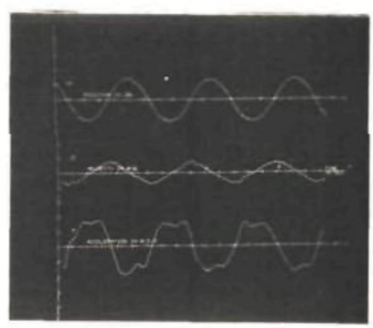

Fig. 6.3 a. Humeral rotation, frontal view b. Z, dZ/dt, d^2Z/dt^2

In a documented study Dijkstra (1973) focused on complex arm motion, involving both the shoulder and elbow joint, at the Medical and Physiological Physics Lab.(J.J. Denier van der Gon) University of Utrecht.

The guiding hypothesis was that in the central nervous system the control process is basically, in any case at its output, reflected in on-off activation signals (Denier van der Gon et al. 1965). Activation signal parameters were (at least) starting time, duration, intensity. On-off activation to the α, γ innervation to the musculoskeletal system was, by measurements and simulations, shown to be compatible with EMG, the acceleration patterns and the trajectories observed.
An early version of the TV-based motion recording system of chapter 2 had been adapted in the Utrecht lab. by van der Wildt (1971).
Fig. 6.4 shows a view of the subject in the transverse plane, while fig. 6.5 is illustrative of the time course of angles, angular velocities and accelerations of a movement approximating that of fig. 6.4a.

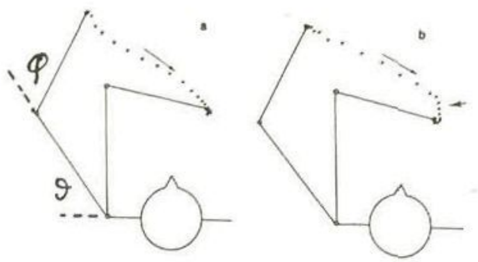

Record with digitised television signals of a fast arm movement without disturbance (a) and with a disturbance during the movement (b).
The arrows indicate the direction of the movement.
The arrow in fig. b shows the slow phase in which the correction on the disturbance takes place.

Fig. 6.4 Wrist trajectories in arm motion *(courtesy Sj. Dijkstra)*

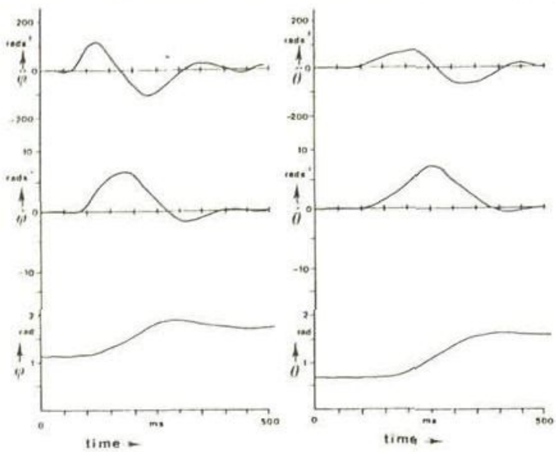

Fig. 6.5 angular values, velocities and accelerations of a movement like that in fig. 6.4a *(courtesy Sj. Dijkstra)*

6.2 Locomotion studies in the cat

As reflected in (Nieukerke 1974), (Furnée et al. 1974) and (Halbertsma 1975), we have been involved in the recording and analysis of aspects of treadmill locomotion in the cat. This concerned a major project at the Anatomy Dept. (S. Miller), Erasmus University of Rotterdam, which phased out only with the remigration of dr Miller to the UK [1].

The main research programme and hypothesis was formulated as follows (Miller et al. 1975b):

"Observations in cats of flexion and extension movements of the four limbs have led to the conclusion that the different forms of alternative locomotion (e.g. walking, trotting, swimming) and in-phase locomotion (galloping, jumping) result from the interaction of 'programs' for the coordination of 1) the homologous limbs (pair of hindlimbs or pair of forelimbs) and 2) the homolateral limbs (hind- and forelimb of the same side of the body). The movements of the homologous pairs of limbs are coupled out of phase in alternate locomotion and approximately in phase in the in-phase form of locomotion. The movements of homolateral pairs of limbs occur approximately out of phase in the trotting type of coupling and approximately in phase in the pacing type of coupling. Transitions between the different forms of coupling occur abruptly over 1 or 2 steps. Therefore, for each type of coupling (homologous or homolateral) there are two distinct forms or 'programs' of movement.

The hypothesis is advanced that a) all the characteristic patterns of locomotion in the cat result from different combinations of these 'programs' of homologous and homolateral limb coupling; b) 'programs' are mutually self-reinforcing in the gaits in which the coordination of the four limbs is bilaterally symmetrical; c) the 'programs' act in competition in certain gaits which are not bilaterally symmetrical, giving rise at times to a changing gait pattern. The results together with those in preceding and following papers (from the Miller group) have led to the suggestion that these basic patterns of movements involving different pairs of limbs have their origin in functional subsets of neural activity in the spinal chord, which can interact in different combinations to meet the varying demands for locomotion."

note

1 *Not without a profitable extension (Halbertsma 1983) to a twinned project run at the Physiology III Dept. (S. Grillner), Karolinska Institutet, Stockholm.*
This group availed themselves of a SELSPOT system, cf section 3.5

The quest for the fundamental properties of the hypothesized step generators, and for their mutual coupling (Miller et al. 1973), was mainly by investigating timing relations in the onset and duration of flexion and extension in the relevant joints of the two or four limbs that could be observed. This was supported by the timing analysis of concomitant muscle activity (EMG) as a reflection of motoneuron inputs from the spinal chord.

The 2-D film recording was superseded by our **TV/computer system**, with the intermediate digital tape recording of landmark coordinates as reviewed in section 2.5. The same section mentions the digitizer/ serializer which was added to allow the acquisition of external data, in the form of smoothed and rectified muscle action potentials (EMG), synchronously with the movement data. As reviewed in section 2.7, we used stroboscopically pulsed UV fluorescent light inside the treadmill cage (Furnée et al. 1974), where one of the cats is shown in fig. 6.6.

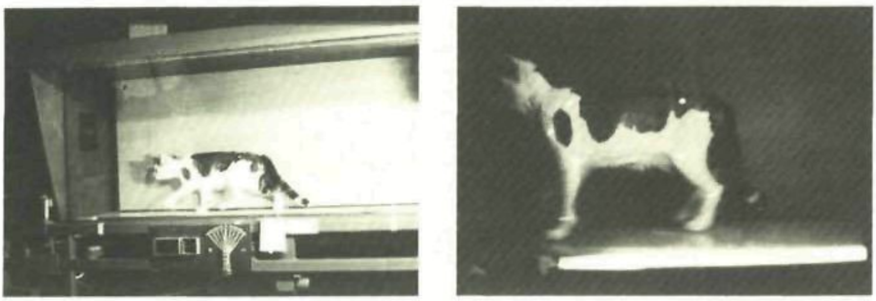

Fig. 6.6. Cat with UV-pulsed reflective markers in treadmill cage.

As described in a companion paper (Miller et al. 1975a) the **correspondance** of the markers with bony landmarks of the underlying skeleton was checked by X-ray cinematography with the skin markers replaced by miniature lead discs. Especially at the shoulder, the skin will shift in a complicated fashion, though the timing of elbow flexion/extension changeover was not affected. The onset of shoulder flexion/extension could not reliably be estimated from the skin markers.

One of the techniques for guiding the investigators to those timing relations that showed the least variability, so as to suggest the primary parameters of step generators and mutual coupling, resembled **average response** methods in superimposing traces with a common trigger point. The trigger, however, was not by an external signal.
Fig. 6.7, from (Furnée et al. 1974) is illustrative of early work.

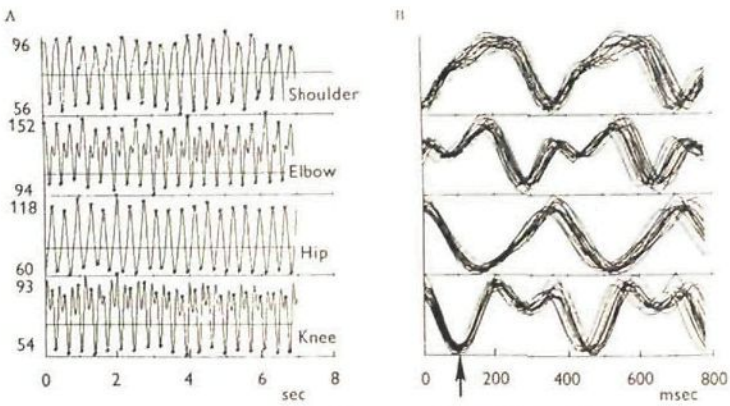

Variation of angles at shoulder, elbow, hip and knee of limbs of same side during stepping on treadmill at 2·0 m.sec^{-1}. Upward excursion indicates extension, downward flexion. Numbers in ordinate indicate extremes of angles in degrees. *A*, 19 successive steps. Stars mark the turning points of flexion and extension. Horizontal lines drawn through the traces represent windows set by the operator during the recognition procedure for the turning points. *B*, the same steps superimposed. The onset of extension of the knee joint (arrow) has been used as the starting point of each step.

Fig. 6.7. Limb angles vs. time in cat locomotion, cf. caption.

Fig. 6.8 shows the additional EMG recordings of four muscles relevant in elbow and knee flexion and extension. Horizontal bars in the superimposed records denote the duration of the corresponding EMG activity.

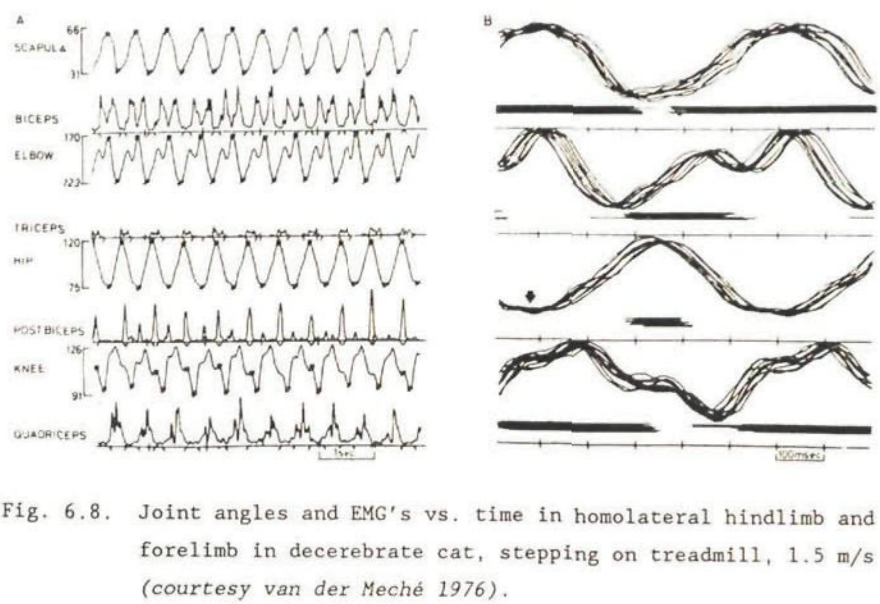

Fig. 6.8. Joint angles and EMG's vs. time in homolateral hindlimb and forelimb in decerebrate cat, stepping on treadmill, 1.5 m/s *(courtesy van der Meché 1976)*.

6.3 Human movement disorders, ballistic arm movement

Our involvement in neurogenic movement disorders was in an ongoing project at the Dept. of Clinical Neurophysiology (O.J.S. Buruma), University of Leiden. The problem area had been defined as follows (Kemp et al. 1982):

"Choreoathetoid syndromes, resulting from disorders of the basal ganglia of the brain, are characterized by involuntary movements. These movements, ranging from a single twitch of the face or the little finger to large movements of the trunk and the extremities, vary in velocity and trajectory and may occur simultaneously. The movements have a strong desocialising effect on the patient. A drug for adequate symptomatic relief has still to be found and, as always, the search for an effective drug has stimulated numerous drug-assessment studies. In this case, objective quantification of the movements is required.
The burden exerted by an involuntary movement on a patient depends on the extent of the motion trajectory, and also on the size of the body part involved. Adequate quantification methods should take these factors into account."
The short-range Doppler radar device developed by Kemp (op.cit.) came a long way to satisfy the above quantization requirements. Additional signal processing yielded a quantity of motion Q that within a certain observation period was proportional to the number of movements, the length of their trajectory and the size of the involved body parts.
It was however realised that only the radial component of velocity was taken into account. It soon became less satisfactory that this overall measurement method was unspecific as to the momentary affected part(s) of the body, and this is where TV got in.

Though a 2-D TV-system, as used in the pilot experiments, only yields the marker positions and velocity components in the transverse plane, the identification of any desirable number of anatomical sites permits the investigator to differentiate e.g. between gross and local motion or between focal points and secondary emanation of incident spasms.

Fig. 6.9 is illustrative of a seated sufferer of **Huntington's chorea**, with markers at the feet, knees, hands, elbows, shoulders, chin and forehead. Head and shoulders show some slow sideways swaying, the feet are shuffled, there is a large knee unrest, of the supported hands the right one shows isolated insults, larger ones emanating to the elbow.

In (Buruma et al. 1983) the opportunities are described of TV/computer systems for the assessment of human movement disorders in neurology.

Fig. 6.10 concerns the involuntary facial movement in a female patient suffering from **focal dystonia**. Superimposed on a cranial rotation, one of the typical gaping movements of the mouth is shown.

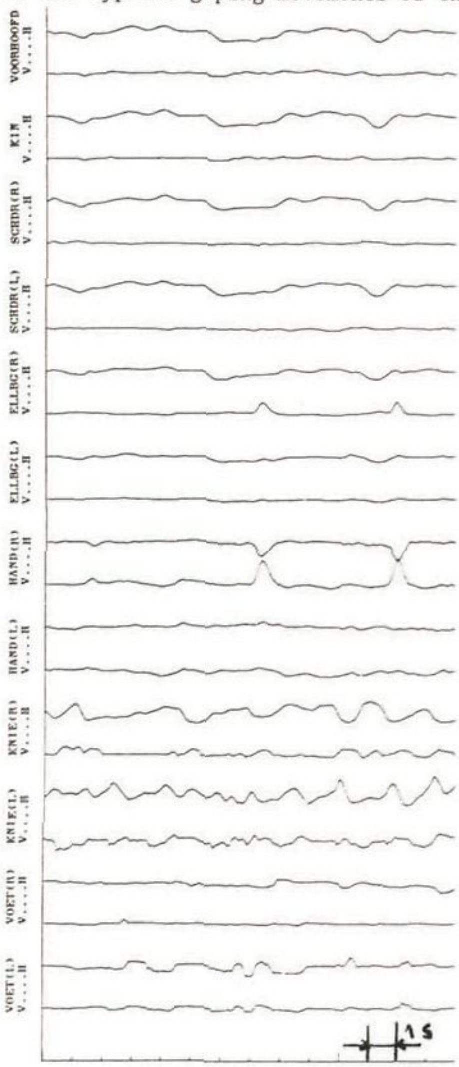

Fig. 6.9. Huntington's chorea; Movements in frontal plane, horizontal and vertical, of forehead, chin, shoulders, elbows, hands, knees and feet; cf. text *(courtesy G. van Antwerpen)*

Fig. 6.10a.A sufferer of focal dystonia of the face

Fig. 6.10b. Marker trajectories 12-fold blow-up *(courtesy H. Demper)*

On the subject of **ballistic hand motion**, where the basal ganglia have a crucial initiating function (Marsden 1982), and where there appears to be no effective feedback for controlling or adapting the movement during its execution, and where typical EMG patterns are observed of sequential agonist/antagonist/agonist activation, with sometimes the latter lacking (Denier van der Gon et al. 1977), findings like those of Fisk and Goodale (1985) have prompted clinical interest in the differences between fast reaches made to ipsilateral and contralateral targets.

As reported in (van Dijk et al. 1986, 1988) we were involved in a range of experiments to test the hypothesis that ipsilateral ballistic hand movements are faster than contralateral ones. With a righthanded subject using his right hand, ipsilateral movement is executed in the space right of the body midline. Another distinction which may be made is that of adducting or abducting movement, which refers to the use of the adductor or abductor musculature. Performed by the right hand e.g. movement from the midline to the left is contralateral and adducting.

The fast hand movements were made with the index finger, identified with a low-inertia marker and sampled by the 60 Hz TV/computer system, moving between a vertical bar placed at the midline in front of the subject and another vertical bar placed at 10, 30 or 50 cm distances. With this setup, movements, cf. <u>fig. 6.11</u>, consisted typically of a fast initial reach bringing the finger close to target, followed by a slower phase to contact the bar, most likely under visual feedback.

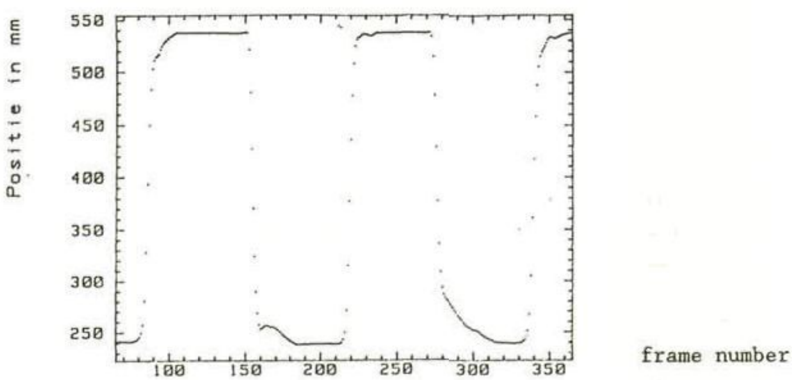

Fig. 6.11. Ballistic hand motion example, cf. text *(ctsy. Demper 1986)*

<u>Fig. 6.12</u> shows an average speed profile, with 95 % confidence bounds.

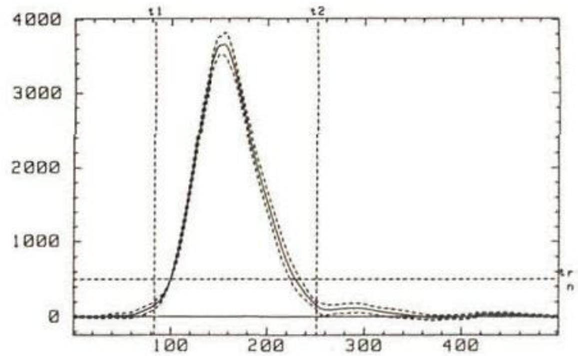

Fig. 6.12. Averaged speed profile (mm/s) vs. (ms), cf. fig. 6.11, one direction *(courtesy Demper 1986)*.

Results from one of the four subjects are summarized in fig. 6.13, showing peak velocity vs. target distance, with ipsilateral movements represented at the right, contralateral ones at the left side, while points in adducting movement are connected by full lines, abducting by dotted lines. Vertical bars denote standard deviation.

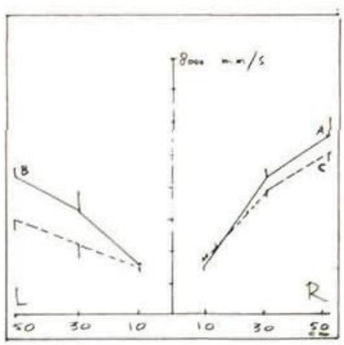

Fig. 6.13. Peak velocities vs. target distance, ballistic hand motion *(courtesy van Dijk et al. 1988)*

As a general result, peak velocity increased with increasing distance. Equally in line with (Fisk op.cit) the ipsilateral movements performed faster than contralateral ones. As a new finding, adducting movements were generally faster than abducting ones.
Apparently the hypothesized, commonly structured, motor programmes do not fully compensate for the mechanical disadvantages involved.

The subject is discontinued till the advent of in-house motion analysis facilities for patient work at the Clinical Neurophysiology Dept.

6.4 Human gait disorders

Also at Leiden University human gait is studied by the Anatomy, Rehabilitation and Orthopedic Depts.(A. Huson, P.M. Rozing) with treadmill, footcontact and EMG facilities. Routine motion recording was based on electrogoniometry, where **pelvic rotation** in the frontal and sagittal plane were derived from a potentiometer system attached to an external pelvis girdle. This girdle was strapped firmly onto the pelvis so to reduce skin motion with respect to the bony structures. The potentiometer angles were referred to a system of parallelogram guiding wires, the system being kept taut by springloading from the ceiling. Reliable recordings were possible up to 2.5 Hz (van Leeuwen et al. 1988), which was considered not quite satisfactory, as frequencies up to 10 Hz were judged to be required even to record walking with a 1 Hz cadency.

As a pilot study for introducing **TV-based methods**, the pelvic girdle *was retained for the above reasons, but the goniometer attachment was* abandoned for a low-inertia object plane with 4 coplanar markers. The assembly was not far unlike the pelvic rig used by Thurston (1982).
Again for reasons of skin slippage, the upper leg was not instrumented but the lower legs and feet carried low-inertia fixed reference marker clusters. These were not of the drastic kind literally introduced by the Inman group in cyclophotography at Berkeley (cf. section 1.1, and Levens et al. 1948 on the bone cortex pins).
An impression is given by fig. 6.14 from (Melein 1987), where also the trunk coordinate axes and anatomical planes are designated.

Representative results from (Melein 1987) are in fig. 6.15 for pelvic rotation in the frontal (YZ) plane and fig. 6.16 for pelvic rotation in the transverse (XZ) plane. Moreover, fig. 6.17 shows forward (X) pelvic translation while fig. 6.18 shows forward translation of both feet. Forward foot motion represents (part of) the swing phase, the extremum is at touchdown, while the backward motion is (part of) the stance phase in moving along with the treadmill surface.
The 3-D PRIMAS system was run at 50 Hz. Noisy behaviour in transverse rotation records (fig. 6.16) is due to the untoward disposition of the two cameras, where the cramped surrounds admitted a convergence angle of no more than 45°.
Otherwise, the system already provides information on more body angles than the goniometer device, which moreover records no translations.

The programs for **3-D calibration** of the camera setup, using a 0.5 m^3 cube with 40 markers, and for the subsequent **3-D reconstruction** were due to preliminary work of Zandbergen (1986) in the gait project. This software, partially based on (Spoor et al. 1980), included routines not only for 3-D point reconstruction, but for the 3-D location and attitude of solid objects and for the angulation between articulating segments, each of which is identified by a marker cluster.

The project concerned ambulation by subjects with a **leg length differential**. This could be compensated or exaggerated by raised orthopedic shoes.

The main problem addressed was in which way the walking subject compensates for the uncompensated (or increased) leg length differential. One of the tasks, even in normal gait, is to prevent the foot hitting the ground in mid-swing phase before the actual touchdown. Mechanisms involved like pelvic rotation and vertical translation, knee and ankle flexion, and circumduction of the complete leg (by femoral abduction), but also step size were hypothesized to show left-right asymmetries in case of leg length discrepancy. This would be a way to identify which modalities are predominantly used. The interest in pelvic rotation was motivated by the association with the functions of the lumbar muscles (Vink 1989) and the low back pain syndrome (Vink and Huson 1987).

In each of the records of <u>figs. 6.15 to 6.18</u>, the nine traces show, in groups of three for three different speeds from stroll to normal walk, treadmill gait with a) a compensated leg length differential, b) an uncompensated 1 cm leg length differential and c) an increased 3 cm leg length differential. The left leg, except if compensated, is the longer one. Block traces within every record identify footcontact (right foot is denoted by upper trace).

Superimposed on the cyclical forward/backward pelvic translation as well as on that of the feet is a gross and less regular displacement of the subject back and forth on the treadmill. This trend should have been subtracted for a proper understanding of <u>figs. 6.17 and 6.18</u>.
The unreproduced record of transverse pelvic displacements, combined with those of the feet indicates a relative outward motion of the foot during the swing phase, which at low speeds is mostly due to an inward pelvic shift toward the stance leg, with little swing foot deviation.

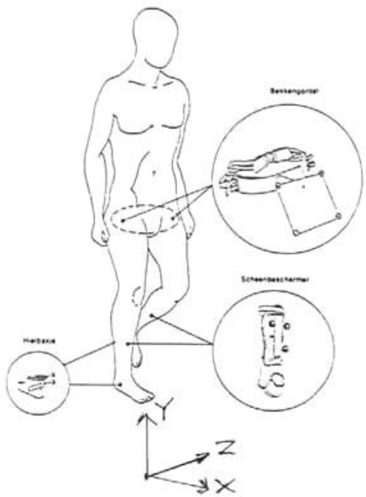

Fig. 6.14. Homunculus, showing shape and location of pelvic brace, shin protector and heel cup, with attached markers. *(courtesy J.B.F. Melein)*

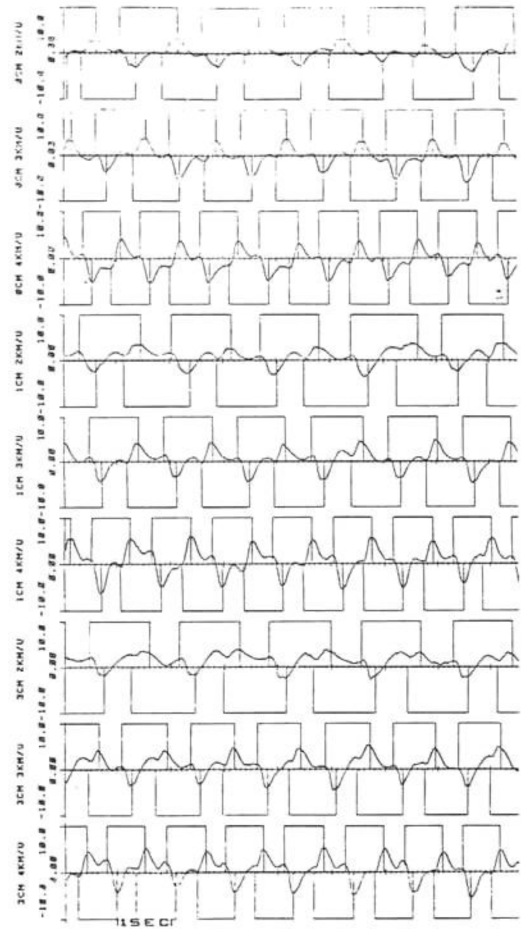

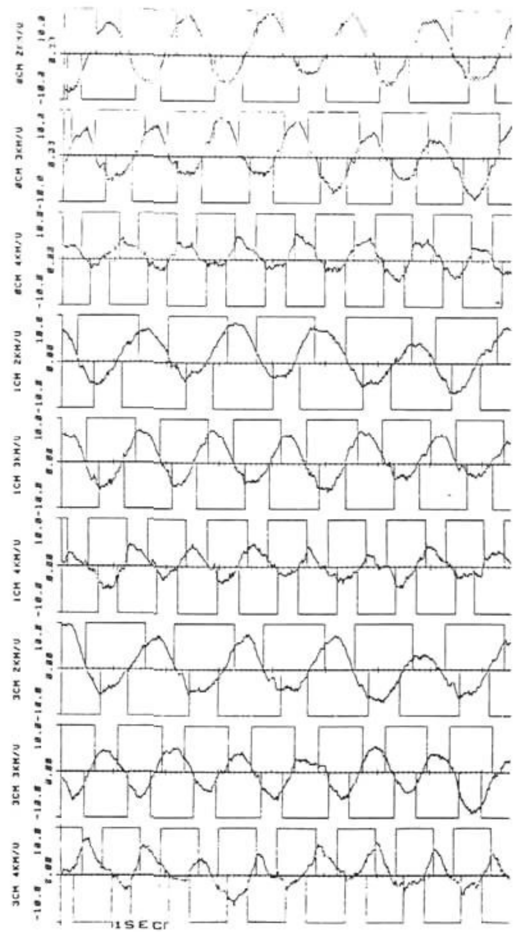

Fig. 6.15. Pelvic frontal rotation, degrees   Fig. 6.16. Pelvic sagittal rotation, degrees

speeds 2, 3, 4 km/h, leg length inequalities 0, 1, 3 cm *(courtesy J.B.F. Melein)*

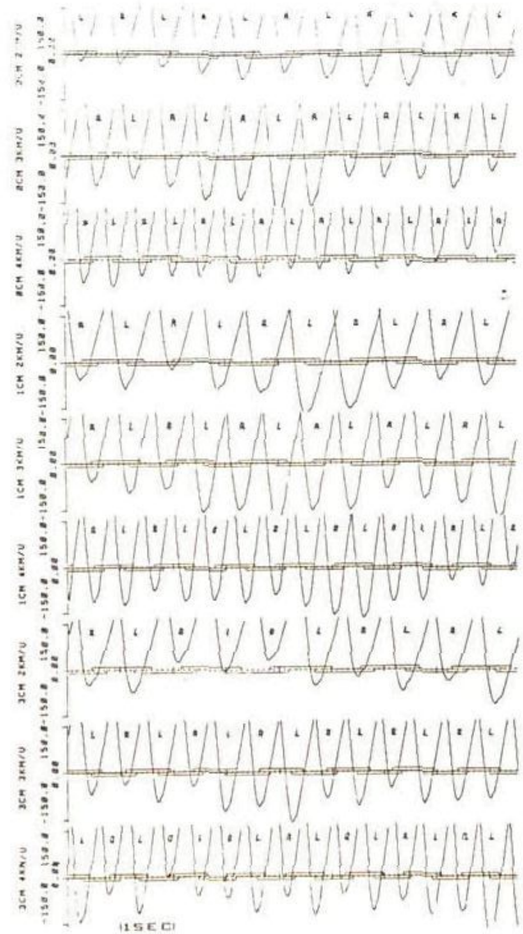

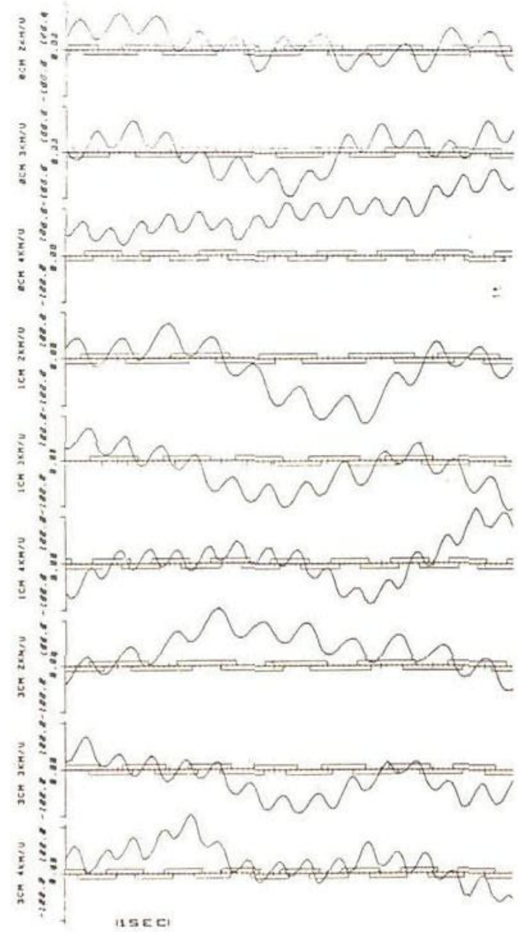

Fig. 6.17. Forward feet placement, mm

Fig. 6.18. Forward pelvic motion, mm

speeds 2, 3, 4 km/h, leg length inequalities 0, 1, 3 cm *(courtesy J.B.F. Melein)*

Higher, but still walking, speeds show a reduced pelvic sway with more pronounced circumduction of the feet, albeit without clear preference for the longer leg. But that there are various compensation modes, is indicated in part of the low-speed uncompensated walk where there is a switchover to marked circumduction of the longer leg.

Some of the other records carry a clearer message. Fig. 6.15 indicates a difference in pelvic tilt amplitude during the swing phases of left or right foot, which grows more marked with increasing speed. However, the maximum pelvic tilts, at the end of stance phase are symmetrical, and again these increase at higher speeds. This suggests the need of additional compensation, e.g. by knee flexion, only at the onset of the swing phase of the longer leg. The sagittal ankle records show no additional ankle dorsiflexion. Pelvic tilt asymmetry during the swing phase may be taken as one of the compensation mechanisms for the leg length differential.
Fig. 6.16, showing transversal pelvic rotation, exhibits left-right asymmetries at all speeds, and mildly so even in the compensated case. It should be noted here, that all records are displayed with reference to rest positions separately recorded at standstill. At the side of the short leg, the pelvic joint is rotated less forward than at the other side. At the same time fig. 6.17, together with fig. 6.18, shows an at first sight corresponding asymmetry in forward foot placement. The short leg is carried less forward than the long one, step lengths being equal in the compensated case. However, the differences in forward foot placement are bigger than can be explained by transverse pelvic angle alone, other factors such as hip flexion being equal.

The speculative consequence is, that the shorter step with the shorter leg is a mechanism to prevent the pelvic joint from sagging too much. And with the frontal pelvic rotation discussed above, this keeps the pelvic joint at the long leg side at an advantageous height for the start of its swing phase. This would obviate overdue knee flexion of the longer leg, as postulated above.

Clearly a treadmill disposition more accessible to a multi-camera view so that the full foot strides may be recorded, together with linearization procedures for increased confidence with wide-angle lenses, as well as means to identify the upper leg, would promise to complete the parameters discussed towards interesting and more convincing results.

6.5 Mandibular motion

In a collaborative project of the Oral Surgery Dept. (G. Boering) at the University of Groningen and the Biomechanical Dept. (J.C. Cool) of Twente University, human jaw movement is investigated from the design viewpoint of temporo-mandibular joint replacement. Already the planar opening and closing of the mouth is a complex phenomenon in rotation and translation. The simple pivot prosthesis offers no durable relief, as the intact neural control and musculo-skeletal organisation of the jaw conflict with an artefact unable of translation, whether this be by design or by consequence of the implant surgery (Kent et al. 1983, Sonnenburg et al. 1983).

With the PRIMAS system we got involved in the motion analysis part of the project (Falkenström 1988), which is being continued as PhD work.

In the primary context of 2-D **jaw motion** in the sagittal plane, focus of the in-vivo experiments is on the description by the polar plot as the locus of instantaneous centres of rotation ICR (Chissin 1906), and on the translational motion of the condylar head vs. the mandibular rotation. Fig. 6.19 a shows a polar plot superimposed on the skeletal diagram, annotated with the anatomical terms, together with the marker trajectories in a series of mouth openings and closings. Some of the complex motion is obvious as markers C and D approximate circular arcs while markers A and B do not.

Movement of the jaw as a solid object was recorded by the attachment of a low-inertia rig as shown in fig. 6.19 b, carrying four markers, and mounted on a slim rod which protruded between the lips, connecting to dental braces temporarily fitted to each of 20 volunteer subjects. An X-ray photograph identified the leaded marker positions relative to the jaw and to the condylar head CH in particular.

Position and attitude of the head was similarly identified, first with two markers on a spectacle-frame, later with five markers on a special brace fitted to the skull to allow the monitoring of cranial rotation.

Fig. 6.20 a shows the reconstructed movement of the condylus centre, it is seen that this snugly tracks the curvature of the initial part of the temporal articulating joint surface. Closer inspection has even confirmed that the condylar trajectory in mouth opening is some mm below the closing path, due to the absence of closing force activity.

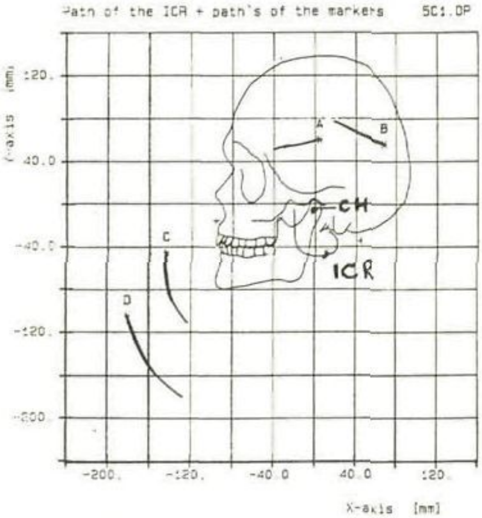

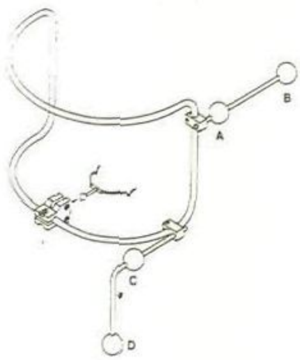

Fig. 6.19 a. Sample polar plot in mouth opening and closing; CH denotes condylar head, ICR is polar locus of ICR

b. Dental brace and markers

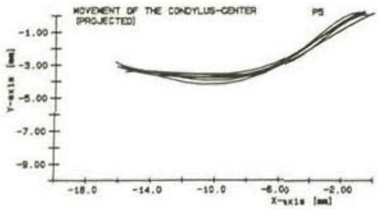

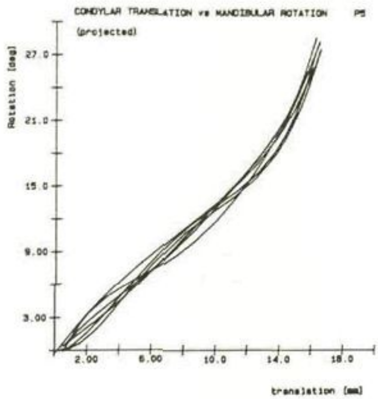

Fig. 6.20 a. Trajectories of condylus in mouth openings/closings

b. Mandibular rotation vs. hor.condylar translation.

(figs. 6.19 and 6.20 courtesy C.H. Falkenström)

Finally fig. 6.20 b seems to resolve a controversy (Smith 1985) on the question if mandibular translation occurs concurrently with rotation, in favour of an at least initially linear relation. With the tendency that only at large mouth openings, rotation continues with a slight further condylar translation. The concurrent vertical translation is seen in fig. 6.20 a.

These findings, already, pose quite a challenge to prosthetic design. Ongoing analysis of these and planned PRIMAS sessions is by programs written in ASYST. Papers by Falkenström and the author were submitted.

6.6 Real-time object tracking

Further automation in ship-to-shore unloading offers promising rewards as to crane efficiency and safety in the handling of bulk material and containers. After hoisting, the horizontal transport of the load, with its acceleration and deceleration, tends to induce inertial phenomena, even oscillations, which should dampen before the load may be dumped, deposited or transferred.

The ASEA Pendulum Control System (ASEA AB, Västeras, Sweden) is an **open loop controller** for the horizontal trolley speed in a bulk crane, like fig. 6.21. An on-line simulator of the trolley and grab movements enables the use of maximum machine acceleration and deceleration with independence of the rope length. The optimized trolley speed profile, shown in fig. 6.22, even allows unloading the grab on-the-fly near its return point, as an additional speed saver.

Fig. 6.21. Bulk crane *(courtesy ASEA)*

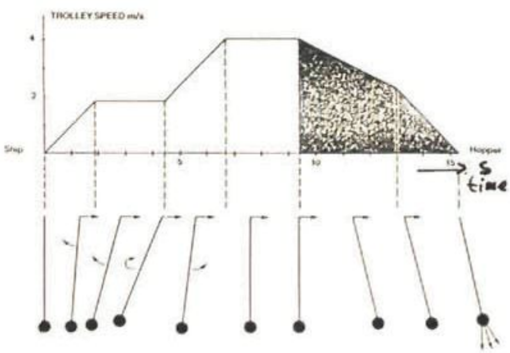

fig. 6.22. Speed profile *(courtesy ASEA)*

This ballistic approach presents a perhaps unexpected parallel to the on-off activation expounded in (Denier van der Gon et al. 1965, 1977) for the control of fast goal-directed human movement.

However, much as visual input is needed for the fine tuning of human movement near its intended goal, ASEA engineers considered the design-in of a position sensing subsystem for **feedback** purposes in container cranes. With containers, the stacking or the positioning on shoreside trailers demands, for obvious safety reasons, an optimally accurate descent and deposition. Human operators work an only four hours shift.

Through Remplir Optoelectronics, Stenkullen S (former manufacturers of the IROS system, cf. section 3.7) we got involved in pilot experiments at a container crane in Gothenburg harbour, may 1987, with ASEA and Lulea University staff.

A 50 Hz Primas system, with our prototype stroboscopic camera equipped with high efficiency red LED's, and a Compaq II portable PC, was set up in the trolley and control cabin. This, with the crane operator and us a bit giddy experimenters, rode back and forth across a windy crane beam at 30 m above ground, cf. fig. 6.23.
Like the precipice view of fig. 6.24, the TV camera looked down at the spreader (container clutch and hold device) which for the occasion carried four retro-reflective markers, assembled from the roadmarking plastic variety.

Fig. 6.23. Container crane *(courtesy Remplir)*

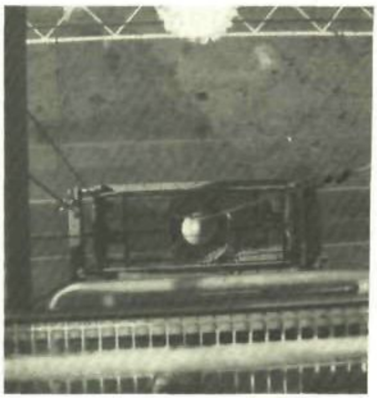

fig. 6.24. View on spreader *(courtesy Remplir)*

In bright sunny weather, the markers were picked up well enough, also out over the water, in a wide range of spreader hoisting heigths.

The marker disposition was such that two large outer ones were in the field of view with the lowered spreader, while two smaller interior markers took over with the spreader coming up. The marker pairs served the software estimation of projected horizontal position and attitude of the spreader, as well as its height, with the single camera.

The 50 Hz sampling rate allowed a fair degree of coordinate smoothing in view of the low frequencies involved.

The unpublished results, analysed at Lulea University, where another telemetric feedback system had been proposed, favoured the selection of the TV-based system over competing remote sensory media. The merger of Asea with the Swiss company of Brown Boveri has apparently delayed regaining of the initiative.
Within the SPIN-funded project with High Technology Holland bv we are entering discussions with another crane manufacturer.

The tentative real-time marker identification software by M. le Gal (1988), referred to in section 4.5, primarily concerned the container crane project. It allowed two sets of four markers, instead of the two pairs described above, to introduce redundancy in the estimation of position and yaw of the container, or to allow the estimation also of the roll and pitch angles in the case of unsymmetric hoisting.
Again, in view of the large inertias involved, the processing rate was not at a premium.

For generality's sake, the real-time marker identification as taken up by Schilt (1989), cf. section 4.5, is concerned with speed indeed, as it assigns markers to coordinates as these are being acquired at the TV field rate. The routine does also allow for relative marker motion.

6.7 Miscellaneous

Bordering the above industrial transport application, is the excursion of PRIMAS towards a multi-purpose **barcode teledetection** system. This was demonstrated at the University's Traffic and Transport Fair, 1988. The 5*30 cm coded tags were assembled with the bars being of retro-reflective sheeting separated by covering material. The stroboscopic PRIMAS camera, equipped with a telelens and the strobed infrared LED illuminator, viewed the tags at some 15 m distance. Standard operation delivered the centroid coordinates of each of the bars in real time, it was by software running on the host that the barcodes were recognized. In this respect, any video frame grabber with the proper camera subsystem may be programmed to perform the job, no subpixel resolution or real-time TV-rate operation being required [2].
Features of the TV-based system, apart from the facility of bridging large distances, are the immunity to tag orientation, discrimination of multiple tags in the field of view, and the additional capacity of exact tag location and tracking.

Closer to the original task of position and movement recording was the *pilot application in* ***stress-strain materials research*** *at the* Fundamental Mechanics Dept. (J. Jansen), University of Eindhoven. Here minute creep was recorded with 8 marker dots of retro-reflective 3M sheeting stuck to a 2 cm dia. lead cylinder sample, subjected to an increasing axial compression force.
Fig. 6.24 a shows the X,Y excursions of the markers, with a sketch of the sample pellet and the identification of marker number 8. The scale values refer to the basic pixel grid. Total X-excursion of marker # 8 amounted to 1 mm. Fig. 6.24 b displays X-displacement vs. field number for marker # 8. The 1986 PRIMAS prototype was run at the reduced rate of 6¼ fields/s, so 2000 fields cover a 320 s experiment. Processing of these data took a mere 5 minutes.
The merits of contactless multi-marker recording, up to a 10*10 marker grid, at high resolutions in space and time, with on-site reduction of large experimental runs, favour the dynamic stress-strain analysis in metallurgy as well as in biological and artificial tissues. The modest pilot project, demonstrating some of the way to go, was instrumental in the application for the *SPIN* grant mentioned in section 4.5.

note
2 *With Philips Norway in the vanguard, TV-based barcode detector boards have been seen to appear on the market.*

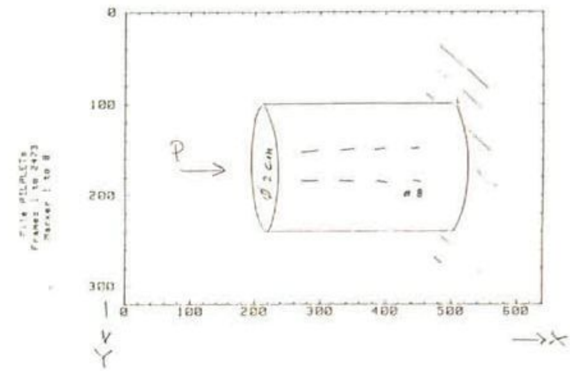

Fig. 6.24 a. Axial compression of metal pellet, marker trajectories.

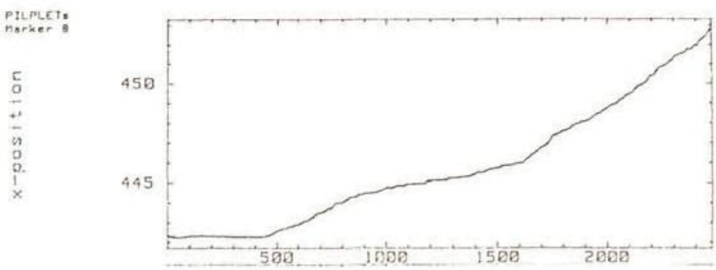

Fig. 6.24 b. Same, marker #8 axial creep vs. field number, cf. text.

Projects under consideration range from underwater models of flexible risers in the offshore industry to eyelid blink in neurology.

At MARIN, the Maritime Research Institute Netherlands, the behaviour of **flexible risers** is studied with realistic models as well as by simulation. Riser systems provide a compliant link between subsea well and floating surface vessels like production and storage facilities, cf. fig. 6.25. A subsea floater is shown to maintain riser curvature. Fatigue risk is incurred by the 3-D motion of the riser piping, that may be induced by current, wave forces and floater motion.
In considering a TV-system for underwater model studies, to supplement the mathematical simulations, MARIN [3] investigators are interested in the real-time identification and extraction of at least some of the markers, though not necessarily at the PRIMAS rated 100 Hz.

note
3 *For MARIN effort in multi-frequency PSD systems, cf. section 5.4*

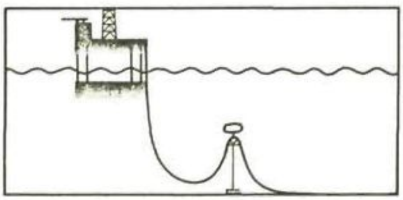

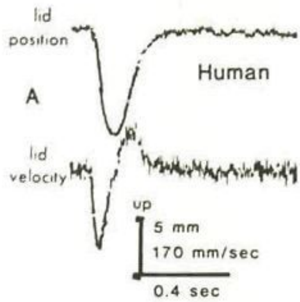

Fig. 6.25. Flexible riser diagram *(courtesy MARIN)*.

Fig. 6.26. Vertical eyelid blink. *(courtesy C. Evinger)*

At the time of formulating a project with the Clinical Neurophysiology Dept. (O.J.S. Buruma), University of Leiden, there was no literature on the non-contacting recording and analysis of **eyelid blink** dynamics, other than by high-speed photography. A major contribution by (Evinger et al. 1984) depends on recording vertical motion of the upper eyelid by a lever and silk thread system of low inertia, transferring its displacement to a single miniature LED imaging on a PSD sensor system. Fig 6.26 presents an illustrative result, where the downward motion is accomplished in some 0.15 s. Horizontal motion, which is thought to be functional in the eyeball cleaning, has been still less accessible to recording. Interest should well be focused on blink, if it were easier to record, for a range of research and diagnostic aspects in neurology and psychology. And next to the saccade it presents one of the fastest motions designated as ballistic, in the sense of a probable open loop control, with a biphasic agonist and antagonist muscle activity.

The PRIMAS 200 Hz scanning option at half-image height, described in section 4.4, is eminently suited for binocular recording of blink, in both directions in the projected image plane. Dual camera 3-D analysis offers exciting prospects. Preliminary effort (with J.G. van Dijk) has concentrated at the retro-reflective marker(s), for this should attach safely and surely to the eyelid, and remain well visible while travelling across the spherical eye surface. This tends to change the angle of incidence to the LED and lens assembly, unless a tiny ball be made.

Summing-up and extrapolating this application chapter, the exhortation by Kruse (1964), quoted in section 2.10, would seem fully to apply.

CHAPTER 7. CONCLUSION

7.1 Early and alternative systems

An introductory sketch has summarized historic development in movement recording for subsequent analysis, motivated by scientific interest in human and animal motion. Film analysis of landmark points, originating from Marey's great invention (1888), has benefited from the advent of the digital computer, and not only in the biomedical field. But, as reviewed, systems for other than manual, frame by frame transcription of the abundant marker coordinate data emerged only by the 1970's.

As a research tool in prosthetics control, we developed an original multi-marker TV-based coordinate data acquisition system to interface a minicomputer in real time at the standard TV field rate. This non-contacting measurement device obviated the intermediate stage of film recording and processing. Two binary counters, synchronized with the TV scan, and read out at video threshold crossings, were at the heart of the new video-digital coordinate converter. Basic X,Y resolution was 8+8, later 9+9 bit.

Chapter 2, dealing with the early Mark I versions of this automated movement recording system, has much of the detail reviewed in a synopsis section, to be consulted for completeness.
Already the 1967 prototype had the option of suppressing all but one upper point on each of the marker image contours, thus providing the additional data reduction which remained a hallmark of all subsequent development. The inherent first stage data reduction is the processing of no other than the edges of above-threshold video signal.
Notably these features distinguish the system from much of the later video frame grabbers for computer analysis of mostly (quasi-)static pictures. As an initial lead however towards greyscale frame grabbing, a system enhancement was implemented for the on-line computer input of black-white, detailed pictorial data as early as 1969.
As a facility to improve accuracy and resolution, our later prototypes had the option of digitizing two or four diagonal points on the marker contours, with software to estimate marker midpoint coordinates.

Low-lag Plumbicon ® tube cameras were used to prevent streaking of the marker images, but the introduction of a synchronous rotating shutter did more than that. It also provided the equidistant and simultaneous sampling of the markers, regardless of position in the image field.
The first prototype already had the choice of using active markers in the form of subminiature lamps or passive reflective paper disks. With the latter, synchronous stroboscopic illumination by fluorescent UV tubes replaced the mechanical shutter contraption as early as 1974.
By that time, viability of the TV/computer motion analysis system was documented in collaborative projects, such as on cat locomotion.

Concurrently with the hardware, software was pioneered that remained characteristic for all subsequent TV-based motion analysis systems. It concerns the identification of the moving markers, where coordinate data must be reassigned if and when the marker projections change in their relative vertical positions. This need for reordering is due to the fact that the TV image is scanned from top to bottom, implying a primary ordering of the raw data coordinate pairs in increasing values of Y. Coordinate assignment by prediction, by extrapolating the marker trajectories is the basic method implemented right from the beginning. A-priori knowledge, such as the geometric distribution of the markers at rest, was also used in early times, though at a loss of generality.

Intermediate stages in the Mark I system series were the interfacing to digital tape storage for motion studies outside the laboratory, the interfacing to the in-house HP-1000 series of minicomputers and the adoption of buffering and multiplexing to accommodate more cameras and to allow the synchronous acquisition of other than kinematic data.

In chapter 2, one section reviews the rather fragmented literature as to the previous use of TV cameras on-line with computers, revealing no comparable real-time multi-marker coordinate data acquisition systems.
Chapter 3 discusses a crop of later configurations, which have emerged as derived or independent, abortive, follow-up or alternative efforts. These latter include commercial systems based on non-TV sensors.
The early merits of TV-based marker coordinate acquisition were most clearly stressed by its adoption in a collaborative project with the Bioengineering Unit at Strathclyde University, Glasgow. Expanded to a multi-camera configuration and with dedicated DMA interfacing to a DEC PDP-12 host computer, new system design was first reported in 1974.

The Strathclyde system, still in place today, gave rise to VICON, the first commercial TV-based motion analysis system, manufactured and marketed by Oxford Instruments, later Oxford Metrics Ltd. UK in 1981. VICON offers a multi-camera turnkey system hosted by the PDP(LSI)-11. Both systems lack the data-reduction from marker contours, marker centroids being assessed by software. Buffering, DMA and large disk requirements or a limitation to short runs are among the consequences. Similarly with later competitors ELITE (1985) and ExpertVision (1988).

To the Strathclyde system developers, TV-based motion analysis owes the use of retro-reflective markers assembled with Scotch 3M ® tape, followed by the use of LED's for marker illumination.
Of other early TV-based work, only the CINTEL system, though abortive, deserves the credit of novelty and real motion analysis applications.

In the non-TV commercial marker motion analysis arena, main contest-tants are the SELSPOT system (1974) and OPTOTRAK (1988). The OPTOTRAK manufacturer draws heavily on the CoStel (1979) system, after having dropped its WaTSMART (1986) near copy of the SELSPOT system. All these systems use active markers in the form of IR LED's, switched in time-multiplex. This provides inherent marker identification, but entails non-simultaneous sampling of the markers, which should be compensated by software to attain rated accuracy. Smoothing, incurred by non-ideal interpolation, tends to compromise the benefit of these systems' high sampling rate, which is between 2.500 and 10.000 samples/marker/s.
The overall sampling rate, indeed, depends on the number of markers.

OPTOTRAK, using linear CCD photodiode arrays and non-linear anamorphic optics, attains its rated accuracy by real-time lens correction, which involves all of the 4 Mpixels per dual-axis camera. SELSPOT, which uses a non-addressable PSD sensor in its best approximation to linear operation, has the additional problem of spurious reflections from the marker LED's. These tend to bias the measured marker image position.

The CODA-3 system has merited a discussion in chapter 3, concluding that for scientific and commercial impact this mechano-optoelectronic system offers too few advantages to offset the serious drawbacks.

Chapter 4 returns to the author's work with reviewing the more recent contributions in TV/computer motion analysis systems.

7.2 PRIMAS Precision Motion Analysis System

In recognizing the merits of marker centroid estimation in software, as in (Taylor et al. 1982), it was in line with our unique feature of data reduction to mechanize centroid estimation in real-time hardware. This meant the elimination of the early contour suppressor. From a 16-bit microprocessor board, with dual-port RAM buffering and additional high-speed arithmetic VLSI chips (1984), the centroid unit developed (1987) into a faster 32-bit board, while dropping the arithmetic chips (1989), to accomodate up to 50 markers, sized 10 TV-lines, at the elevated 100 Hz TV rate.
Marker centroid estimation yields the benefit of sub-pixel resolution, as corroborated by the tests reviewed at the end of chapter.

Interfacing to the host computer was modified, to hook up first to an HP-9000 series desktop, to yield a mobile system for projects outside the laboratory. The present PRIMAS system (1986) is hosted by IBM-AT compatible PC's.
For both system implementations, the data acquisition, control and all subsequent analytical software was written mainly as students' contributions. It should be added that these include marker identification routines, as well as 3-D camera calibration plus 3-D point and marker cluster reconstruction. The latter routines serve the position and attitude estimation of articulating segments, examples of which are given in chapter 6.
Returning to the system and host configuration, some alternatives are discussed for multi-camera, multi-marker multi-processor applications, part of this belongs to work in the near future.

Having used a solid-state matrix camera by 1984, the benefits of a stable pixel geometry, deposited with a high degree of accuracy and linearity, were convincingly apparent, as already indicated by the end of chapter 2. Distorsion correction would only concern the radially symmetric non-linearities of a quality 16 mm cinecamera lens.
Moreover, adopting the frame transfer CCD sensor it was found amenable to a doubling of the TV scan rate to 100 fields/s, so to improve the PRIMAS system sampling rate.

At the same time, it was managed to tailor the frame transfer control pulses, so to make a new reduced-integrationtime, stroboscopic camera.

This electronically-shuttered PRIMAS camera (1986) boasted an aperture time of 1:20 of the field period (by 1988 1:100 or 0.1 ms), without recourse to an opto-electronic variable opacity device in the optic pathway. Main feature of the 100 Hz stroboscopic TV camera is contrast enhancement of the already stroboscopically lit retro-reflective markers against the ambient or background scene highlights. This has allowed PRIMAS to relax the ambient light conditions or background clutter, so to operate even in outdoors broad daylight or in demanding industrial circumstances.
This feature obviates the need for real-time video processing, such as crosscorrelation and template matching in the ELITE system as a means of separating clutter from circular marker images of a certain size.

With the CCD camera's pixelclock being provided from the system, the synchronization at all levels of camera and video-digital coordinate converter has led to the low-noise, high-precision operation witnessed in the performance section of this chapter. Another contribution to the remarkable specification is the excellent video amplifier stage in the measurement-quality MX-type cameras by High Technology Holland bv. These have incorporated the reduced-integrationtime feature, within a SPIN-funded collaboration project (1988).

After reviewing some of the literature on sampling rate requirements in biomechanics applications, as well as on noise propagation in the case of differentiating measured position data to obtain the often desired (angular) velocities and accelerations, the figure of merit for spatio-temporal resolution is introduced in the revised form of $Q = (\sqrt{f})/p$. Here f denotes the sampling rate and p the precision.
The conclusion is that increasing the sampling rate is effective only under the square root, while precision is of direct influence. This is where PRIMAS improvement has been mainly aimed.
Based on the performance tests reviewed and on the commercial systems' datasheets, PRIMAS scores highest in the final systems comparison of spatio-temporal resolution. Moreover some provisos, as reviewed above, apply to the other high-scoring non-TV commercial systems.

Reliance on the TV-category of sensors, especially of the solid-state variety, would seem to have been the best choice and a guarantee for affordable progress in system performance just by keeping in step with rapid development of this worldwide mass-produced precision part.

7.3 Synchronous detection PSD system

Contrasting with the above, chapter 5 reports a sideline activity to improve on some of the SELSPOT system's shortcomings, while retaining the high sampling rates typical of the PSD sensor (non-TV) camera.
Using frequency-multiplex instead of switching for identifying the LED markers, the method of synchronous detection was applied to retrieve the distinct LED signal amplitudes which, like in the SELSPOT system, correspond to the projected marker image coordinates.
It is shown that with moving markers the algorithm of periodic multi-frequency synchronous detection works out to the simultaneous sampling of the frequency component amplitudes, or marker positions.
Moreover, constant ambient or background illumination is absolutely rejected, and the interference of electric light severely suppressed. This in its turn, permitted the use of visible-light LED's, to reduce the problem of spurious reflections.
With respect to sensor noise, synchronous detection is seen to behave like a narrow bandfilter, the equivalent noise bandwidth equalling the marker sampling rate. The (240 Hz) marker sampling rate is the inverse of the summation period in periodic synchronous detection.
Basic LED frequencies, in the 10 kHz range, being chosen as harmonics of the sampling rate, it is seen that (even within a relatively narrow band) a selection may be made of a number of LED marker frequencies, such that none equals a higher harmonic of the other. Harmonics risk to be produced by non-linearities of the LED emission characteristic. This arrangement ensures zero crosstalk with synchronous detection in the case of multiple stationary markers.
A separate investigation has yielded the phase relations for these anharmonic LED marker frequencies, such as to obtain a minimum crest factor in the summed multi-frequency PSD signal. With a margin for the case of moving markers, this aims to prevent saturation of the PSD.
With a moving marker, the relatively low frequency components involved are amplitude modulating the PSD signal frequency, and synchronous detection was shown to behave like a low-pass zero-phase filter.
Tapered windowing of the synchronous detection signals, may flatten out the transfer function towards higher movement frequencies.
Furthermore, windowing impressively reduces the crosstalk from moving markers, with a further suppression of ambient electric light.
A progression of prototype systems, yet without windowing, is reported together with tests of their low-noise, low-interference performance.

7.4 Synopsis of contemporary systems

In the following overview the systems encountered in previous chapters are tabulated according to a selection of viewpoints and features.

1. **non-TV systems** — sampling rate
   - inherent marker identification
   - high speed

1.1 active markers

1.1.1 non-simultaneous marker sampling:

PSD sensors	SELSPOT (1975), SELSPOT-II	10	kHz/marker
	WatSMART	5	"
CCD line sensors	CoStel (1979, 1988)	1	kHz/marker
	OPTOTRAK (1988)	2.5	"

1.1.2 simultaneous marker sampling:

Delft Synchronous Detection PSD system (1977/88) — 240 Hz

1.2 passive markers
non-simultaneous X,Y and marker sampling,
and non-equidistant marker sampling:

electro-mech.scanner CODA-3 (1981) — 300 Hz

2. **TV-based systems**

   - passive markers

2.1 software marker identification
moderate speed
simultaneous marker sampling
(w. strobed illumination and/or strobed TV cameras)

Delft Mark I system	(1967)	50/60 Hz
Strathclyde system	(1974)	"
VICON	(1981)	"
ELITE	(1985)	50 Hz
Delft PRIMAS system	(1986)	50,100 Hz
ExpertVision	(1986)	60 Hz

(most systems have 200 Hz, taped or directview upgrades by 1989)

2.2 inherent marker identification
high speed (small amplitudes)
non-simultaneous marker sampling
(w. random access image dissector camera)

HENTSCHEL	(1988)	7.5 kHz/marker

Cf. table 4.4 for a comparison of spatio-temporal resolution qualities.

Not tabulated is the Kodak Ektapro, a 1kHz TV tape recording system, where the off-line replay mode offers some analytical features.

7.5 Discussion

To return to the mainstream of TV-based motion analysis systems, the final application chapter 6 reviews a cross-section of collaborative projects in the biomedical and industrial fields. Upgraded sampling rate, improved resolution and precision, enhanced contrast of the passive retro-reflective markers, multi-camera operation and versatile 3-D software have left their mark in a range of demanding topics.

Concurrently, this decade's literature abounds of rewarding research projects in human, animal and industrial movement, accomplished with either TV-based or original and derived SELSPOT systems.
Now we have seen that, besides inherent marker identification, the only real advantage of non-TV systems resides in the sample rate. But also, oversampling was seen to be less effective than enhancing system precision, to improve spatio-temporal resolution and combat noise.

Summing up the TV story from another viewpoint, we were at the cradle of a viable brainchild, which developed throughout infancy, soon made foreign friends and through these went into business at the age of 13, begot some 30 VICON offspring in a 5 year period, then with the family branching out to include some new names and adding the input of clever uncles or aunts, grew into what today totals an estimated $ 20 million business of some 200 units installed in science and industry.

The prospects of this successful family look bright, and already some future improvement was discussed, where we are planning to contribute.

The real-time marker centroid estimation, which already outputs height and width bytes next to the coordinates, should be refined to cater for the rare case of pathological markers, which risk to occur as the connected images from separate marker projections.
To bring accuracy to the point of meeting the geometric accuracy of CCD's, a thorough camera calibration routine is called for, which takes care of internal parameters like lens distorsion, sensor skew and sub-pixel location of the principal point.
Marker identification routines are beginning to use dual-camera data, to resolve apparent ambiguities in the single projection plane. These would seem to be the most pressing software areas. First results were already discussed of performing the marker assignment in real time.

Concurently, commercial systems focus on user-friendly, full-blown software packages, from data acquisition to final 3-D analysis. This drive to market packages, developed in collaboration with a few main customers, may prove to be one of their main competitive strengths.

Now our hardware projection is, that in the high-speed arena SELSPOT, though more original and with a longstanding customer and software base, will lose out to the high-accuracy OPTOTRAK, mainly because of the spurious LED reflection problems.

The LED reflection, though minimized, is a reason for not pursuing our synchronous detection PSD system with the vigour devoted to PRIMAS.

In bridging the gap with systems like OPTOTRAK, TV-systems will indeed be achieving higher sampling rates. One of the reasons being sheer technology push, as HDTV will bring higher pixelrates to the industry. This should reflect in still other rapid-scan devices than the Ektapro chip. Meanwhile we will probably not be alone in making a smarter use of the present crop of mosaic sensor chips.

On the other hand, one sees a new acceleration of microcomputer and PC number crunching power, of memory size and speed, joined to an immense interest in picture processing. A host of talented people in dedicated enterprises, or enterprising universities, is working at sophisticated TV frame grabbers and associated software. Constant drive for robotics applications pushes the demand for real-time operation unto realistic timescales, set by at least the standard TV framerate.
There should be no surprise, if real-time frame grabbing and feature extraction algorithmics would succeed to converge upon high-resolution sub-pixel estimation of marker centroids within a few years. The first limited-performance systems have been leaving university environment.

That would, after 25 years, tend to obsolete the direct approach of marker-oriented data reduction, that was introduced by the binary video-digital coordinate converter, basically just two counters on a pixel grid, the leading theme of this book.

REFERENCES

AALDERINK, B.J. (1970). Automatische chromosoomanalyse: inleidend onderzoek (Dutch). MSc thesis june 1970, Faculty of Applied Physics, Delft University of Technology.

ABDEL-AZIZ, Y.I. and H.M. KARARA (1971). Direct linear transformation from comparator coordinates in object-space coordinates in close-range photogrammetry. In: Proc. ASP Symp. Close-range Photogramm. Urbana Ill jan. 1971, p 1-18.

ALLEN, J.R., A. KARCHAK, V.L. NICKEL and R. SNELSON (1966). The Rancho Electric Arm. In: Proc. 3rd Annual Rocky Mountain Bioeng. Symposium, may 2-3, 1966, p 79-82.

ANDREWS, B.J. and D. JONES (1976). A note on the differentiation of human kinematic data. In: Dig. 11th Int.Conf.on Med.& Biol.Eng.,Ottawa 1976, p 88-89.

ANDREWS, B.J., G. THYNNE, S.M. NICOL and A.Q. BEALE (1981). The Strathclyde tv/computer system for 3-D human motion analysis. In: Computing in Medicine, J.P. Paul et al. (eds), MacMillan London 1982, 6 p

ANDREWS, B.J. (1982). On-line locomotion analysis using television techniques. PhD thesis july 1982, Univ. of Strathclyde, Glasgow, 301 p

ANDRIESSE, B. (1977). Analyse van de armbeweging (Dutch). MSc thesis jan. 1977. Faculty of Applied Physics, Delft University of Technology.

ANONYMOUS (1973). A vidicon to minicomputer converter. Digital Design **3** # 5, may 1973, p 32-34.

ANTONSSON, E.K. and R.W. MANN (1985). The frequency content of gait. J.Biomechanics **18**, p 39-47.

van ANTWERPEN, G. (1983). Digitale signaalverwerking ten behoeve van bestudering van de lichaamsbewegingen van patienten met de chorea van Huntington (Dutch). MSc thesis june 1983, Faculty of Applied Physics, Delft University of Technology.

ARZBAECHER, R.C., D.I. CHEIFETZ and D.C. CARRON (1970). A digital system for the study of eye-movements. Med.Res.Eng. oct-nov.1970, p 23-25

ASEA Pendulum Control System, trade literature, Västeras, Sweden.

AYLOR, J.H., R.L. RAMEY, B.W. JOHNSON and S.I. REGER (1984). Motion analysis by raster-scan image source and image processing techniques. IEEE-IM **33** # 4, dec.1984, p 301-306.

AYOUB, M.A., M.M. AYOUB and J.P. RAMSEY (1970). A stereometric system for measuring human motion. Human Factors **12** # 6, p 523-535.

BAHNIUK, E. and M.J. WIJNSCHENK (1964). Design parameters for an orthotic arm aid. In: ASME Winter Annual Meeting, Philadelphia nov. 17-22, 1963, 12 p.

BAKX, J. (19777). Positiedetektiesysteem (Dutch). Trainee report, 1977 Faculty of Applied Physics, Delft University of Technology.

BATTYE, A., A. NIGHTINGALE and J. WHILLIS (1955). The use of myo-electric currents in the operation of prostheses. J.of Bone & Joint Surg., **37B** # 3, aug. 1955, p 506-510.

BAUM E. (1978). Motografie - Grundzüge einer arbeitswissenschaftlichen Methode zur Bewegungsaufzeichnung. Z.f.Arbeitswiss.sch. **32** # 2,p 71-76

BAUM E. (1986). Motografie - Eine Methode zur Betrachtung und Messung von Bewegungen. In: Motografie, herausg. E. Dorrer u. J. Peipe, Schriftenreihe UBW Heft 23, München 1987 ISSN 01731009, p 43-52.

BAUMANN, J.U., Ph. PROCTER and Th. KLOSSNER (1983). Camera speeds in gait analysis. In: Proc. IX ISB, D. Winter ed., Waterloo, Canada, 6 p.

BERGER, N. and C.R. HUPPERT (1952). The use of electrical and mechanical muscular force for the control of an electric prosthesis. Am.J. of Occup. Therapy, **6** # 3, p 110-114.

BERNSTEIN, N. (1930). Analyse der Körperbewegungen und Stellungen im Raum mittels Spiegel-Stereoaufnamen. Arbeitsphysiologie **6** # 3.

de BIE, J. (1980). Analyse van de armbeweging (Dutch). MSc thesis feb. 1980, Faculty of Applied Physics, Delft University of Technology.

BIJLSMA, J. (1970). Een televisie registratiesysteem voor bewegende objecten (Dutch). MSc thesis june 1970. Faculty of Applied Physics, Delft University of Technology.

BLACKMAN, R.B. and J.W. TUKEY (1958). The measurement of power spectra from the point of view of communications engineering. Bell Syst. Tech. J. **37**, jan./march 1958, reprint New York Dover 1959.

BOEKHORST, J.C.A. (1966). Enkele beschouwingen over de realisering van een objecten-klassificerende machine (Dutch). MSc thesis jan. 1966, Faculty of Applied Physics, Delft University of Technology.

BOERHAAVE, H. (1703). De usu ratiocinii mechanici in medicinae. Leiden Verbessel 1703 (French & Dutch translations in: Opuscula selecta Neerlandicorum de arte medica, van Rossum, Amsterdam 1905).

BORELLI (1679). De motu animalium. Rome 1679.

BOS, A. van den (1987). A new method for synthesis of low-peak-factor signals. IEEE-Trans.ASSP **35** # 1, jan. 1987, 120-122.

BOS, A. van den (1989). Estimation of Fourier coefficients. Accepted paper, IEEE-Trans.IM.

BOTTOMLEY, A.H. (1962). Working model of a myoelectric control system. In: Proc. Symp. on Automatic Control in Prosthetics. Belgrade, ETAN.

BOTTOMLEY, A.H. and T.K. COWELL (1964). An artificial hand controlled by the nerves. New Scientist **282**, 12 march 1964, p 668-671.

BRAUNE, C.W. and O. FISCHER (1891). Die Bewegungen des Kniegelenkes nach einer neuen Methode am lebenden Menschen gemessen. Abhandlunge Math.-Physische Classe d. Kön.Sächs.Ges.f.Wissensch. **17** # 2, p 1-76.

BRAUNE, C.W. and O. FISCHER (1895). Der Gang des Menschen I. Abhandl. Math.-Physische Classe d. Kön.Sächs.Ges.f.Wissensch. **21**, p 153-322.

BRESLER, B. and J.P FRANKEL (1950). The forces and moments in the leg during level walking. Trans.ASME **72**, paper 48-A-62, p 27-36.

BROWN, D.A. (1969). Advanced methods for the calibration of metric cameras. In: Proc.1969 ASP Symp.Computat. Photogramm. Syracuse NY.

BRUEGGER, W. and M. MILNER (1978). Computer-aided tracking of body motions using a c.c.d. image sensor. J.MBEC **16**, march 1978, p 207-210.

BRYANT, C.D. (1962). Non-contact dimensional measurements by optical and electronic techniques. IRE Trans. Indust.El., may 1962, p 1-6.

BURUMA, O.J.S., R.A.C. ROOS, G. VAN ANTWERPEN and E.H. FURNÉE (1983). Assessment of Dyskinesia. In: Dyskinesias, Proc. Japanese-Dutch workshop Leiden, oct. 1983, Actua Sandoz **7**, Alphen 1984 ISBN 9060162358, p 138-141.

CARLET, M.G. (1872). Essai experimental sur la locomotion humaine - étude de la marche. Ann.d.Sc.Nat.Zoöl. **16**, (series 5) art. 6, p 1-92.

CHARLIER, J.R. and J.C. HACHE (1982). New instrument for monitoring eye fixation and pupil size during the visual field examination. J.MBEC **20**, jan.1982, p 23-28.

CHENG, I.S. (1974). Computer-television analysis of biped locomotion. PhD thesis 1974, Ohio State University, Columbus.

CHENG, I.S., S.H. KOOZEKANANI and M.T. FATEHI (1975). Simple computer-television interface system for gait analysis. IEEE-BME, may 1975, p 259-260.

CHISSIN, C. (1906). Ueber die Oeffnungsbewegung des Unterkiefers und die Beteilung der auesseren Pterygoidmuskeln bei derselben. Arch.Anat. Entwicklungsgesch. 1906, p 41-67.

CODA-3 trade literature (1981 on). Movement Techniques ltd. Loughborough Leics. UK.

COLLET, M. (1985). Frame-transfer, X/Y and interline image sensors: how do they compare? Photonics Spectra sept. 1985, p 103-112.

COLLET, M. (1986). Solid-state image sensors. Sensors and Actuators **10** p 287-302.

COLLEWIJN, H., F. VAN DER MARK and T.J. JANSEN (1975). Precise recording of human eye movements. Vision Res. **15**, p 447-450.

CONNORS, W.P. (1971). Lateral photodetector operating in the fully reverse-biased mode. IEEE-Trans.ED **18**, p 591-596.

CoSTEL trade literature (1989). LOG.IN srl, Roma.

DEMPER, H. (1985a). Koppeling van het rekenend meetinstrument aan een HP-9816 personal computer (Dutch). BSc report sept. 1985. Faculty of Applied Physics, Delft University of Technology.

DEMPER, H. (1985b). Simulatie van middelpuntsschattingen van ronde markeringen (Dutch). BSc report, dec. 1985. Faculty of Applied Physics Delft University of Technology.

DEMPER, H. (1986). Onderzoek aan ballistische armbewegingen bij gezonde proefpersonen en bewegingsstoornissen bij patienten met neurologische aandoeningen (Dutch). BSc report april 1986, Faculty of Applied Physics, Delft University of Technology.

DEMPER, H. (1987). Verbeterd rekenend meetinstrument voor bewegingsanalyse (Dutch). MSc thesis aug. 1987. Faculty of Applied Physics, Delft University of Technology.

DENIER VAN DER GON, J.J., J.Ph. THURING and J. STRACKEE (1962). A handwriting simulator. Physics in Med.& Biol. **6** # 3, p 407-414.

DENIER VAN DER GON, J.J. and J.Ph. THURING (1965). The guiding of human writing movements. Kybernetik, **2** # 4, p 145-148.

DENIER VAN DER GON, J.J. and W.J. WADMAN (1977). Control of fast ballistic human arm movements. Proc.Physiol.Soc. **271**, june 1977, p 28-29.

DERCUM, F.X. (1888). The walk in health and disease. In: Trans. Col. Physicians **10**, p 308-338.

DIJKSTRA, Sj. (1973). Evaluation and simulation of fast arm movements. PhD thesis jan. 1973, Faculty of Mathematics and Physics, University of Utrecht, 83 p.

van DIJK, J.G, O.J.S. BURUMA, E.L.E. BOLLEN, H. DEMPER and E.H. FURNÉE (1986). Variability and goal-dependance of velocity and accelaration of fast hand movements. In: Abstr.1986 Congr.Int.Med.Soc.Motor Disturbances. Lausanne, 19-21 june 1986, p 55.

van DIJK, J.G., E.L.E. BOLLEN, E.H. FURNÉE, H. DEMPER, E.A. VAN DER VELDE, R.A.C. ROOS and O.J.S. BURUMA (1988). Movement direction as well as laterality influences peak velocity of fast hand movements. Funct.Neurology 1988 # 3, p 69-78.

DINN, D.F., D.A. WINTER, B.G. TRENHOLM (1969). CINTEL: computer interface for television. Presented at: Int.El.Conf. Toronto, 6-8 oct.1969.

DINN, D.F., D.A. WINTER, B.G. TRENHOLM (1970). CINTEL: computer interface for television. IEEE-Trans Comp. nov. 1970, p 1091-1095.

DUIN, R.P.W., J.A. DE VOS, J.G.M. BAKKER, R.R. DE BOER and E.H. FURNÉE (1977). The recognition of muscle activity patterns for prosthesis control. In: Proc.SITEL-ULG Pattern Recognition Seminar, Liège Belgium 19-20 nov. 1977, p 8.1.1-8.1.9.

EDGERTON H.E., R. BONAZOLI and J.T LAMB (1954). Duration and peak candle power of some electronic flashlamps. J. SMPTE **63**, p 15 et seq.

EDGERTON, H.E. and D.A. CAHLANDER (1961). Holdover in Xenon flashlamps J.SMPTE **70**, p 7 et seq.

EKTAPRO-1000 / SPIN PHYSICS 2000, trade literature (1980 on). Eastman Kodak, Rochester NY, USA.

ELFTMAN, H. (1938). The measurement of the external forces in walking. Science **88**, p 152 et seq.

ELFTMAN, H. (1939). Forces and energy changes in the leg during walking. Am.J.o.Physiol. **125**, p 339 et seq.

ELITE trade literature (1986 on). BTS sprl, Milano, Italy.

EMR PHOTOELECTRIC/SCHLUMBERGER, trade literature ODD 658 (1973). Princeton NJ USA.

ENDEN, A.W.M van den, and N.A.M. VERHOECKX (1989). Discrete-time signal processing. Prentice Hall International (UK) ISBN 0132167638.

ENGEN, T. and L.F. OTTNAT (1967). Upper extremity orthotics: a project report. Orthopedic & Prosthetic Appliance J., june 1967, p 112-127.

EVINGER, C., M.D SHAW, C.K. PECK, K.A MANNING and R. BAKER (1984). Blinking and associated eye movements in humans, guinea pigs and rabbits. J.of Neurophysiology **52** # 2, p 323-339.

EXPERTVISION Trade lierature (1986 on). Motion Analysis Co. Santa Rosa CA, USA.

FALKENSTROEM, C.H. (1988). Aanzet tot het ontwerpen van een kaakgewrichtsprothese: orientatie en bewegingsanalyse (Dutch). MSc thesis june 1988, Faculty of Mechanical Engineering, Twente University.

FEDDERN, U. and S. ZUR FERTH (1984). The frame transfer sensor: an attractive alternative to the camera tube. El.Components & Applic. **6** # 4 p 223-229.

FERRIGNO, G. and A. PEDOTTI (1985). A digital dedicated hardware system for movement analysis via real-time TV signal processing. IEEE-Trans BME **32** # 11, nov. 1985, p 943-950.

FERRIGNO, G. and M. GUSSONI (1988). Procedure to automatically classify markers in biomechanical analysis of whole-body movement in different sports activities. J.Med.& Biol.Eng.& Comp. may 1988, p 321-324.

FINLEY, F.R. (1965). Electromyographic patterns of multiple muscle sources. In: The control of external power in upper-extermity rehabilitation (ed. J. Lyman), Warrenton, april 8-10, 1965, NAS-NRC Washington DC 1966, p 61-83.

FINLEY F.R. and R.W. WIRTA (1967). Myocoder-computer studies of electro-myographic patterns. Arch.Physical Medic. & Rehab. **48** # 1, jan. 1967, p 20-24.

FISCHER, O. (1904). Der Gang des Menschen, VI. Abh.Math-Phys.Cl.d.Kön. Sächs.Ges.f.Wissensch. **28**, p 533-623.

FISHER, C. (1967). An image analysing computer. Bio-Med.Eng. aug. 1967 p 351-357.

FISK, J.D. and M.A. GOODALE (1985). The organisation of eye and limb movements during unrestricted reaching to targets in contralateral and ipsilateral visual space. Exp. Brain Res. **60**, p 159-178.

FRUENGEL, F. (1956). Ein neues Hochfrequenzblitzgerät für lange Blitzserien sowie Anwendungen gesteuerter Einzelblitze in der Spannungstechnik. Z.f.angewandte Physik **8** (1956), p 86-90.

FUCHS, H, J. DURAN and B. JOHNSON (1977). A system for automatic acquisition of three dimensional data. In: Proc. AFIPS Conf. 46, p 49-53

FURNÉE, E.H. (1961). Hoogfrequent telketen (Dutch). MSc thesis oct. 1961, Faculty of Electrical Eng., Delft University of Technology.

FURNÉE, E.H. (1967). Hybrid instrumentation in prosthetics research. In: Proc. 7th Int.Conf.on Med.& Biol.Eng., Stockholm 1967, p 446.

FURNÉE, E.H. (1969). Beeldinvoer voor computers met behulp van TV-camera en video-digitaal-omzetter (Dutch). Polytech.Journal (Holland) 24 # 23, 14 nov. 1969, p 976-978.

FURNÉE, E.H. (1969). Handleiding 11-kanaals interface (XIO) voor IBM-1130 rekenmachine (Dutch). Internal rept. dec.1969, Faculty of Applied Physics, Delft University of Technology.

FURNÉE, E.H. (1970). Graphic input to a digital computer by means of a TV-camera. In: Abstr. IMEKO V, 25-30 may 1970, Versailles, p B-509.

FURNÉE, E.H., J.J.T. HENDRIKS and G.J. VAN INGEN SCHENAU (1972). Movement studies of human extremities by means of a TV-camera interfaced to a digital computer. Unpubl. paper Bioméca I, Paris 7-10 sept. 1972.

FURNÉE, E.H., J.M. HALBERTSMA, G. KLUNDER, S. MILLER, K.J. NIEUKERKE, J. VAN DER BURG and F.G.A. VAN DER MECHÉ (1974). Automatic analysis of stepping movements in cats by means of a television system and digital computer. Proc. Physiol.Soc 22-23 mar.1974; J.of Physiol. **240**, p 3-4 P

FURNÉE, E.H. (1984a). Intelligent movement measurement devices I: video converter with real-time marker processor. In: Proc. 8th Int. Symp.Ext.Control Human Extremities, ETAN Belgrade 1984, Supp. p 39-41.

FURNÉE, E.H. (1984b). Intelligent movement measurement devices II: position-sensitive photocell with multifrequency synchronous detector. In: Proc. 8th Int.Symp.Ext.Control Human Extremities, ETAN Belgrade 1984, Supp. p 41-53.

FURNÉE, E.H. (1986a). Real-time, high resolution estimation with high-speed, stroboscopic TV-cameras. Poster. In: Abstr.ISPO UK Annual, Glasgow, 19-21 march 1986.

FURNÉE, E.H. and B.W.H. KLEISS (1986b). Single-electrodes control of multi-function Otto Bock hand prosthesis by EMG-autocovariance estimation. Poster. In: Abstr.ISPO UK Annual, Glasgow, 19-21 march 1986.

FURNÉE, E.H. (1986c). Innovation in video-digital coordinate measurement for movement analysis. In: Motografie, herausg. E.Dorrer/J.Peipe, Schriftenreihe UBW Heft 23, München 1987 ISSN 01731009, p 127-130.

FURNÉE, E.H. (1986d). Innovation in video-digital coordinate measurement for movement analysis. In: Abstr. Study Inst.& Conf. Biomechanics of human movement. Formia, 16-21 june 1986, p 27-29.

FURNÉE, E.H. (1986e). High-resolution real-time movement analysis at 100 Hz. In: Proc. North Am.Conf.Biomech. Montreal 1986 p 273-274.

FURNÉE, E.H. (1986f). Real-time, high-resolution estimation with high-speed, stroboscopic TV. In: Abstr.5th ESB. Berlin 8-10 sept.1986 p 134

FURNÉE, E.H. (1988a). Motion analysis by tv-based coordinate computing in real time. Invited paper. In: Proc.IEEE-EMBS 10th Ann.Int.Conf., New Orleans, LA USA, IEEE CH2566-8-88,p 656.

FURNÉE, E.H. (1988b). Speed, precision and resolution of a tv-based motion analysis computer. Invited paper. In:Proc.IEEE-EMBS 10th Ann. Int.Conf.,New Orleans, LA USA, IEEE CH2566- 8-88, p 1745.

FURNÉE, E.H. (1988c). Principles and performance of some opto-electronic motion analyzers. In: Proc. 5th Int.Conf.Biomed.Eng., Singapore, 8-10 dec.1988, p 179-182.

FURNÉE, E.H. (1988d). On camera speeds for human movement analysis. In: Proc. 5th Int.Conf.Biomed.Eng.,Singapore, 8-10 dec.1988, p 193-196

FURNÉE, E.H. (1989a). TV/computer motion analysis systems: the first two decades. Symp.on Biolocomotion: a century of research using moving pictures. Formia, april 14-17, 1989. Abstr.in: ISB Newsletter # 34 p 8

FURNÉE, E.H. (1989b). Advances in TV/computer motion monitoring. Invited paper. In: Proc. IEEE-EMBS 11th Ann.Int.Conf., Seattle WA USA, 2 p

GAL, M. le (1988). Détermination de la position et de l'orientation d'un objet solide par l'aide du système PRIMAS pour l'analyse de mouvement. Trainee report (IAESTE) june 1988, Faculty of Applied Physics, Delft University of Technology / Institut Universitaire de Technologie le Creusot France.

GEMMINK, G.W. (1971). Een video digitaal omzetter voor vier helderheidsniveaus. BSc report june 1971, Faculty of Applied Physics, Delft University of Technology.

GILBRETH, F.B. (1911). Motion study. Van Nostrand Co, New York 1911.

GILBRETH, F.B. and L.M. GILBRETH (1919). Fatigue study. Routledge and Sons, London 1919.

GILBRETH, F.B. & L.M. GILBRETH (1920). Motion study for the handicapped. Constable, London 1920.

GLEW, N.L. (1963). Closed-circuit television and the stroboscope. Industrial Electronics, nov. 1963, p 711 et seq.

GODEFROY, J.C.L. (1917). Light-line registration of movement (Dutch), Psychiatr. & Neurol. Bladen **21**, p 431-439.

GODEFROY, J.C.L. (1921). Dystaxia epileptica - an experimental psychological study regarding motor disturbances (Dutch). Psychiatr.&Neurol. Bladen **25**, p 68-129, 272-275.

GOMBERT, S. (1970). Een vierkanaals cycle-steal interface voor de IBM-1130 (Dutch). MSc thesis oct. 1970, Faculty of Applied Physics, Delft University of Technology.

GOODALL, J. (1964). Tool-using and aimed throwing in community of free living chimpanzees. Nature **201** (492), p 1264 et seq.

GREATOREX, C.A. (1960). Image intensification using a flying spot X-ray tube. Advances in Electronics & Electron Physics **12**, New York, p 327 et seq.

GREAVES, J.O.B. (1986). State of the art in automated motion tracking and analysis systems. In: Proc. SPIE **693**, aug. 1986, 5 p.

GRIEVE, D.W. (1969). A device called the Polgon for the measurement of the orientation of parts of the body relative to a fixed external axis In: Proc. Physiol.Soc. 10-11 jan.1969, J.of Physiology **201**, p 70 P.

GROEN, F.C.A. (1969). Het herkennen van enige visuele objecten met behulp van contourvolgers (Dutch). BSc report jan. 1969, Faculty of Applied Physics, Delft University of Technology.

GROEN, F.C.A. (1971). Onderzoek naar het herkennen van menselijke chromosomen (Dutch). In: Proc.IFAC Symp.Aut.Control & Comp. in the medical field, Brussels, 1971.

GROEN, F.C.A., P.W. VERBEEK, N.J. ZIMMERMAN, JJ. HEUSDENS, R. SNIJDER, P.A. VIS, P.H.M. WICHERN, H.J.G. WOLFF, Th. HOEKSMA, W.L. KNOOP and W.T. van BEEKUM (1976). A universal measurement and processing system for two-dimensional images. In:Proc. IMEKO VII, London 1976, p 259-267

GUSTAFSSON, L. and H. LANSHAMMAR (1977). ENOCH - An integrated system for measurement and analysis of human gait. PhD thesis sept. 1977, Uppsala University, UPTEC 7723R, ISBN 9150601202, 230 p.

GUETH, V., F. ABBINK and W. HEINRICHS (1973). Eine Methode zur chrono-zyklographischen Bewegungsaufzeichnung mit einem Prozeszrechner. Int. Zeit.f.Angewandte Physiologie **31**, p 151-162.

HAAS, R.B. (1976). Muybridge - Man in motion. Univ. of Calif. Press, Berkeley CA 1976.

HALBERTSMA, J.M. (1974). Het ontwerp van een helder punt (Dutch). BSc report oct. 1974, Faculty of Applied Physics, Delft University of Technology.

HALBERTSMA, J.M. (1975). Registratie en analyse van bewegingen en spierpotentialen voor het onderzoek naar de neuronale besturing van het lopen bij de kat (Dutch). MSc thesis april 1975, Faculty of Applied Physics, Delft University of Technology.

HALBERTSMA, J.M. (1983). The stride cycle of the cat: the modelling of locomotion by computerized analysis of automatic recordings.PhD thesis june 1983, Delft University of Technology; Acta Physiol. Scandinavica Suppl. **521**, p 1-75.

HAMAMATSU TV CO. trade literature C1181 (1974), Hamamatsu, Japan.

HAMAMATSU TV CO. trade literature C1000, C1055, Hamamatsu, Japan.

HARRIS, F.J. (1978) . On the use of windows for harmonic analysis with the discrete Fourier transform. Proc.IEEE **66** # 1, jan. 1978, p 51-83.

HARVEY, W. (1627). De motu locali animalium. Edited and translated by G. Whitteridge, Cambridge Univ.Press 1959.

HENDRIKS, J.J.T. (1972). Bewegingsstudie van armen en benen door middel van televisie gekoppeld aan een digitale rekenmachine (Dutch). MSc thesis april 1972, Faculty of Applied Physics, Delft University of Technology.

HENTSCHEL trade literature (1988). HENTSCHEL SYSTEM GmbH, Hanover, FRG van 't HOF, F. (1970). An economic and accurate XY-tablet and stylus for the digital conversion of graphical data. In: Physics Exhibition Handbook, Inst. of Physics & Physical Society, London 1970, p 107.

HOLZAPFEL, C. (1981). High-speed color video system for data acquisition at 200 fields per second. SPIE **291**, Biomech.Cinematogr. p 35-36.

HOOPER, C.W. and G.A. STICKLER (1968). Quality measurement on yarn bobbins using TV video waveforms. Meas.& Control 1, mar.1968, p 84-86.

HOUTKOOPER, J.M. (1968). Enkele technieken voor patroon herkennen (Dutch). MSc thesis june 1968, Faculty of Applied Physics, Delft University of Technology.

HYZER, W.G. (1981). High-speed video system provides instant images. Industr.Res.& Developm. feb. 1981, p 180-185.

van INGEN SCHENAU, G.J. (1972). Een televisie registratiesysteem voor bewegingsstudie van armen en benen (Dutch). BSc report jan. 1972, Faculty of Applied Physics, Delft University of Technology.

van INGEN SCHENAU, G.J. (1973). Bewegingsstudie van de arm door middel van televisie gekoppeld aan een digitale rekenmachine (Dutch). MSc thesis april 1973, Faculty of Applied Physics, Delft University of Technology.

van INGEN SCHENAU, G.J., R.W. de BOER and G. de GROOT, (1987). On the technique of speed skating. Int.J.of Sport Biomech. 3, p 419-431.

IROS, trade literature (1985). Remplir Optoelectronics, Stenkullen, S.

JANSSEN, M. (1876). Bull. de la Soc. franç. de la Photogr. 14 dec 1876

JARRETT, M.O., B.J. ANDREWS and J.P. PAUL (1976).A television-computer system for the analysis of human locomotion. In: Proc. IERE Golden Jubilee Conf., Univ.Southampton, 6-8 april 1976, p 357-370.

JARRETT, M.O. (1976) A tv/computersystem for human locomotion analysis PhD thesis june 1976, University of Strathclyde, Glasgow, 312 p.

JARRETT, M.O. and H.J. WOLTRING (1982). Photogrammetric calibration of a TV-based gait analysis system. Suppl.Abstr.(stand-in paper), 3rd ESB Meeting, Nijmegen, jan. 21-23, 1982.

JARRETT, M.O. (1983). Comment on "An automated motion measurement system for clinal gait analysis". Letter to Ed. J.Biomech. **16** # 4, p 301.

KASVAND T., M. MILNER and L.F. RAPLEY (1971). A computer-based system for the analysis of some aspects of human locomotion. In: Proc. Human Locomotor Engineering, 7-10 sept. 1971, Inst.of Mechanical Eng.London p 297-306.

KASVAND, T. and M. MILNER (1972). Pattern recognition applied to measurement of human limb positions during movement. J.o.Cybernetics 2 # 1 p 66-78.

KEMP, B., J.M. FRANZEN, O.J.S. BURUMA and R.A.C. ROOS (1982). Quantification of random body movements by a Doppler radar device. J.of Med. & Biol. Eng.& Comp. **20**, p 539-544.

KENT, J.N., D.J. MISIEK, R.K. AKIN, E.C. HINDS and C.A. HOMSEY (1983). Temporo-mandibular joint condylar prosthese: a 10 year report. J.Oral Maxillofac.Surg. **41**, p 245-254.

KEPPLE, T., S.J. STANHOPE and A.H. RICH (1988). The presentation and evaluation of a video based, six degree-of-freedom approach for analyzing human motion. In: Proc.IEEE-EMBS 10th Ann.Int.Conf., CH2566-8-88, p 649-650.

KLUNDER, G. (1973/1982). Video-digital coordinate converter (Dutch and English). Internal reports and System documents. Motion Studies Lab., Faculty of Applied Physics, Delft University of Technology.

KOBRINSKII, A.E., S.V. BOLKHOVITIN, L.M. VOSKOBOINIKOVA, D.M. IOFFE, E.P. POLYAN, B.P. POPOV, Ya.L. SLAVUTSKI, A.Ya. SYSIN, Ya.S. YAKOBSON. Problems of bioelectric control. In: Proc. 1st IFAC, Moscow, 1960, p 619-623.

KOFSKY, I.L. (1966). Reduction of pictorial data by microdensitometry. In: Symp.o.Aerospace Meas.Techn., Mass.Inst.o.Technol., 7-8 july 1966.

KRUG, W. (1954). Die Anwendung des Aequidensitenverfahrens in der Feinmesstechnik. Feingerätetechnik **3** # 9, p 387-390.

KRUSE, J.R. (1964). Automatic tracker keeps eye on missiles. Electronics, april 6, 1964, p 82-87.

LABAW, K.B. (1970). Theoretical model of the lateral photodiode. In: NCW-IDP 3161, Aviation Ordn.Dept., China Lake CA USA.

LANSHAMMAR, H. (1982). On precision limits for derivatives numerically calculated from noisy data. J. Biomechanics **15**, p 459-470.

LAPPALAINEN, P. and M. TERVONEN (1975). Instrumentation of movement analysis by raster-scanned image source. IEEE-Trans.IM **24** # 3, sept. 1975, p 217-221.

LEDLEY, R.S. (1964). High-speed automatic analysis of biomedical pictures. Science **146**, p 216-223.

LEDLEY, R.S., L.S. ROTOLO, T.J. GOLAB, J.D. JACOBSEN, M. GINSBURG and J.B. WILSON (1965). FIDAC: film input to digital automatic computer and associated syntax-directed pattern-recognition programming system. In: Optical and electro-optical information processing, ed. Tippett, J.T., MIT Press, Massachusets 1965, p 591-613.

LEEUWEN, J.L. van, P. VINK, C.W. SPOOR, W.C. DEEGENAARS, H. FRATERMAN and A. VERBOUT (1988). A technique for measuring pelvic rotations during walking on a treadmill. IEEE-Trans BME **35** # 6, p 485-488.

LENSTRA, A.J. (1987). Simulated annealing toegepast op de synthese van lage-piekfactorsignalen (Dutch). MSc thesis april 1987, Faculty of Applied Physics, Delft University of Technology.

LEO, T. and V. MACELLARI (1979). On-line microcomputer system for gait analysis data acquisition based on commercially available optoelectronic devices. In: Biomechanics VII-B, PWN-Polish Scientific Publishers, Warszawa, p 163-169.

LEVENS, A.S., C.E. BERKELEY, V.T. INMAN and J. BLOSSER (1948). Transverse rotation of the segments of the lower limb in locomotion. J.Bone &.Joint Surg. 30A # 4, p 859-872.

LINDHOLM, L.-E. and K.E.T. OEBERG (1974). An optoelectronic instrument for remote on-line movement monitoring. In:Proc. 2nd Int.Symp.Biotelemetry; P.A. Neukomm ed., Karger, Basel 1974.

LINDHOLM, L.-E. and G.P. PETERSSON (1976). Position sensitive photodetectors with high linearity. In Proc. IEEE-ED Conf., Washington DC, 1976, p 408-411.

LOK, K. (1988). Ontwerp van een seriële interface tussen een VME board en een PC-AT (Dutch). Trainee report july 1988, Faculty of Applied Physics, Delft University of Technology.

LYMAN, J. (1966). Afterword in : The control of external power in upper-extremity rehabilitation (ed. J. Lyman), NAS-NRC, Washington DC, 1966, p 339-344.

MACELLARI, V. (1983). CoSTEL - a computer peripheral remote sensing device for 3-dimensional monitoring of human motion. J.Med.& Biol.Eng. & Comp. 21 # 3, p 311-318.

MAREY, E.-J. (1868). Le mouvement dans les fonctions de la vie. Paris, Ballière, 1868, 480 p.

MAREY, E.-J. (1873). De la locomotion terrestre chez les bipèdes et les quadrupèdes. J.de l'Anatomie et de la Physiologie 9 # 42.

MAREY, E.-J. (1873). La machine animale, locomotion terrestre et aérienne. Paris, Ballière, 299 p, 3e ed. 1882.

MAREY, E.-J. (1885). La méthode graphique dans les sciences expérimentales et particulièrement en physiologie et en médecine. Paris, Masson 1872. 2nd Ed. with supplement: Le développement de la méthode graphique par l'emploi de la photographie. Paris, Masson 1885, 500 + 60 p.

MAREY, E.-J. (1890). Le vol des oiseaux. Paris, Masson, 394 p.

MAREY, E.-J. (1894). Le mouvement. Masson, Paris 1894.

MARQUARDT, E. (1959). Indication for application of the pneumatic arm prosthesis, Part 1 & Part 2. Prostheses, Braces and Technical Aids, autumn 1959 # 6 p 3-10, and spring 1960 # 7 p 4-11.

MARQUARDT, E. (1962). Aktive Prothesenversorgung eines armloses Kleinkindes im 2. Lebensjahr. Jahrbuch d.Fürsorge f.Körperbehinderte, p 245 et seq.

MARSDEN, C.D. (1982). The mysterious motor functions of the basal ganglia. The Robert Wartenberg Lecture. Neurology, may 1982.

McGHEE, R.B., S.H. KOOZEKANANI, S. GUPTA and I.S. CHENG (1976). Automatic estimation of joint forces and moments in human locomotion from television data. In:Proc.4th IFAC Symp.Ident.&SystemParam.Est.,Tbilisi USSR, 21-27 sept. 1976, p 368-376.

MECHÉ, F.G.A. van der (1976). Locomotion in the cat: a behavioural and neurophysiological study of interlimb coordination. PhD thesis april 1976, Erasmus University of Rotterdam, 111 p.

MELEIN, J.B.F. (1987). Driedimensionale registratie van lopen met been lengte verschil (Dutch). MSc thesis sept. 1987, Faculty of Applied Physics, Delft University of Technology.

MERCHANT, J., R. MORRISSETTE and J.L PORTERFIELD (1974). Remote measurement of eye direction allowing subject motion over one cubic foot of space. IEEE-Trans.BME **21** # 4, july 1974, p 309-317.

MESQUI, F. and P. NIEDERER (1981). Motion analysis of simulated vehicle-pedestrian impacts using automated highspeed cinephotogrammetry. In: SPIE **427**: high speed photography, videography and photonics, 1981, p 250-257.

MESQUI, F. and P. NIEDERER (1984). Accuracy aspects of a digital image processing system for recovering spatial trajectories from high-speed film recordings in impact studies. In: Abstr. 4th ESB, Davos, p 328.

MILLER, S., D.J. REITSMA and F.G.A. van der MECHÉ (1973). Functional organisation of long ascending propriospinal pathways linking lumbosacral and cervical segments in the cat. Brain Res. **62**, p 169-188.

MILLER, S., J. van der BURG and F.G.A. van der MECHÉ (1975a). Coordination of movements of the hindlimbs and forelimbs in different forms of locomotion in normal and decerebrate cats. Brain Res. **91**, p 217-235

MILLER, S. and F.G.A. van der MECHÉ (1975b). Locomotion in the cat: basic programs of movement. Brain Res. **91** p 239-253.

MITCHELSON, D.L. (1975). Recording of movement without photography. In: The Human Movement Studies. ed. Whiting, H.T.A. Series Lepus Books London 1975.

MITCHELSON, D.L. (1988). Automated three dimensional movement analysis using the CODA-3 system. Biomedische Technik (FRG) **23** # 7, aug. 1988 p 179-182.

MOON R.J. (1950). Amplifying and intensifying fluoroscopic image by means of scanning X-ray tube. Science **112**, p 389 et seq.

MORECKI, A., R.B. McGHEE, S.H. KOOZEKANANI, J. OLSZEWSKI, C.N. BURNETT and K. JAWOREK (1978). Two methods for automatic computer analysis of human motion from optical images. In: Biomechanics VII, Proc. ISB 1978 p 67-68.

MOZLEY, A.V., R.B. HAAS and F. FORSTER-HAHN (1972). Eadweard Muybridge The Stanford Years, 1872-1882. Stanford CA, Stanford University Museum of Art, 1972.

MURPHY, W.W., R.G. BIRD and D.H. GARCIA (1966). Measurement of body motions. In: Proc. ASME Winter Annual Meeting, 66-WA/BHF-2, 8 p.

MURRAY M.P., B.A. DROUGHT and R.C. KORY (1964). Walking patterns of normal men. J.Bone & Joint Surgery **46A** # 2, p 335-360.

MUYBRIDGE, E. (1887). Animal locomotion. Reprint in: Animals in motion London, Chapman & Hall, 1899, 264 p; re-edited L.S. Brown, Dover 1957.

MUYBRIDGE, E. (1901). The human figure in motion. Chapman & Hall, London 1901; Reprint Dover, New York 1955.

NAC trade literature HSV-200 (1982), HSV-400 (1987). Int. Instrument Marketing Co. Ltd, Thame, Oxon UK (A NAC/Photo-Sonics company).

NIEUKERKE, K.J. (1974). De analyse van het loopgedrag van katten (Dutch). MSc thesis jan. 1974, Faculty of Applied Physics, Delft University of Technology.

NOORLAG, D.J.W. and S. MIDDELHOEK (1979). Two-dimensional position-sensitive photodetector with high linearity made with standard IC-technology. IEE J.Solid-State and Electron Dev. 3, p 75-82.

NOORLAG, D.J.W. (1982). Lateral-photoeffect position-sensitive detectors. PhD thesis sept. 1982, Delft University of Technology, 211 p.

d'OMBRAIN, G.L., L. ROSZA and L.A. COX (1966). Graphical to digital converter. In: Record 1966 IEEE Int.Conv. pt 10, p 66-73.

OOSTINJEN, P. (1980). Het Selspot data-acquisitiesysteem (Dutch). BSc report aug. 1980, Faculty of Applied Physics, Delft University of Technology.

OOSTINJEN, P. (1982). Een synchrone detector voor positiebepaling met een Selcom halfgeleidercamera (Dutch). MSc thesis jan. 1982, Faculty of Applied Physics, Delft University of Technology.

OPPENHEIM, A.V., A.S. WILLSKY and I.T. YOUNG (1983). Signals and Systems. Prentice-Hall, Englewood Cliffs NJ, 796 p, ISBN 0138097313.

OPTOTRAK trade literature (1989). Northern Digital Inc. Waterloo, CDN.

OWEN, R.B. and M.L. AWCOCK (1968). One- and two-dimensional position sensing semiconductor detectors. IEEE Trans.Nucl.Sc. **15**, p 290-303.

PASECKI, E. (1967). Application of TV to the measurement of linear dimensions. Pomiarz Automat. Kontrola (Poland) **13** # 7, 1967, p 309-311

PAUL, J.P. (1967a). Forces transmitted by joints in the human body. In: Proc. Inst.Mech.Eng. **181**, 3J p 8-15.

PAUL, J.P. (1967b). Forces at the human hip joint. PhD thesis, dec. 1967, University of Glasgow.

PAUL, J.P. (1967c). The patterns of hip joint force during walking. In: Proc. 7th Int.Conf.Med.&Biol.Eng. Stockholm 1967, p 516.

PAUL, J.P., M.O. JARRETT and B.J. ANDREWS (1974).Quantitative analysis of locomotion using television. In: Abstr.World Congr.ISPO, Montreux 8-12 oct.1974, p 43. (17 pages unpubl. manuscript in our possession).

PEPOE, R. (1970). Manual for automatic film scanner developed at Children's Hospital in Iowa City, Iowa USA.

PHILIPPENS, M. (1980). Aspects of load acquisition and analysis in the index finger. Internal report Bioeng.Unit, Univ.of Strathclyde Glasgow

POULSON, J. (1973). Biomechanics of the leg. PhD thesis. University of Strathclyde, Glasgow.

PRIESTLEY, M.B. (1981). Spectral analysis and time series. Academic Press, London 1981, ISBN 012549223.

REITER R. (1948). Eine neue Elektrokunsthand. Grenzgebiete der Medizin 4, p 133-135.

RESWICK, J.B. (1965). Signal Processing, introduction. In: The control of external power in upper-extremity rehabilitation (ed. J. Lyman), NAS-NRC, Washington DC 1966, p 203-207.

ROBINSON, D.A. (1963). A method of measuring eye movement using a scleral search coil in a magnetic field. IEEE-Trans BME **40**, p 137-145.

ROEHRLE, H., R. SCHOLTEN, C. SIGOLOTTO, W. SOLLBACH and H. KELLNER (1984). Joint forces in the human pelvis-leg skeleton during walking. J.Biomech. **17** # 6, p 409-424.

SABEL, J.C. (1989). Driedimensionaal schatten: algoritmes in ASYST voor verwerking van TV-camerabeelden (Dutch). MSc thesis aug. 1989, Faculty of Applied Physics, Delft University of Technology.

SAITO, S., H. YAMANOBE and A. TSUKAHARA (1974). A photoelectronic device for recording of 3-D positional changes and its application to analysis of human motions. Tohoku J.Exp.Med. **113**, p 25-35.

SANGSTER, F.L. and K. TEER (1969). Bucket brigade electronics - new possibilities for delay, time axis conversion and scanning. IEEE-J.SC 4, p 131-136.

SAPRYKIN, K.V. (1968).Control of measurement of linear dimensions with the help of television. Indian J.of Technol. **6** # 1, jan. 1968, p 1-7.

SCHILT, B.J. (1989). Vooronderzoek naar het gebruik van de transputer voor real-time dataverwerking van een bewegingsregistratiesysteem (Dutch). In partial fulfilment of MSc thesis, feb/sept. 1989, Faculty of Applied Physics, Delft University of Technology.

SCHLESINGER G. (1917). Die Mitarbeit des Ingenieurs bei der Durchbildung der Ersatzglieder. Verein Deutscher Ingen., Berlin Zeitschr. **61**, p 6 et seq.

SCHOTTKY, W. (1930). Ueber den Entstehungsort der Photoelektronen in Kupfer-Kupferoxydul-Photozellen. Phys.Z., Leipzig **31**, p 913-925.

SCHROEDER, M.R. (1970). Synthesis of low-peak-factor signals and binary sequences with low autocorrelation. IEEE-Trans.IT, p 85- 89.

SCHUCK, W.H. (1966). Vidicon star tracker. Applied Optics **5** # 4, april 1966, p 489-496.

SELCOM AB, Mölndal, Swedish Patent Application 10165/72.

SELCOM AB, Mölndal, Sweden, Dutch Patent Application 7310666. Werkwijze en toestel voor het bepalen van de plaats van een punt.

SELSPOT trade literature (1975 on). SELCOM AB, Mölndal/Partille, S.

SERLÉ, E.J. (1983). Ruisonderzoek in een op video gebaseerd positiebepalingssysteem (Dutch). BSc report may 1983. Faculty of Applied Physics, Delft University of Technology.

SERLÉ, E.J. (1984). Rekenend meetinstrument voor op TV gebaseerde bewegingsregistratie (Dutch). MSc thesis nov. 1984. Faculty of Applied Physics, Delft University of Technology.

SIKKENK, H. (1986). Ontwerp en bouw van een synchrone detektor voor positiebepaling van LED's (Dutch). BSc report, Faculty of Applied Physics, Delft University of Technology.

SIKKENK, H. (1988). Synchrone detektor voor positiebepaling van aktieve markers met een Selspot halfgeleiderkamera (Dutch). MSc thesis may 1988, Faculty of Applied Physics, Delft University of Technology.

SIMPSON, D.C. (1965). The control of a multi-movement powered upper limb prosthesis. In: Proc. Eur.Symp. on Medical Electronics, Brighton 1965, p 296-297.

SIMPSON, D.C. (1971). E.p.p. (extended physiological proprioception) control of a complete arm prosthesis. Report of 6th Int.Course, Schweiz.Arbeitsgemeinsch.f.Prothesen u.Orthosen, Zürich 1971.

SIMPSON, D.C. and G. KENWORTHY (1973). The design of a complete arm prosthesis. Biomedical Engineering, feb. 1973, p 56-59.

SLEPIAN, D. (1976). On bandwidth. Proc. IEEE **64** # 3, p 292-300.

SMITH, R.J. (1985). Functions of condylar translation in human mandibular movements. Am.J.Orthodonty **88**, p 191-202.

SOERJANTO, R. (1971). On the application of the myoelectric handprosthesis in the Netherlands. PhD thesis Univ. of Amsterdam 1971, 184 p.

SONNENBURG, I. and K. FETHKE (1983). Zur Problematik der alloplastischen Kiefergelenkersatzes. Dtsch.Z.Mund Kiefer Ges. Chir. **7**, p 410-417

SORENSEN, E. (1966). Electronic measurement of area. Ingenioren (Denmark) **75** # 3, 1 feb. 1966, p 171-173.

SPOOR, C.W. and F.E. VELDPAUS (1980). Rigid body motion calculated from spatial coordinates of markers. J.Biomechanics **13**, p 391-393.

STEILBERG, P.C. (1967). Het ontwerp van een video-naar-digitaal omzetter voor de analyse van armbewegingen (Dutch). BSc report oct. 1967 Faculty of Applied Physics, Delft University of Technology.

STEILBERG, P.C. (1968). Televisieregistratiesysteem voor de analyse van armbewegingen (Dutch). MSc thesis oct. 1968. Faculty of Applied Physics, Delft University of Technology.

SYDENHAM, P.H. (1968). Linear and angular transducers for positional control in the decametre range. Proc.IEE **115** # 7,july 1968,p 1057-1066

SYDENHAM, P.H. (1982). Handbook of measurement science, **1**, Theoretical fundamentals. John Wiley, Chichester, 654 p, ISBN 0471100374.

TANENBAUM, A.S. (1981). Computer networks. Prentice Hall, Englewood Cliffs NJ USA, 517 p, ISBN 0131646990.

TAYLOR, F.W. (1911). The principle of scientific management. Harper, New York 1911.

TAYLOR, K.D., F.M. MOTTIER, D.W. SIMMONS, W. COHEN, R. PAVLAK JR, D.P. CORNELL and B. HANKINS (1982). An automated motion measurement system for clinical gait analysis. J.Biomech. **15** # 7, p 505-516.

TEXAS INSTRUMENTS (1972). The opto-electronics data book.

THURSTON, A.J. (1982). Repeatability studies of a TV/computer system for measuring spinal and pelvic movements. J.Biomed.Eng. **4**, april 1982 p 129-132.

TICHAUER, E.R. (1966). Gilbreth revisited. In: Proc. ASME 1966 Winter Annual Meeting, paper 66-WA/BHF-7, New York 1966, 17 p.

TOMOVIC, R. (1960). Human hand as a feedback system. In: Proc.1st IFAC Congress, Moscow, p 624-628.

TOMOVIC, R. and G. BONI (1962) An adaptive artificial hand. IRE-Trans. AC, april 1962, p 3-10.

TOMOVIC, R. and M. PETROVIC (1965). Cybernetic rendezvous problems. IEEE-Trans.AC **10**, jan. 1965, p 22-27.

TOMOVIC, R. (1965). Control theory and signal processing in prosthetic systems. In: The control of external power in upper-extremity rehabilitation (ed. J. Lyman), Warrenton, april 8-10, 1965, NAS, Washington DC, 1966, p 221-226.

VELTMAN, B.P.Th. and H. KWAKERNAAK (1961). Theorie und Technik der Polaritätskorrelation für die dynamische Analyse niederfrequenter Signale und Systeme. Regelungstechnik **9** # 9, p 357-364.

VELTMAN, B.P.Th. and A. van den BOS (1963). The applicability of the relay correlator and the polarity coincidence correlator in automatic control. In: Proc. 2nd IFAC World Congr., Basel, Butterworth, London 1964, p 620-626.

VICON trade literature (1980 on) Oxford Medical Systems,Oxford Medical Computers, Oxford Metrics UK.

VIERORDT, K.H. (1881). Das Gehen des Menschen in gesunden und kranken Zuständen nach selbstregistrierenden Methoden dargestellt. Laupp, Tübingen 1881.

VINK, P. and A. HUSON (1987). Lumbar back muscle activity during walking with a leg inequality. Acta Morphol. Neerl.-Scand. **25**, p 261-271.

VINK, P. (1989). Functions of the lumbar back muscles. PhD thesis april 1989, University of Leiden, 111 p.

WALLMARK, J.T. (1957). A new semiconductor photocell using lateral photoeffect. Proc. IRE **45**, p 474-483.

WALTON, J.S. (1986). The accuracy and precision of a video-based motion analysis system. In: Proc. SPIE **693**, aug. 1986, 13 p.

WALTON, J.S. (1988). ExpertVision: a video-based non-contact system for motion measurement. In: Proc.19th Ann.Symp.Soc.Flight Test Engs., aug. 1988, Arlington Texas USA.

WATSMART trade literature (1986 on). Northern Digital Inc. Waterloo, Ontario, Canada.

WEBER, W. and E. WEBER (1836). Mechanik der menschlichen Gehwerkzeuge. Dieterich, Göttingen 1836.

WHITTLE, M.W. (1982). Calibration and performance of a 3-D TV system for kinematic analysis. J.Biomechanics **15** # 3, p 185-196.

WIJNSCHENK, M.J. (1967a). Regeltechnische aspecten van armprothesen (Dutch), Ned.Tijdschr.v.Natuurk. **33**, 1967, p 271-294.

WIJNSCHENK, M.J. (1967b). Optimal control in arm prosthis design. In: Proc. 7th.Int.Conf.Med.& Biol.Eng. Stockholm 1967, p 447.

WIJNSCHENK, M.J. and E.H. FURNÉE (1968). De besturing van armprothesen (Dutch). Ned.Tijdschr.v.Fysiother. **78** # 3 4 p.

WILDT, H. van der (1971). Video-digitaal meetsysteem (Dutch). Int.Rep. Phys.Lab. University of Utrecht.

WILLMANN, - (1882). The horse in motion as schown by instantaneous photography; sic; (from Muybridge). Turner, London 1882.

WINTER, D.A., S.A. MALCOLM and B.G. TRENHOLM (1968). Real-time conversion of video fluoroscopic images. In: Dig.2nd Can.Med.&Biol.Eng.Conf. Toronto 9-1 sept.1968.

WINTER, D.A., R.K. GREENLAW and D.A. HOBSON (1970).A clinical approach to the study of human locomotion. In: Dig.3rd Cdn.Med.&Biol.Eng.Conf., Halifax NS, sept. 1970.

WINTER, D.A., and G.D. REIMER (1972a). Quantization errors in calculation of volumes, areas and coordinates in medical images. In:Proc.16th SPIE Conf., San Fransisco.

WINTER, D.A., R.K. GREENLAW and D.A. HOBSON (1972b). TV - computer analysis of kinematics of human gait. Comp.& Biomed.Res. **5**, p 498-504.

WINTER, D.A., H.G. SIDWALL and D.A. HOBSON (1974). Measurement and reduction of noise in kinematics of locomotion. J. Biomech. **7**, p 157-159

WINTER, D.A. (1982). Camera speeds for normal and pathological gait analyses. J.Med.& Biol.Eng.&Comp. **20**, p 408-412.

WISNIEFF, R.E. (1961). An automatic TV tracking theodolyte for range instrumentation. IRE-Trans. Mil.El. oct. 1961, p 326-330.

WOLTRING, H.J. (1975). Single- and dual-axis lateral photodetectors of rectangular shape. IEEE-Trans.ED 22, p 581-590.

WOLTRING, H.J. and E.B. MARSOLAIS (1980). Optoelectric (Selspot) gait measurement in two- and three-dimensional space - preliminary report. Bull.of Prosthetics Res. 10-34 (Vol. **17** # 4) Fall 1980.

WOLTRING, H.J. (1981). 3-D Utility software for S.M.A.C. at the Dundee Limb Fitting Centre. Internal report on behalf of the Dundee Limb Fitting Centre/Scottish Home and Health Department. 28 oct.1981.

WOLTRING, H.J. (1984). Meting en modelvorming rond het menselijk bewegingsproces (Dutch). Medica Physica 1984 # 7, p 27-42.

WOLTRING, H.J., I.S. McCLAY and P.R. CAVANAGH (1989). 3-D Photogrammetric camera calibration without a calibration object. Abstr.# 197 in Proc. 12-th Congr. Int.Soc.Biomech. (26-30 june 1989) Los Angeles, USA

YAKOBSON, Ya.S., A.E. KOBRINSKII, B.P. POPOV, E.P. POLYAN, Ya.L. SLAVUTSKI and A.Ya. SYSIN (1958). A forearm prosthesis with an electrical servo controlled by muscle currents and fitted with a means of sensing the gripping force. Authors' certificate No 120300, with priority from 24 october 1958, 2 p.

ZAMZOW, H. (1988). Schnelle Bewegungen in Echtzeit erfassen: Bewegungs Analyse mit dem randomaccess tracking System. Elektronik 4, feb. 19, 1988, p 107-110.

ZANDBERGEN, A. (1984). Opwarm-karakteristiek van tv-camera's (Dutch). BSc report dec. 1984. Faculty of Applied Physics, Delft University of Technology.

ZANDBERGEN, A. (1986). 3-D Analyse van een loopbeweging met behulp van TV-camera's (Dutch). MSc thesis aug. 1986, Faculty of Applied Physics, Delft University of Technology.

ZUIDHOF, M. (1989). Marker identificatie in twee en drie dimensies bij een TV-computer bewegingsmeetsysteem (Dutch). MSc thesis oct.1989, Faculty of Applied Physics, Delft University of Technology.

SCIENTIFIC EXHIBITS

7th Int. Conf. on Med. & Biol. Eng., Stockholm, aug. 14-19, 1967.

IMEKO V, Versailles, may 25-30, 1970.

Physiological Society London, march 22-23, 1974.

Workshop Gait Analysis, University of Dundee, march 30-april 1, 1981.

Sport'84, Nationaal Sportcentrum, Arnhem, may 16-19, 1984.

Studiedag toepassing bewegingsanalyse in de sport, Nat.Sportcentrum, Arnhem, 25 jan. 1986.

Symposium Motografie, Univ.d.Bundeswehr, München, march 11-12, 1986.

5th ESB, Berlin, sept. 8-10, 1986.

Flanders Technology International, Gent, may 5-11, 1987.

Het Instrument, Utrecht, may 2-6, 1988.

Ident/Vision, Stuttgart, may 30-june 1, 1989.

Curriculum vitae E.H. Furnée

aug. 1933	born in the Hague
june 1951	final exam, Maerlant Lyceum
oct. 1961	degree, Electrical Engineering, Delft University of Technology
nov. 1961	military service, Electronic Development Lab. Armed Forces (LEOK) Oegstgeest
nov. 1963	Cooperation Centre for Measurement and Control, c/o Faculty of Applied Physics, Delft University of Technology
jan. 1981	Signal Processing Department, Faculty of Applied Physics, Delft University of Technology.

Samenvatting

Het onderwerp van het proefschrift wordt gevormd door op televisie-camera's gebaseerde computergekoppelde meetsystemen voor bewegings-analyse, vanaf de introductie van de oorspronkelijke video-digitale coordinatenomzetter door de auteur, tot de hedendaagse ontwikkelingen waaraan eveneens is bijgedragen.

Het inleidend **hoofdstuk 1** schetst eerst historische ontwikkelingen van het waarnemen en registreren van voornamelijk menselijke en dierlijke beweging. Hier nemen vooral de vroege toepassingen van fotografie door Muybridge (1877) en Marey, en in het bijzonder de uitvinding van de filmcamera door de fysioloog Marey (1888) een belangrijke plaats in. De filmcamera, die niet alleen in de wetenschap een uitzonderlijk groot toepassingsgebied heeft gevonden, was als meetinstrument het eerste bemonsteringssysteem dat de acquisitie en opslag van een in aanleg willekeurige hoeveelheid bemonsteringen toeliet. Numerieke uitwerking van met fotografie verkregen bewegingsdata vond al plaats door Braune en Fischer (1891).

De inleiding vervolgt met een overzicht van latere numerieke bewerking middels computer invoer van fotografische en filmgegevens, eerst door menselijke waarnemers met projectie- en ponsband-apparatuur, later met de eerste flying-spotscanners.

Een schets van enige vroege ontwikkelingen in ledemaatvoorziening bij gehandicapten, met name in extern bekrachtigde arm- en handprotheses, illustreert de achtergrond van de behoefte bij de onder auspiciën van het toenmalige Ontmoetingscentrum voor Meet- en Regeltechniek opge-richte werkgroep Prothesebesturing aan een nieuwe, niet-fotografische meetmethode voor on-line registratie van armbewegingen.

Hoofdstuk 2 beschrijft de diverse stadia van ontwikkeling van dit, op standaard closed-circuit TV gebaseerde, optoelektronische meetsysteem, dat de digitaal gecodeerde coordinaten levert van bovendrempelig hel-dere beeldpunten. Deze dusgenoemde video-digitaal coordinatenomzetting gebeurt in real time ten aanzien van de TV beeldaftasting.

De uitvoer van beeldpuntcoordinaten betreft in het algemeen slechts omtrekspunten van contrasterende markers, aangebracht op strategische punten aan de bewegende delen. De coordinatenconversie van een tiental markers ter grootte van 10 beeldlijnen betekent op een rooster van bv. 256 * 256 pixels al een 300-voudige datareductie.

Echter, de eerste versie (Furnée 1967) heeft al in de vorm van de z.g. contour onderdrukker een voorziening, die de hoeveelheid data beperkt tot één coordinatenpaar per marker, dus nog eens een 20-voudige data-reductie. Later werd terwille van de nauwkeurigheid overgegaan op twee cq vier coordinatenparen per marker, waarvan het middelpunt vervolgens in de gastheercomputer wordt geschat. Datareductie al in het real-time domein blijft tot de kenmerken van het meetsysteem behoren.

Vanaf het begin is het meetprincipe van de video-digitale coordinaten omzetter het, onder besturing van de binaire video helderheidspulsen, uitlezen van de momentane stand van twee binaire 8 bit (later 9 en 10 bit) tellers. Voor de verticale coordinaat is dat een lijnteller, voor de horizontale coordinaat een intervalteller. Bij de tot 1985 benutte electronenbuis camera's betrof dit de telling van tijdintervallen, waarin de lijntijd werd verdeeld. Het kristalgestuurde tellersysteem leverde tevens de synchronisatiepulsen naar de camera(s).
Een aantal interfaces werd ontwikkeld voor koppeling aan de voorhanden minicomuters, met daarnaast besturingen voor digitale bandrecorders voor gebruik van het meetsysteem bij de eerste samenwerkingsprojekten buiten het eigen laboratorium.

Middels een voorziening in de video-digitaal coordinatenomzetter konden óók, met een normale camera waargenomen, detailrijke foto's worden ingelezen. Als aanpassing aan de beperkte invoersnelheid van de computer gebeurde dat, door een voortschuivende traliegewijze onder-drukking, in 16 achtereenvolgende beelden. Uitbreiding tot boven de twee videoniveaus lag voor de hand. Deze aanloop naar de latere z.g. framegrabbers voor stilstaand beeld, o.a. voor patroonherkennen in chromosoomfoto's, is in het hier beschreven werk niet voortgezet.
Dit vormde de enige afwijking van het (tot heden) leidend meetprincipe dat bij optoelektronische bewegings-registratie het objekt wordt geabstraheerd tot een aantal welgekozen en zo goed mogelijk gefixeerde markeringspunten. Aldus worden terwille van de real-time verwerking detail-arme, contrastrijke beelden verkregen.

Eveneens in hoofdstuk 2 wordt de introductie besproken van de voor de TV camera geplaatste roterende sluiter om te komen tot equidistante bemonsteringstijdstippen, ondanks de aftasting van boven naar beneden van het camerabeeld. Met hetzelfde doel, nu zonder de synchrone camera sluiter, is stroboscopische belichting ingevoerd van passieve, reflecterende markers, eerst bij loopstudies van de kat.

Met de verticale en horizontale aftasting van TV wordt tevens, naast de *in eerste aanleg beperkte snelheid, een niet onaanzienlijk* bezwaar van deze in een vast patroon adresserende sensor gegeven. Bij gebruik in het TV meetsysteem zijn, tenzij er bijzondere restricties worden opgelegd, de markers onderling niet onderscheidbaar. Tevens is de *volgorde van de real-time uitvoer van de coordinatenparen bepaald door* de plaats van de markerprojekties ten opzichte van elkaar. Daar i.h.a. het beeld en dus de marker volgorde bij beweging zal veranderen, is er de noodzaak om programmatisch de coordinatenparen toe te wijzen aan de juiste *markers. Ook de hiervoor ontwikkelde, in het algemeen op baan*-predictie van de afzonderlijke markers berustende, programmatuur wordt besproken. Evenals de correcties voor niet-lineariteiten, die met name bij buizencamera's en in mindere mate bij lensdistorsie vereist zijn.

Tenslotte bevat dit hoofdstuk een terugblik op het vroegste gebruik van videosignalen in meetsystemen, waarbij de belangstelling minder uitgaat naar analoge verwerking van dimensionele of plaats informatie. Van een aanzet tot digitale coordinatenconversie bevat de literatuur vóór 1967 nauwelijks enige gedocumenteerde voorbeelden, terwijl van de verwerking van meer dan één punt en anders dan met slow-scan TV alleen een vermoeden bestaat, zonder opheldering over de gebruikte methode.

Dat met de video-digitaal coordinaten omzetter nieuw gebied betreden werd, vindt in de o.a. door Sydenham (1968) en Andrews (1982) gecompileerde literatuur geen tegenspraak. Niettemin is dit instrument weinig anders dan een interface tussen bestaande sensor- en computertechniek. Over de jaren werd aan dit interface intelligentie en verwerkingscapaciteit toegevoegd, zoals in hoofdstuk 4 besproken wordt.

In **hoofdstuk 3** komen van het Delftse prototype afgeleide systemen ter sprake, evenals latere onafhankelijk gerapporteerde alternatieven van een veelal gelijksoortige opzet.

Samenwerking met de Bioengineering Unit van de University of Strathclyde (Glasgow) heeft geleid tot een, o.a. ten aanzien van het gebruik van meer camera's wat uitgebreider bewegingsregistratie- en analysesysteem (Paul e.a. 1974). Dit is zeer sterk op interfacing aan de DEC-PDP/11 (later LSI/11) gericht. Tevens via Jarrett (1976) geinstalleerd bij het Dundee Limb Fitting Centre, was het Strathclyde systeem op zijn beurt prototype voor het commerciële VICON systeem, dat in 1981 werd uitgebracht door Oxford Instruments (UK).
Pas in 1986 is dit weer met enige innovaties cq aanpassingen nagevolgd door ELITE van BTS (Italie) en ExpertVision van Motion Analysis (USA).
Aan de Strathclyde groep (Andrews e.a. 1981) is het gebruik van Scotch 3M retro-reflecterende markers, en belichting met LED's te danken.

Hoofdstuk 3 bespreekt ook een aantal bijdragen van andere auteurs, waaronder het gebruik van TV voor het bepalen van de blikrichting.
Aandacht wordt gericht op met de gastheercomputer verrichte middelpunt bepaling van markers uit filmbeelden (Winter e.a. 1970) en de bepaling van geometrische zwaartepunten vanuit de marker omtrekscoordinaten (Taylor e.a. 1982). Deze methode, waarbij resoluties beneden de pixel-afmetingen te behalen zijn, werd in het Delftse systeem en in VICON overgenomen. Dan komt in hoofdstuk 4 bij het PRIMAS "Precision Motion Analysis System" de implementatie in real time aan de orde van dit data-reductie en precisie verhogende algoritme.

Tenslotte wordt in hoofdstuk 3 ook een alternatieve optoelektronische methode (SELSPOT), waarin een niet-geadresseerde Position Sensitive Device sensor en actieve geschakelde LED markers worden gebruikt, aan de orde gesteld. Ook wordt een mechano-optisch sensorsysteem (CODA-3) besproken. Deze twee commerciële systemen uit 1975 resp. 1981 worden, evenals het OPTOTRAK systeem van 1988, vergeleken met de TV methodes.

Na deze rondblik gaat **hoofdstuk 4** weer over het eigen werk, behalve paragraaf 8 waar, voorafgaande aan een beschouwing van de te stellen eisen en een vergelijking van de specificaties, de recente versies van VICON, ExpertVision, ELITE en het HENTSCHEL systeem worden besproken.

Inleidende metingen bevestigden de voordelen, mede uit het oogpunt van ruis onderdrukking, van zwaartepuntsbepaling uit de omtrekscoordinaten van de afzonderlijke markers. Voor real-time zwaartepuntsbepaling werd dit algoritme ondergebracht in een 16 bit microprocessor subsysteem.

Het daarmee verkregen rekenend meetinstrument biedt een optimum aan datareductie. Middels de IEEE-488 instrumentatiebus werd het systeem gekoppeld aan een desktop personal computer, waarmee de opstelling gemakkelijk verplaatsbaar werd.

Een optimum aan stabiliteit is verkregen met een nieuw ontwikkelde niet-geinterlinieerde CCD-camera, die tot op het niveau van de videofrequente pixelklok met het meetsysteem is gesynchroniseerd.
Tevens heeft deze, op de frame-transfer sensor gebaseerde, camera de voorziening van een geheel electronisch bekorte integratietijd, ofwel (gezien als bemonsteringssysteem) een bekorte apertuur, aanvankelijk van 5 %, later van 1 % van de rasterperiode.
Deze stroboscopische camera werking is vanzelfsprekend synchroon met de stroboscopische LED belichting van de retroreflecterende markers. Hierdoor is het contrast van de markers tegen de omgevings- en objectverlichting dermate vergroot dat het meetsysteem onder sterk verruimde condities, tot buitenshuis in daglicht kan worden toegepast.
Ter verhoging van de bemonsteringsfrequentie werkt de camera als optie op 100 Hz. Als bijzondere voorziening is er de strip-scan optie van 200 halfhoge beeldjes/s.

In een samenwerking in het kader van een SPIN-gesubsidieerd onderzoek wordt een aantal van deze eigenschappen thans ondergebracht in de, op basis van dezelfde sensor, uit te brengen commerciële meetcamera van High Technology Holland bv (Eindhoven). Daar wordt ook aan een marktversie van het PRIMAS bewegingsmeetsysteem gewerkt.

Een aantal gerealiseerde en voor multi-camera gebruik nog voorgenomen *strukturen van het PRIMAS rekenend meetsysteem wordt in dit hoofdstuk* besproken. Daaronder het gebruik van digitale signaalbewerkingschips (vervallen bij de thans gebruikte 32 bit microprocessor), de dual-port geheugens als interface tussen onderscheiden subsystemen, en de koppeling met IBM-AT compatibele personal host computers.

De prestaties van het meetsysteem worden getoetst aan de z.g. spatiotemporele resolutie, waarin de precisie bij stilstaande markers wordt gerelateerd aan de bemonsteringsfrequentie. Deze kwaliteitsfactor is in gewijzigde vorm ontleend aan (Lanshammar 1982).

Hierbij blijkt het PRIMAS systeem aan de kop te staan van de hedendaagse competitie. Ook wordt het onderzoek besproken van de resolutie in de zin van standaard deviatie van de meetfout bij een reeks incrementele markerverplaatsingen. Hier zijn eveneens superieure resultaten behaald.

Hoofdstuk 5 is gewijd aan een geheel ander coordinatenmeetsysteem, waaraan is gewerkt, op basis van een Position Sensitive Device sensor. Hier zijn de LED markers amplitude-gemoduleerd op verschillende frequenties, in tegenstelling tot SELSPOT waar de LED's in tijdmultiplex worden geschakeld. Met coherente detectie vanuit de multifrequente sensorsignalen worden de coordinaatwaardes voor de onderscheiden LED markers bepaald. Anders dan bij SELSPOT, CODA-3 en OPTOTRAK worden de markers simultaan bemonsterd. De detectiemethode is equivalent aan een zeer nauw bandfilter ten opzichte van de sensorruis, terwijl ook de invloed van omgevingslicht wordt geminimaliseerd. Een reeks van in digitale technieken uitgevoerde prototypes passeert de revue en als voornaam testresultaat wordt de lage meetruis besproken.
Aangetoond wordt, dat het toepassen van een vensterfunctie gunstig is voor het beloop van de overdrachtsfunctie, die een laagdoorlaat karakter heeft voor de frequentiecomponenten van bewegende markers.

In **hoofdstuk 6** wordt een aantal toepassingen, i.h.a. in de vorm van samenwerkingsprojekten, besproken.
Daarbij illustreren de eerste metingen aan doelgerichte armbewegingen, met hoek- en snelheidsberekening, de mogelijkheden van het prototype.

Met de Erasmus Universiteit (Anatomie) is gewerkt aan gangbeeldanalyse van katten op de lopende band. Gelijktijdig met de ledemaatbewegingen werd EMG geregistreerd als uitdrukking van motoneuron activiteit. Het aldaar plaatsvindende onderzoek was gericht op de tot stereotype bewegingen leidende vuurpatronen en de poot- en segmentsgewijze koppeling van hypothetische stapgenerators in het ruggemerg.

Met de Leidse Universiteit (Neurologie) is vooronderzoek verricht aan onwillekeurige bewegingen bij de mens bij zekere aandoeningen van het centraal zenuwstelsel. De bedoeling was om te komen tot klassifikatie van de stoornissen en evaluatie van de medicatie effecten. Eveneens is gewerkt aan bewegingskarakteristieken van snelle, z.g. ballistische armbewegingen, o.m. inzake correlatie met links- en rechtshandigheid.

Gangbeeldonderzoek bij de mens is verricht op de lopende band bij de Leidse Universiteit (Bewegingswetenschappen), waar met een 3-D opstelling rotaties en translaties van het bekken, en van het loopapparaat, zijn gemeten. Dit onderzoek was gericht op links- rechts asymmetrieën bij het lopen van proefpersonen met beenlengteverkorting.

Tot het onderhanden onderzoek behoren de metingen aan het kaakgewricht in samenwerking met Universiteit Twente (Mechanica) bij de Groningse Universiteit (Mondziekten en Kaakchirurgie). Hier wordt een analyse verricht van het rotatie/translatie gedrag van de onderkaak. Daartoe wordt een uitwendige beugel met markers gebruikt, die bevestigd is aan de dentuur van de onderkaak. Ook worden de inwendige bewegingen gereconstrueerd van het kaakkopje (t.o.v. de markers vastgelegd middels één röntgenfoto). Doel is ontwerp van de ideale kaakgewrichtsprothese.

Bij de TU Eindhoven (Fundam. Mechanica) is enig vervormingsonderzoek verricht aan metalen pellets voorzien van een aantal minuscule markers, onder axiale druk. Resultaten van het pilot-experiment riepen de vraag op naar hogere-resolutie systemen voor een 10 * 10 marker matrix, een van de doelstellingen van het SPIN-subsidieprojekt.

Tenslotte worden enige voorstudies besproken voor andere technische toepassingen, waaronder real-time tracking van de last bij containerkranen (ASEA, NELCON), bewegingen bij offshoresimulatoren (MARIN) etc.

Bij de **conclusies** in hoofdstuk 7 worden de ontwikkeling van computergekoppelde bewegingsmeetsystemen en de bijdragen van de auteur samengevat. Tevens wordt een overzicht gegeven van de karakteristieken van de gangbare systemen, waarna in een discussie ook de blik op verdere ontwikkelingen wordt gericht.

OFFSETDRUKKERIJ HAVEKA B.V., ALBLASSERDAM